Mécanisme d'action antidépresseur rapide de la kétamine et de son principal métabolite (2R,6R)-hydroxynorkétamine : rôle de la balance excitation-inhibition chez la souris

Thu Ha Pham

université PARIS-SACLAY

NNT : 2018SACLS086

Mécanisme d'action antidépresseur rapide de la kétamine et de son principal métabolite (2*R*,6*R*)-hydroxynorkétamine: rôle de la balance excitation-inhibition chez la souris

Thèse de doctorat de l'Université Paris-Saclay
préparée à l'Université Paris-Sud

École doctorale n°569 innovation thérapeutique:
du fondamental à l'applique
Spécialité de doctorat: Sciences pharmacologiques

Thèse présentée et soutenue à Châtenay-Malabry, le 30 Mars 2018, par

Thu Ha Pham

Composition du Jury :

Michel Hamon Pr, UPMC Univ. Paris 6 (– INSERM UMR894)	Président
Isabelle Leroux-Nicollet Pr, Université de Normandie (– INSERM U1245)	Rapporteur
Raymond Mongeau Dr, Université Paris-Descartes (– EA4475)	Rapporteur
Hervé Daniel Pr, Université Paris-Saclay (– CNRS UMR9197)	Examinateur
Philippe Fossati Pr, UPMC Univ. Paris 6 (– Gh Pitié-Salpêtrière, ICM-A-IHU)	Examinateur
Alain Gardier Pr, Univ. Paris-Sud, Université Paris-Saclay (– UMRS1178)	Directeur de thèse

Thèse de doctorat

Je dédie cette thèse

À mes chers parents

À mon très cher mari

À ma chère future fille

Remerciements

- ***Aux membres du jury,***

Je remercie **Monsieur le Professeur Michel Hamon**, à l'unité INSERM UMR 894, Sorbonne Universités, UPMC Université Paris 6, d'avoir accepté de présider ce jury de thèse.

Je remercie **Madame le Professeur Isabelle Leroux-Nicollet**, à l'unité INSERM U1245, Université de Normandie, Rouen, pour son suivi et ses conseils depuis mon comité de mi-thèse et pour avoir accepté de juger mon travail final en tant que rapporteur.

Je remercie **Monsieur le Docteur Raymond Mongeau**, à l'unité EA4475, Université Paris-Descartes, pour avoir accepté de juger mon travail final en tant que rapporteur.

Je remercie **Monsieur le Professeur Hervé Daniel**, CNRS UMR9197, Institut des Neurosciences, Université Paris-Saclay, Orsay et **Monsieur le Professeur Philippe Fossati**, Service de Psychiatrie d'adultes, Gh Pitié-Salpêtrière, ICM-A-IHU, Sorbonne Universités, UPMC Université Paris 6, d'avoir accepté de participer à ce jury de thèse en tant qu'examinateur.

- ***À Monsieur le Professeur Alain Gardier,***

Je te remercie du fond du coeur pour tous les enseignements que tu m'as apportés en tant que directeur de thèse pendant ces quatre ans et demi de thèse. Tu m'as donné l'opportunité de travailler au sein de ton équipe mais aussi toutes les instructions importantes pour faire évoluer ma thèse en particulier et ma carrière en général. Tu es aussi un professeur de français exemplaire doté d'une grande patience. Merci pour ta présence tout au long de mon séjour en France. Je te suis extrêmement reconnaissante pour toutes tes relectures et tes corrections concernant mes publications, ma revue et ma thèse qui t'ont prises énormément de temps et d'énergie. Ensemble, nous avons eu des réussites importantes dans notre domaine de recherche. Tes connaissances scientifiques, ta disponibilité et ta compréhension ont été pour moi une source d'inspiration et d'énergie pour surmonter tous ces défis. Ton dévouement est sans nul doute le pilier fondateur qui m'a permis de mener à bien mon travail de thèse.

- ***À Monsieur le Professeur Denis David,***

Je te remercie sincèrement pour ton soutien et ta grande disponibilité tout au long de mon travail. Ta passion pour la recherche m'a vraiment impressionnée et m'a encouragée à poursuivre ce travail de thèse. Merci pour le temps que tu as consacré à analyser tous mes résultats comportementaux, ainsi que mes données finales et la correction de mes manuscrits. Grâce à ton aide, j'ai pu avancer énormément dans mon travail. Je te remercie aussi de m'avoir donné l'opportunité de travailler avec des collaborateurs américains, avec lesquels nous avons pu réaliser des travaux intéressants avec le HNK.

- ***À Monsieur le Docteur Jean-Philippe Guilloux,***

Je te remercie pour ta présence qui m'a fait très plaisir pendant ces années. Tu as été le premier à me montrer la technique de microdialyse, qui m'a servie tout au long de mon travail. Tes conseils en statistiques ont facilité les analyses de mes données et m'ont fait gagné beaucoup de temps. J'ai aussi beaucoup aimé les jeux que tu as organisés. Grâce à toi, j'ai appris plein de choses et je te remercie encore pour toute ton aide.

- ***À Monsieur le Docteur Laurent Tritschler,***

Un grand merci à toi pour m'avoir enseigné toutes ces techniques, ainsi que tes astuces extraordinaires qui m'ont fait gagner du temps et de l'énergie. Tes conseils sur la partie optogénétique m'ont appris plein de choses. Tu es une personne très sympathique avec qui j'ai toujours eu plaisir à parler.

- ***À Madame le Docteur Indira Mendez-David,***

En dehors de tout ton soutien scientifique important pendant mon travail de thèse, je te remercie particulièrement d'être une amie merveilleuse qui est toujours à l'écoute. Merci pour tous ces bons moments partagés au laboratoire comme à l'extérieur.

- ***À Madame le Docteur Céline Defaix,***

Je te remercie pour toutes les manips de spectroscopie de masse et ta participation importante à mon travail de thèse. Tu m'as accompagnée tout au long de mes manips, en particulier pendant tous ces étés passés au laboratoire. J'ai beaucoup apprécié travailler avec toi.

- ***À mes collègues avec lesquels j'ai pu travailler durant ma thèse au laboratoire,***

Je remercie en particulier **Charlène** car tu m'as beaucoup aidé pendant ces années d'une part avec le français, d'autre part avec les manips, mais aussi pour le "service" de transport et les aides familiales. Ça a été une grande joie de pouvoir travailler avec toi.

Je remercie aussi **Julie** pour tous ses conseils de français et ses histoires drôles que nous avons partagées pendant cette année. Je remercie **Maryam** pour ses conseils, ses superbes gâteaux délicieux qui m'ont beaucoup fait plaisir. Merci à **Françoise** et **Louise** pour leur présence et leur bonne humeur pendant mon séjour en France, ainsi que pour tous les services qu'elles m'ont rendus. Merci à *Karim* pour ses encouragements et son soutien. Je remercie *Daniela*, *Flavie*, *Yannick* et *Gaël,* même si vous êtes partis, vous m'avez donné beaucoup de conseils au début de ma thèse. Merci à *Valentine*, la gentille stagiaire, qui est une amie très sympathique.

- ***Aux personnes avec lesquelles j'ai pu collaborer durant ma thèse,***

Je tiens à remercier tous mes collaborateurs dont l'équipe du Docteur Christine Denny, l'équipe du Professeur René Hen (Université de Columbia, USA), l'équipe du Professeur Jean-Claude Alvarez (Hôpital Raymond-Poincaré, France), l'équipe du Professeur Mothet (LAC CNRS, Orsay), le

Professeur François Coudoré (UMR-S 1178) et le Docteur Bruno Guiard (Université de Toulouse) qui m'ont fourni de nombreux conseils et outils et qui m'ont enseigné des techniques importantes pour la réalisation de ce travail de thèse.

Je remercie en particulier le **Docteur Audrey Solgadi** et le **Professeur Pierre Chaminade** de la plateforme SAMM pour toutes les discussions intéressantes sur la rédaction de l'article méthodologique et pour avoir fourni les résultats de spectrométrie de masse de ma thèse.

Je remercie le personnel de la plateforme Animalerie qui a permis que mes études de comportements se déroulent dans les meilleures conditions possible.

- ***À mes amis,***

Je remercie mes amis de l'ADIT : Chloé, Doumet, Rami, Hélène et Julie d'avoir été présents pendant ces années. C'est un plaisir de vous connaître.

Je remercie tous mes amis vietnamiens et français. Merci pour vos attentions et vos encouragements qui m'ont accompagnée tout au long de mon travail. Merci sincèrement pour vos présences dans ma soutenance et des souhaites que vous m'avez envoyé de loin.

Je remercie les professeurs vietnamiens de l'Université de Pharmacie de Hanoi, en particulier **le Docteur Nguyen Thanh Hai** pour m'avoir donné l'envie de faire de la recherche mais aussi pour m'avoir donné de très bons conseils pour la réussite de mes études en France.

- ***À ma famille,***

Merci à mes parents de m'avoir soutenue et encouragée du début à la fin dans ce choix de carrière. Merci aussi de m'avoir aidé en m'offrant toutes les conditions nécessaires pour réussir aujourd'hui. Con cám ơn bố mẹ nhiều!

Merci à ma petite sœur Thu Huong d'avoir pris soin de moi pendant cette période difficile et stressante. Merci à ma belle-sœur Ha My et au copain de ma sœur Viet d'être venus en France pour ma soutenance et de m'avoir aidée pour le pot. Merci à mes beaux-parents pour tous leurs encouragements pendant ces années.

Last but not least, Tung Nam, my wonderful husband, thank you so much for all your supports and all the happiness that you have been giving me every single day since we met, especially our little angel that is coming to life very soon. Thanks for having shared with me every moment of my life during these 6 years. I couldn't have overcome these difficulties without you. You are my soulmate, my ideal husband and for sure a perfect future papa of our little girl. This thesis is undoubtedly dedicated to you ☺ .

Publications scientifiques

Revue

T.H.Pham, A.M.Gardier. *« Fast-acting antidepressant activity of ketamine: highlights on brain glutamate, GABA and serotonin neurotransmission in preclinical studies »*

Articles de recherche

T.H. Pham, I. Mendez-David, C. Defaix, B.P. Guiard, L. Tritschler, D.J. David, A.M. Gardier. *« Ketamine treatment involves medial prefrontal cortex serotonin to induce a rapid antidepressant-like activity in BALB/cJ mice » - Neuropharmacology,* 2017 **(Article 1)**

T.H. Pham, C. Defaix, X. Xu, S-X. Deng, D. Landry, R.A. Brachman, C.A. Denny, A.M. Gardier. *« Common neurotransmission recruited in (R,S)-ketamine and (2R,6R)-hydroxynorketamine-induced sustained antidepressant-like effects » - Biological Psychiatry, 2017* **(Article 2)**

R.A. Brachman, J.C. McGowan, J.N. Perusini, S,C. Lim, **T.H Pham**, C. Faye, A.M. Gardier, I. Mendez-David, D.J. David, R. Hen, C.A. Denny. *« Ketamine as a Prophylactic Against Stress-Induced Depressive-Like Behavior » - Biological Psychiatry, 2015*

T.H. Pham, C. Defaix, L. Tritschler, D.J. David, A.M. Gardier. *« Role of cortical and raphe $GABA_A$ and AMPA receptors in ketamine-induced fast antidepressant-like activity »* (en préparation) **(Article 3)**

C. Defaix, A. Solgadi, **T.H. Pham**, A.M. Gardier, P. Chaminade, L. Tritschler. *« Rapid analysis of glutamate, glutamine and GABA in mice frontal cortex microdialysis samples using HPLC coupled to electrospray tandem mass spectrometry » - Journal of Pharmaceutical and Biomedical Analysis, 2018* **(Matérial et méthode)**

L. Tritschler, A.M. Kheirbek, L.Y. Dantec, I. Mendez-David, J-P. Guilloux, C. Faye, J. Doan, **T.H. Pham**, R. Hen, D.J. David, A.M. Gardier. *« Optogenetic activation of granule cells in the dorsal*

dentate gyrus enhances dopaminergic neurotransmission in the Nucleus Accumbens » - *Neurosci Res,* 2017

Communications affichées

T.H. Pham, C. Defaix, X. Xu, S-X. Deng, D. Landry, R.A. Brachman, C.A. Denny, A.M. Gardier. « Common neurotransmission recruited in (*R,S*)-ketamine and (2*R*,6*R*)-hydroxynorketamine-induced sustained antidepressant-like effects »

- Travel Grant Award au 30ème Congrès international d'ECNP, 2017, Paris, France et
- Travel Grant Award au 19ème Meeting Régional de FENS, 2017, Pécs, Hongrie

T.H. Pham, C. Defaix, A. Solgadi, P. Chaminade , L. Tritschler, I. Mendez-David, D.J. David, A.M. Gardier. *« Mechanism of ketamine rapid antidepressant-like activity in mice: Role of the excitatory and inhibitory imbalance in mice »*. Journée de la Recherche, 2016, Châtenay-Malabry, France

T.H. Pham, I. Mendez-David, C. Defaix, B.P. Guiard, L. Tritschler, D.J. David, A.M. Gardier. *« Ketamine treatment involves medial prefrontal cortex serotonin to induce a rapid antidepressant-like activity in BALB/cJ mice »*. GDR3545, 2016, Tours, France; et Journée de l'École Doctorale 569, 2016, Châtenay-Malabry, France

A.M. Gardier, I. Mendez-David, B. Guiard, **T.H. Pham**, D.J. David. *« Acute ketamine treatement induced long lasting behavioral effects in anxio-depressive mice »*. SFN Neuroscience Meeting 2014, Washington DC ; et Journée de la Recherche, 2015, Châtenay-Malabry, France

Communications orales

T.H. Pham, C. Defaix, X. Xu, S-X. Deng, D. Landry, R.A. Brachman, C.A. Denny, A.M. Gardier. « Common neurotransmission recruited in (*R,S*)-ketamine and (2*R*,6*R*)-hydroxynorketamine-induced sustained antidepressant-like effects ». Journée de l'École Doctorale 569, 2017, Châtenay-Malabry, France

T.H. Pham, I. Mendez-David, C. Defaix, B.P. Guiard, L. Tritschler, D.J. David, A.M. Gardier. *« Ketamine treatment involves medial prefrontal cortex serotonin to induce a rapid antidepressant-like activity in BALB/cJ mice »*. Le 5ème séminaire annuel de brainstorming entre les collaborateurs de l'équipe UMRS1178, 2016, Châtenay-Malabry, France

Sommaire

Abréviations

5-HIAA	L'acide 5-hydroxy-indolacétique
5-HT	5-hydroxytryptamine, sérotonine
5-HIAA$_{ext}$	La concentration extracellulaire de 5-HIAA
5-HT$_{ext}$	La concentration extracellulaire de 5-HT
AMPA	L'acide α-amino-3-hydroxy-5-methyl-4-isoxazole propionique
ASC	Aires sous la courbe
DA	Dopamine
ESM	L'écart-type standard à la moyenne
FCx	Frontal cortex
FST	Forced Swim Test
GABA$_{ext}$	La concentration extracellulaire de GABA
Glu$_{ext}$	La concentration extracellulaire de glutamate
Gln$_{ext}$	La concentration extracellulaire de glutamine
Hr	Heure
ISRS	Inhibiteurs sélectifs de recapture de la sérotonine
J1 (J2)	Le 1er jour (le 2ème jour)
KET	Kétamine
LCR	Liquide céphalo-rachidien artificiel
mPFC	Cortex médian préfrontal
NMDA	N-méthyl-D-aspartate
NRD ou DRN	Noyau du raphé dorsal
PCP	Phencyclidine
R	Récepteur
SERT	Transporteur de la sérotonine
SNC	Système Nerveux Central
TDM	Trouble dépressif majeur
TRD	La dépression résistante au traitement
UCMS	Unpredictable Chronic Mild Stress
Veh	Véhicule

Liste des figures

Liste des tableaux

Liste des box

Résumé

Le trouble dépressif majeur (TDM) est un problème majeur de santé publique et un des troubles psychiatriques les plus courants, avec une prévalence de 350 millions de personnes dans le monde (WHO, 2012). Les antidépresseurs classiques (cf. inhibiteurs sélectifs de la recapture de la sérotonine, ISRS) constituent les traitements pharmacologiques les plus largement prescrits pour le TDM. Cependant, leurs effets thérapeutiques retardés associés aux nombreux patients résistants à ces traitements soulignent l'urgence de trouver de nouveaux médicaments plus efficaces.

Récemment, il a été montré que la kétamine, antagoniste non compétitif du récepteur ionotropique N-méthyl-D-aspartate (R-NMDA) du L-glutamate et anesthésique général dissociatif, avait un effet antidépresseur étonnant chez les patients victimes de dépression résistante à un traitement classique (TRD). Toutefois, le mécanisme d'une telle activité antidépressive rapide et soutenue n'est pas complètement compris. Par ailleurs, les nombreux effets indésirables de la kétamine limitent son utilisation en clinique. Face à ces défis, nous nous sommes intéressés au rôle de la balance excitation-inhibition sur les effets neurochimiques liés aux comportements de type antidépresseur induits par la kétamine chez la souris.

La première question de ma thèse a été d'étudier l'interaction entre l'effet antidépresseur de la kétamine et le système sérotoninergique, en évaluant l'implication du circuit neuronal du cortex médian préfrontal (mPFC), jouant un rôle indispensable dans les effets pharmacologiques et moléculaires de la kétamine, vers le noyau du raphé dorsal (NRD), où se trouvent les corps cellulaires des neurones sérotoninergiques. La microdialyse intracérébrale *in vivo* chez la souris éveillée est la principale technique utilisée dans mon étude car elle permet de suivre les changements simultanés de divers neurotransmetteurs cérébraux, i.e. des concentrations extracellulaires de la sérotonine, du glutamate, de la glutamine et du GABA (5-HT_{ext}, Glu_{ext}, Gln_{ext} et $GABA_{ext}$). J'ai réalisé en parallèle le test de la nage forcée (forced swim test, FST) puisqu'il s'agit du test comportemental de référence pour prédire l'effet de type antidépresseur d'une molécule. Tous mes travaux ont été réalisés 24 heures (24h, effet soutenu) après l'administration d'une dose unique, faible (infra-anesthésique) de kétamine. J'ai choisi d'effectuer tous mes travaux chez des souris BALB/cJ car

elle possède un phénotype anxio-dépressf – un modèle reconnu dans la littérature scientifique.

Après avoir vérifié les effets antidépresseurs de la kétamine, 24h après une administration unique par voie systémique (10 mg/kg, i.p.), chez la souris, nous avons trouvé que la kétamine (systémique ou locale intra-mPFC) est plus efficace que la fluoxétine (ISRS) car elle accroit la durée de nage (un paramètre sérotoninergique dans le FST), corrélée positivement avec une augmentation des concentrations 5-HT_{ext} dans le mPFC. Cette corrélation, associée à l'absence d'effets de la kétamine sur la nage chez des souris déplétées en 5-HT centrale (par la pCPA, un inhibiteur de synthèse de la 5-HT), a confirmé l'implication du système sérotoninergique cortical, en particulier dans le mPFC, dans le mécanisme d'action antidépressive de la kétamine. Par ailleurs, le blocage de son effet par le NBQX, un antagoniste du récepteur AMPA (R-AMPA du glutamate), injecté intra-NRD, souligne le rôle de l'activation de ce récepteur situé dans le NRD (**Article 1**).

Par la suite, nous avons évalué l'effet antidépresseur du (2*R*,6*R*)-hydroxynorkétamine (HNK), un des métabolites principaux du mélange racémique (*R,S*)-kétamine. Actuellement, les résultats concernant cette molécule sont controversés (Yang *et al.*, 2016; Zanos *et al.*, 2016). Ce métabolite, différent de sa molécule mère, agirait directement sur le R-AMPA pour induire une décharge neuronale glutamatergique. Grâce à la microdialyse *in vivo* couplée au FST chez la même souris, nous avons montré que le (2*R*,6*R*)-HNK est aussi efficace que la (*R,S*)-kétamine pour augmenter la durée de nage et la 5-HT_{ext} dans le mPFC. Cependant, il possède un effet plus particulièrement glutamatergique et moins GABAergique que sa molécule mère. De plus, nous n'avons pas retrouvé de traces de ces deux molécules dans le plasma des souris 24h après leur administration, période où les tests neurochimiques et comportementaux ont été réalisés. Cela souligne une adaptation neuronale plus complexe prolongeant leurs effets "thérapeutiques" (**Article 2**).

Fort de ces résultats concernant l'implication des systèmes sérotoninergique, glutamatergique (excitation) et GABAergique (inhibition) corticaux dans le mécanisme d'action antidépressive de la kétamine, nous avons ensuite réalisé une étude associant pharmacologie et optogénétique pour déterminer le rôle de la balance excitation-inhibition dans le circuit mPFC-NRD et aussi pour tenter d'expliquer les cascades de signalisation qui sous-tendent ce mécanisme. L'antagoniste du R-AMPA, le NBQX, injecté par voie intra-NRD et l'agoniste du récepteur $GABA_A$ (R-$GABA_A$), muscimol, injecté par voie intra-mPFC ont tous deux bloqué

l'effet antidépresseur de la kétamine sur la durée de nage et sur la 5-HT_{ext}. La bicuculline, antagoniste du R-$GABA_A$, injecté en intra-NRD n'a ni bloqué, ni renforcé les effets de la kétamine. De ce fait, leurs effets sur le système glutamatergique/GABAergique sont surprenants. L'acide dihyroxykainique (DHK), inhibiteur sélectif du transporteur EAAT2/GLT1 de glutamate, induit à lui seul un effet de type antidépresseur dans le FST, en augmentant toutes les concentrations de Glu_{ext}, Gln_{ext}, $GABA_{ext}$ et 5-HT_{ext}. Selon les données obtenues, nous avons observé que l'effet antidépresseur comportemental est visible uniquement après une augmentation simultanée de 5-HT_{ext} et de Glu_{ext} ou encore de 5-HT_{ext}, Glu_{ext} et $GABA_{ext}$. Cette hypothèse est renforcée par le fait que la stimulation des neurones pyramidaux glutamatergiques du mPFC grâce à la technique d'optogénétique semble reproduire l'effet de la kétamine dans le FST et sur la 5-HT_{ext} (résultats préliminaires). L'inhibition par optogénétique du circuit mPFC-DRN a réduit de 30% le temps de nage forcée ainsi que le taux de 5-HT dans ces deux régions, soulignant ainsi l'implication partielle de ce circuit dans les effets de la kétamine. Nous pouvons ainsi conclure que l'effet antidépresseur est induit plutôt par une augmentation de l'excitation cérébrale impliquant la (*R,S*)-kétamine et son principal métabolite cérébral, le (2*R*,6*R*)-HNK, soulignant l'importance du rôle des interneurones GABAergiques et de la libération du glutamate endogène dans le mPFC (**Article 3**).

Mes travaux de thèse apportent des nouvelles connaissances sur l'interaction étroite entre l'effet antidépresseur de la kétamine et les systèmes de neurotransmetteurs centraux dans un modèle animal d'anxiété/dépression. Ces résultats soulignent l'importance de la balance excitation-inhibition dans son mécanisme d'action antidépressive. Nos travaux expérimentaux, associés à la "revue" dans laquelle nous avons analysé de nombreux articles sur ce sujet et résumé en figures illustrées, permettront les chercheurs d'avoir une vue générale de l'activité antidépresseur rapide de cette molécule originale (**Revue**, *soumise pour publication*).

Introduction

1 Le trouble dépressif majeur (TDM)

Le trouble dépressif majeur (TDM) est une maladie grave, débilitante, qui réduit l'espérance de vie et une des principales causes de handicap dans le monde. Selon l'Organisation Mondiale de la Santé, environ 350 millions de personnes sont touchées par la dépression, avec un risque plus élevé pour les femmes que pour les hommes (WHO, 2012). Nous prévoyons également que le TDM sera la deuxième cause d'invalidité en 2020 (C. J. Murray & Lopez, 1996). Le TDM est caractérisé par au moins un épisode dépressif discret d'une durée d'au moins 2 semaines et entraînant des changements nets de l'humeur, d'intérêts et de plaisir, des changements de la cognition et des symptômes végétatifs (Otte *et al.*, 2016). Les critères de diagnostic actuels sont décrits dans le Tableau 1 selon la 5ème édition de "Diagnostic and Statistical Manual of Mental Disorders" (DSM-5), publié en 2013. D'après le DSM-5, un individu doit présenter au moins cinq symptômes parmi ceux décrits pour définir le TDM chaque jour pendant au moins deux semaines, qui sont nouvellement présentés ou clairement aggravés avant le début de l'épisode dépressif, afin d'être diagnostiqué avec un TDM. Selon l'étude de Bromet *et al.*, 2011, la prévalence des épisodes dépressifs majeurs au cours des 12 derniers mois affecterait 5,9% des Français et 8,3% des Américains, avec un pic de 10,4% chez des Brésiliens.

Le TDM apparaît environ deux fois plus souvent chez les femmes que chez les hommes et affecte environ 6% de la population adulte dans le monde chaque année. Le TDM est associé à un risque accru de développer des comorbidités telles que, un trouble anxieux, un diabète, une pathologie cardiaque et un accident vasculaire cérébral, ce qui augmente encore son fardeau. De plus, le TDM peut entraîner la mort par suicide. Il est estimé que jusqu'à 50% des 800 000 suicides par an dans le monde surviennent dans le cadre d'un épisode dépressif et que les patients atteints de TDM sont près de 20 fois plus susceptibles de décéder par suicide que la population générale. La contribution génétique au TDM est estimée à environ 35%. En outre, les facteurs environnementaux, tels que des violences sexuelles, physiques ou émotionnelles durant l'enfance, sont fortement associés au risque de développer un TDM, bien que la compréhension de l'interaction des facteurs environnementaux avec les facteurs génétiques et épigénétiques soit loin d'être complète (Otte *et al.*, 2016).

Major Depressive Disorder (DSM-5th Diagnostic Criteria)
A. Five (or more) of the following symptoms have been present during the same 2-week period and represent a change from previous functioning; at least one of the symptoms is either (1) depressed mood or (2) loss of interest or pleasure. 1. Depressed mood most of the day, nearly every day, as indicated by either subjective report (e.g., feels sad, empty, hopeless) or observation made by others (e.g., appears tearful). (Note: In children and adolescents, can be irritable mood.) 2. Markedly diminished interest or pleasure in all, or almost all, activities most of the day, nearly every day (as indicated by either subjective account or observation.) 3. Significant weight loss when not dieting or weight gain (e.g., a change of more than 5% of body weight in a month), or decrease or increase in appetite nearly every day. (Note: In children, consider failure to make expected weight gain.) 4. Insomnia or hypersomnia nearly every day. 5. Psychomotor agitation or retardation nearly every day (observable by others, not merely subjective feelings of restlessness or being slowed down). 6. Fatigue or loss of energy nearly every day. 7. Feelings of worthlessness or excessive or inappropriate guilt (which may be delusional) nearly every day (not merely self-reproach or guilt about being sick). 8. Diminished ability to think or concentrate, or indecisiveness, nearly every day (either by subjective account or as observed by others). 9. Recurrent thoughts of death (not just fear of dying), recurrent suicidal ideation without a specific plan, or a suicide attempt or a specific plan for committing suicide.
B. The symptoms cause clinically significant distress or impairment in social, occupational, or other important areas of functioning.
C. The episode is not attributable to the physiological effects of a substance or to another medical condition.
D. The occurrence of the major depressive episode is not better explained by schizoaffective disorder, schizophrenia, schizophreniform disorder, delusional disorder, or other specified and unspecified schizophrenia spectrum and other psychotic disorders.
E. There has never been a manic episode or a hypomanic episode.

Tableau 1. Les critères de diagnostic actuels du TDM selon la 5ème édition de DSM-5 (2013)

La psychothérapie et la psychopharmacologie sont toutes les deux efficaces dans le traitement du TDM. Cependant, environ 30 à 60% des patients ne répondent toujours pas de manière adéquate à un traitement antidépresseur et souffrent toujours de symptômes résiduels incapacitants, même après plusieurs tentatives de traitement (Trivedi *et al.*, 2006). Les nouveaux développements en psychothérapie comprennent l'utilisation de technologies d'intervention comportementale. En ce qui concerne les approches pharmacologiques, les antidépresseurs glutamatergiques tels que la kétamine (0,5 mg/kg perfusion i.v.), sont actuellement étudiés après des résultats préliminaires d'efficacité prometteurs.

Malgré les progrès dans la compréhension de la neurobiologie du TDM, aucun mécanisme établi ne peut expliquer tous les aspects de la maladie. Cependant, le TDM est associé à de plus petits volumes hippocampiques ainsi qu'à des changements dans l'activation ou la connectivité des réseaux neuronaux. De plus, les altérations des principaux systèmes neurobiologiques qui interviennent dans la réponse au stress sont évidentes dans le TDM, notamment celle de l'axe hypothalamo-hypophyso-surrénalien (HPA), du système nerveux autonome et du système immunitaire et de l'inflammation.

1.1 Un bref rappel des traitements pharmacologiques classiques de TDM

L'hypothèse monoaminergique de la dépression date de 50 ans et propose que les patients souffrant de dépression aient des concentrations cérébrales diminuées de sérotonine, noradrénaline et dopamine (Hirschfeld, 2000). En 1958, le premier traitement pharmacologique réussi pour la dépression est un inhibiteur de la monoamine oxydase (IMAO) – une enzyme dégradant des amines biogènes tels que la sérotonine, la dopamine et la noradrénaline. En 1959, l'imipramine, le premier médicament de la classe des antidépresseurs tricycliques (TCA), a été approuvé pour le traitement de TDM. Les TCAs inhibent la recapture sélective de la noradrénaline et de la sérotonine par leurs transporteurs respectifs.

La découverte de ces antidépresseurs et de leurs cibles moléculaires a conduit à la conception de médicaments antidépresseurs de deuxième et troisième génération, tels que les Inhibiteurs Sélectifs du Recapture de la Sérotonine (ISRS) et les Inhibiteurs Sélectifs du Recapture de la Noradrénaline (ISRN) et les Inhibiteurs du Recapture mixtes, sérotonine/noradrénaline. La mise sur le marché successif de ces antidépresseurs a renforcé l'hypothèse monoaminergique de la dépression. Les ISRSs et ISRNs sont devenus les

médicaments prescrits en 1ère intention par les psychiatres pour traiter le TDM. Des exemples de différentes classes d'antidépresseurs figurent dans Figure 1..

Cependant, les limites thérapeutiques de ces agents pharmacologiques - notamment un important délai d'action retardé, un faible taux d'efficacité et les effets indésirables - soulignent la nécessité de découvrir de nouvelles pistes thérapeutiques (Tableau 2). Les limites des antidépresseurs monoaminergiques seraient notamment dues au fait qu'ils activent des récepteurs inhibiteurs qui se désensibilisent progressivement lors de leur administration chronique (ex : l'autorécepteur 5-HT_{1A}) et qu'ils n'influencent pas de manière significative la synaptogenèse et/ou la neurogenèse dans l'hippocampe adulte (discuté au 2.1).

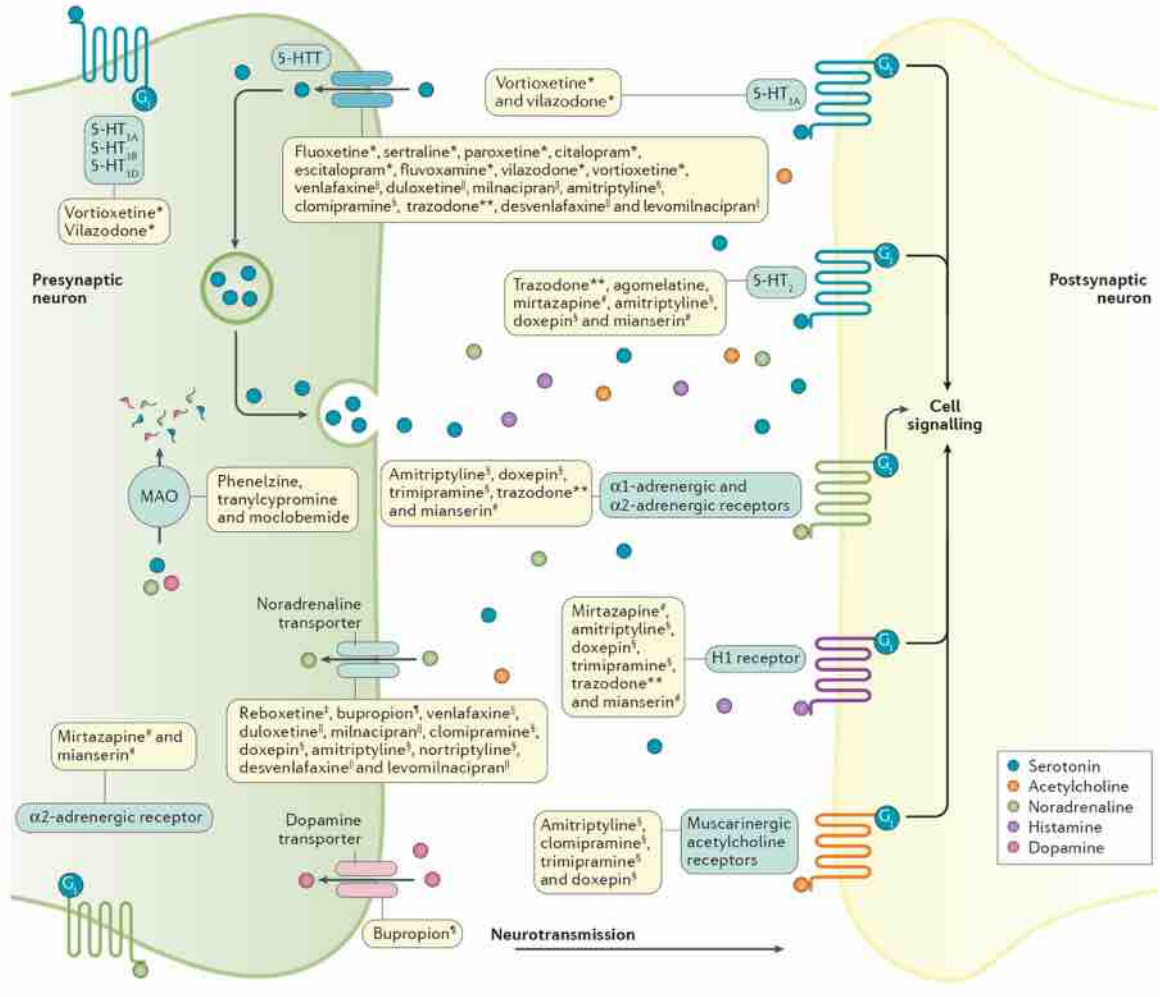

Figure 1. Les différentes cibles d'action des antidépresseurs classiques (d'après Otte et al., 2016).

MAO : monoamine oxydase
§ : TCA - antidépresseurs tricycliques
* : ISRS - inhibiteurs sélectifs de la recapture de la sérotonine
‡ : NRI - inhibiteurs de la recapture de la noradrénaline relativement sélectifs
‖ : IRSN - inhibiteurs de la recapture de la sérotonine-noradrénaline
¶ : NDRI - inhibiteurs de la recapture de la noradrénaline-dopamine
# : Les antagonistes des récepteurs α2-adrénergiques
** : Antagoniste de la sérotonine et inhibiteur de la recapture
5-HTT : transporter sérotonergique.

Tableau 2. Mécanisme, début d'action et statut clinique des médicaments antidépresseurs commercialisés aux États-Unis et/ou en Europe, ou en essais cliniques (d'après Duman *et al.*, 2016)

Traitements antidépresseurs	Mécanisme	Délai d'action	Usage clinique
Agents précoces : inhibiteur de la recapture (IR) tricyclique, inhibiteur de la monoamine-oxydase (IMAO) et autres			
Imipramine, Amitriptyline, Amoxapine, Protriptyline, Trimipamine	Noradrénaline (NE) et 5-HT IR	Semaines - mois	Approuvé aux États-Unis et en Europe
Desipramine	NE IR	Semaines - mois	Commercialisés
Doxepine, Maprotiline	NE IR et Histamine 1 antagoniste	Semaines - mois	Commercialisés
Tranylcypromine, Phenelzine, Isocarboxazide, Sélégiline	IMAO	Semaines - mois	Approuvé par la FDA
Bupropion	NE et dopamine IR	Semaines - mois	Approuvé par la FDA
Trazodone, Nefazadone	5-HT IR et 5-HT_{2A} antagoniste	Semaines - mois	Commercialisés
Mirtazapine, Miansérine	α2-adrénergique/5-HT_{2A-3} antagoniste	Semaines - mois	Commercialisés
Générations ultérieures de IRs			
Fluoxétine, Sertraline, Citalopram, Paroxétine, Vortioxétine, Vilazodone	ISRS	Semaines - mois	Commercialisés
Duloxétine	ISRS, 5-HT_{1A} antagoniste partiel	Semaines - mois	Commercialisés
Venlafaxine, Levomilnacipran	NE/5-HT IR	Semaines - mois	Commercialisés
Antipsychotiques atypiques (approuvés pour l'utilisation en tant que traitements complémentaires pour les patients prenant déjà un ISRS)			
Quetiapine, Olanzapine	5-HT_{2A} et dopamine D_2 antagoniste	Jours - semaines	Approuvé par la FDA
Aripiprazole, Brexipiprazole	5-HT_{2A} antagoniste, D_2 agoniste partiel	Jours - semaines	Approuvé par la FDA
Les modalités de stimulation cérébrale			
ECT (la thérapie par électrochocs)	BDNF – plasticité de circuit	Semaines	Approuvé par la FDA
TMS (stimulation magnétique transcrânienne)	Plasticité de circuit	Semaines - mois	Approuvé par la FDA
VNS (stimulation vagale)	Plasticité de circuit	Mois	Approuvé par la FDA
Médicaments à action rapide			
Kétamine, Lanicémine	Bloqueur de canal de NMDA-R	Heures - jours	Essais cliniques
CP 101,606 (= traxoprodil)	NMDA-R : NR2B sous-unité sélective NAM	Heures - jours	Essais cliniques - arrêté
GLYX-13 (= rapastinel)	NMDA-R : site co-agoniste Glycine NAM	Heures - jours	Essais cliniques
AV-101 (L-4-chlorokyurenine or 4-CI-KYN)	NMDA-R : Glycine modulateur	Inconnu	Essais cliniques
Scopolamine	Acétylcholine-muscarinique antagoniste	Heures - jours	Expérimentation

NMDA-R : récepteur NMDA ; NAM : modulateur allostérique négative ; ISRS : inhibiteur sélectif de la recapture de sérotonine ; FDA : agence américaine des produits alimentaires et médicamenteux.

1.2 Modèles animaux de dépression

L'investigation chez l'animal possède un fort potentiel pour découvrir de nouvelles cibles thérapeutiques et, peut-être apporter de meilleurs traitements aux patients. Trouver les modèles animaux appropriés pour reproduire certains symptômes d'une maladie humaine donnée est toujours difficile, en particulier pour les troubles psychiatriques. Le développement de modèles animaux est encore compliqué par le faible nombre de facteurs de risque génétiques identifiés à ce jour de la dépression chez les humains (ex : polymorphismes du SERT et du R-5-HT_{1A}). De plus, bon nombre de symptômes généralement ressentis par les patients atteints de TDM sont hautement subjectifs (comme une humeur dépressive) et seuls quelques-uns peuvent être objectivement observés et évalués chez les animaux (troubles du sommeil, de l'alimentation, perte de poids, comorbidité anxieuse, hyper-corticostéronémie chez les rongeurs/hyper-cortisolémie chez l'homme, etc…). Malgré ces défis, les modèles animaux ont permis de découvrir plusieurs voies susceptibles de contribuer à la compréhension de la pathogenèse du TDM ont facilité l'étude des processus moléculaires impliqués et/ou le mécanisme d'action des médicaments et des ECT. Ces voies comprennent, mais sans s'y limiter, les mécanismes neuroendocrines, inflammatoires et immuns, l'épigénétique, les réseaux moléculaires et le transcriptome, le microbiote intestinal (en plein essort actuellement) et l'axe intestin-cerveau, le dysfonctionnement synaptique, et la neurogenèse (Otte *et al.*, 2016).

Un modèle animal pertinent permet de comprendre les facteurs moléculaires, génétiques et épigénétiques pouvant mener à la dépression. Il est certain que ce n'est pas un seul gène "dépressif" qui est impliqué dans la survenue de la maladie, mais plutôt un réseau de gènes expliquant la multiplicité des symptômes. D'après Yan *et al.*, 2010, les critères à prendre en compte pour mettre au point un modèle animal des pathologies dépressives sont: (i) – fortes ressemblances phénoménologiques, (ii) – similarités physiopathologie, (iii) – étiologie comparable et (iv) – traitement antidépresseur commun avec l'humain. Malheureusement, la dépression est un trouble hétérogène et l'homogénéité chez l'animal est un point négatif de ce type de modèle. Des modèles animaux actuellement utilisés sont listés ci-dessous d'après Yan *et al.*, 2010, dont les symptômes sont inversés par les traitements des antidépresseurs :

Learned helplessness (LH) paradigme : l'état de stress chez l'animal est provoqué par une succession de chocs électriques aux pattes de manière imprévisible pendant plusieurs jours (Seligman *et al.*, 1975). Le comportement impuissant "helpless" est évalué en analysant la performance de l'animal dans un paradigme d'échappement actif, tel que la latence pour appuyer sur un levier ou franchir une porte. Ce modèle manifeste des changements neuro-végétatifs similaires aux troubles dépressifs tels que des troubles du sommeil, une diminution du poids corporel, des troubles sexuels et une augmentation des taux de corticostérone plasmatique (Cryan & Mombereau, 2004).

Chronic mild stress (CMS) : cette procédure implique une exposition des rongeurs de façon relativement continue à divers facteurs de stress légers, tels que des périodes de privation de nourriture et d'eau, de faibles réductions de température, des changements de compagnons et d'autres changements inoffensifs, mais d'imprévisibles manipulations, sur une période (généralement 3 semaines). La CMS provoque l'apparition de nombreux symptômes de type dépressif, tels que l'agressivité, la diminution des comportements sexuels, d'investigation, et de l'activité locomotrice. Le test de préférence au sucrose et l'état du pelage sont les deux tests fréquemment utilisés pour évaluer l'état de stress chez ces animaux (Willner, 2005).

Modèle de défaite sociale "**Social defeat stress"** : ce modèle est le plus utilisé chez les rongeurs. A la différence des deux modèles ci-dessus, il permet une approche de nature sociale dans le stress. Un mâle est introduit dans le territoire des mâles agressifs. L'intrus est rapidement examiné et attaqué par les résidents. Après quelques minutes d'exposition physique, l'intrus est séparé des résidents par une paroi en plastique avec trous pour permettre les contacts visuels, olfactifs et auditifs pendant 24h. L'animal est ensuite exposé aux différents résidents agressifs chaque jour pendant quelques jours (Krishnan *et al.*, 2007).

Corticostérone (CORT) modèle : ce modèle est le plus simple car il est établi après l'administration orale chronique de CORT, une hormone surrénale associée au stress, qui va induire des comportements persistants, reproductibles et durables (y compris l'anhédonie et l'impuissance). L'exposition chronique à la CORT provoque également chez le rongeur adulte une réduction de la neurogenèse hippocampique, de l'expression de facteur neurotrophique dérivé du cerveau (BDNF) et de la protéine de liaison à l'élément de réponse à l'AMPc phosphorylée (pCREB) dans l'hippocampe (David *et al.*, 2009; Mendez-David *et al.*, 2014).

➢ Commentaire : Le LH paradigme a une haute validité prédictive, mais les symptômes dépressifs ne persistent pas suffisamment. Le modèle CMS est critiqué du fait de son faible taux de reproductibilité et le modèle de défaite sociale ("Social Defeat") reflète plutôt un phénotype d'anxiété. Le modèle CORT utilisé au laboratoire à haute reproductibilité et haute validité prédictive. Pourtant, il est critiqué pour être un modèle induit par un agent pharmacologique (CORT), ce qui limiterait sa concordance avec la maladie décrite chez l'homme.

Modèle génétique chez l'animal : avec le développement des approches génétiques (ex : élevage puis génotypage des lignées de souris "knock-out" - KO constitutives, KO inductibles, tissus spécifiques ; souris "knock-in" ; souris transgéniques), les stratégies mutantes offrent une approche particulièrement utile pour découvrir les cibles potentielles des troubles dépressifs. Cependant, ces stratégies sont très coûteuses et demandent beaucoup de temps pour disposer d'une cohorte d'animaux assez grande et faire une évaluation phénotypique. Ainsi, l'utilisation des lignées de souris "sauvages/wild-type" avec un phénotype hyper-anxieuse, comme le BALBc/J (Dulawa *et al.*, 2004) que j'ai utilisé dans mes travaux de thèse, est plus simple. Cette souche de souris est immédiatement disponible et permet d'obtenir des résultats reproductibles.

1.3 La dépression résistante au traitement (TRD)

La dépression résistante au traitement (TRD) touche plus de 1% des individus aux États-Unis et environ 30% de tous les patients déprimés peuvent être classés comme affectés par la TRD (Rush *et al.*, 2006). C'est un trouble invalidant associé à une déficience psychosociale persistante et à de faibles impacts sociaux/professionnels. La TRD peut généralement être définie comme l'absence de réponse à au moins deux types d'antidépresseurs différents (comme précisé dans la célèbre étude collaborative STAR*D (Sequenced Treatment Alternatives to Relieve Depression) terminée en 2006 et ayant évalué la réponse aux antidépresseurs) pendant plus de quatre semaines à la dose maximale recommandée (Serafini *et al.*, 2014). À ce jour, la pathogenèse de TRD reste incertaine.

Un groupe de cliniciens a élaboré un plan stratégique pour la dépression résistante au traitement, appelée traitement séquentiel alternatif pour soulager la dépression (STAR*D) (Rush *et al.*, 2006). STAR*D fournit un plan de traitement en quatre étapes, dans lequel un

patient passe à l'étape de traitement suivante s'il ne parvient pas à une rémission complète dans l'étape de traitement en cours. Les ISRSs sont la première étape du traitement et, au fur et à mesure que les patients progressent dans les étapes de traitement, ils reçoivent un nouvel antidépresseur ayant un mécanisme d'action différent. Les patients qui obtiennent une rémission complète et tolèrent un traitement à une étape spécifique reçoivent ensuite un traitement à long terme avec ce médicament. Les résultats d'une étude à long terme à grande échelle ont révélé un taux de rémission cumulatif de 67% (pour les quatre étapes de traitement). Cependant, les patients qui ont progressé au cours d'un plus grand nombre d'étapes de traitement ont présenté des taux de rechute plus élevés que les patients ayant obtenu une rémission dès la première étape (Rush *et al.*, 2006).

2 Kétamine comme traitement de la TRD

La kétamine (2-(2-chlorophényl)-(1-méthylamino)-cyclohexanone) est un antagoniste non compétitif du récepteur ionotropique N-méthyl-D-aspartate (R-NMDA) du L-glutamate qui se lie au site “phencyclidine” de ce canal calcique. C’est un anesthétique général dissociatif d’action rapide dont les propriétés hallucinogènes en ont fait une drogue populaire addictive du nom de “Special K”. Récemment, l’étude de Berman *et al.*, 2000 confirmée par d’autres depuis cette a date, a montré que la kétamine a un effet antidépresseur étonnant. En effet, plusieurs essais cliniques en double-aveugle contre placebo ont suggéré qu'une seule dose faible de kétamine (0,5 mg/kg administrée par voie intraveineuse en 40 minutes, une dose inférieure à la dose anesthésique) exerce une activité antidépressive rapide (dans les 72 heures après son injection) et persistante (pour 1 semaine) chez des patients déprimés résistants à un traitement antidépresseur classique (Zarate *et al.*, 2006). De plus, la kétamine diminuerait également les pensées suicidaires et donc le risque suicidaire (Price *et al.*, 2009).

Toutefois, les mécanismes conduisant à une telle action antidépressive sont probablement plus complexes que le simple blocage des récepteurs NMDA du L-glutamate et n'ont pas été clairement définis jusqu'à présent (Li *et al.*, 2010).

2.1 Mécanisme moléculaire proposé pour l'effet antidépresseur de la kétamine

2.1.1 Atrophie neuronale et perte synaptique dans la dépression

Les études d'imagerie cérébrale de patients déprimés fournissent des arguments solides car constants d'une diminution du volume des régions cérébrales corticales et limbiques - comme le cortex médian préfrontal (mPFC) et l'hippocampe - qui contrôlent les émotions, l'humeur et la cognition, suggérant qu'une atrophie neuronale est liée à la durée de la maladie et au délai de prescription du traitement (MacQueen & Frodl, 2011).

Les études sur les rongeurs ont fourni des éléments détaillés de l'atrophie neuronale, de la réduction de la densité synaptique et de la perte de cellules dans les modèles de dépression et de stress (CMS) (Duman & Aghajanian, 2012). Le BDNF a été d'un intérêt particulier en ce qui concerne l'atrophie des connexions neuronales car ce facteur neurotrophique est requis pour le développement neuronal précoce et pour la survie et la fonction neuronale, y compris la plasticité synaptique, dans le cerveau adulte (Duman & Voleti, 2012).

Dans des conditions normales, la stimulation du neurone présynaptique libère le glutamate neuronal, entraînant l'activation des récepteurs AMPA du glutamate postsynaptique et la dépolarisation membranaire; cela provoque l'activation de plusieurs voies intracellulaires, y compris la voie de signalisation BDNF-TrkB (kinase liée à la tropomyosine B), et la voie mTORC1 (cible du complexe 1 de la rapamycine) dans l'hippocampe et le mPFC (Duric *et al.*, 2010). Ces voies sont essentielles pour la régulation de la plasticité synaptique, un mécanisme d'apprentissage adaptatif fondamental qui comprend la maturation (augmentation du diamètre des épines dendritiques) et l'augmentation du nombre de synapses (synaptogenèse) (Duman *et al.*, 2016). Ce processus nécessite une synthèse protéique *de novo* médiée par mTORC1 de protéines synaptiques neuronales, y compris les sous-unités GluA1 de récepteurs glutamatergique AMPA et PSD95. Le stress répété diminue la signalisation de BDNF et de mTORC1 en partie via la régulation positive du régulateur négatif REDD1 (régulant les dommages et les réparations de l'ADN), qui diminue la synthèse des protéines synaptiques et contribue ainsi à une diminution du nombre de synapses. D'autres protéines impliquées dans la régulation de la plasticité synaptique comprennent GSK3 et la protéine phosphatase 1 (PP1) (Figure 2).

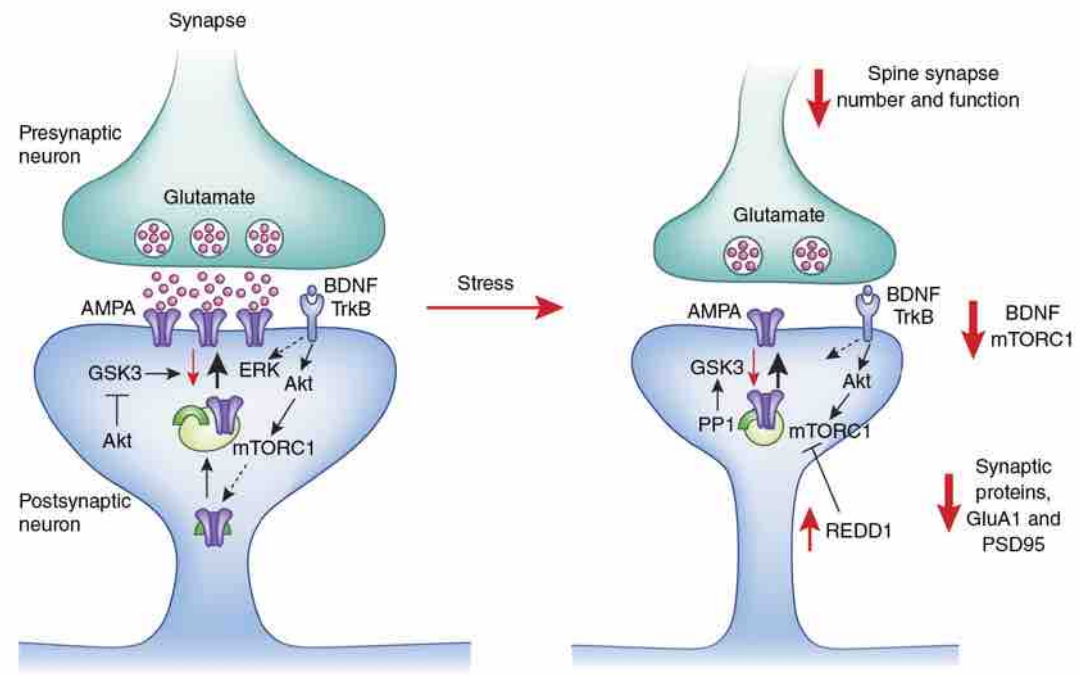

Figure 2. Le stress chronique provoque une atrophie des processus neuronaux et diminue le nombre de synapses (d'après Duman et al., 2016)

2.1.2 Mécanisme moléculaire d'action antidépresseur rapide de la kétamine dans le mPFC

L'hypothèse la plus connue du mécanisme de la kétamine est qu'elle provoque des "bursts" de glutamate suite à la désinhibition des interneurones GABAergiques corticaux: le déclenchement tonique de ces interneurones GABAergiques serait piloté par les récepteurs NMDA, et l'état actif du canal ouvert (i.e., après libération des ions Mg^{2+} du canal) permettrait à la kétamine de se fixer sur le site du PCP et de bloquer l'activité du canal (Miller *et al.*, 2016). D'après Duman *et al*., 2016, ces bursts de glutamate auraient pour conséquences de stimuler les récepteurs AMPA post-synaptiques, ce qui provoquerait la dépolarisation de la membrane des neurones et l'activation des canaux Ca^{2+} (VDCC), conduisant à la libération de BDNF et à la stimulation du signal TrkB/Akt. Cela activerait la signalisation mTORC1 et déclencherait une synthèse accrue des protéines nécessaires à la maturation et la formation des synapses (e.g, GluA1 et PSD95) (Figure 3). Dans des conditions où la libération de BDNF est bloquée (comme chez les souris knock-in possédant l'allèle $BDNF^{Val66Met}$ avec un risque accru de dépression) ou neutralisée (en utilisant un anticorps), ou dans laquelle la signalisation mTORC1 est bloquée (perfusion de rapamycine dans le mPFC), nous observons bien que les effets synaptiques et comportementaux de la kétamine sont bloqués (Li *et al.*, 2010; Liu *et al.*, 2012). La rechute vers un état dépressif serait associée à une diminution des synapses sur les neurones du mPFC,

ce qui pourrait se produire lors d'un stress chronique, d'un déséquilibre en hormones endocrines (cortisol), en œstrogènes, en cytokines inflammatoires ou lors de maladies métaboliques et cardiovasculaires (Duman *et al*., 2016).

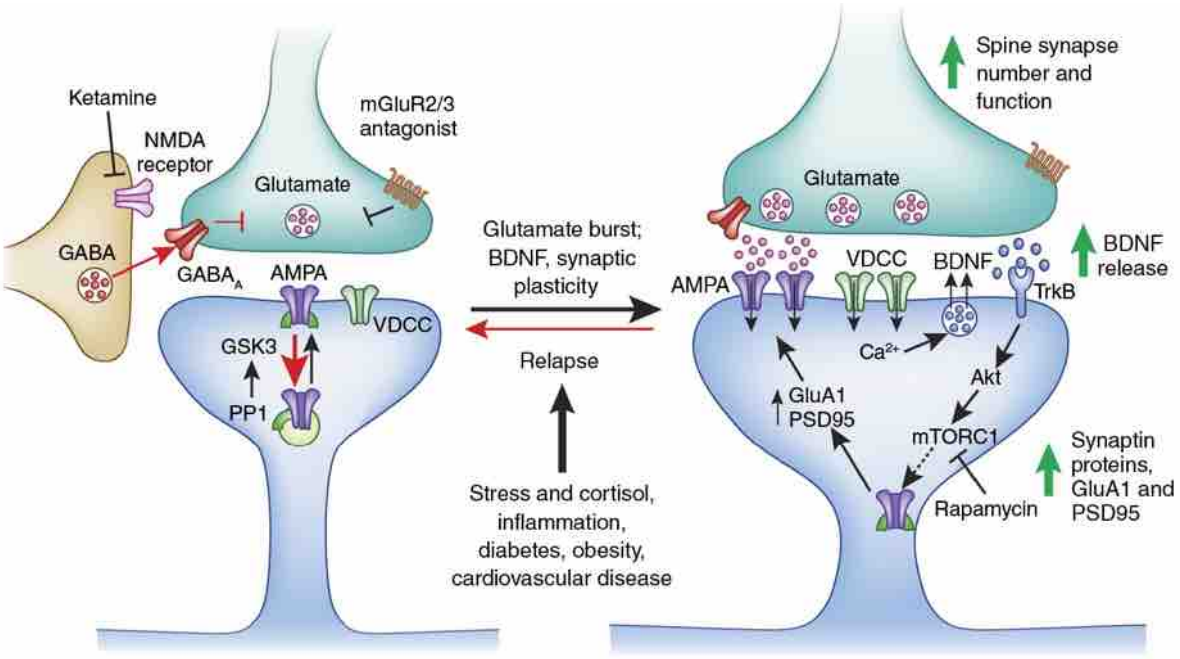

Figure 3. Mécanisme d'action de la kétamine, un antidépresseur d'action rapide dans le mPFC (d'après Duman et al., 2016)

2.2 Mécanisme d'action antidépresseur de la kétamine : lien avec la neurotransmission du glutamate, du GABA et de la sérotonine dans les études précliniques

Les modifications neurochimiques (glutamate, GABA et 5-HT) et comportementales induites par l'administration d'une dose infra-anesthésique de kétamine sont discutés dans la revue ci-dessous, en se focalisant sur les rongeurs, les modèles d'animaux de la pathologie dépressives et les tests d'anxiété/dépression utilisés dans les nombreuses études publiées chez le rat ou la souris. La réponse antidépressive rapide à l'antagoniste de récepteur NMDA serait associée à des "bursts" de glutamate et à une synaptogenèse dans le mPFC (Duman & Aghajanian, 2012; Duman *et al.*, 2016; Li *et al.*, 2010). L'implication de la balance de la neurotransmission excitatrice (glutamate, sérotonine) et inhibitrice (GABA) dans le circuit du glutamate - mPFC / sérotonine - noyau du raphé dorsal (NRD) dans les études chez les rongeurs a donc été analysée dans cette revue.

De plus, l'ordre d'apparition des changements neurochimiques (glutamate, GABA et 5-HT) sera proposé à la fin de cette revue avec une figure illustrée, en fonction des données collectées dans la littérature et des résultats que j'ai obtenu pendant mon M2 et ma thèse. L'objectif principal de ce travail est d'aider à mieux imaginer une vue d'ensemble de l'effet antidépresseur "soutenu" (i.e., à 24hr) de la kétamine sur la balance excitation-inhibition corticale.

Revue

Soumise au journal "Current Neuropharmacology".

Current Neuropharmacology
BENTHAM SCIENCE

Fast-acting antidepressant activity of ketamine: highlights on brain glutamate, GABA and serotonin neurotransmission in preclinical studies

Journal:	*Current Neuropharmacology*
Manuscript ID	CN-2018-0021
Manuscript Type:	Thematic Issue Article
Date Submitted by the Author:	02-Mar-2018
Complete List of Authors:	Pham, Thu Ha; CESP/UMR-S 1178, Univ. Paris-Sud, Fac Pharmacie, Inserm, Université Paris-Saclay Gardier, Alain; CESP/UMR-S 1178, Univ. Paris-Sud, Fac Pharmacie, Inserm, Université Paris-Saclay
Keywords:	ketamine, antidepressant, resistance, excitation, inhibition, medial prefrontal cortex, neurotransmitter

Fast-acting antidepressant activity of ketamine: highlights on brain glutamate, GABA and serotonin neurotransmission in preclinical studies

Thu Ha Pham, Alain M. Gardier*

CESP/UMR-S 1178, Univ. Paris-Sud, Fac. Pharmacie, Inserm, Université Paris-Saclay, Chatenay Malabry, 92290, France.

Abstract: Ketamine, a non-competitive antagonist of N-methyl-D-aspartate (NMDA) receptor, displays a fast antidepressant activity in treatment-resistant depression and in rodent models of anxiety/depression. A large body of evidence about the cellular and molecular mechanisms underlying its fast antidepressant-like activity comes from animal studies. Although structural remodeling of frontocortical/hippocampal neurons has been proposed as being critical, the role of excitatory/inhibitory neurotransmitters in this behavioral effect is unclear. Neurochemical and behavioral changes are maintained 24h after ketamine administration, well beyond its plasma elimination half-life. Thus, ketamine initiated a cascade of cellular mechanisms supporting its fast antidepressant-like activity. To date, the underlying mechanism involves glutamate release, then downstream activation of AMPA receptors, which trigger mammalian target of rapamycin (mTOR)-dependent structural plasticity via brain-derived neurotrophic factor (BDNF) and protein neo-synthesis in the medial prefrontal cortex (mPFC), a brain region strongly involved in ketamine therapeutic effects. However, these mPFC effects are not restricted to glutamatergic pyramidal cells, but extend to other neurotransmitters (GABA, serotonin), glial cells and brain circuits (mPFC/dorsal raphe nucleus-DRN). It could be also mediated by one or several ketamine metabolites (e.g., (2*R*,6*R*)-HNK). The present review focuses on evidences for mPFC neurotransmission abnormalities in major depressive disorder and their potential impact on neural circuits (mPFC/DRN). We will integrate these considerations with results from recent preclinical studies showing that ketamine, at antidepressant relevant doses, induced neuronal adaptations that involve the glutamate-excitatory/GABA-inhibitory balance. Our analyses will help directing future studies in elucidating the mechanism of action of a new fast-acting antidepressant drugs generation.

Keywords: ketamine, antidepressant, resistance, excitation, inhibition, medial prefrontal cortex, neurotransmitter

1. INTRODUCTION

Clinical studies have first demonstrated that ketamine, a non-competitive antagonist of the N-methyl-D-aspartate subtype of excitatory amino acid receptor (NMDA-R), is a dissociative anaesthetic [1]. Then, ketamine was found to display antidepressant efficacy in treatment-resistant depression (TRD) [2, 3].

Different methods have been used for staging TRD [4]. Each staging method has its own criteria for treatment duration, classes and number of antidepressant trials and severity of depression. Although there is a lack of consensus regarding these criteria of TRD, failure to respond to more than two classes of antidepressant drugs (among them monoaminergic ones) with adequate dosage and for an adequate duration is defined as TRD [5]. More than fifty percent of depressed patients would meet this definition [6], among them, those taking monoaminergic antidepressant drugs of the serotonergic/noradrenergic class. However, low response rates to the first antidepressant prescription suggest that there are other strategies/mechanisms of action that may help patients with a TRD [7, 8]. Ketamine could be one of them.

*Address correspondence to this author at Laboratoire de Neuropharmacologie. CESP/UMR-S 1178, Univ. Paris-Sud, Fac Pharmacie, Inserm, Université Paris-Saclay. 5, rue J-B Clement, Tour D1, 2e etage, F-92296 Chatenay Malabry cedex. tel: (33) 1 46 83 54 16E-mail: alain.gardier@u-psud.fr

Recently, results of twelve randomized clinical trials confirmed that ketamine is the only NMDA-R antagonist to date consistently demonstrating such an antidepressant efficacy in treatment-resistant depression. Its antidepressant effects following an intravenous infusion are both rapid and robust, but it has a short-lived action. In most cases, the remission peaks obtained at post-infusion day 1 and fainted at day 7 (see meta-analysis reviews: [9-13]).

Although downstream neuronal adaptations might be involved in its antidepressant activity [14], the mechanisms underlying ketamine's effects remain unclear. Analyzing in detail brain regions and circuitry involved in its mechanism of action is important because: First, major depressive disorder (MDD) is a serious, debilitating, life-shortening illness and a leading cause of disability worldwide. According to the World Health Organization, about 350 million people are affected by depression, with a higher risk for females than males [15]. MDD is also predicted to be the second leading cause of burden in 2020 [16]. Second, limitations of the most currently prescribed drugs for MDD treatment, i.e., selective serotonin reuptake inhibitors (SSRIs) and serotonin–norepinephrine reuptake inhibitors (SNRIs) targeting the brain monoaminergic system, such as the delay between drug administration and antidepressant efficacy. Divergent roles of serotonin (5-HT) autoreceptors and heteroreceptors in modulating responses to antidepressant drugs explain, at least in part, this long delay of action [17]. Third, an up-to-20% of resistance and non-response rate has made these current treatments less reliable [18]. Therefore, it is necessary to clarify the mechanisms underlying ketamine's fast antidepressant-like activity [19]. It

has been postulated that ketamine exerts its therapeutic effect with limited direct interactions with 5-HT systems. Our recent studies performed in BALB/cJ mice suggested evidence of activation of 5-HT neurotransmission in the medial prefrontal cortex (mPFC) [20, 21].

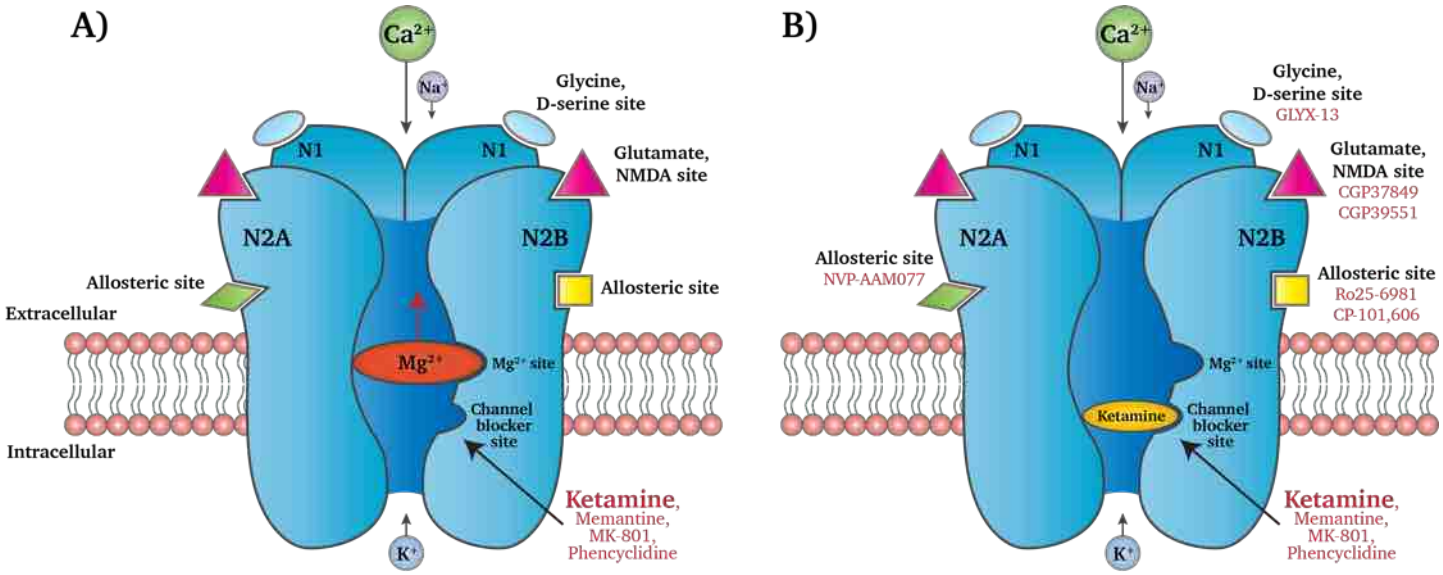

Figure 1. NMDA receptor channel as target of rapid antidepressant drugs

New antidepressant drugs targeting NMDA receptor (NMDA-R) have shown promising results in both clinical trials and preclinical studies. Identification of their specific binding sites could help explaining the mechanism of their neurochemical and behavioral effects. NMDA-R is tetrameric ionotropic glutamate receptor, which is often composed of four subunits: two GluN1 and two GluN2 (GluN2A and GluN2B). NMDA-R has high permeability for Ca^{2+} ions.

A) Under physiological conditions, Mg^{2+} induces a voltage-dependent blockade of the channel and prevents totally Ca^{2+} flux through this channel.

B) When the channel is open, one Ca^{2+} and one Na^{+} ions will enter the pore in exchange for one K^{+} ion. NMDA-R can only be activated by a simultaneous binding of glutamate to its site located on the GluN2 subunits and of glycine/D-serine, as co-agonists, binding on GluN1 subunit. CGP37849 and CGP39551 are known as competitive NMDA-R antagonists on GluN2 subunit. GLYX-13, known as functional partial agonist of NMDA-R on the glycine-site, has been shown lately to induce antidepressant-like effects without ketamine-like side effects [384]. Only a significant depolarization leads to Mg^{2+} release from its binding site and allow other channel blockers to enter. Ketamine and other channel blockers (e.g., memantine, MK-801) are known to block this channel in an uncompetitive manner, by a specific binding to the phencyclidine-binding site. This channel also possesses allosteric binding sites, located extracellularly, with Ro25-6981 and CP-101,606 (traxoprodil) on GluN2B subunit, and NVP-AAM077 on GluN2A subunit.

The present review will focus on preclinical data regarding cellular and molecular mechanism of ketamine underlying its antidepressant-like activity rather than clinical data on ketamine's benefits on TRD. Indeed, a lot of clinical reviews has already been published, many of them have used a small number of patients in TRD (see a meta-analysis: [22-24]). In addition, some clinical and biological predictors of ketamine's response are often identical to other therapeutics used in MDD, thus we are waiting for more specific biomarkers of this response [25].

Preclinical studies have begun to elucidate the mechanism underlying the rapid antidepressant-like activity of ketamine in animal models/tests of anxiety/depression. The rapid antidepressant response to the NMDA-R antagonist has been associated with a glutamate burst and activity dependent synapse formation in the mPFC [7, 26, 27]. Thus, the involvement of the balance between excitatory (glutamate, 5-HT) and inhibitory (γ-aminobutyric acid - GABA) neurotransmission within the glutamate mPFC/5-HT dorsal raphe nucleus (DRN) circuitry in rodent studies is addressed. Since ketamine is comprised of a mixture of two optical isomers: (*S*)-ketamine and (*R*)-ketamine, several active metabolites such as (*2R,6R*)-HNK may potentially make an important contribution to its antidepressant-like activity [28]. A possible direct activation of α-amino-3-hyroxy-5-methyl-4-isoxazolepropionic acid receptor subtype (AMPA-R) by (*2R,6R*)-HNK, the main brain active metabolite [29], is also discussed. The role of several factors, including species, route and dose of administration, and timing of measures (30 min., 24hr or 7 days prior to testing) are described and evaluated. For example, sub-anaesthetic ketamine doses display a broad range of behaviors and cognitive deficits that resemble aspects of endogenous psychosis: a single dose (25 mg/kg, intraperitoneal - i.p.) has been used for the past two and a half decades as an pharmacological animal model of schizophrenia at sub-anesthetic doses (in rats: [30-32]). Such stereotypies limit the ability to analyze the antidepressant-like activity of ketamine in the forced swimming test (FST) shortly after its systemic administration, for example, and to compare the results across studies. The behavioral response of rodents in the FST has strong predictive validity for antidepressant drug activity in patients [33]. Thus, understanding the reason for ketamine's short-lived action and how antagonism of NMDA-R can alter synapse and

circuit function is important to developing circuit-based pharmacotherapy of depression [34].

2. PHARMACODYNAMICS AND PHARMACO-KINETICS OF KETAMINE

Ketamine is described as a powerful NMDA-R antagonist: *in vitro* EC50 = 760 nM, *in vivo* ED50 = 4.4 mg/kg in rodents cortex or hippocampus [35, 36]. Ketamine is an NMDA-R open channel blocker: under physiological conditions, the channel is closed (in the presence of Mg^{2+}), and the drug has little or no ability to enter into the Ca^{2+} channel and to bind to its PCP-like site (Figure 1). An electrophysiological *in vitro* study performed in cultured hippocampal neurons has shown that ketamine can still block NMDA-R and reduce post-synaptic currents under physiological conditions (i.e., in the presence of Mg^{2+}) [37], which suggests that ketamine readily exceeds the physiologic capacity of the NMDA-R's Mg^{2+}-dependent voltage gating to impede ion flow through the receptor channel.

Ketamine is a racemic mixture containing equal parts of (*R*)-ketamine and (*S*)-ketamine. Compared to (*R*)-ketamine, (*S*)-ketamine has about four-fold higher analgesic and anesthesic potency, in agreement with its four times higher affinity to NMDA-R [38]. (*S*)-ketamine is considered having twice the therapeutic index of racemic ketamine, which means that side effects may be reduced when only half of the usual racemic dose is administered [39].

Ketamine has a short elimination half-life (t1/2 = 30 min in mice; [40]) and is rapidly transformed into various metabolites such as norketamine and HNKs immediately after it enters the body circulation [28]. In our recent study [20], we reported that, at 30 mins after an i.p. administration, the plasma concentration of the major brain metabolite, (2*R*,6*R*)-HNK is already five times the one of racemic ketamine. While norketamine is considered as an NMDA-R antagonist (Ki = 0.6 – 0.9 μM), HNK only shows a moderate inhibition of this receptor in the (2*S*,6*S*)- isoform (Ki = 7 μM), but not the (2*R*,6*R*)- isoform (Ki >100 μM) [41]. Interestingly, (2*R*,6*R*)-HNK, has been demonstrated to have antidepressant-like properties in rodents, while (2*S*,6*S*)-HNK does not [29]. These raise the question whether looking in NMDA-R blockade is the future direction for new fast-acting antidepressant drug discovery. In fact, the antidepressant activity of the parent drug, ketamine, depends on AMPA-R activation [21, 42].

3. QUICK VIEW OF EFFECTS OF AN ACUTE KETAMINE ADMINISTRATION

The pioneer experimental work of Moghaddam *et al.* (1997) [43] demonstrated that a single sub-anesthetic dose of ketamine activated glutamatergic neurotransmission in the prefrontal cortex (PFC). Ketamine induced a rapid increase (starting at 40 min after an i.p. injection of 10, 20 or 30 mg/kg, and lasting for 100 min for the 30 mg/kg dose) in extracellular levels of glutamate (Glu_{ext}) as measured by *in vivo* microdialysis in rats. This effect was blocked by an intra-PFC application of the AMPA-R antagonist, CNQX. Consequently, such an NMDA-R blockade led to cognitive disruptions.

Thirteen years latter, the rapid antidepressant-like activity of ketamine was supported by another pre-clinical study also performed in rats: Li *et al.* (2010) [26] were the first to suggest that the antidepressant effects of ketamine (10 mg/kg, i.p.) require activation of the mammalian target of rapamycin (mTOR) pathway and induction of synaptogenesis (synaptic formation/maturation) in the mPFC in an AMPA-R-dependent manner. Indeed, AMPA-R activation is required for the antidepressant actions of ketamine because a pretreatment with a selective AMPA-R antagonist, NBQX, blocked the rapid induction of mTOR signaling pathway in the mPFC [26]. These authors then investigated the underlying cellular and molecular mechanisms involved in the rapid antidepressant-like activity of ketamine. Using whole-cell voltage clamp in cortical slices from rats that have been chronically stressed, Li *et al.* (2011) [44] demonstrated that such a low ketamine dose ameliorated chronic stress-induced anhedonia and anxiogenic behaviors and reversed decreases in excitatory postsynaptic current responses in slices of layer V pyramidal neurons in the mPFC.

In addition, the effects of a single dose of ketamine depend upon the inhibitory phosphorylation of glycogen synthase kinase-3 (GSK-3) [45]. Complementary electrophysiological data have been obtained measuring excitatory postsynaptic current either in cortical or hippocampal slices [26]. Taken together, these data are consistent with the hypothesis that ketamine blocked a subset of NMDA-R located on GABA-releasing interneurons in the mPFC, thus decreasing GABA release, which facilitates glutamate release and the induction of a long-term potentiation (LTP)-like synaptic plasticity [26]. In addition, this indirect disinhibition hypothesis of glutamate signaling suggests that ketamine induces rapid increases in cortical excitability *via* the selective blockade of inhibitory GABA interneurons, thus increasing glutamate release in the mPFC [34]. The subsequent activation of AMPA-R signaling located on glutamatergic neurons has since been described by many authors to explain how ketamine can increase protein synthesis, synaptogenesis and induce cortical disinhibition (see [27, 34, 46]).

Ketamine responses were impaired in Val66Met knock-in mice, among them synaptogenesis in the mPFC, suggesting that activation of brain-derived neurotrophic factor (BDNF) release and its high affinity receptor, tropomyosin receptor kinase B (TrkB) are necessary for ketamine to exert its antidepressant-like activity [45]. In addition, 3 mg/kg of ketamine did not produce antidepressant-like effects as measured 30 min and 24h after administration to homozygous BDNF knockout mice (rapid and sustained effects, respectively) [47]. This later group focusing on the hippocampus, proposed another synaptic plasticity process in C57BL/6 mice: the fast antidepressant effects of NMDA-R antagonists would depend on deactivation of eukaryotic elongation factor 2 (eEF2) kinase (also called CaMKIII), thus reducing eEF2 phosphorylation and leading to de-suppression of translation of BDNF. Monteggia's group used extracellular field potential recordings and hippocampal slices dissected from mice to describe changes in glutamate neurotransmission and signaling

cascade induced by ketamine following NMDA-R blockade [37, 48]. Ketamine applied to these slices potentiated within 30 min AMPA-R-mediated neurotransmission in the CA1 region of the hippocampus. Ketamine-mediated synaptic potentiation would require a **direct** involvement of NMDA-R blockade, an increased expression of both GluA1 - GluA2 subunits of postsynaptic AMPA-R, protein synthesis, BDNF expression and a tonic activation of eEF2 kinase. This cascade of events would lead to ketamine's antidepressant response [48]. However, contrasting results quickly appear in the literature regarding the role of BDNF in this cascade of events. For example, unlike monoamine drugs (i.e., SSRI, SNRI), in heterozygous $BDNF^{+/-}$ C57 mice (with up to 50% reduction of central BDNF), ketamine at a higher dose than Monteggia's group (50 *vs* 3 mg/kg, i.p.) still produced a characteristic antidepressant-like response without activating BDNF signaling in the hippocampus [49]. Perhaps more pronounced reductions in BDNF levels are required to block the behavioral effects of ketamine. On the other hand, Liu *et al.* (2012) studied the role of the Val66Met (rs6265) single nucleotide polymorphism (SNP), a putatively functional polymorphism within the first exon of BDNF, and ketamine response in BDNF knock-in mice [50]. They found different synaptogenesis levels in the mPFC after ketamine administration. Homozygous Val/Val mice exhibited high increases in spine density, while homozygous Met/Met carriers responded the least. Indeed, the antidepressant effects of ketamine in Met/Met mice were attenuated in the FST compared to Val/Val or Val/Met carriers. These data suggests that the weakened antidepressant response to ketamine typically seen in approximately 30% of patients might be, at least partialy related to the Val66Met polymorphism [51]. However, the Val66Met variant may play a different role with monoaminergic antidepressant drugs as opposed to fast-acting antidepressants such as ketamine as suggested by Laje et al. (2012) [51].

Thus, converging findings suggest that ketamine-induced fast antidepressant-like activity is related, at least in part, to neuroplasticity changes in the frontocortical/hippocampal networks via activation of AMPA-R-dependent glutamate transmission. However, ketamine effects could be also mediated by one or several ketamine metabolites and activation of other neurotransmitters (GABA, 5-HT) and brain circuits (mPFC/DRN). It is even more difficult to clarify the mechanism of action of an acute sub-anesthetic dose of ketamine knowing that the time of observation is an important parameter to analyze its rapid (30 min), sustained (24h post-injection) or long term (one week) antidepressant-like activity in adult rodents. Studying the sustained effect of ketamine *in vivo* offers several advantages: it can be analyzed in various preclinical behavioral tests in rodents because its side effects (i.e., psychotomimetic, stereotypies) are no longer observed at this time point [49]. For the same reason, only low sub-anesthetic doses (less than 25 mg/kg, i.p.) would be relevant to measure ketamine antidepressant-like activity in rodents since higher doses were used to develop a model of schizophrenia (25 mg/kg: [31]).

Still, it is unclear whether specific brain regions, cell types or circuits are selectively more sensitive to ketamine [52] and to what extent glutamatergic and monoaminergic systems (mainly 5-HT) play a role in ketamine's antidepressant-like activity. Ketamine binding parameters to glutamatergic NMDA-R (Ki = 0.25 μM in rat cortical and hippocampal preparation: [41]) suggest that glutamate, the major excitatory neurotransmitter in the brain could play an important role for guiding future therapeutic strategies. In addition, there is currently a debate to compare binding affinities of ketamine enantiomers and metabolites to NMDA-R or AMPA-R and their pharmacological properties (i.e., putative antidepressant-like activity in the FST in rodents): (*R*)-ketamine *vs* (*S*)-ketamine, or *vs* numerous ketamine metabolites: norketamine, hydroxynorketamines (HNKs) and others [53-56].

In summary, the current knowledge regarding different steps involved in the mechanism of action of an acute ketamine dose (leading to its *fast antidepressant-like activity)* can be summarized as follows (Figure 2):

1 - Ketamine binds to NMDA-R located on GABAergic interneurons

2 - Burst of glutamate neurons (LTP), thus glutamate release from pyramidal cells located in the mPFC

3 - Stimulation of post-synaptic AMPA-R, which is ligand-dependent Na^+/Ca^{2+} channel

4 – Increases in BDNF synthesis and release, activation of TrkB/Akt

5 - Activation of the mTORC1 signaling pathway [26] in the mPFC [27], but deactivation of the eEF2 kinase in the ventral hippocampus (v-Hipp) [47]

6 - Synapse maturation and synaptogenesis, plasticity

7 - *Fast antidepressant-like activity*

We have been interested to know whether GABA and 5-HT release participate to this pathway (Figure 3).

Here, we review the connections between ketamine and neurotransmitter systems that could possibly explain its surprising fast antidepressant-like activity in rodents (naïve *vs* animal models of anxiety/depression). The excitatory/inhibitory balance provided by glutamatergic/GABAergic systems in the mPFC is likely to participate to this activity. Indeed, alterations in both neurotransmitter systems may contribute to the pathophysiology of MDD [57]. As to the importance of serotonergic system throughout the history of antidepressant drug research, we will also resume and discuss recent results regarding ketamine's interaction with the brain serotoninergic system.

4. ACUTE-ADMINISTRATION OF KETAMINE & MOLECULAR ALTERATIONS

4.1. Glutamate neurotransmission

Modern stereological methods have estimated that approximately 60% of neurons in human brain use glutamate as primary excitatory neurotransmitter [58]. Glutamate exerts its actions via its binding to three different ionotropic receptor subtypes, which are classified as NMDA-R, AMPA-R and kainate receptor, and through metabotropic receptors

(mGluR) [59]. Ionotropic receptors are post-synaptic, while mGluR are located on the membrane of both post- and pre-synaptic neurons. Initial studies on glutamate were focused on the neurotoxic effects of glutamate following calcium influx [60]. However, subsequent studies have reported that, while excessive stimulation is neurotoxic, physiological stimulation of glutamate receptors is involved in cell growth and neuronal plasticity [61].

Under normal conditions, glutamate plays a key role in regulating neuroplasticity, learning and memory. Indeed, the balance between glutamate and GABA, the primary inhibitory neurotransmitter in the brain is essential for the physiological homeostasis in the central nervous system (CNS) [62]. Abnormalities in this excitatory/inhibitory neurotransmitter systems may lead to aberrant functional connectivity and altered synaptic levels of both neurotransmitters mainly in the cortex, thus playing a critical role in anxiety and depression [63-65]. Glutamatergic neurons and synapses by far outnumber all other neurotransmitter systems in the brain with the only exception of the GABAergic system [66]. As an example, it has been estimated that, in the whole human brain, there are roughly two hundred thousand serotonergic neurons out of ninety billion total neurons [67, 68]. In mouse brain, there are only twenty six thousand serotonergic neurons out of seventy million total neurons, of which sixteen thousand cells were found in the raphe system [69, 70]. Therefore, excessive increases in glutamatergic neurotransmission are known as a potent neuronal neurotoxicity [71].

In the brain, glutamatergic neurotransmission and metabolism are united by the conceptualization of the tripartite synapse (Figure 2), which consists of a presynaptic neuron, a postsynaptic neuron, and an astrocyte (glial cell). Glial cells have all of the necessary components for synthesis, release, and reuptake of glutamate [72, 73]. Glutamate released from neurons is taken up by glial cells, via excitatory amino-acid transporter (EAAT 1&2), where it is converted into glutamine. When necessary, glutamine is then transported out of the glia and taken up by neurons where it is converted back to glutamate, thereby complete the glutamate-glutamine cycling [74]. This neuronal-glial cycling serves as a reservoir to limit an excess of synaptic glutamate levels, which could lead to excitotoxicity [75, 76]. Thus, it has been suggested that astroglial dysfunction may have a considerable role in neuropsychiatric diseases such as MDD [77].

4.1.1. The glutamatergic deficit hypothesis of depression

The hypothesis of glutamate abnormalities in MDD has become more and more consistent. Indeed, higher glutamate levels in the blood and cerebrospinal fluid (CSF) have been found in patients with MDD [78-82]. In addition, there is a positive correlation between plasma glutamate levels and severity of depressive symptoms in patients with MDD [81]. Interestingly, a five-week treatment with antidepressant drugs (SSRIs) significantly decreased the levels of glutamate in serum in depressed patients [83, 84], suggesting the possible role of glutamate in the action of antidepressants. The dosage of glutamate levels *in vivo* in the human brain has been developed with the non-invasive magnetic resonance spectroscopy (MRS) to quantify glutamate and glutamine together as a composite measurement labeled "Glx". Decreased Glx levels have been found in the anterior cingulate [85-87] or PFC [88, 89] of depressed patients. Thus, altered Glx in MDD can be reversed by antidepressant treatment [57, 90]. Unipolar depressed patients treated with antidepressant drugs or electroconvulsive therapy (ECT) had increases in cortical Glx to levels no longer different from those of age-matched controls [88, 91].

Comparison of quantitative data between rodent and human brains are difficult due to the lack of refined *in vivo* assays measuring brain glutamate levels, thus reducing the understanding of the pathophysiology of the glutamatergic activity and effects of drug treatment. The hypothalamic–pituitary–adrenal axis (HPA axis) has been shown to be associated with stress. Long term exposed to high level of glucocorticoids (hyperactivities of HPA) involved the activation of forebrain glutamate neurotransmission, e.g., by four-fold in the hippocampus [63, 92]. Indeed, both stress and glucocorticoids (often elevated in depressed patients) increase Glu_{ext} in the rat mPFC [93, 94].

Studies in animals also described a glutamate hypothesis of depression [66, 95] and have confirmed these alterations in glutamate neurotransmission. Acute stress is associated with increased glutamatergic neurotransmission mainly in the PFC, hippocampus and amygdala as measured by *in vivo* microdialysis [96-98], while treatment with antidepressants attenuated stimulation-evoked glutamate release [99-101].

Chronic stress has been developed in different animal models of anxiety/depression such as chronic unpredictable stress (CUS) or chronic unpredictable mild stress (UCMS) and social defeat. Using *ex vivo* ^{1}H-MRS in a chronic stress model of depression in rats, a decrease in both glutamate and Glx in the PFC and hippocampus was measured [102]. Similarly, *ex vivo* liquid chromatography tandem-mass spectrometry detected a decreased glutamate in the mPFC in the chronic social defeat stress mice model of depression [103]. Interestingly, CUS is associated with dendritic atrophy and decreased glutamate receptor expression in the mPFC [104]. UCMS mice display an increase in glutamate and a decrease of glutamine contents in the hippocampus, which were reversed by a chronic fluoxetine treatment [105]. Noteworthy, in animals and depressed individuals, there **are regional differences in glutamatergic neurotransmission** with a hypofunction in the PFC and a hyperfunction in the hippocampus, amygdala, locus coeruleus [106]. These regions are interconnected (e.g., mPFC-vHipp pathway: [107]) and influence each other via direct and indirect neural activities in the control of stress response. Therefore, chronic stress is associated with more complex neuronal changes, different from normal, physiological response to acute stress. Indeed, by modifying glutamate release and reuptake, chronic stress affects the cortex by reducting synaptic AMPA-R and NMDA-R availability, synapse density and diameter and dendritic arborization and length, thus consistenly leading to neuronal atrophy in the PFC and hippocampus and to a decrease in synaptic functioning (see review [108]). Stress induced by UCMS in mice caused a hypofunction of the PFC, which could initiate an increased

glutamatergic neurotransmission from amygdala onto prefrontal parvalbumin interneurons that contributed to their behavioral impairment following UCMS [109].

Alternatively, there has been increasing interest in the role of glutamate in mood disorders, especially knowing the effects of ketamine in improving depressive symptoms in patients with TRD. Glutamatergic alterations may occur in mood disorders through inflammation [110]. Recent data have elucidated the mechanisms by which the innate and adaptive immune systems interact with neurotransmitters and neurocircuits to influence the risk for depression [111]. Increased inflammation has been observed in a significant subgroup of patients with mood disorders, and inflammatory cytokines have been shown to influence glutamate metabolism through effects on astrocytes and microglia [112]. In addition, the administration of the inflammatory cytokine interferon-alpha has been shown to increase brain glutamate levels in the basal ganglia and dorsal anterior cingulate cortex as measured by MRS in patients with MDD [113]. Thus, it was proposed that an exaggerated release of glutamate by glial cells during an immune activation promotes aberrant signaling through stimulation of extrasynaptic glutamate receptors, ultimately resulting in synaptic dysfunction and loss [114].

Overall, normalization of glutamate neurotransmission is likely a common effect of antidepressant drugs. In addition, decrease number of glia cells may contribute to depression, due to the crucial role of glutamate uptake by glial cells in removing glutamate from synapses.

4.1.2. Ketamine influences on glutamate content

Ketamine, as blocker of NMDA-R, induces an immediate increase in Glu_{ext}, neuronal excitability and spontaneous oscillations after an acute administration [115]. Various tools and experimental protocols have been used to analyze these changes, some of them being used in both human and rodents. For example, a rapid and transient increase in mPFC glutamate cycling (Glx) in response to a single dose of ketamine (0.5 mg/kg, intravenous - i.v.) was demonstrated in *ex vivo* studies using ^{1}H-[^{13}C]-nuclear MRS in depressed patients with MDD [116]. At such a low ketamine dose, ten of eleven patients remitted having a 50% reduction in the HAMD-24 scale. In addition, using pharmaco-metabolomics in human, an increase in plasma glutamate levels was found two hours after ketamine i.v. administration [117].

Preclinical evidence also using *ex vivo* ^{1}H-MRS, confirmed these data, i.e., a rapid and transient increase in glutamate, glutamine and GABA levels in the mPFC was found in rats immediately after ketamine injection (3, 10 and 30 mg/kg, i.p.) [118]. Performance in the FST 24h after ketamine administration at 30 mg/kg (but not at 3 and 80 mg/kg) partially mirrors the dose-dependent effects on rat glutamate/GABA-glutamine cycling. Using neurochemical assay in dissected brain regions of stressed CUS rats, Melo *et al.* (2015) [119] have found a significant decrease in post-mortem brain tissue homogenates levels of glutamate in the nucleus accumbens (NAcc, a brain region involved in anhedonia), but not in the PFC, and a combination treatment of ketamine (10 mg/kg for 3 days) and fluoxetine or imipramine (10 mg/kg for 14 days) reversed this effect.

To access the Glu_{ext}, *in vivo* microdialysis is the most relevant tool when performed in freely moving rodents because a correlation can be drawn between changes in neurotransmitter levels in dialysates and responses to a behavioral test (e.g., the FST). The Glu_{ext} monitored by *in vivo* microdialysis reflects the balance between neuronal release and reuptake into the surrounding nerve terminals and glial elements [120]. Moghaddam *et al.* (1997) [43] have first tested a range of ketamine doses (from 10 to 200 mg/kg, i.p.) and found that only low subanesthetic doses (less than 30 mg/kg) increased Glu_{ext} in rat mPFC. This effect was confirmed by Lorrain et al. (2003) [121], using also a low dose (18 mg/kg, i.p.) in rats. Interestingly, this study found that only a systemic, but not a local intra-mPFC dose of ketamine, increased local Glu_{ext}, indicating that ketamine might also act outside of the mPFC to enhance glutamate release.

In the dorsal hippocampus, ketamine decreased Glu_{ext} in UCMS rats, at doses 10, 25 and 50 mg/kg, i.p., together with a decrease in depressive-like behavior [122]. These results suggest, one more time, regional differences in glutamatergic neurotransmission: a hypofunction in the PFC and a hyperfunction in the hippocampus, amygdala, locus coeruleus in mood-related disorders in animals and depressed individuals [106].

4.1.3. Glutamate receptors as targets of ketamine antidepressant actions

4.1.3.1. NMDA-R

Physiology. NMDA-Rs are tetrameric ionotropic glutamate receptors. NMDA-R dysfunction has been implicated in neurologic and psychiatric disorders including Alzheimer's disease, Huntington's disease, depression, schizophrenia, chronic and neuropathic pain, epilepsy, and neuron death following stroke [123]. NMDA-Rs are composed of a combination of GluN1 subunits with GluN2 and/or GluN3 subunits. The GluN1 subunit is encoded by a single gene; four genes encode the GluN2 ubunits (GluN2A, GluN2B, GluN2C, and GluN2D); two genes encode the GluN3 subunits (GluN3A and GluN3B). Most NMDA-Rs are composed of two GluN1 subunits together with either two GluN2 subunits or a combination of GluN2 and GluN3 subunits. NMDA-Rs activation requires simultaneous binding of both glutamate (binding to GluN2 subunits) and glycine (binding to GluN1 and GluN3 subunits) (see a review [124]). The biophysical properties of the NMDA-R channel that determine its specific involvement in physiological synaptic processes are: (i) a high permeability for Ca^{2+} ions and (ii) a voltage-dependent blockade by Mg^{2+} ions. Only a significant depolarization (for instance, induced by activation of AMPA-type receptors) leads to release of Mg^{2+} and allows Ca^{2+} entry through NMDA-R channels. In turn, Ca^{2+} influx can trigger numerous physiological and pathological intracellular processes [125].

Pathophysiology of NMDA-R in depression. To test for the role of glutamate neurotransmission in specific neurons *in*

vivo, genetic manipulations using conditional knockout mice and cell type specific promoters have been set up. Some negative results have been obtained regarding gene deletion of NMDA-R or its GluN1 subunit: mice lacking NMDA-R in parvalbumin interneurons displayed normal depression-related behaviors [126]. By contrast, developmental, selective

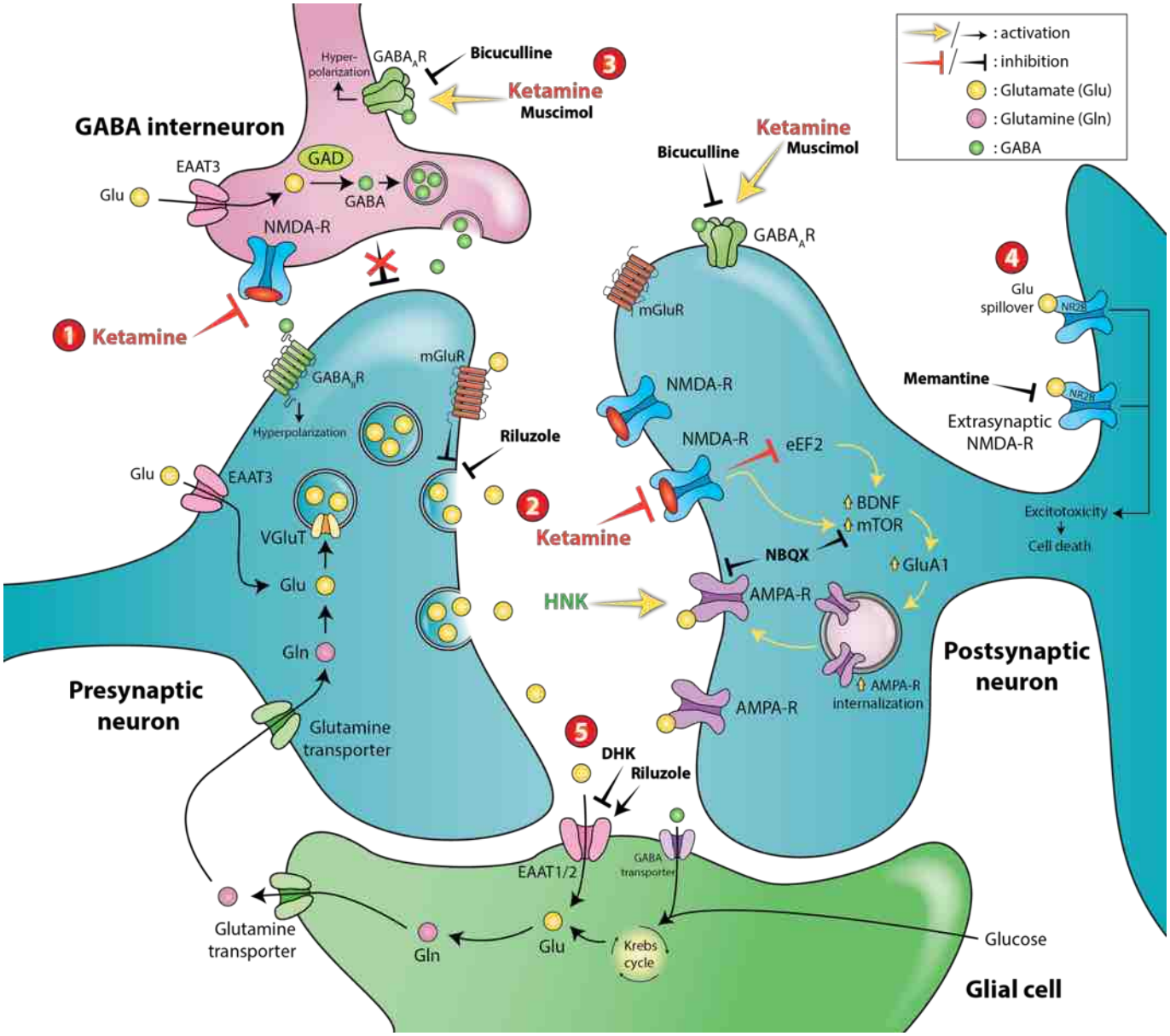

Figure 2. Potential mechanisms of action of ketamine rapid antidepressant-like activity involved glutamatergic neurons (pyramidal cells), GABAergic interneurons and astrocytes in the medial prefrontal cortex.

(1) Ketamine has been first proposed to block pre-synaptic NMDA receptor (NMDA-R) located on GABAergic interneurons, which induces a disinhibition of these inhibitory GABAergic interneurons on glutamatergic pyramidal neurons. This disinhibition allows an increase in firing activity in pyramidal cells, leading to an increase in glutamate release. As a result, extracellular level of glutamate increased and consequently activates the post-synaptic AMPA receptor (AMPA-R), prolonging the excitatory effects to other neurons and triggering other neurotransmitters release (e.g., 5-HT, dopamine).

(2) Ketamine could also block post-synaptic NMDA-R located on glutamatergic neuron. This blockade is demonstrated to block the eukaryotic elongation factor 2 (eEF2) thus reducing eEF2 phosphorylation and leading to de-suppression of BDNF translation in the hippocampus [47]. Ketamine also requires activation of the mammalian target of rapamycin (mTOR) pathway in the medial prefrontal cortex (mPFC) in an AMPA-R-dependent manner, as NBQX, AMPA-R antagonist, is reported to block this pathway and ketamine antidepressant-like activity in the mPFC [26]. The activation of mTOR pathway and de-suppression of BDNF lead to an increased translation of synaptic proteins, including GluA1, which reinforces the AMPA-R internalization to traffick more AMPA-R to the synapse and increases synapse spine numbers and stabilization, a process called synaptogenesis [7]. (2R,6R)-hydroxynorketamine (HNK), a metabolite of ketamine, has gained a lot of interest lately for its amazing antidepressant activity. Different from ketamine, HNK activates directly post-synaptic AMPA-R to induce its effects, which involves an increase of extracellular glutamate level [20]. Continued…

genetic deletion of the NMDA-R GluN2B subunit only from forebrain parvalbumin interneurons revealed a critical role of this receptor in ketamine's antidepressant-like activity [127].

Mood disorders could be underlined by an increased inhibition (the GABAergic system) or a decreased excitation (the glutamatergic system). The impact of stress and glucocorticoids on glutamate neurotransmission involved a sustained activation of ionotropic NMDA-R [66, 95, 128]. Indeed, chronic stress could enhance glutamate release [122], which overactivated NMDA-R and consequently impaired AMPA-R activity. Chronic stress also decreased expression of GluN1, GluN2A and GluN2B subunits of NMDA-R in rat PFC [129]. Such changes of NMDA-R and AMPA-R function can exert two opposite effects depending on the synaptic or extrasynaptic receptor concentration [66]. Recent evidence suggests that the extrasynaptic glutamatergic receptor signaling pathway mainly contributes to the detrimental effects of TRD [8].

Drug treatment. The disinhibition hypothesis of the glutamatergic transmission is based on the efficacy of NMDA-R antagonists in TRD, and was drawn to understand the cellular and molecular mechanisms underlying its fast-acting glutamatergic antidepressant drugs such as ketamine (see below; [34]). Chronic antidepressant drugs treatment can regulate glutamate receptors via reducing NMDA-R function by producing region-specific decreases in the expression of transcripts for GluN1 subunits [128, 130], and conversely by potentiating AMPA-R-mediated transmission [131]. Various studies have shown that treatment with antidepressant drugs decreased plasma glutamate levels in depressed individuals and reduced NMDA-R function by decreasing the expression of its subunits and by potentiating AMPA-R-mediated transmission [106]. In addition, defects in GABAergic synaptic transmission can have an impact on glutamatergic transmission. Indeed, $GABA_A$ receptor ($GABA_A$-R) $\gamma 2$ subunit heterozygous ($\gamma 2^{+/-}$) mice displayed a homeostatic-like reduction in the cell surface expression of NMDA-R and AMPA-R, and functional impairment of glutamatergic synapses in the hippocampus and mPFC. A single subanesthetic dose of ketamine normalized these deficits mainly in the mPFC [65].

Recent evidence indicates that the major determinant of ketamine effects is not the degree of calcium influx, **but the location of NMDA-R** [8]. The complexity of NMDA-R modulation has escalated with the knowledge that receptors can traffic between synaptic and extrasynaptic sites, and its location on the plasma membrane profoundly affects the physiological function of NMDA-Rs [132]. The balance between synaptic and extrasynaptic NMDA-R activity is crucial as the two receptor populations can differentially signal to cell survival and apoptotic pathways, respectively [71] (Figure 2). In fact, extrasynaptic NMDA-Rs are activated by excessive Glu_{ext}, which cause overstimulation of NMDA-Rs. This leads to an increased calcium influx into neuronal cells and an elevation of intracellular calcium levels, which activate toxic metabolic processes and trigger cell death [133]. Typically, NMDA-Rs are found at postsynaptic sites. In the adult forebrain, synaptic NMDA-Rs are predominantly di-heteromeric GluN1/GluN2A and tri-heteromeric GluN1/GluN2A/GluN2B receptors, although their ratios may vary between inputs. By contrast, peri- and extrasynaptic sites are enriched in GluN2B-containing receptors, while normal (non-pathological) parvalbumin-positive interneurons are enriched in GluN2A subunits (for more details, see below on GABA; [134]). NMDA-Rs are mobile (at least in cultured neurons), particularly the GluN2B-containing ones, and probably exchange through lateral diffusion between synaptic and extrasynaptic sites [134]. Therefore, GluN2B subunit receptor antagonists preferentially target extrasynaptic receptors composed of GluN1/GluN2B subunits, which constitute a major hub for signalling pathways that lead to neuronal death [134].

Studies of glutamatergic transporters dysfunction have demonstrated that chronic stress may impair the effective clearance of glutamate from synapses by glial EAATs, thus leading to excessive extrasynaptic NMDA-R function [95, 135]. The physiological function of extrasynaptic NMDA-Rs is not fully understood, but their activation by glutamate spillover may contribute to long-term depression (LTD) [71]. Extrasynaptic NMDA-Rs are involved in excitotoxicity because a selective activation of these receptors in hippocampal neurons triggers the same amount of cell death as activation of all NMDA-Rs [136]. Thus, it is plausible to consider that the effects of NMDA-R-mediated glutamatergic neurotransmission form an 'X' shape, which means that increased synaptic NMDA-R and decreased extrasynaptic NMDA-R may influence neuronal survival and synaptogenesis [71].

NMDA-R antagonists (e.g., MK-801, CGP37849 and CGP39551) can potentiate the effects of antidepressant drugs (see [137, 138] for a review). More evidences insisted on a role for NMDA-Rs containing GluN2B, the subunit usually found in extra-synapses, in the rapid antidepressant actions of ketamine. Indeed, some studies have supported the antidepressant-like effects of GluN2B selective blockers in rodents such as Ro25-6981 [139] and eliprodil [140] or in human (CP-101,606 - [44]). *In vivo* deletion of GluN2B, only in cortical pyramidal neurons, mimics and occludes ketamine's actions in depression-like behavior and excitatory synaptic transmission [127]. To support this theory, evidences pointed out that chronic stress might also enhance GluN2B-containing NMDA-Rs in the hippocampus and suppress synaptic plasticity [141]. However, another study suggested that memantine, a more potent NMDA-R antagonist compared to ketamine, predominantly targets extrasynaptic NMDA-Rs, whereas the NMDA-Rs inhibited by ketamine would be mainly synaptic [142]. Moreover, both ketamine and memantine antagonize the NMDA-R at rest when Mg^{2+} is absent, but only ketamine blocks the NMDA-R at rest when physiological concentrations of Mg^{2+} are present [37]. These data come together with the fact that memantine fails to induce any antidepressant-like activities [143, 144], suggesting that memantine and ketamine display different mechanisms of action: location of NMDA-Rs could explain this disparity.

An interesting study [145] testing selective antagonists of GluN2A (NVP-AAM077) and GluN2B (Ro25-6981) subunits of NMDA-R for their antidepressant-like activities and stereotypies in rats have shown that: antagonism of both subunits concomitantly induced psychotomimetic symptoms, while antagonism of only one subunit (GluN2A or GluN2B) induced an antidepressant-like effect in the FST. Moreover, only NVP-AAM077 and the non-selective channel blocker MK-801

Figure 2. continued…
(3) Ketamine has shown $GABA_A$ receptor ($GABA_AR$) agonistic property. $GABA_AR$ could be found on both GABAergic and glutamatergic neurons. The combination of a lower dose of ketamine with muscimol, $GABA_AR$ agonist, induced antidepressant effect in mice [240]. Bicuculline, $GABA_AR$ antagonist, on the other hand, provoked seizures that could be reversed by ketamine [241, 245]. GABA is synthesized from glutamate by enzyme glutamic acid decarboxylase (GAD), which is only found in neuron, not in glial cells. The role of $GABA_B$ receptor ($GABA_BR$) in ketamine actions is still unknown, since it is a G protein-coupled receptor found presynaptically on neurons. This receptor is activated by GABA to induce neuronal hyperpolarization that limit the release of glutamate. This could participate in the control of GABAergic interneurons to limit glutamatergic neuronal firing activity, until ketamine blocked the inhibitory control of GABA on pyramidal cells. Glutamate metabotropic receptors (mGluR) are G protein-coupled receptors, and could be found both pre- and post-synaptically. Activation of this family of receptor blocks glutamate release. Antagonists of this receptor (e.g., LY341495) also display antidepressant-like activities, while its agonism has neuroprotective quality.
(4) The excessive increase of extracellular glutamate could lead to neuronal excito-toxicity, which could be limited by glial cells. Indeed, the glutamate spillover is thought to bind to extrasynaptic NMDA-Rs, which are rich of GluN2B subunit, thus activating the apoptotic pathway and subsequently, neuronal death. Memantine, NMDA-R channel blocker, targets predominantly these receptors [142].
(5) The excessive level of glutamate could be reuptaken by excitatory amino acid transporters (EAATs), located on glial cells (EAAT 1/2) and on presynaptic neurons (EAAT3). In glial cells, glutamate is transformed into glutamine and stocked until necessary. Herein, GABA could also be transformed into glutamate by using glucose and entering the Krebs cycle. The utility of glucose has been shown to be increased after ketamine intravenous injection [116]. Glutamine stocked inside glial cells could be transported back into presynaptic neuron by glutamine transporters to re-produce glutamate. Glutamate will be stocked inside vesicles by vesicular glutamate transporters (VGluT) and then released to the extracellular compartment at cell depolarization. Dihydrokainic acid (DHK), a selective inhibitor of EAAT2 was demonstrated to have antidepressant-like activity in rats [197], with a huge increase of extracellular glutamate. Meanwhile, ketamine failed to reduce EAATs function [20]. On the other hand, riluzole, a glutamate positive allosteric modulator (PAM) of EAAT2, has shown neuroprotective properties by facilitating the function of this transporter and prevent the release of glutamate by presynaptic neurons. The use of riluzole as an 'add-on' to ketamine treatment in treatment-resistant depression is still under debate.

were capable of increasing Glu_{ext} and $5\text{-}HT_{ext}$ in the mPFC (*in vivo* microdialysis), but not Ro25-6981, indicating that increasing neurotransmitters efflux is not the key element for antidepressant effects of GluN2B selective antagonists. One important remark is that in this study these antagonisms targeted predominantly pyramidal cells. In addition to this finding, micro-injection of Ro25-6981 intra-mPFC was sufficient to induce antidepressant effect, but selective genetic removal of GluN2B subunit on interneurons did not occlude this response [139]. These data suggest that the consequences of GluN2B blockade are different depending on where they are located, i.e., either on glutamatergic pyramidal cells or on GABAergic interneurons, thus underlining the importance of neuronal types (glutamatergic *vs* GABAergic ones) in studying ketamine responses.

On the other hand, restricted deletion of GluN1 in forebrain interneurons did not significantly affected FST behavior [126], meaning that these animals retained their antidepressant-like behavioral response to ketamine despite lacking the putative target responsible for its NMDA-R antagonism. This argues against the hypothesis that antidepressant-like effects are produced by loss of interneuron NMDA-R activity, leading to the disinhibition of pyramidal neuronal firing. However, this conclusion is tempered by the fact that GluN1 is only deleted on a subset of (primarily parvalbumin-expressing) interneurons – leaving open the possibility that the remaining interneuron receptors were sufficient to maintain normal FST behavior in these mutants.

Whether or not NMDA-R antagonism is essential for ketamine antidepressant activity is still a matter of debate. Interesting clinical results from [115] showed an increase in cortical excitability at 6.5 h after ketamine infusion in a group of depressed patients responding to ketamine, but not in non responders. Since this time point occurs much later than psychotomimetic effects associated with the drug, these data are consistent with the hypothesis that the direct NMDA-R antagonism is not sufficient to explain therapeutic effects of ketamine, but rather enhanced non-NMDA receptor-mediated glutamatergic neurotransmission via synaptic potentiation is crucial to ketamine's antidepressant effects (see below for AMPA-R). Such residual effects were also observed in rodents 24h after ketamine administration [20, 21, 26].

4.1.3.2. AMPA-R

Physiology. Not only NMDA-Rs, but also other components of the glutamatergic synapse are involved in the development of depression or its treatment. Importantly, AMPA-R was consistently and repeatedly demonstrated among these components, suggesting that this receptor sub-type might be a central mediator in the pathophysiology and treatment of depression. Lately, the importance of AMPA-R in depression has been largely investigated. Indeed, it was shown that:

AMPA-R, together with kainate receptors, play a major role in excitatory synaptic transmission and plasticity by mediating fast postsynaptic potentials [133]. AMPA-R channel properties are largely determined by subunit composition of the tetrameric receptor, assembled from GluA1-4 subunits [131]. In synapses of hippocampal principal neurons, most AMPA-R are heteromers of GluA1 and GluA2 (80%) and the remaining 20% are assembled from GluA2 and GluA3 subunits [146]. The GluA4 subunit is only expressed in interneurons and in juvenile principal neurons [147]. Binding of endogenous glutamate to at least two of the receptor subunits is required to trigger rapid channel opening, allowing depolarizing current carried mostly by Na^+ ions to enter into the cell [108]. AMPA-R functionally links to a variety of signal transduction events to induce synaptic changes that exceed the basic conception of ketamine as ligand-gated ion channels [148]. Interestingly, the number of AMPA-R at synapses is dependent on

relative rates of exocytosis and endocytosis at the post-synaptic membrane: this process is called "AMPA-R trafficking" [149]. AMPA-R can be trafficked into and out of synapses to increase or decrease synaptic transmission, in order to induce LTP or LTD, respectively [150, 151].

Pathophysiology of AMPA-R in depression. Changes to synaptic plasticity are further coordinated with those to structural plasticity within the tripartite synapse. On pyramidal neurons, LTP and LTD induce dendritic spine growth and retraction respectively, whilst AMPA-R expression is positively related to the size of the spine head [152]. In depression, subregions of the PFC and hippocampus structural and synapse-related findings seem consistent with a deficit in LTP and facilitation of LTD, particularly at excitatory pyramidal synapses [153]. Among all subunits, the GluA1 seems to be of particular importance in LTP as GluA1/A2 heteromers are trafficked to synapses during LTP [150]. Especially, using GluA1-knockout mice, Zamanillo *et al.* (1999) reported the essential role of this subunit in LTP establishment, most likely due to a selective loss of extrasynaptic AMPA-R reserve pools, thus preventing activity-dependent synaptic insertion of AMPA-Rs [154, 155]. Interestingly, the duration of stress exposure seems to modify GluA1 differently: short-term exposure to stress increased GluA1 [156, 157], while long-term (28 days) exposure decreased its expression in hippocampal neurons [158-160]. AMPA-R is strongly involved in synaptic plasticity, in particular those containing GluA1-subunit. Using *in situ* hybridization studies [161, 162], it was shown that repeated electroconvulsive shock (ECS) in rats increased GluA1 mRNA expression in hippocampus areas that are connected to the LTP and consequently increased synaptic efficacy. Compelling evidences suggest that classical antidepressant drugs up-regulate AMPA-R function, which in turn may lead to changes in synaptic strength and plasticity. Indeed, chronic fluoxetine (SSRI) or reboxetine (SNRI) treatment increased the expression of all AMPA-R subunits both in the PFC and hippocampus in a time-dependent manner that was consistent with their antidepressant-like efficacy in rats [163, 164].

In patients with MDD, the results of recent studies on the involvement of AMPA receptors in post-mortem brain tissue (cortex, hippocampus) are heterogeneous: increase in radioligand binding [165] or decrease in mRNA expression levels of AMPA receptor subunits [158]. Clearly, additional studies are required to solve these inconsistencies [166].

Interestingly, AMPA-R activation is capable of promoting neuronal survival (i.e., protects cells from apoptosis). This process involves a powerful activation of BDNF synthesis and release, which activates dendritic spine development [106]. Antidepressant drugs induced marked increases of AMPA-R subunits expression in rat hippocampus, suggesting the targetting of AMPA-R as a therapeutic approach for the treatment of depression [163, 167].

The role of AMPA-R in depression is accompanied by the regulation of NMDA-R. A model of GluA1-knockout mice displayed increased learned helplessness, decreased hippocampus 5-HT and norepinephrine levels, and disturbed glutamate homeostasis with increased glutamate tissue levels and increased NMDA-R GluN1 subunit expression [168], thus indicating a particular interaction between GluA1 and several neurotransmitter systems in provoking depression-like behaviors. The up-regulation of glutamate levels in this study is possibly due to a compensatory mechanism in response to the lack of GluA1-containing AMPA-Rs. On the other hand, the increased expression of GluN1 subunit agrees with downregulation of this subunit by SSRI and SNRI treatment in mouse brain [128, 130]. These data support the notion that physiological and pharmacological properties of NMDA-R play a critical role in the therapeutic actions of structurally diverse antidepressants.

In the absence of GluN2B subnit, the synaptic levels of AMPA-R are increased and accompanied by a decreased constitutive endocytosis of GluA1-containing AMPA-R [169], which is in accordance with findings regarding the concomitant role of GluN2B in mood disorders and the antidepressant effects of GluN2B-selective antagonism (see NMDA-R).

Treatment (ketamine and other AMPA-R agonists). Recent evidences have confirmed that ketamine requires an activation of AMPA-R to exert its antidepressant-like activity. NBQX, an AMPA-R antagonist, blocked the antidepressant-like effects of ketamine in rodents [21, 26, 44, 170-172]. This has led to the glutamate hypothesis of depression and its treatment, e.g., an enhanced glutamate release in the mPFC following ketamine administration results in an activation of AMPA-R, which is necessary for the antidepressant-like activity of NMDA-R antagonists [20, 170]. An up-regulation of AMPA-R GluA1 subunit expression was observed in stressed rodents after an acute ketamine treatment [173, 174]. Interestingly, this upregulation of the hippocampal cell-surface AMPA-R expression is selective to this GluA1 subunit since ketamine did not alter the localization of GluA2, GluA3 and GluA4 subunits [173], indicating that sub-anesthetic doses of ketamine affected a very precise cell-surface AMPA-R GluA1 subunit in the hippocampus.

It is important to remember here the previous findings on classical SSRI antidepressant drugs. For instance, GYKI52466, an AMPA-R antagonist, blocked the antidepressant-like effects of fluoxetine [175] in stressed mice. Up-regulation of GluA1, GluA2/A3 subunits was found in rats PFC and hippocampus [163, 164, 167, 176] and in mice [177] after chronic treatment with classical antidepressants. Meanwhile, the observation of upraised GluA1 following antidepressant drug treatment is more consistent as it was still elevated at 72h post-treatment, while upregulated effects on the GluA2/3 subunits was transient [167, 176]. Moreover, the increase was found on the membrane fraction, not the total extract, suggesting a facilitation of AMPA-R trafficking from intracellular pools to synaptic sites following antidepressant drug treatment. An upregulation of AMPA-R surface expression [26, 65, 170] is therefore a strong candidate mechanism underlying the antidepressant-like effects of ketamine. The drug could trigger critical synaptic changes at excitatory synapses that mediate the relatively long-lasting increases in cortical excitability [115].

Whether or not ketamine exerts its antidepressant-like effects via a direct activation of AMPA-R remains unknown. An

increase in population activity was observed in AMPA-R located in the dorsal hippocampus of anesthetized rats immediately, but not two days after an i.p. administration of ketamine (10 mg/kg) indicating that this may contribute to ketamine immediate therapeutic effects, but not to its substained effects [178]. Interestingly, this study found that this low dose of ketamine significantly increased the AMPA-, but not NMDA-, evoked firing at 30 min post-injection. The lack of blockade of NMDA-R-evoked firing of glutamatergic pyramidal neurons by ketamine may appear puzzling since ketamine is an NMDA-R antagonist, but it could stem from the fact that ketamine exerts its effect through GABA interneuron disinhibition. Indeed, ketamine and MK-801, the most potent NMDA-R antagonist, selectively target NMDA-R located on GABA neurons and lead to decreased inhibition (disinhibition) following a surge in glutamate, thus resulting in an enhancement of AMPA-R activation [179, 180].

In summary, AMPA-R is essential for inducing LTP and LTD, through its trafficking process in and out of post-synaptic membranes. Targetting GluA1 subunit has brought new insights into the function of AMPA-R in depression. Importantly, the antagonism of AMPA-R has become a popular approach in highlighting the necessary stimulation of AMPA-R in fast antidepressant drugs' action, especially ketamine. Here, we underline the importance of distinguishing between the acute, 30 min post-injection and the sustained, 24h post-administration, of ketamine. While the acute effect seems to potentiate AMPA-R and glutamate release, even though the choice of a ketamine dose and subsequently its responses to behavioral tests are highly questionable when performed 30 min post-treatment, the sustained one has, by far, still remained questionable. Understanding how AMPA-R impacts other receptor subtypes and other neurotransmitter system might be the key to understand how ketamine expresses its sustained antidepressant-like activities.

There are potential toxicological concerns associated with chronic activation of AMPA-R (e.g., neurotoxicity, seizures) that could either limit the therapeutic range or preclude the long-term use of such agonists [138]. However, using drugs acting as positive allosteric modulators (PAMs) could offer several advantages, among them no intrinsic agonist activity, it avoids permanent synaptic activation, thus, a weak role in excitotoxic processes is expected [181]. For example, LY392098, an AMPA-R PAM, would act downstream of the NMDA-R/GABAergic interneuron/glutamatergic axis engaged by ketamine. LY392098 potentiated AMPA-R-mediated currents of PFC neurons [182] and also possessed an antidepressant-like activity in the FST and TST, which required AMPA-R activation, unlike imipramine [183]. Surprisingly, it exerted little influence on extracellular NA and 5-HT levels in mPFC dialysates in rats at doses that were active in the FST [184], indicating a different mechanism involved in AMPA-R PAMs that is not commonly seen in SSRI.

4.1.4. Glutamate transporters interacts with the antidepressant-like activity of ketamine

Glutamate transporters play an important role in regulating Glu_{ext} to maintain dynamic synaptic signalling processes. There are a number of transporter families for glutamate, including the plasma membrane EAATs, the vesicular glutamate transporters (VGLUTs), and the glutamate-cysteine exchanger (reviewed by [185]). Excessive glutamate receptor stimulation is toxic to neurons, and glutamate transporters rapidly clear glutamate from the synapse to avoid deleterious consequences. An appropriate reuptake of glutamate by astrocytes is thus crucial for preventing 'spill-over' of synaptic glutamate concentrations and binding to the extrasynaptic NMDA-R [8].

There are three classes of VGLUTs: VGLUT1, VGLUT2 and VGLUT3, ensuring the vesicular uptake of glutamate in the CNS. VGLUTs can be found on many types of neurons such as glutamatergic, GABAergic and serotonergic ones (reviewed by [186]). VGLUT1 and VGLUT2 are often used as markers of presynaptic glutamatergic transmission since glutamate is released into the synapse via these vesicular glutamate transporters in the forebrain [187, 188]. Recent clinical studies reported decreased levels of VGLUT1 in the entorhinal cortex of depressed patients [189]. In addition, the number of synapses containing VGLUT1 and VGLUT2 was decreased in stressed mice [190].

EAATs divide into five subtypes: EAAT1 (or GLAST1), EAAT2 (or GLT-1), EAAT3 (or EAAC1), EAAT4 and EAAT5. EAAT1 is highly abundant and is the major glutamate transporter in the cerebellum, being about 6-fold more abundant than EAAT2. Moreover, EAAT1 is responsible for 90-95% of glutamate uptake in the forebrain. EAAT1 and EAAT2 are both predominantly localized on astrocytes and abundant in the hippocampus and cerebral cortex [191]. In contrast, EAAT3 is a neuronal transporter and also abundant in the cerebral cortex. Meanwhile expression of EAAT4 and EAAT5 is restricted to the cerebellum and retina, respectively [192].

Using a microarray analysis, a down-regulation of glutamate transporters in glial cells (EAAT-1 & EAAT-2/GLT-1) was found in post-mortem cerebral cortex of patients who had suffered from MDD [193]. Deficits in these glutamate transporters could impair glutamate reuptake from synaptic cleft by astrocytes, thus prolonging activation of postsynaptic receptors by the endogenous glutamate. Increases in Glu_{ext} could then perturb the balance between excitatory/inhibitory neurotransmitter levels [194]. Moreover, the reduced levels of glial cell number and density in the brain of patients with mood disorders are one of the most consistent pathological findings in psychiatric research, suggesting that a decrease in glial-cell function could help to explain the altered glutamate content observed in several brain regions of these patients [14]. In addition, the blockade of astrocytic glutamate uptake (EAAT2/GLT-1) in rat mPFC followed by an increase in Glu_{ext} and neuronal activity, is sufficient to produce anhedonia, a core symptom of depression [195], indicating a critical involvement of prefrontal glial dysfunction in anhedonia-like outcomes.

In rats receiving a different regimen of UCMS and ketamine treatment (10, 25, and 50 mg/kg once a day for 5 days), the

expression of EAAT2 and EAAT3 was downregulated. In addition, the stress-induced increase in Glu_{ext} in the hippocampus was reversed by the three doses of ketamine, which also upregulated the expression of glutamate transporters EAAT2 and EAAT3 [122]. Similarly, EAAT2 level in this brain region was downregulated in CUS-exposed rats, which is reversed by an acute dose of ketamine (10 mg/kg, i.p.) at 24h post-treatment [196]. These data suggest that the antidepressant-like effect of ketamine would link to the regulation of EAATs expression and the enhancement of glutamate uptake in the hippocampus of depressive-like rats.

Recently, dihydrokainic acid (DHK), a selective inhibitor of EAAT2 (GLT-1) displayed antidepressant-like effects in rats [197]. Micro-infusion of DHK into the infralimbic cortex (IL-PFC) decreased the immobility duration in the FST and the latency to feed in the NSF, and increased Glu_{ext} and $5\text{-}HT_{ext}$ in the IL-PFC. These effects were reproduced by s-AMPA, a synthetic agonist of AMPA-R, and blocked by the pretreatment with para-chloro-phenylalanine (pCPA), a selective and irreversible trytophan hydroxylase inhibitor that blocked 5-HT synthesis. DHK seems to share the same pharmacological properties as ketamine in mice, since an increase in Glu_{ext} and $GABA_{ext}$ in the mPFC together with an increase in swimming duration in the FST were observed during DHK perfusion intra-mPFC (Pham *et al.*, 2018, in preparation) (Figure 2). However, ketamine failed to reduce the function of EAATs in the zero-net-flux experiment, a method of quantitative microdialysis that allows verifying the reuptake function of neurotransmitter transporters [20]. These results indicate that the increase in Glu_{ext} observed at 24h post-injection of ketamine is likely due to an increase in glutamate release in the mPFC. A combination of ketamine with VGLUTs inhibitors would bring interesting results to complete this observation.

On the other hand, riluzole, glutamate PAM, GLT-1, an FDA-approved medication for the treatment of amyotrophic lateral sclerosis, has been shown to potently and rapidly inhibit glutamate release in both *in vitro* and *in vivo* studies [198]. It has both neuroprotective and anticonvulsant properties due to its ability to inhibit glutamate release and enhance both glutamate reuptake and AMPA-R trafficking [199], thus protecting glial cells against glutamate excitotoxicity (Figure 2). Clinical evidences from several, mostly open label and observational studies, have suggested efficacy of riluzole as an 'add-on' in treatment-resistant major depression (see the review of [200]), eventhough riluzole alone was insufficient for clinical response in these patients [201]. However, using riluzole as an 'add-on' to ketamine treatment in TRD patients did not significantly alter the course of antidepressant response to ketamine alone [202].

Together, these data point out that rapid enhancement of glutamate transporters following an inhibition of glutamate release may not contribute to ketamine's therapeutic action. It seems more likely that the blockade of these transporters goes in the same direction as ketamine. The brain regions (e.g., mPFC or hippocampus) plays an important role in defining specific roles of EAATs that interact with ketamine. Meanwhile, VGLUTs should be studied more to have a better understanding of the link between glutamate release and reuptake in the antidepressant-like activities of ketamine. These effects of ketamine involved glutamatergic system in preclinical studies are summarized in Table 1.

4.2. GABA

GABA is the principal neurotransmitter mediating neural inhibition in the brain. GABAergic neurons represent between 20 and 40% of all neurons depending on brain regions and are known to balance and fine-tune excitatory neurotransmission of various neuronal systems, including the monoaminergic projections to the forebrain.

There are two major classes of GABA receptors: ionotropic $GABA_A$ and metabotropic $GABA_B$. $GABA_A$-Rs are known as key control elements of anxiety states based on the potent anxiolytic activity of benzodiazepines, which act as positive allosteric modulators of a major subset of $GABA_A$-Rs [203]. Structurally, $GABA_A$-Rs represent heteropentameric GABA-gated chloride channels, and can be found at synapses, extrasynapses, or at axon terminals.

The $GABA_B$ receptor ($GABA_B$-R) is a heterodimeric, metabotropic, class C of G protein-coupled site, which represents a more complex structure than other G protein-coupled receptors (GPCRs) [204]. This receptor subunit is implicated in affective disorders based on altered anxiety- and depression-related behavioral measures in mice subjected to pharmacological and genetic manipulations of these receptors (see the review by [203]). In the CNS, $GABA_B$-Rs are presynaptic receptors (auto- and heteroreceptors), inhibiting the release of neurotransmitters from nerve terminals, as well as postsynaptic receptors, which are stimulated by GABA release to hyperpolarize pyramidal cells. Activation of $GABA_B$-R causes downstream changes in K^+ and Ca^{2+} channels, mainly through an inhibition of the cAMP synthesis [205].

A systematic classification of cortical GABAergic interneurons was recently published [206]. Three groups of interneurons account for nearly all cortical GABAergic interneurons [207]. The three markers are the Ca^{2+}-binding protein parvalbumin (PV), the neuropeptide somatostatin (SST), and the ionotropic 5-HT receptor $5\text{-}HT_{3A}$. Each group includes several types of interneurons that differ in morphological and electrophysiological properties, thus having different functions in the cortical circuit. The most numerous group is the PV accounting for ≈40% of GABAergic interneurons and includes fast spiking cells. PV interneurons, also called fast-spiking interneurons, regulate the activity of cortical pyramidal neurons and provide the inhibitory postsynaptic potential to these neurons [208]. The other two groups represents ≈30% of GABAergic interneurons [207]. All these interneurons are modulated by 5-HT and acetylcholine via ionotropic receptors [209].

4.2.1. The GABAergic deficit hypothesis of MDD

In patient with MDD and patients with TRD. The GABAergic deficit hypothesis of MDD has been well established as one of the four causes of depression, together with altered monoaminergic neurotransmission, altered HPA axis function

and glutamatergic hypofunction. This hypothesis is reinforced by reports of decreased GABA levels in the plasma [210, 211] and CSF [212] of depressed patients. More recently, brain imaging approaches using ^{1}H-MRS show dramatic reductions of GABA in the PFC region of MDD patients [89, 213, 214]. Interestingly, GABA deficits are more pronounced and severe in TRD patients [215].

The GABAergic deficit hypothesis in depression also includes diminution of GABA neurons quantity. Postmortem studies report a decrease in PFC GABA neurons density in patients with MDD [216, 217]. These cellular changes are consistent with recent neuroimaging studies revealing a reduction in the cortical levels of GABA in depression. These data pointed out that the GABAergic neurons are vulnerable to the pathological factors, thus their dysfunction may be the primary changes for the pathogenesis and prognosis of MDD [203, 218]. By contrast, post-mortem cerebral cortex from MDD patients who died by suicide displayed up-regulation of $GABA_A$-R subunit gene expression, which controls the function of the $GABA_A$-R complex [193]. Together with down-regulation of glutamate transporters found in glia cells of these MDD patients, these data are in line with the tight coupling of the GABA synthesis with glutamate cycling, which involves the isoform of glutamate decarboxylase-67, GAD67. Recently, a proteomic approach in post-mortem cingulate cortex found persistent MDD effects on some proteins such as GAD67 and EAAT3 across current episodes or remission [219]. These persistent effects of the disease seem to involve dysregulation of GABA and glutamate signaling-related proteins.

Together, these heterogeneous data point out that the elucidation of the molecular mechanisms underlying GABAergic neuron involvement is critically important to develop an efficient strategy for the treatment of MDD [220].

In animal models of anxiety/depression. Studies in rodents are in line with these clinical results, i.e., depressive-like phenotypes of $GABA_A$-R mutant mice can be reversed by treatment with conventional antidepressant drugs, as well as with ketamine. Thus, GABAergic deficits may causally contribute to anxiety/depression-like phenotype in mice [221]. In addition, a sub-anesthetic dose of ketamine can exert an antidepressant-like activity and enhance GABAergic synaptic transmission in the mPFC in BALB/cJ mice [20]. A selective inactivation of the γ2 subunit gene of $GABA_A$-Rs in SST-positive GABAergic interneurons increased excitability of SST-positive interneurons, and in turn, increased the frequency of spontaneous inhibitory postsynaptic currents of targeted pyramidal cell [221].

Role of $GABA_A$ and $GABA_B$ receptors in anxiety/depression. Of the two classes of GABA receptors, the $GABA_A$-R is better studied in MDD, and strong evidence for co-morbidity of anxiety and depressive disorders has already been described. Indeed, partial deficit of this receptor in mice induced depression-like behavior. In particular, forebrain-specific $GABA_A$-R γ2 subunit ($\gamma2^{+/-}$) heterozygous mice were characterized as an animal model of anxiety-depression that includes anxious- and depressive-like emotional behaviors in seven different tests [222, 223]. Behavioral deficits in this mouse model involved a reduction in hippocampal neurogenesis and an elevation in corticosterone levels. UCMS of rats results in a marked reduction in the frequency, but unaltered amplitude, of GABAergic inhibitory synaptic currents recorded from PV-positive GABAergic interneurons, suggesting presynaptic deficits in GABA release in this animal model of depression [224]. In addition, the modest reductions in $GABA_A$-Rs function and GABAergic synaptic transmission in $\gamma2^{+/-}$ mice resulted in a decreased expression of NMDA-R and AMPA-R, and impaired glutamatergic synapses in the mPFC and hippocampus [65]. A single sub-anesthetic dose of ketamine fully restored synaptic function of pyramidal cells in $\gamma2^{+/-}$ mice along with antidepressant-like behaviour. In parallel, GABAergic synapses of $\gamma2^{+/-}$ mice were potentiated by ketamine, but only in the mPFC [65]. The antidepressant-like effects of MRK-016, a negative allosteric modulator of $GABA_A$-R containing the α5 subunit are also observed in rodents [225, 226]. These data suggest that antidepressant drug treatments can normalize the causal imbalance between the major excitatory and inhibitory neurotransmission, mainly in the mPFC (see [203]).

$GABA_B$-Rs have also been studied as a target of antidepressant drugs. Indeed, preclinical studies showed that mice lacking functional $GABA_B$-Rs exhibited an antidepressant-like phenotype, but displayed an increased anxiety [227, 228]. In addition, pharmacological blockade of $GABA_B$-Rs resulted in an antidepressant-like response [228-230].

In summary, literature data dealing with the role of GABAergic system in mechanisms involved in antidepressant-like activity point to the activation of $GABA_A$-Rs and a selective blockade of $GABA_B$-Rs in the brain.

Acute *vs* chronic stress. While acute stress enhanced GABAergic synaptic transmission in the hippocampus, chronic stress reduced GABAergic synaptic currents and affect the integrity of hippocampal PV-positive interneurons [231]. In UCMS model of depression in mice, GABA release by presynaptic terminals, and genes and proteins related to GABA synthesis and uptake (i.e., GAD67 and GABA transporters) decreased specifically in the mPFC [220]. Moreover, this latter study showed decreased innervations from GABAergic axons to glutamatergic neurons. The stress-induced incoordination between GABAergic and glutamatergic neurons lead to imbalanced neural networks in the mPFC, which may be the pathological basis of MDD [218, 220].

4.2.2. The GABAergic system as target of ketamine's antidepressant-like action

Ketamine-induced changes of GABA levels. Recent clinical studies have demonstrated that fast antidepressant-like activity of ketamine impacted the GABAergic system. Using ^{1}H-MRS method in patients with MDD, Milak *et al.* (2016) [116] reported a rapid and robust *ex vivo* increases in both mPFC Glx and GABA in response to a single subanesthetic dose of ketamine intravenously. This up to 40% increase in cortical Glx and GABA concentrations may be explained by changes in brain glucose utilization**.** Virtually all the glucose entering into the brain is metabolized through glutamate because one molecule of glucose gives rise to two molecules of acetyl-

CoA, which enter the tricarboxylic acid cycle to become α-ketoglutarate and then glutamate. In GABAergic neurons, this same process feeds GABA synthesis because glutamate is the precursor of GABA. Thus, the robust correlation between increases in Glx and GABA concentrations in this study supports the hypothesis that glucose utilization drives the glutamate/GABA neurotransmitter balance. These effects of ketamine support the GABAergic deficit hypothesis in depression [203]. Clinical reports also showed lower CSF, blood or *in vivo* brain imaging measuring GABA levels in MDD patients, and monoaminergic antidepressant drugs reversed these effects. Indeed, depressive patients had lower serum GABA levels compared with healthy individuals, and one ECT increased baseline GABA levels [232]. Using ^{1}H-MRS in patients with MDD, the decreased cortical GABA concentration was reversed either after treatment with repetitive transcranial magnetic stimulation [233], or following SSRI treatment and ECT [234-236].

Similarly in preclinical studies, microinjection of bicuculline (a $GABA_A$-R antagonist) increased local cerebral glucose utilization in rats, while muscimol (a $GABA_A$-R agonist) did the opposite [237]. This pharmacological study suggests that the brain GABAergic system could limit ketamine-mediated glutamate release and reduce excessive spread of glutamatergic excitation. To our knowledge, increases in GABA levels in rodents after ketamine administration has also been reported: using *ex vivo* ^{1}H-MRS, Chowdhury *et al.* (2017) [118] reported a rapid and transient increase in GABA concentration in post-mortem mPFC homogenates after a single i.p. ketamine injection in rats. Using a 4.7-T magnetic resonance system in anesthetized rats, both doses of ketamine (10 and 25 mg/kg) increased BOLD image contrast in the mPFC and hippocampus, but not in the ventral pallidum [238]. Using *in vivo* microdialysis in freely moving mice, ketamine also increased extracellular GABA levels ($GABA_{ext}$) in the mPFC at 24h post-administration [20].

Taken together, these results suggest that ketamine produced a dose-dependent GABA release, thus could correct the deficit in the GABAergic system found in MDD, most effectively in the mPFC, a region highly implicated in MDD, underlining an important role of GABAergic interneurons in this brain region in the fast/sustained antidepressant activity of ketamine.

Conversely, CUS model in rats shown an increase in GABA levels *ex vivo* in post-mortem brain homogenates, measured with ^{1}H-MRS, and a subanesthetic dose of ketamine (40 mg/kg, i.p.) normalized this effect [239]. This emphasizes the biphasic effect of different doses of ketamine on the GABAergic system, depending on different techniques applied and brain regions studied in rodents.

Ketamine effects in combination with GABA modulators. More studies are digging into the role of $GABA_A$ and $GABA_B$ receptors. Recently, a combination of low doses of ketamine (0.1 mg/kg, i.p.) and muscimol (0.1 mg/kg, i.p.) was sufficient to induce an antidepressant-like effect in the TST, suggesting that ketamine would activate $GABA_A$-R to induce its antidepressant-like activity [240]. Similarly, sub-anesthetic (15 mg/kg, i.p.) dose of ketamine would possess a $GABA_A$-R agonistic property in mice as it antagonized the seizure induced by bicuculline (a $GABA_A$-R antagonist) [241]. In rat cortical neurons in culture, muscimol opened GABA-Cl(-)-channel, permitted inward Cl^- fluxes and increased basal glutamate release by potentiating intracellular Ca^{2+}, an effect reversed by bicuculline [242], suggesting a role of $GABA_A$-R agonism in inducing neuronal excitation. Similar to muscimol and baclofen (a $GABA_B$-R agonist), ketamine as well reduced bicuculline influence on spontaneous proximal discharges on rat cortical slices [243], indicating that ketamine also would possess a $GABA_B$-R agonistic property. Activation of $GABA_A$-R in the rat mPFC has been recently demonstrated to produce an anxiolytic-like response in the elevated plus maze test (EPM), while antagonism of this receptor by bicuculline produced an anxiogenic-like behavior [244]. Indeed, bicuculline-induced convulsant symptoms in rats at 7.5 mg/kg was prevented by pre-treatment with ketamine (40 mg/kg) [245]. It is important to notice that, if a receptor antagonist induces a cellular response when administered alone (as bicuculline 8 mg/kg i.p.: [241]), it suggests that $GABA_A$-Rs are tonically activated by endogenous GABA levels.

Ketamine reduced NMDA-R-mediated responses and enhanced $GABA_A$-R-mediated responses on rat hippocampal slices, indicating specific actions on inhibitory synaptic events and changes in the balance between glutamate (excitatory) and GABA (inhibitory) synaptic transmission *in vitro* [246]. Thus, agonism of $GABA_A$-R, even indirectly, could possibly contribute to ketamine mechanism of antidepressant-like activity, as suggested by increases in c-Fos immunoreactivity in the rat hippocampus, a non specific marker of neuronal activation [247]. Combining $GABA_A$ or $GABA_B$ receptors pharmacological activation with ketamine also produced intriguing results, e.g., muscimol and baclofen can cause impaired memory acquisition and aggravate the negative effects of ketamine [32, 248].

Ketamine may have different influences on GABAergic system depending on the brain regions. By increasing γ power in the rat hippocampus, low dose of ketamine (3 mg/kg, s.c.) increased local pyramidal cell firing possibly by disinhibition of local inhibitory interneuron, which are the causes of psychosis-relevant behaviors [249]. This effect is blocked effectively by local injection of muscimol into this region, pointing out that agonism of $GABA_A$-R in brain regions other than mPFC is conversely necessary to limit ketamine's psychosis effect.

Role of PV interneurons in ketamine's action. Ketamine as an NMDA-R antagonist, is attracted predominately to this target located on GABAergic interneurons [180]. PV interneurons receive the largest glutamatergic input among all GABA-releasing neurons in the cortex. This class of interneurons is highly sensitive to NMDA-R antagonists and enrich of GluN2A subunit [134, 250], which could be the primary target of ketamine. However, several selective subunit NMDA-R antagonists did not demonstrate efficacy in TRD [251]. Alterations of PV-positive cells by ketamine have been well established in schizophrenia [252-254], but the role of PV in ketamine-induced antidepressant-like activity needs to be further investigated. Recently, Wang *et al.* (2014) [255] reported that ketamine down-regulated the activity of PV interneurons by reducing the levels of PV and GAD67, thus down-regulating the GABA levels and up-regulating glutamate levels in the rat

hippocampus and PFC, suggesting that PV interneurons may be involved in ketamine's antidepressant-like activity. Moreover, Zhou *et al.* (2015) [256] confirmed that an acute dose ketamine (10 and 30 mg/kg) displayed an antidepressant-

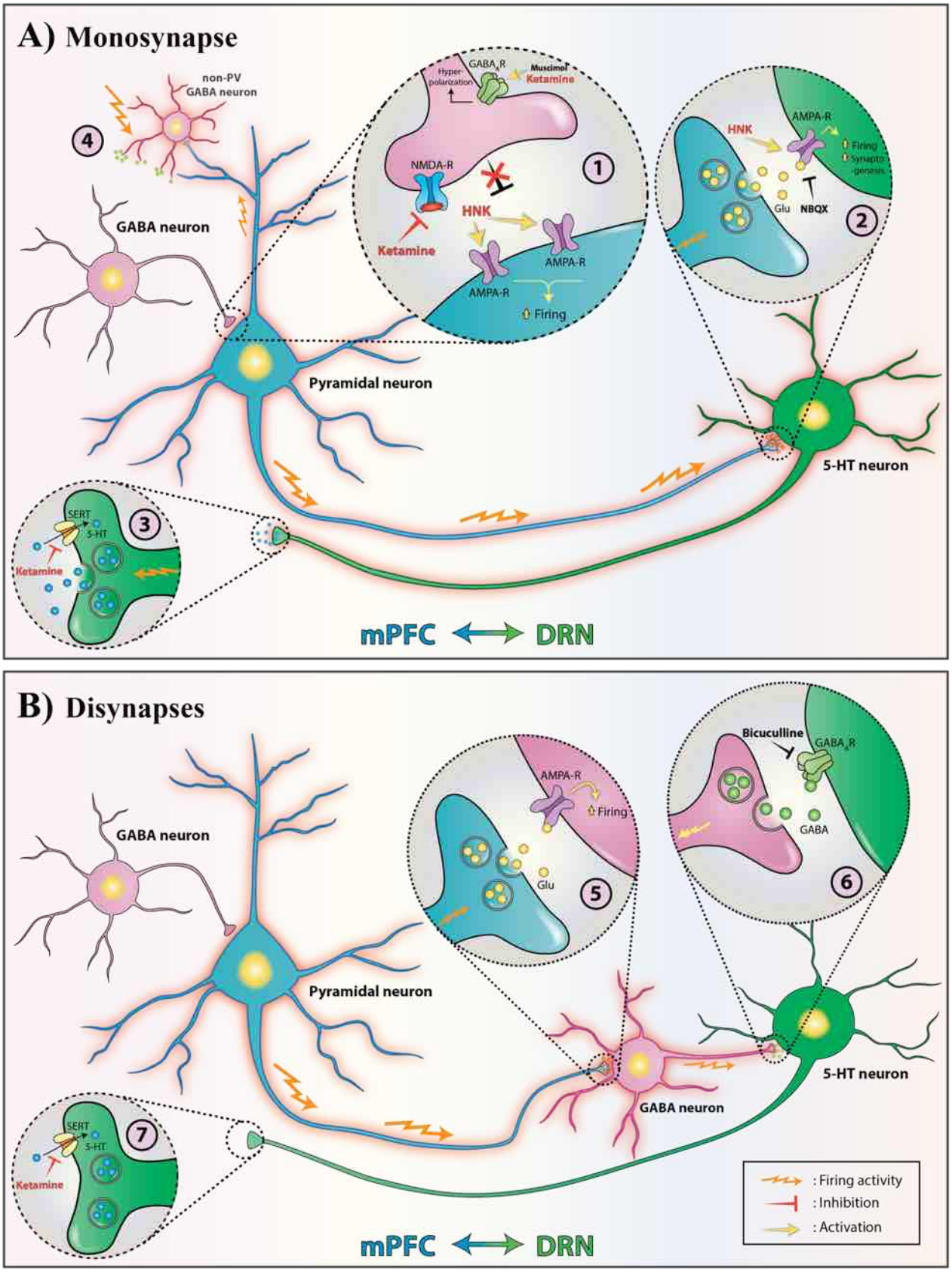

Figure 3. Hypothesis of ketamine and its active metabolite (2*R*,6*R*)-hyrdoxynorketamine (HNK) antidepressant mechanisms based on the direct (monosynapse) and indirect (disynapses via GABA neuron) pathways of medial prefrontal cortex – dorsal raphe nucleus (mPFC-DRN) circuit, with the involvement of glutamatergic, GABAergic and serotonergic neurotransmissions.
A) Monosynaptic pathway: mPFC pyramidal cells are controlled by GABA interneurons (mostly parvalbumin (PV)-positive ones) directly on the cell bodies. These glutamatergic neurons have projections toward 5-HT neurons located in the DRN, while their dendrites synapse with other non-PV-positive GABA neurons in the mPFC. **(1)** Ketamine blocks selectively NMDA receptor (NMDA-R) located on GABA neurons controlling the action potential of pyramidal cells, leading to a disinhibition of these neurons and subsequently facilitating their action potential – firing activity. This induces a burst of glutamate release by presynaptic neurons to activate postsynaptic receptors, such as AMPA receptor (AMPA-R), to initiate further neurotransmission enhancement. Ketamine also possesses $GABA_A$ receptor ($GABA_AR$) agonistic quality so it could activate this presynaptic receptor on GABA neurons, like $GABA_AR$ agonist muscimol, to be further hyperpolarized. This disinhibition induced by ketamine is considered indirect since HNK is demonstrated to active directly AMPA-R to induce neuronal firing and glutamate burst. **(2)** The excitatory signal is transferred to the DRN, where it synapses with 5-HT cell bodies. This stimulates postsynaptic AMPA-R on 5-HT neurons and facilitates the synaptogenesis as well as the release of 5-HT in the terminals (mPFC). This hypothesis is reinforced by a loss of ketamine antidepressant effects in rodent's behaviors as well as on 5-HT levels by intra-DRN injection of AMPA-R antagonist NBQX. **(3)** 5-HT extracellular level is increased, possibly due to 5-HT release or an indirect blockade of serotonin transporters (SERT) by ketamine. **(4)** mPFC pyramidal cells could also transfer excitatory signals locally to non-PV-positive GABA neurons to induce a GABA burst, as observed in many clinical and preclinical studies.
B) Disynaptic pathway: mPFC pyramidal cells is also known to synapse onto GABA-rich area of the DRN. Thus, it could be GABA interneurons that control 5-HT neurons in this later region. **(5)** After being stimulated by the ketamine-induced disinhibition (or HNK-induced activation), pyramidal cells send the excitatory signals to DRN GABA neurons, which induces a local GABA burst. **(6)** The GABA burst subsequently activates postsynaptic $GABA_AR$ located on 5-HT neurons to inhibit their neuronal activity. This could explain for an unchanged or even decrease of DRN 5-HT neuronal firing after ketamine injection. An intra-DRN injection of bicuculline, $GABA_AR$ antagonist, could block this inhibition and facilitate the neuronal response [299]. **(7)** 5-HT release in the mPFC might not be accelerate, but ketamine could still weaken the serotonin reuptake by SERT indirectly to maintain the 5-HT level.

like activity in the FST at 30 min and 2 hr post-treatment and reduced PV and GAD67 tissue levels at 30 min in the mPFC of 'naïve', non stressed rats. It also increased glutamate levels and decreased GABA levels in the mPFC. In addition, only the higher dose of ketamine (30 mg/kg) at repeated administration (5 days) reduced PV and GAD67 cortical tissue levels at 2 hr post-treatment, but this regime elicited stereotyped behaviours and hyperlocomotion, and a longer duration of PV and GAD67 loss, higher glutamate levels and lower GABA levels in the mPFC, which may mediate a disinhibition of glutamatergic neurotransmission in 'naïve' rat PFC. In support of these findings, stress induced by UCMS in mice increased mPFC PV expression, which could originate from activation of glutamatergic circuit from amygdala onto frontal PV neurons [109]. Indeed, glutamatergic afferents from the amygdala to the PFC a drive robust inhibition through monosynaptic activation of PV interneurons [257]. Unfortunately, Shepard *et al.* (2017) [109] did not use any antidepressant drugs, i.e., ketamine or SSRI, to reverse these observed alterations of PV in UCMS mice, which could bring interesting insights to the subject. Intriguingly, Yang *et al.* (2015) [258] has reported that (*S*)-ketamine, but not (*R*)-ketamine, induced PV-positive cells loss in a social defeat stress model of mice, which displayed a lack of antidepressant-like effects compared to the (*R*)- enantiomer.

Remarkably, a study used genetically modified C57Bl/6 mice lacking NMDA-R specifically in PV cells to probe directly the connection between NMDA-R-dependent function of PV neurons and depression-like behaviour. The mutation itself did not provoke a depression-like behavior, but did attenuate ketamine antidepressant-like effect in the FST [126]. This study used constitutive adult knockout mice, thus compensatory events may have occurred during the development. However, these results highlight that NMDA-R located on PV interneurons might play a primary role in the mechanism of action of ketamine. Interestingly, the same decrease in PV and GAD67 was observed with the GluN2A-, but not the GluN2B-subunit selective antagonist in cortical PV interneuron in culture [259], suggesting the activity of GluN2A-containing NMDA-Rs plays a pivotal role in the maintenance of the GABAergic function of PV interneurons and subsidizes ketamine actions. On the other hand, degradation of PV interneurons before ketamine administration (10 mg/kg, i.p.) even diminished its long-term antidepressant-like activity in rat [260], indicating that ketamine requires these interneurons to have its actions. Taken together, these data suggest that upregulation of PV interneurons are implicated in anxiety/depression-like symptoms and are regulated by ketamine in rodents. Even though the alteration of PV precisely in depression still remains unclear, these evidences indicate that loss of PV interneurons contributes to the antidepressant-like activity of ketamine. Meanwhile, there has been little to no information about how other classes of interneurons (SST and $5\text{-}HT_{3A}$) would be involved in ketamine's action. Their locations as well as their functions in controlling neuronal activities are distinct from that of PV interneurons. More studies targetting individual class of interneurons could bring more insights into how ketamine functions as a fast-acting antidepressant drug as well as how to improve its safety profile in regard of psychotomimetic and addictive effects. It also underlines the key role of the balance between glutamate/GABA systems in its mechanism of action.

Ketamine increases GABA synaptic transmission. NMDA-R blockade is known to acutely increase spontaneous γ oscillations activity [261], including ketamine [262-264]. Computational modeling supports the hypothesis that these abnormal oscillations result directly from ketamine-induced reducing NMDA-R-mediated inputs to fast-spiking PV-positive GABAergic interneurons in TRD [115], which leads to enhanced cortical excitability. In this study, the NMDA-R antagonists-

induced increase in spontaneous γ activity was limited to the period just after drug intake, when psychotomimetic symptoms were most prominent. Thus, ketamine-related increases in spontaneous γ cortical activity might be more relevant to the acute, dissociative than the antidepressant effects. Moreover, NMDA-R activation exerts a control on inhibitory GABAergic neurotransmission, e.g., in CA1 pyramidal neurons: NMDA increased firing of GABAergic interneurons, thereby leading to GABA release from GABAergic axons in mouse hippocampal slices [265]. In addition, the NMDA-R antagonist, MK-801 suppressed NMDA-induced increase in spontaneous inhibitory post-synaptic currents (IPSC). Thus, ketamine may have a similar mechanism of action.

Taken together, these studies confirm the implication of the GABAergic system in ketamine induced fast-antidepressant-like activity. There is a consensus in the literature for a decrease in the inhibitory role of cortical PV interneurons elicited by ketamine. It is now clear that ketamine is efficient in enhancing glutamatergic transmission, but its influence on GABAergic transmission still diverges between non-stress and stress models in rodents. These effects of ketamine involved GABAergic system in preclinical studies are summarized in Table 2.

4.3. Serotonin (5-HT)

This part of the review will focus on the knowledge that links ketamine to the brain serotonergic system, but not on molecular proteins/events that specifically occurred in 5-HT neurons such as tryptophan hydroxylase 2 - TPH2, Pet1, DRN signalling cascade behind 5-HT receptors, and so on…, because there are many recent publications detailing these points.

Serotonergic neurons of the mammalian brain comprise the most extensive and complex neurochemical network in the CNS after that of glutamate, which makes up the basic wiring of the brain [266, 267]. It has been estimated that the human brain contains about 250 000 5-HT neurons of a total of hundred billion total neurons [268]. CNS 5-HT modulates, in particular, stress, food intake, sleep-wakefulness, pain control, and at the cellular and molecular levels, neurogenesis, apoptosis, dendritic and spine refinement, cell migration, and synaptic plasticity [269], therefore implicated in the aetiology of many mental illnesses, especially MDD [270]. Indeed, all effective antidepressants share the ability to enhance 5-HT transmission, which appears to be necessary for their antidepressant effect [271]. With the recent knowledge of the role of glutamatergic and GABAergic drugs in anxiety/depression, the unique implication of 5-HT in depression now seems impossible [270]. There are various 5-HT receptor types, with the three main families: 5-HT_1, 5-HT_2 and 5-HT_3, and four smaller ones: 5-HT_4, 5-HT_5, 5-HT_6 and 5-HT_7 [272]. These subtypes have become subjects to many studies in depression and other psychotic disorders, in which the use of pharmacological (i.e., agonists and antagonists) and genetic (i.e. mutant models) tools are of favors. All these subtypes are GPCRs (except 5-HT_3, which belongs to the ionotropic receptor family) and could be found both pre- and post-synaptically in the CNS. Interestingly, in the hippocampus and mPFC, most 5-HT receptor subtypes are found on both pyramidal cells and interneurons [266, 273, 274]. For example, 5-HT_{1A} receptors direct the orientation of plasticity in layer V pyramidal neurons of the mouse mPFC [275]. Thus, an inter-communication between glutamatergic and GABAergic systems must be involved in modulating serotonergic transmission to induce antidepressant responses. In addition, to understand how discrete raphe cells subpopulations account for the heterogeneous activities of the midbrain serotonergic system, recent findings defined anatomical and physiological identities of 5-HT raphe neurons (e.g., dorsal and median raphe 5-HT neurons project to the medial mPFC, amygdala and dorsal hippocampus). 5-HT neurons projecting to these brain regions form largely non-overlapping populations and have characteristic excitability and membrane properties [276].

Serotonergic system dysfunction in depression. Abnormalities in serotonergic function have been believed to be a common factor in several related mental illnesses since the 1950s [277]. A deficit of the serotonergic system is defined as a factor of increasing vulnerability in MDD. Indeed, clinical studies found reduced CSF and plasma concentrations of the 5-HT major metabolite – 5-hydroxyindoleacetic acid (5-HIAA) – in drug-free depressed patients that was associated with higher suicidal attempts [278-280], suggesting an altered 5-HT turnover rate in MDD. Remarkably, treatment with pCPA, a tryptophan hydroxylase inhibitor, that depleted central 5-HT system, caused a rapid relapse in depressed patients who had responded to the antidepressant drug medication [281]. The strongest evidence for the role of the serotonergic system in MDD is the widespread prescription of antidepressant drugs that target the serotonin transporter (SERT) – namely, the selective serotonin reuptake inhibitors (SSRIs) and the dual serotonin and norepinephrine reuptake inhibitors (SNRIs) – which account for more than 90% of the global antidepressant drugs on the market [266]. The concentration of synaptic 5-HT is controlled by its reuptake into the pre-synaptic terminal by SERT, and by 5-HT_{1A} and 5-HT_{1B} autoreceptors [282]. Therefore drugs SSRIs have been successfully used for the treatment of depression [279]. Reduced post-mortem SERT availability in depressed patients reinforced these findings [283]. However, a long delay onset of action (from 4 to 6 weeks) and a high rate of non-response/resistance have limited the efficacy of these classical antidepressant drugs.

At clinically relevant doses, SSRIs increase extracellular 5-HT levels (5-HT_{ext}) in the midbrain raphe nuclei, thereby activating inhibitory somatodendritic 5-HT_{1A} autoreceptors in pre-clinical studies. Consequently, the firing activity of 5-HT neurons is reduced and the enhancement of 5-HT_{ext} in forebrain is dampened. Blocking this negative feedback control by using 5-HT_{1A} autoreceptor antagonists (such as WAY 100635) permits SSRIs to produce a marked increase in 5-HT_{ext} in the forebrain [284]. These results provided a neurobiological basis for the potentiation of certain antidepressant drugs by pindolol, a 5-HT_{1A}/beta-adrenoceptor antagonist, in MDD. The treatment of these patients using an SSRI and pindolol, markedly reduced the latency of the antidepressant response in previously untreated patients and induced a rapid improvement in TRD [120, 285-291].

Nevertheless, no clear image has been emerged for 5-HT receptors alterations (i.e., 5-HT_1 and 5-HT_2 receptors) as post-mortem reports in depressed patients (suicide victims with/without psychiatric diagnoses) were heterogeneous (reviewed by [281, 292]). The appearance of new drugs with rapid and effective antidepressant activities that target prominently the glutamatergic/GABAergic system leaves the role of 5-HT in depression a matter to debate. As most of commercialized antidepressant drugs share the ability to enhance brain 5-HT neurotransmission, understanding the interaction between ketamine and the serotonergic system will bring more insights into their molecular and cellular mechanism of action.

4.3.1. Ketamine alters 5-HT levels

The most used technique to access the level of 5-HT in rodents brains is *in vivo* microdialysis in rodents. By far, the mPFC has been the most brain region studied for ketamine's influence on 5-HT neurotransmission (e.g., infralimbic *vs* pre-limbic cortex in rats [197]). At sub-anesthetic doses, ketamine increased mPFC 5-HT_{ext} in rats. Indeed, using systemic (25 mg/kg, s.c.) and intra-mPFC (3 mM) routes of administration, an increase in 5-HT_{ext} was described in the mPFC [293]. Interestingly, bilateral, but not monolateral, local injection of ketamine intra-mPFC altered 5-HT_{ext} levels, suggesting that a bilateral activation of the mPFC is required to induce an effect of ketamine on 5-HT efflux. Moreover, only systemic, but not local injection of ketamine, provoked hyperlocomotion and stereotypies, thus indicating a role of other brain regions in these behavioural effects. Several teams confirmed that a dose-dependent effect of ketamine occurred on mPFC 5-HT_{ext} in naïve, non stressed rats [30, 294, 295], except in rodents subjected to cortical depletion of 5-HT levels by pCPA (in rats: [296]; in mice: [21]) or following a combination of 5-HT depletion and a restraint stress [296]. Acute low doses of ketamine (3 and 10 mg/kg, i.p.) also increased 5-HT levels in *ex vivo* brain tissue homogenates from the PFC, hippocampus and striatum, which correlated with an increase in the number of head movements in the head-twitch-response (a serotonin-dependent test) in rats [297].

These observations are consistent with a role for cortical 5-HT in mediating neurochemical effects of ketamine as measured 1 or 24h prior to test. This time point was chosen to avoid the acute schizophrenia-like effects of ketamine. However, it underlines the importance of the experimental models used in these studies. In addition, the interaction between ketamine and the serotonergic system is mostly described after an acute ketamine injection. We have therefore recently reported changes in 5-HT_{ext} at 24h post-injection of ketamine (10 mg/kg, i.p. [20, 21]). At this time point, when compared to fluoxetine (an SSRI), we found a significant increase in 5-HT_{ext} that correlated positively with increases in the swimming duration (i.e., a serotonin-dependent parameter) in male BALB/cJ mice. Our data brought up interesting evidences of the link between neurochemical and behavioral changes that could contribute to the overall image of ketamine mechanism of antidepressant-like actions. The range of doses is also very important in ketamine's actions, since the higher doses were developed as a model of schizophrenia (as already mentioned above in "quick view of effects of an acute ketamine administration" section [31, 256].

4.3.2. Implication of the mPFC-DRN circuit

Recently, two optogenetic studies brought very interesting elements to the mechanism of ketamine-induced antidepressant-like activity, both performed in naïve, unstressed rats [298, 299]. In addition, some interesting information help to understand the role of the mPFC, e.g., in social defeated mice expressing a strong depressive-like phenotype, optogenetic stimulation of mixed excitatory and inhibitory neurones in the mPFC induced potent antidepressant-like effects [300].

Using an optogenetic approach to analyse a brain circuit, Warden *et al*. (2012) were the first to demonstrate that the selective stimulation of mPFC cells projections to the DRN induced potent antidepressant-like effects in rats [301]. Given that the mPFC is one of the few forebrain areas projecting densely to the DRN, where the majority of 5-HT cell bodies are located, the circuit mPFC-DRN has been largely studied to confirm its implication in depression [302-304]. However, these glutamatergic inputs from the mPFC to DRN serotonergic neurons could be direct monosynaptic or indirect through DRN GABAergic interneurons, thus leading to different outcomes of 5-HT neurotransmission. Indeed, using electron microscopy, Varga *et al.* (2001) found that the mPFC projection to the DRN preferentially targets local circuit GABAergic neurons [305], which are well known to synapse with 5-HT neurons [306, 307].

Microcircuits implicated in top-down control of 5-HT neurons in the DRN by excitatory inputs from the mPFC have been then identified. Thus, a combination of cFos mapping (i.e., a marker of neuronal activation) with *in vivo* optogenetic stimulation of mPFC terminals expressing channelrhodopsine (ChR2) was used to determine DRN neuronal activation. It was for the first time demonstrated that excitatory mPFC axons project to GABA-rich areas of the DRN, and drive the synaptic activity of these DRN GABA neurons via an AMPA receptor-dependent mechanism [308]. These data agree with a study demonstrating that the control of dorsal raphe serotonergic neurons by the mPFC involves 5-HT_{1A} and $GABA_A$-Rs [309]. It is also consistent with mPFC projections to the DRN preferentially target local-circuit GABAergic neurons [307, 310, 311]. In addition, identification of monosynaptic glutamatergic inputs from the PFC to serotonergic neurons in the DRN was reported [312], indicating that direct mPFC-DRN pathway that exerts excitatory control over serotonergic neurons in the DRN also exists.

Up to now, there has been two major studies using optogenetic to investigate the pathways involved in ketamine actions: the mPFC by [298] and the circuit mPFC-vHipp by [299]. To identify the precise cellular mechanisms underlying ketamine rapid and sustained antidepressant-like activity, Fuchikami *et al.* (2015) [298] used an optogenetic stimulation of IL-PFC, a sub-region of the mPFC involved in emotional processes in rats. Neuronal inactivation of the IL-PFC by muscimol completely blocked the antidepressant and anxiolytic effects of systemic ketamine (10 mg/kg). By contrast, optogenetic

stimulation of glutamatergic neurons in the IL-PFC produced rapid and sustained antidepressant-like effects, which were associated with increased number and function of spine synapses of layer V pyramidal neurons (as in [26]). Thus, local intra-IL-PFC ketamine infusions or optogenetic stimulation of IL-PFC produced behavioral and synaptic responses similar to the effects of systemic ketamine administration. These *in vivo* optogenetic results support a role for cortical neuronal activity in the mPFC in the antidepressant-like activity of ketamine. The authors also pointed out that (i)-several specific brain circuits could contribute to the cortical optogenetic stimulation because connections between of IL-PFC and amygdala, DRN and NAcc were described [313]; (ii)-depending on the neuronal cicuit, optogenetic stimulation of mPFC terminal fields can produce either antidepressant (DRN) or prodepressive responses [301]. This was the first study using optogenetics to investigate the mechanism of ketamine's actions so there are still some limits: only one virus (ChR2 for activation, but a pharmacological tool, muscimol, to block the antidepressant-like effects of ketamine) was used in this study, in non-stressed animals, thus no brain circuit was identified. In addition, ketamine was used as an anesthetic for the surgery, which could compromise the results.

The second study by Carreno *et al.* (2016) [299] was published one year later and brought new insights into ketamine action. Using two different viruses (ChR2 for activation and halorhodopsine for inhibition) to activate and inactivate the neuronal circuit mPFC-vHipp in rats, they confirmed that this circuit is essential for ketamine's antidepressant-like activity in the FST. The vHipp is connected to the limbic system with afferents to the mPFC and NAcc in rats [314]. Furthermore, the hippocampus is implicated in the effects of stress, depression and antidepressant drug response [313]. In this optogenetic study, the FST was performed in rats 30 min or one week following a single administration of ketamine (10 mg/kg, i.p.). Both optogenetic and pharmacogenetic specific activation of the vHipp-mPFC pathway using Designer Receptors Exclusively Activated by Designer Drugs, DREADD) mimicked the antidepressant-like response to ketamine (10 mg/kg, i.p.). Interestingly, (i)- this activation could only took place when the feedback response in the DRN was blocked (by bicuculline, to block the control of GABA interneurons on 5-HT neurons), thus underlining an involvement of the disynaptic pathway, via GABA interneurons, in the mPFC-DRN circuit that connected glutamatergic, GABAergic and serotonergic neurons together. However, it would have been nice to use several behavioral tests, instead of one (the FST) to verify this "DRN feedback inhibition" hypothesis; (ii)- vHipp-mPFC circuit is specific because its activation of the vHipp/NAcc circuit did not reproduce this response. Furthermore, optogenetic inactivation of the vHipp/mPFC pathway (using halorhodopsine virus) at the time of FST reversed ketamine's antidepressant-like response. In this experiment, only one ketamine dose was administered, and the test was performed immediately one week after. Thus, these data demonstrate that activity within the vHipp-mPFC pathway and early transient activation of vHipp TrkB receptors are essential for the sustained antidepressant-like response to ketamine. Another point raised by these authors is that activity-dependent BDNF signaling in the vHipp initiated a unique cellular cascade leading to plasticity, which had occurred one week following ketamine administration.

To know whether 5-HT synthesis is involved in the antidepressant-like effects of ketamine, a pre-treatment with pCPA was performed. Ketamine response in the FST was blocked by pCPA at 24h post-treatment thus indicating a role of serotonergic system in the antidepressant mechanism of ketamine [21, 296]. Meanwhile, paroxetine, a classic antidepressant drug that acts mainly by blocking SERT, failed to induce a sustained effect similar to ketamine, suggesting that the role of the serotonergic system is different between these two antidepressant drugs [42]. Interestingly, micro-injection of ketamine intra-mPFC also lost its antidepressant-like effects in the FST after PCPA pretreatment, emphasizing a particular modulation of mPFC in ketamine action. Furthermore, in this latter study, systemic administration of ketamine also increased c-Fos immunoreactivity in DRN 5-HT neurons, which were blocked by microinjection of NBQX into the mPFC. Collectively, these findings suggest that activation of a subset of DRN 5-HT neurons modulated by mPFC projections may have an important role in the antidepressant effects of ketamine. Thus, the serotonergic systems selectively modulated by the mPFC-DRN projections may be involved in the antidepressant effects. This hypothesis was underpinned by the finding that deep brain stimulation (DBS) of the mPFC exerted an antidepressant effect in animal models of depression, which was abolished by 5-HT depletion [315]. These studies demonstrated the functional complexity of mPFC circuitry in depression and antidepressant drug responses. Many ketamine studies used unstressed animals. More studies using chronic stress or performed in rodent models of anxiety/depression (social defeat, CORT model, or BALB/cJ mice) before ketamine administration are needed.

Activation of DRN neurons itself does not induce antidepressant effects. Contrary to intra-mPFC injection of ketamine, its local intra-DRN injection had no effect on 5-HT release [295]. By contrast, acute application of high doses of ketamine (100 μM) on raphe slices decreased the 5-HT_{ext} [295] and reduced basal 5-HT neuronal firing rate [316]. In rat DRN slices, application of same dose of ketamine (100 μM) increased both 5-HT release (up to 80%) and reuptake (up to 200%) [317]. According to this study, the stimulation of 5-HT reuptake, which overcame the increase in electrical stimulation inducing 5-HT efflux, could explain the decrease in 5-HT levels. We have also reported a similar decrease in 5-HT neuronal activity using electrophysiology in anesthesized mice, 24h after a 10 mg/kg dose of ketamine, i.p. [21]. At this dose, no alteration of 5-HT neurons firing activity in rat DRN was observed, whereas significant changes were found on firing activity of noradrenaline, dopamine neurons [178]. Ketamine modulation of 5-HT neuronal firing occurred via AMPA and NMDA receptors, since applications of AMPA and NMDA (10-100 μM) in rat brain slices dose-dependently increased 5-HT firing activity that was enhanced by $GABA_A$-R antagonist bicuculline, suggesting that both AMPA and NMDA evoked local release of GABA [318]. Interestingly, in this study, only the direct effect of NMDA on 5-HT neurons was blocked by AMPA-R antagonist DNQX, indicating that NMDA evoked local release of glutamate, which subsequently activated

AMPA-R located on 5-HT neurons. The indirect implication of NMDA in 5-HT neuronal firing is intriguing, since ketamine is an NMDA-R antagonist. Further studies are needed to elucidating this mechanism of action.

Remarkably, subsequent preclinical studies using microdialysis *in vivo* have demonstrated that NMDA has a dose-dependent effect that varied according to the brain region. Infusion of low doses of NMDA (25 μM) into the rat raphe nucleus decreased 5-HT_{ext} locally and increased 5-HT_{ext} in the frontal cortex. Conversely, infusion of 100 μM NMDA into the rat raphe increased local 5-HT_{ext} and decreased cortical release of 5-HT [319-321]. Interestingly, while the 5-HT_{1A} receptor antagonist WAY100635 had no influence on NMDA (100 μM)-induced changes in 5-HT_{ext} in these experiments, an NMDA-R antagonist reversed the increase and decrease in 5-HT_{ext} in the DRN and PFC, respectively [320]. This observation is similar to the data we obtained with ketamine [21], underlining complex interactions between NMDA-R, AMPA-R and $GABA_A$-R to modulate 5-HT neurotransmission, as well as a profound involvement of mPFC-DRN pathway in these alterations.

4.3.3. Ketamine blocks the serotonin transporter (SERT)

The intriguing increases in 5-HT levels induced by ketamine raise the question whether this is due to a blockade of the selective 5-HT transporter (SERT), similar to classical SSRIs antidepressant drugs. Ketamine competitively decreased [3H]-paroxetine binding from rat brains synaptosomes at Ki = 18.8 μM [322], indicating that ketamine can bind to SERT. In accordance with these data, ketamine inhibited up to 63 % of 5-HT uptake at 10^{-3} M (EC50 = 125 μM in HEK-hSERT cells), which was significantly reduced by desipramine and fluoxetine. A downregulation of SERT binding was demonstrated in a positron emission tomography (PET) study in non-human primates following an acute ketamine i.v. injection [323], indicating an interaction between SERT and ketamine that might be involved in its antidepressant action. However, the affinity of ketamine for SERT occurred at a much higher dose than treatment-relevant doses [324, 325], indicating an indirect interaction with SERT that could be modulated by other factors.

4.3.4. Ketamine interacts with serotonergic receptors

Serotonin mediates a wide variety of physiological functions by activating multiple receptors, and abnormalities of them have been implicated in many psychiatric disorders including anxiety, depression (see [326] for a review). All the 14 serotonin receptor subtypes have not been evaluated in pre-clinical ketamine studies. We are going to focus this last part of the review mainly on some 5-HT receptor types.

Ketamine and 5-HT_1 receptor. At least five 5-HT_1 receptor subtypes have been identified: 5-HT_{1A}, 5-HT_{1B}, 5-HT_{1D}, 5-HT_{1E} and 5-HT_{1F}. All are seven transmembrane GPCR (via Gi or Go) and negatively coupled to adenylyl cyclase (see the official classification of receptors from the International Union of Basic and Clinical Pharmacology (IUPHAR) at http://www.guidetopharmacology.org). By far, there have been some pre-clinical evidences about the interaction between ketamine and two receptor subtypes: 5-HT_{1A} and 5-HT_{1B}. Each subtype divided into auto-receptors (presynaptic) and heteroreceptors (postsynaptic). The inhibitory 5-HT_{1A} receptor exists in two separated populations with distinct effects on serotonergic signalling: (i)- 5-HT_{1A} autoreceptor is localized on the soma and dendrites of serotonergic neurons in the DRN and its activation by endogenous 5-HT or receptor agonists limit 5-HT release at 5-HT nerve terminals throughout the brain and (ii)- 5-HT_{1A} heteroreceptors located on the membrane of non serotonergic neurons and mediating an inhibitory response [120].

The gap in timing between the immediate blockade of SERT *in vitro* [327], increases in the synaptic 5-HT levels in the brain mediated by SSRIs [328-330] and the long delay to observe an antidepressant activity *in vivo* in clinical studies [331] and in animal models [332] has not been completely explained yet. It is well known that the activation of 5-$HT_{1A/1B}$ autoreceptors limits the effects of SSRIs at serotonergic nerve terminals [289]. Thus, the functional desensitization of the presynaptic DRN 5-HT_{1A} receptor sub-type induced by a chronic SSRI treatment partially explains this phenomenon [286, 288]. Somatodendritic 5-HT_{1A} autoreceptors activated by SSRI-induced increases in endogenous 5-HT levels in raphe nuclei that limits 5-HT release at nerve endings (i.e., in the PFC) are gradually desensitized after 4 to 6 weeks of SSRI treatment ([329]; see the pindolol story in "Serotonergic system dysfunction in depression" section). For example, WAY100635 (0.5 or 1 mg/kg), a selective somatodendritic 5-HT_{1A} antagonist, potentiated fluoxetine-induced increases in 5-HT_{ext} in rat v-Hipp or PFC [333, 334]. This functional adaptation of 5-HT_{1A} autoreceptors that occur after a chronic SSRI treatment would be related to a decrease in the transcription of the gene coding for 5-HT_{1A} receptors, decoupling of Galpha (i3) subunit protein isoforms in the anterior raphe, and/or internalization into DRN 5-HT neurons [335, 336]. Such molecular events do not occur in postsynaptic brain regions, such as the hippocampus because 5-HT_{1A} receptors are likely coupled to different G proteins compared to the DRN [337].

WAY100635 (3 mg/kg, s.c.) blocked ketamine (30 mg/kg, i.p.) effects in the NSF in mice [338]. However, at such a high dose, WAY100635 is non-selective for 5-HT_{1A} because it also blocked dopamine D4 and 5-HT_7 receptors [339, 340]. Rivera-Garcia *et al.* (2015) [297] has therefore reported no effect of WAY100635 (1 mg/kg, i.p.) on ketamine (3 and 10 mg/kg, i.p.) positive effects in the head-twitch response (a serotonin-dependent test) and 5-HT levels in post-mortem rat brain tissue homogenates, indicating that 5-HT_{1A} autoreceptors unlikely play a significant role in ketamine-induced increases in 5-HT neurotransmission.

Presynaptic 5-HT_{1B} autoreceptors located at serotonergic nerve terminals are involved in a negative feedback control of 5-HT release [341, 342]. In contrast, 5-HT_{1B} heteroreceptors are involved in the regulation of the release of various neurotransmitters, e.g., inhibitory activity on glutamatergic, GABAergic, dopaminergic, noradrenergic and cholinergic neurons [343]. Microdialysis data obtained in knockout 5-HT_{1B}

mice brought additional information by suggesting that 5-HT_{1B} autoreceptors limit the effects of SSRIs on dialysate 5-HT levels at serotonergic nerve terminals in the PFC [344]. In the PET study described above with macaques [323], ketamine increased 5-HT_{1B} receptor binding in the nucleus accumbens and ventral pallidum, and a pretreatment with NBQX blocked this effect. It suggests that AMPA-R activation exerts a critical role in ketamine-induced upregulation of postsynaptic 5-HT_{1B} receptors in these brain regions, which may be involved in the antidepressant action of ketamine.

Ketamine and 5-HT_2 receptor. The 5-HT_2 receptor family comprises three specific subtypes: 5-HT_{2A}, 5-HT_{2B} and 5-HT_{2C}, all of them being positively coupled to phospholipase C [345]. In the CNS, the subtypes 5-$HT_{2A/2C}$ are implicated in psychotic pathology and found predominantly post-synaptical on non-serotonergic neurons. Antagonism of 5-$HT_{2A/2C}$ is one of the critical features of atypical antipsychotic drugs in treatment-resistant schizophrenia patients [346]. An indirect hypothesis of the 5-HT_2 receptor role in the antidepressant drug activity has recently been suggested. Antidepressant drugs that increase 5-HT_{ext} (such as SSRIs) desensitize 5-HT_{2C} receptors that activate GABAergic interneurons inhibiting serotonergic neurons [347, 348]. 5-HT_{2C} receptors may also participate to stress-induced changes in serotonergic neurotransmission. The negative effect of 5-HT_{2C} receptor activation is reduced during a chronic SSRI treatment. This modulation likely underlies anxiolytic properties of SSRIs [349].

Ketamine (10 and 20 mg/kg, i.p.) enhanced the head-twitch response, in mice, which was blocked by cyproheptadine, a 5-HT_2 receptor antagonist, and NMDA [350]. It suggests an interaction between NMDA-R blockade and post-synaptic 5-HT_2 activation in ketamine-induced enhancement of serotonergic pathway. In agreement with these findings, electrophysiological studies in rat brain slices have shown that the activation of 5-HT_{2A} receptors in the cerebral cortex, a region where these receptors are enriched, produced a dramatic increase in glutamatergic excitatory postsynaptic potentials in the apical dendritic region of layer V pyramidal cells [302]. Co-application of 5-$HT_{2A/2C}$ receptor antagonists with ketamine diminished its schizophrenic effects. Indeed, 5-$HT_{2A/2C}$ receptor antagonists blocked ketamine-induced increase in dialysate 5-HT_{ext} levels (at schizophrenic-relevant dose: 25 mg/kg, s.c.) [30]. Disruption of prepulse inhibition (PPI), a phenomenon linked to abnormalities found in rodent models of schizophrenia that caused impaired cognition, was induced by ketamine (10 mg/kg, s.c, 15 min prior to testing) and was attenuated by ziprasidone, a novel clozapine-like antipsychotic 5-HT_{2A} receptor antagonist [351]. Discriminative stimulus in rats induced by ketamine (5 and 30 mg/kg, i.p.) was also blocked by ketanserin, a 5-HT_2 receptor antagonist, and clozapine [352]. Together, these data suggest that the combination of ketamine with atypical antipsychotics could limit its psychotomimetic effects that occur shortly after its administration. Interestingly, another 5-HT_{2A} receptor antagonist, ritanserin (0.5 mg/kg, i.p.) did not impede ketamine antidepressant-like effect in the NSF in mice [338]. Therefore, finding a range of ketamine dose in which 5-HT_2 receptor antagonists could help to reduce its side effects, without affecting its antidepressant-like activity is a necessary good research direction that might bring promising results.

Ketamine and 5-HT_3 receptor. 5-HT_3 receptors are unique among the 5-HT receptors' family as they are non-selective Na^+/K^+ ion channel receptors [353]. They modulate fast synaptic transmission. The putative antidepressant-like activity of 5-HT_3 receptor antagonists has been studied in the learned helplessness rat model of depression. Chronic administration of 5-HT_3 receptor antagonists such as zacopride and ondansetron reduced the number of escape failures [354]. Given acutely, ICS205-950, another 5-HT_3 receptor antagonist, dose-dependently decreased the duration of immobility in the FST [355]. Interestingly, 1-(m-Chlorophenyl)-biguanide (mCPBG), a 5-HT_3 receptor agonist attenuated the decrease in immobility produced by classical antidepressants [355]. In the study of Kos *et al.* (2006), a 5-HT_3 receptor antagonist, MDL72222, co-administered with a high dose of ketamine (40 mg/kg, given i.p. immediately prior to testing) failed to reverse ketamine-induced behavioral deficits in rats (i.e., discriminative stimulus, PPI and cognitive disruption), but potentiated ketamine antidepressant-like effects in the TST (12.5 mg/kg, i.p.) [356]. Taken together, the blockade of 5-HT_3 receptor may contribute to the action of antidepressant drugs.

Ketamine and 5-HT_6 receptor. 5-HT_6 receptors in the rat brain appear to be localized in the CNS system and positively coupled to adenylyl cyclase. This receptor fam-ily is involved in behavioral disorders and in the mechanism of 5-HT-modulating drugs, including antidepressants and antipsychotics, due to high affinities of these drugs for 5-HT_6 receptors (reviewed by [345]). In a rat study, an acute administration of EMD 386088, a 5-HT_6 receptor agonist, improved ketamine-induced schizophrenia-like deficits in cognition and memory, but did not affect ketamine-evoked PPI disruption in rats [357]. In this study, ketamine (10 or 20 mg/kg) was administered s.c. 75 min before the task. Even with limited available information, 5-HT_6 receptors agonist improved some of the ketamine-induced deficits relevant to schizophrenia, therefore could be an interesting research direction to examine benefits of such a drugs' combination to overcome ketamine side effects.

Ketamine and 5-HT_7 receptor. 5-HT_7 receptors also postively coupled to adenylyl cyclase and share high binding affinity for antidepressant and antipsychotic drugs [345]. Some studies have evaluated the effects of selective 5-HT_7 receptor antagonists on ketamine-induced deficits in recognition tasks in rats. SB-269970, the most used 5-HT_7 receptor antagonist, can block ketamine (30 mg/kg, s.c.)-induced hyperlocomotion in mice [358], and cognition deficits and disruption of social interactions at a lower dose in rats (20 mg/kg, i.p., [359, 360]). Remarkably, 5-HT_7 receptor agonist abolished the reversed ketamine-induced social withdrawal of 5-HT_7 receptor antagonist, suggesting an important participation of this receptor in this side effect. On the other hand, 5-HT_7 receptor antagonists, unlike 5-HT_2 receptor antagonists, did not reverse ketamine-induced PPI deficits, thus underlining the selective involvement of 5-HT_2 receptor in this action.

Overall, the brain serotonergic system appears to interact fully with different aspects of ketamine's pharmacological

properties and side effects. **First**, ketamine increases 5-HT levels in various brain regions in rodents, which is positively correlated with its antidepressant-like activity. This observation is demonstrated mostly in the mPFC, a key region in ketamine's effects, yet not in the DRN, where a high density of 5-HT neuronal cell bodies are located. Moreover, to the best of our knowledge, the 5-HT_{1A} autoreceptor doesn't seem to take part in ketamine antidepressant-like activity, which is an interesting difference with classical antidepressant drugs such as SSRIs. This appears intriguing, but could be explained by an involvement of a complex communication between different neurotransmitters that modulate consequently the outcome of 5-HT levels in the DRN. Indeed, an interaction between glutamatergic-GABAergic-serotonergic systems are strongly implicated in ketamine's actions because: (i)- the majority of mPFC neuronal projections to the DRN are mostly indirect through GABAergic interneurons, which are well-known to synapse with local DRN 5-HT neurons; (ii)- modulation of 5-HT neurons firing activity in the DRN involves both glutamatergic and GABAergic receptors. In addition, further investigation of ketamine effects on the excitatory/inhibitory balance in the mPFC and hippocampus, would give more information than just analysing changes in one neurotransmitter levels. **Second**, ketamine requires activation of the brain serotonergic neurotransmission to exert its antidepressant-like effects, as depletion of this system decreased changes in its antidepressant-like activity as well as in mPFC 5-HT_{ext} levels. **Third**, an indirect rather direct, involvement of SERT might be mandatory to ketamine-induced increases in mPFC 5-HT_{ext} levels. A knockout SERT study in mice could bring more insights into this interaction. In addition, behavioural and neurochemical responses to acute ketamine administration in animal models of anxiety/depression are needed, and if possible, to test for the antidepressant response. **Finally**, except for 5-HT_1 receptors, the other classes of serotonergic receptors seem to take part in regulating ketamine-induced side effects, especially the 5-HT_{2A} antagonists. Combination of these agents with ketamine is a promising direction to not only limit its undersirable schizophrenic symptoms, but also to enhance its antidepressant-like effects at lower and safer doses. These effects of ketamine involved serotonergic system in preclinical studies are summarized in Table 3.

CONCLUSIONS

In this review, we have analyzed current data on ketamine antidepressant-like activity that involved the glutamatergic, GABAergic and serotonergic neurotransmissions.

The current indirect cortical disinhibition hypothesis regarding the cascade of cellular and molecular events leading to a fast antidepressant-like activity of an acute ketamine dose can be summarized as follows: ketamine binds to NMDA-R located on GABAergic interneurons, and induces a selective blockade of inhibitory GABA interneurons, thus increasing glutamate bursts (LTP) and glutamate release from pyramidal cells located in the mPFC. The subsequent activation of a ligand-dependent Na^+/Ca^{2+} channel, i.e., AMPA-R signaling lo-cated on post-synaptic glutamatergic neurons has described by many authors (see [27, 34, 46]). It increases BDNF synthesis and release, which activates TrkB/Akt, then the mTORC1 signaling pathway in the mPFC (Duman's group: [26]), but deactivation of the eEF2 kinase in the ventral hippocampus (Monteggia's group: [47]). These cascade ultimately led to synapse maturation and synaptogenesis, plasticity and a *fast antidepressant-like activity.*

However, several points need to be clarified. One of them is whether, in addition to glutamate, GABA and 5-HT release participate to this pathway. Ketamine is likely to enhance these three neurotransmitters, at least in the mPFC, but several specific brain circuits could contribute to its antidepressant-like activity. Using microdialysis technique in awake, freely moving mice, we found a concomitant increase in the Glu_{ext}, $GABA_{ext}$ and 5-HT_{ext} in the mPFC, while several authors reported increases in one of them. Thus, the question about which neurotransmitter was first modified and lead to further alteration of the others is also pending.

1- Glutamate release. In microdialysis studies, the increase in Glu_{ext} after administration of a single subanesthetic dose of ketamine, was observed in the mPFC either immediately after administration (in rats: [43, 294, 361]) or 24h after (in mice: [20, 21]). So, ketamine rapid antidepressant-like effect may induce quick bursts of glutamate and glutamate release that set off a cascade of subsequent events involving GABA and 5-HT neurotransmission stimulation. Since ketamine binds to glutamate NMDA-R, glutamate release within the mPFC/hippocampus/DRN circuit is likely the first neurotransmitter initiating the cellular cascade leading to plasticity, then fast antidepressant-like activity. Cortical pyramidal neurons belong to two groups: single spiking cells (few) and repetitive bursting cells (present in most cortical areas). Both cell types also differ morphologically. Glutamate-induced bursts require activation of NMDA-R (by contrast, application of AMPA evoked single spikes) [362]. Thus, if bursts of glutamate are necessary for pyramidal neurons to activate GABA interneurons as suggested by Duman *et al.* (2016) [27], ketamine, as an NMDA-R antagonist, may weaken the connections between pyramidal cells and GABA interneurons. Whether or not this mechanism is involved only in the fast antidepressant-like effects of ketamine, but also in its effects against stress [363], pain relief (antalgic) [364], psychotomimetic effects is currently unknown. Brain regions, circuits (amygdala and emotion), neurotransmitters involved in these various properties must be different.

2- BDNF release/TrkB activation. Activity of the mPFC-hippocampus pathway suggests that an early transient activation of BDNF release and its binding to high affinity TrkB receptors in the hippocampus is essential for the sustained antidepressant-like response to ketamine [299]. However, the hypothesis was questioned in heterozygous $BDNF^{+/-}$ mice. They found that neither ketamine nor the AMPA-R PAM LY451656 activated BDNF signaling, but produced a characteristic antidepressant-like response in these mice. Thus, unlike for monoaminergic antidepressants, BDNF signalling would play a minor role in the antidepressant effects of glutamate-based compounds [49].

3- GABA release. Results regarding changes in $GABA_{ext}$ after ketamine have shown either no effect in several rat brain

regions [238, 365], or an increase in the mPFC in BALB/cJ mice [20]. This latter ketamine response in stressed mice is difficult to reconcile with the GABA deficit hypothesis in depression. We can notice that a new multimodal antidepressant, vortioxetine also inhibits GABAergic neurotransmission in some brain regions (mPFC, vHipp) via a 5-HT_3 receptor antagonism-dependent mechanism and thereby disinhibit pyramidal neurons and enhance glutamatergic signalling [366, 367]. However, it was shown that UCMS in mice impaired GABA release and reuptake by upregulating miRNAs and downregulating GAD67 in mouse cortex [220]. It would be interesting to identify the family of GABA interneurons inhibited by ketamine (PV, SST, receptor 5-HT_{3A}). For example, the cellular vulnerability to stress is exacerbated in SST-positive GABAergic interneurons [368]. A functional potentiation of inhibitory GABAergic transmission from SST-positive GABAergic interneurons to pyramidal cells result in reductions in the synaptic excitation/inhibition ratio and was sufficient to elicit an antidepressant-like phenotype [221]. Thus, glutamate/GABA balance, i.e., excitation/inhibition ratio of microdialysate levels reinforced this assertion [20]. These data are consistent with the GABAergic deficit hypothesis of MDD and with an enhancement of GABAergic synaptic transmission by antidepressant therapies. Increases in dialysate levels of both glutamate and GABA could help balancing the brain's neurochemistry since neuronal atrophy and decreases in hippocampal volume are regularly reported in patients with MDD [369]. A sustained activation of glutamate neurotransmission in the cortex and/or hippocampus can induce large increases in dialysate glutamate levels, and a subsequent retrograde excitotoxicity, neuronal degeneration or seizure susceptibility [370]. Studying the contribution of synaptic *versus* extrasynaptic NMDA-R in ketamine responses may help to address this question. In our study [20], ketamine enhanced Glu_{ext} (+100% *vs* control group, in pmol/sample) to a greater extent than $GABA_{ext}$ (+50% *vs* control group, in fmol/sample). Thus, this range of concentration could translate into distinct pharmacological (antidepressant-like activity) or pathological (neuronal death) role for extracellular glutamate [371].

The GABAergic alteration in ketamine's action depends on the type of stress. A chronic stress decreased GABA neurotransmission, and repeated antidepressant therapy (e.g., antidepressant drugs, ECT or ketamine) corrected this deficit. However, the increase in GABA levels seems unusual since GABA is the principal neurotransmitter regulating neural inhibition of the brain. This could be explained as a consequence of glutamate bursts, that could subsequently induce fast-spiking GABAergic interneurons, then activating GABA release by GABAergic vesicular (Figure 2). It might not be an enhancement of GABA synthesis, at least in the PFC and hippocampus, because ketamine downregulated the expression of GAD67 in these brain regions [255, 256]. GAD67 is the enzyme endorsing the degradation process from glutamate to GABA in the glutamine-glutamate-GABA tripartite-synapse cycle. The downregulation of GAD67 expression suggests that GABA synthesis is not the cause of $GABA_{ext}$ increases that we observed in the mPFC. However, this could be only selective to PV-positive (fast-spiking), but not other classes of interneurons (e.g., SST), since PV expression is also reduced in these studies. Downregulation of PV expression facilitated synaptic current in mice [372], thus accelerated glutamatergic neurotransmission. On the other hand, this increase of $GABA_{ext}$ could also be explained by an increase of glucose utilization, which metabolized glutamate – the precursor of GABA or even a blockade of GABA reuptake by transporters located on pre-synaptic neurons or on glial cells.

4- Glutamatergic/GABAergic balance. The modification of ketamine on glutamatergic and GABAergic neurotransmission, together with the glutamate and GABA deficit hypothesis of depression, underline the importance of excitatory:inhibitory (E:I) balance of MDD. Modifying this balance seems to be the key of antidepressant therapies, as shown in a recent study [221]. Here, our review resumes that ketamine is capable of enhancing both glutamate and GABA levels in the brains. The increase in excitability allows the brain to boost its function by increasing neurotransmission and reinforcing connections between brain regions. Increases in GABA levels elevation may limit the excessive increases in glutamate and to maintain the homeostasis of the brain. However, how ketamine induces such an increase still remains unclear. PV-positive interneurons target the proximal regions of pyramidal cells, whereas SST-positive interneurons are dendrite-preferring interneurons [373] (Figure 3). A downregulation of PV, the calcium-binding protein that control greatly the generation and timing of pyramidal cells' action potentials, was observed after treatment of ketamine. However, there has been little information of how ketamine interacts with SST-positive interneurons in the brain. Ketamine-induced downregulation of this protein was already described, but only at anesthetic dose [374]. We could imagine that the downregulation of PV expression will facilitate the action potential of pyramidal cells to occur, leading to an increase in glutamate release. However, how SST-positive interneurons control the dendrites of these cells to transfer the signals further in subcortical regions still require more investigations. Understanding how ketamine modifies particular subtypes of GABA interneurons is an important puzzle pieces to resolve the E:I balance implication in ketamine-induced antidepressant-like actions.

5- Serotonin release. It is likely that impaired cortical glutamate/GABA balance induced by NMDA-R antagonists lead to downstream changes in other neurotransmitters. Thus, several groups described increases in swimming duration in the FST, a serotonergic parameter [375], and in mPFC 5-HT_{ext} following systemic ketamine administration. However, the mechanism underlining ketamine-induced increases in 5-HT neurotransmission is intriguing, since it involved a decrease, but not an increase, in DRN firing rate [21], an effect similar to what was described following an acute SSRI treatment [376, 377]. The firing activity of 5-HT neurons returned to baseline after a chronic SSRI treatment because DRN 5-HT_{1A} autoreceptors gradually desensitized [378, 379]. Activation of AMPA-R located on 5-HT neurons in the in the DRN might have facilitate 5-HT release in the mPFC, since pre-clinical studies found that selective AMPA-R antagonists blocked ketamine antidepressant-like activity together with the 5-HT_{ext} increase in the mPFC. The mPFC projects densely towards the DRN either directly or indirectly via GABA interneurons (Figure 3). When examining glutamate receptor mediated excitatory effects on DRN 5-HT neuronal activity in rat brain

slices, Gartside *et al.* (2007) [318] found that the selective blockade of somatodendritic 5-HT_{1A} receptors failed to enhance the excitatory response of DRN 5-HT neurons to AMPA and NMDA. Taken together, these data suggest that 5-HT could be subsequently modified by ketamine-induced glutamate bursts in the mPFC, without a high degree of tonic activation of 5-HT_{1A} autoreceptors in the DRN.

6- Complex neurotransmission between NMDA-R, AMPA-R, $GABA_A$-R and 5-HT receptors. The mechanism of antidepressant-like effects of ketamine involve many receptors, forming a complicated network that could not be analyzed separately. Herein, we point to NMDA-R, AMPA-R, $GABA_A$-Rs and 5-HT receptors. Ketamine is NMDA-R channel blocker. While GluN1 role is still a matter of debate, the GluN2A and GluN2B are, on the other hand, could be important antidepressant drug target. Ketamine blocks GluN2A- and GluN2B-containing NMDA-Rs equally [380], thus implication of both subunits should be studied in parallel in ketamine antidepressant-like activity. The disinhibition theory of ketamine antidepressant-like activity suggests a selective blockade of NMDA-R located on GABAergic interneurons, which therefore disinhibits pyramidal cells to enhance their electrical activities. This pathway is considered as indirect. Since the PV-postivie interneurons were reported to be enriched with GluN2A subunit of NMDA-R, and the downregulation of PV activity are strongly implicated in ketamine actions, it is possible that ketamine is attracted more to this subunit of NMDA-R to induce the disinhibition effect. On the other hand, the GluN2B subunit could be involved in the direct pathway of ketamine antidepressant-like activity. This direct pathway, according to Miller's team [34], takes place at pyramidal cells' dendrites, which, unlike the indirect pathway, might not involve an increase in Glu_{ext} and 5-HT_{ext}. The selective blockade or removal of this subunit on pyramidal neurons engaged in a rapid increase in excitatory synaptic input onto these neurons to induce antidepressant effects. This is an interesting hypothesis since GluN2B selective antagonists have shown inconsistent results in clinical trials. More studies targeting GluN2B subunits on pyramidal cells will help to better understand this point.

Meanwhile, evidences point out that the activation of AMPA-R is essential for ketamine antidepressant activity. Whether ketamine exerts these effects directly on AMPA-R or indirectly by blocking NMDA-R located on GABAergic interneurons remains unclear. AMPA-R activation might be required for the fast ketamine effect (i.e., when administration occurred 30 min prior testing) to set off the glutamate bursts, while NMDA-R blockade might be involved in its sustained effects. The trafficking process of AMPA-R is demonstrated to be essential for ketamine's sustained effects, since it enhanced synaptogenesis and functional connectivity between brain regions [7]. Moreover, alteration of NMDA-R subunits expression in GluA1-knockout mice and alteration of AMPA-R subunits expression in GluN2B-knockout mice have confirmed an interaction between these two glutamatergic receptor subtypes in regulating depression. These two receptors also modulate 5-HT neuronal firing and local GABA release in the DRN.

It is still unclear to what extent the monosynaptic connection and the disynaptic connection – via GABA interneurons between the mPFC and DRN are involved in ketamine actions. The monosynaptic glutamatergic inputs from the PFC to serotonergic neurons in the DRN could modulate directly the increase in presynaptic 5-HT release. By contrast, the disynaptic pathway via GABA interneurons could involve a more complex pathway in which AMPA-R, NMDA-R and $GABA_A$-Rs interact concomitantly to induce an increase in cortical GABA levels. This could implicate the interneurons in both regions, mPFC and DRN, since ketamine corrected the deficit of GABAergic neurotransmission most effectively in the mPFC, the region known to project densely towards the GABA-rich zone of the DRN (Figure 3).

Optogenetic technique could help differentiating effectively these two distinct pathways. This innovative approach is used extensively today to study brain circuits. Using photosensitive receptors, this technique allows neurobiologists to access specific neuronal pathways with a high selectivity targeting neuronal types. Further studies using an optogenetic approach, in combination with conventional techniques (e.g., microdialysis, electrophysiology) should be conducted to examine the specific role of each neuronal type (glutamate, GABA, 5-HT) in some potential circuits such as mPFC-DRN and mPFC-vHipp to understand more deeply the connections between these neurons and the order in which they are altered in ketamine's actions.

7- Ketamine response rate in TRD. Defining ketamine responders and non-responders in rodent models of anxiety/depression could bring relevant information in line with the clinical interest of ketamine in TRD. Protein expression represents a combination of markers associated with the maintenance of animals in a refractory state, or associated with behavioral improvement [381, 382]. Future preclinical studies will be required to validate whether proteomic changes observed in responders and non-responders ketamine-treated mice mirror biological and imaging changes (e.g., *ex vivo* nuclear magnetic resonance spectroscopy, PET scan, magnetic resonance imaging studies) observed in TRD patients.

In conclusion, the mechanism of ketamine requires complex interactions between different neurotransmitters, receptors, and brain regions. Indirect and direct pathways, as well as the monosynaptic and disynaptic connections, have been suggested to understand ketamine antidepressant mechanism of action. Identifying how all these factors connect together to induce such a rapid and sustained antidepressant-like activity of ketamine, esketamine, their metabolites and AMPA-R agonists require more studies combining several techniques, e.g., the coupling of optogenetic and *in vivo* microdialysis analysis realized during behavioral tests in rodents [383]. The glutamatergic/GABAergic balance must be in the center of these investigations. We need to get more information about the pharmacological properties of NMDA-R and AMPA-R subunit-specific ligands (e.g., GluN2A, GluN2B, GluA1) at particular location (pyramidal cells, interneurons, 5-HT neurons), in particular neuronal circuit (e.g., mPFC-DRN, mPFC-hippocampus) These preclinical discoveries will pave the way for the clinical development of the next generation of antidepressant drugs being fast-acting, more effective and better tolerated.

Table 1: Ketamine antidepressant-like activity involved glutamatergic neurotransmission in preclinical studies (rats and mice).

References	Species (rats or mice) and strain	Ketamine dose and route of administration	Behavioral and neurochemical changes	Molecular/cellular changes, brain region studied
I) Ketamine increases glutamate content				
Moghaddam *et al.*, 1997	Rats	Ketamine 10, 20 and 30 mg/kg, i.p. (acutely)	- Increased Glu_{ext} level (PFC)	
Lorrain *et al.*, 2003a	Sprague–Dawley rats	Ketamine 18 mg/kg, s.c. (acutely)	- Increased Glu_{ext} level (mPFC)	
Melo *et al.*, 2015	Wistar rats, UCMS model	Ketamine alone or combined: ketamine (4 days) + fluoxetine or imipramine (14 days), all at dose 10 mg/kg, i.p.	- Ketamine alone or in combination: reversed UCMS-induced anhedonia in the FST, sucrose preference, EPM. - UCMS-induced decrease Glu levels in the NAc, but not the PFC, and the combination reversed these effects	
Chowdhury *et al.*, 2017	Sprague–Dawley rats	Ketamine 3, 10 and 30 mg/kg, i.p. (30 min and 24h prior testing)	- Increased Glu, GABA and Gln contents only at 30 min post-injection, not at 24h (mPFC) - Reduced immobility duration (FST, only at dose 30 mg/kg, 24h post-injection)	
Zhu *et al.*, 2017	Sprague–Dawley rats, UCMS model	Ketamine 10, 25 and 50 mg/kg, i.p. (5 days)	- UCMS induced an increase of Glu_{ext} (hippocampus), reversed by ketamine	
Pham *et al.*, 2017a	BALBc/J mice	Ketamine 10 mg/kg, i.p., (24h prior testing)	- Increased Glu_{ext} (mPFC) - Increased swimming duration (FST)	
II) Ketamine alters NMDA- and AMPA-R function				
Moghaddam *et al.*, 1997	Rats	Ketamine 10, 20 and 30 mg/kg, i.p. (acutely) + CNQX 50 µM infused intra-PFC (acutely)	- CNQX blocked ketamine-induced increase in $dopamine_{ext}$ level (PFC)	
Wakasugi *et al.*, 1999	Rat hippocampal slices	Ketamine 10 mM (acutely)		- Reduced NMDA-R-mediated responses and enhances $GABA_A$-receptor-mediated responses

References	Species (rats or mice) and strain	Ketamine dose and route of administration	Behavioral and neurochemical changes	Molecular/cellular changes, brain region studied
Maeng *et al.*, 2008	Mice	Ketamine 2.5 mg/kg, i.p. (24h or 2 weeks prior testing) + NBQX (10 mg/kg, i.p., 10 min prior to ketamine)	- NBQX blocked ketamine effects in the FST	- Ketamine reduced p-GluA1 (hippocampus), blocked by NBQX
		Ro 25-6981 (selective NR2B antagonist) 3 mg/kg, i.p. (30 min prior testing) + NBQX (10 mg/kg, i.p.)	- NBQX blocked Ro 25-6981 effects in the FST	
Li *et al.*, 2010, Li *et al.*, 2011	Rats	Ketamine 10 mg/kg, i.p. (24h prior testing) + NBQX 10 mg/kg, i.p. (10 min prior to ketamine)	- Ketamine decreased immobility in the FST, latency to feed in the NSF and number of escapse failure (LH paradigm)	- Ketamine rapidly increase synaptic proteins and spine number (PFC) - NBQX blocked ketamine-induced increase in p-mTOR, p4E-BP1 and pp70S6K expression (PFC)
		Ro 25-6981 (selective NR2B antagonist) 10 mg/kg, i.p. (24h prior testing)	- Produced rapamycin-sensitive behavioral response (FST and NSF)	- Activated mTOR
Autry *et al.*, 2011	C57Bl6 mice	Ketamine 3 mg/kg, i.p. (30 min prior testing) + NBQX 10 mg/kg, i.p. (30 min prior testing)	- NBQX blocked ketamine effects in the FST	
		Ketamine 1, 5, 20 and 50 μM in hippocampal cultures (acutely)		- blocked NMDA-R spontaneous activity (from 1 μM) - increased AMPA-R-mediated synaptic responses (at 20 μM)
Koike *et al.*, 2011	ICR mice (for TST) Sprague-Dawley rats (LH paradigm)	Ketamine 10 mg/kg, i.p. (30 min prior testing) + NBQX 10 mg/kg, s.c. (5 min prior to ketamine)	- NBQX blocked ketamine effects in reducing the number of escape failure (LH paradigm) and immobility duration in the TST	
		Ketamine 30 mg/kg, i.p. : 72h prior testing) + NBQX 10 mg/kg, s.c. (72h prior testing)	- NBQX blocked ketamine effects in the TST	
Koike & Chaki, 2014	Sprague-Dawley rats	Ketamine 10 mg/kg, i.p. (24h prior testing) + NBQX 1, 3 & 10 mg/kg, s.c. (30 min prior testing)	- NBQX (10 mg/kg) blocked ketamine effects in the FST	

References	Species (rats or mice) and strain	Ketamine dose and route of administration	Behavioral and neurochemical changes	Molecular/cellular changes, brain region studied
Miller *et al.*, 2014	NR2B KO mice	Ketamine 50 mg/kg, i.p. (30 min prior to TST and 24h prior to electrophysiology)	- NR2B KO in mice increased immobility duration in the TST, similar to ketamine	- NR2B KO occluded ketamine-induced increase in excitatory synaptic transmission (PFC) - NR2B KO occluded ketamine-induced increase in BDNF, SAP-102, GluA1, p-mTOR expression
Nishitani *et al.*, 2014	Wistar rats	Ketamine 5 and 25 mg/kg, s.c. (acutely) + NBQX 30 nmol intra-DRN (10 min prior to ketamine)	- Increased 5-HT_{ext} (mPFC and DRN), blocked by NBQX	
Bjorkholm *et al.*, 2015	Sprague–Dawley rats	Ketamine 10 mg/kg, i.p. (24 prior testing)		- Increased AMPA- and NMDA-induced current activation
El Iskandrani *et al.*, 2015	Sprague–Dawley rats	Ketamine 10 and 25 mg/kg, i.p. (30 min prior testing)		- Increased AMPA-evoked (from 10 mg/kg) firing and decreased NMDA-evoked firing (only at 25 mg/kg) (hippocampus)
		+ NBQX 3 mg/kg. i.p. (10 min prior to ketamine)		- NBQX blocked ketamine-induced increases in population activity of VTA dopamine neurons and firing rate of LC norepinephrine neurons
Zhang *et al.*, 2015	C57BL/6J mice, Social defeat model	Ketamine 10 mg/kg, i.p. (3h prior testing)	- Decreased immobility (FST and TST) - Long-lasting effects (up to 7 days) on sucrose preference test	- Decreased proBDNF (PFC), increased BDNF, PSD-95 and GluA1 (PFC, hippocampus), at 4 and 8 days post-treatment
Beurel *et al.*, 2016	Mice knock-in GSK3 alpha/beta homozygous	Ketamine 10 mg/kg, i.p. (24h prior testing)		- GSK3 knockin blocked ketamine-induced up-regulation of BDNF. mTOR and GluA1 expression (hippocampus)
Fukumoto *et al.*, 2016	C57BL/6J mice	Ketamine 30 mg/kg, i.p. (30 min prior testing) + NBQX 1, 3 and 10 mg/kg, s.c. OR + NBQX 0.01 and 0.03 nmol/side intra-mPFC (35 min prior testing)	- NBQX (only at 3 and 10 mg/kg or 0.03 nmol intra-mPFC) blocked ketamine effects in the FST	- NBQX (0.03 nmol intra-mPFC) blocked ketamine-induced increase of c-Fos expression on 5-HT neurons (DRN)
Ren *et al.*, 2016	$GABA_AR$ subunit $gamma2^{+/-}$ mice (129X1/SvJ) cell cultures	Ketamine 10 μM (3-6h prior testing)		- Reversed NR1, AMPA-R cell surface expression and glutamatergic synapses density deficit

References	Species (rats or mice) and strain	Ketamine dose and route of administration	Behavioral and neurochemical changes	Molecular/cellular changes, brain region studied
	$GABA_AR$ subunit gamma2$^{+/-}$ mice (C57BL/6J)	Ketamine 3 mg/kg, i.p. (8h prior testing)	- Increased time and entries in open arm (EPM) - Increased swimming time (FST)	
		Ketamine 10 mg/kg, i.p. (24h prior testing)		- Increased NMDA-R (NR2B subunit) surface expression (PFC, hippocampus) - Increased AMPA-R surface and total expression (only hippocampus) - Reversed the deficit of functional glutamatergic synapses
Pham *et al.*, 2017b	BALBc/J mice	Ketamine 2 nmol (intra-mPFC, 24h prior testing) + NBQX 0.1 µg (intra-DRN, 30min prior to ketamine)	- NBQX blocked ketamine-induced decrease in immobility duration (FST) and increase in $5\text{-}HT_{ext}$ level (mPFC)	

Glu: glutamate. Gln: glutamine. Glu_{ext}: extracellular level of glutamate, measured by microdialysis. $5\text{-}HT_{ext}$: extracellular level of glutamate, measured by microdialysis. LH: learned helplessness. TST: tail suspension test. FST: forced swim test. NSF: novelty suppressed feeding. EPM: elevated plus maze. i.p.: intraperitoneal injection. s.c.: sub-cutaneous injection. KO: knock-out. mPFC: medial prefrontal cortex. PFC: prefrontal cortex. DRN: dorsal raphe nucleus. VTA: ventral tegmental area. NAc: nucleus accumbens. NMDA-R: NMDA receptor. AMPA-R: AMPA receptor. UCMS: unpredictable chronic mild stress. BDNF: brain-derived neurotrophic factor.

Table 2: Ketamine antidepressant-like activity involved GABAergic neurotransmission in preclinical studies (rats and mice).

References	Species (rats or mice) and strain	Ketamine dose and route of administration	Behavioral and neurochemical changes	Molecular/cellular changes, brain region studied
Horne *et al.*, 1986	Slices of rat cerebral cortex	Ketamine 100 μM (acutely)		- Reduced spontaneous paroxysmal discharges, similar to muscimol 2μM and baclofen 10 μM
Wakasugi *et al.*, 1999	Rat hippocampal slices	Ketamine 10 mM (acutely)		- Reduced NMDA-R-mediated responses and enhances $GABA_A$-receptor-mediated responses
Irifune *et al.*, 2000	ddY mice	Ketamine 15 mg/kg, i.p. (acutely) + Bicuculline 8 mg/kg, i.p. (5 min after ketamine injection)	- Bicuculline induced tonic seizures, which was blocked by ketamine	
Nakao *et al.*, 2003	Wistar rats	Ketamine 100 mg/kg, i.p. (2h prior to sacrificing) + Propofol 2 mg/kg, i.v. and bicuculline 0.5 mg/kg, i.v., bolus		- Increased c-Fos expression in the posterior cingulate and retrosplenial cortices, inhibited by propofol and disinhibited by bicuculline
Kinney *et al.*, 2006	Cultured cortical PV interneurons of Swiss mice	Ketamine 0.5 μM (exposed during 24h)		- Decreased GAD67 expression specifically on PV+ neurons, similar to NR2A-selective antagonist NVP-AAM077.
Littlewood *et al.*, 2006	Sprague–Dawley rats	Ketamine 10 and 25 mg/kg, s.c.(acutely)	- No alteration in $GABA_{ext}$ (ventral pallidum) was found acutely after ketamine injection	
Pinault, 2008	Wistar rats	Ketamine 2.5 - 10 mg/kg, s.c. (acutely)		- Dose-dependently increased the power (200%–400%) of wake-related gamma oscillations in the neocortex, similar to MK-801
Lazarewicz *et al.*, 2010	CA3 region of mouse hippocampus			- Attenuated theta frequency band and enhanced gamma frequency range in both background and evoked power
Schneider & Rodriguez de Lores Arnaiz, 2013	Wistar rats	Ketamine 40 mg/kg, i.p. (acutely) + Bicuculline 5 mg/kg, i.p. (30 min after ketamine injection)		- Ketamine alone decreased [^{3}H]-QNB binding (a parameter correlated with convulsant seizures), and blocked bicuculline-induced seizures
Perrine *et al.*, 2014	Sprague–Dawley rats (CUS model)	Ketamine 40 mg/kg, i.p. (24h prior testing)	- Decreased immobility (FST)	

References	Species (rats or mice) and strain	Ketamine dose and route of administration	Behavioral and neurochemical changes	Molecular/cellular changes, brain region studied
			- CUS rats showed increase GABA level (ex vivo ^{1}H-MRS, mPFC), reversed by ketamine	
Pozzi *et al.*, 2014	C57BL/6N mice lacking NMDA-R specifically in PV interneurons	Ketamine 3 mg/kg, i.p. (24h et 1 week prior testing)	- Ketamine alone reduced immobility (FST) - The mutation alone didn't induce depression-like behavior but attenuated ketamine's acitiviy in the FST	
Wang *et al.*, 2014	Wistar rats	Ketamine 10 mg/kg, i.p. (30 min prior testing)	- Decreased immobility (FST) and latency to feed (NSF) - Decreased GABA level and increased glutamate level (PFC and hippocampus), detected by ELISA kits	- Decreased NRG1and p-ErbB4 genes expression (marker for pyramidal cells-PV+ interneurons activation) (PFC and hippocampus) - Decreased PV and GAD67 expression (PFC and hippocampus)
Zhou *et al.*, 2015	Wistar rats	Ketamine 10 and 30 mg/kg, i.p. (30 min and 2h prior testing) The dose 30 mg/kg was administered repeatedly for 3 days consecutive	- Decreased immobility (FST) - Ketamine 30 mg/kg induced hyperactivity (Open Field test) - Increased glutamate level (PFC) - Decreased GABA level (PFC): acutely at 30 min for ketamine 10 mg/kg and persistently for ketamine 30 mg/kg	- Reduced PV and GAD67 expression (PFC): acutely at 30 min for ketamine 10 mg/kg and persistently for ketamine 30 mg/kg
Yang *et al.*, 2015	C57Bl6/J social defeat model	(R)- or (S)-ketamine 10 mg/kg, i.p. (24h or 7 days before testing)	- Both induced antidepressant responses in the succrose preference test, TST and FST: (R)-ketamine is more potent in these tests - (S)-ketamine induced hyperlocomotion and PPI	- Increased synaptogenesis, BDNF-TrkB signaling (PFC and hippocampus) - (S)-Ketamine induced loss of PV+ cells (PFC and hippocampus)
Ren *et al.*, 2016	$GABA_AR$ subunit gamma2$^{+/-}$ mice (C57BL/6J)	Ketamine 3 mg/kg, i.p. (8h prior behavioral tests) Ketamine 10 mg/kg, i.p. (24h prior molecular/cellular analysis)	- Gamma2$^{+/-}$ mice responded better to ketamine than wild-type mice in the FST, EPM	- Increased GABAergic synapses number and vesicular GABA transporters expression (only in mPFC) - Increased glutmatergic synaptic function (mPFC and hippocampus) - Down-regulation of NR1, NR2B, GluA2/3 surface expression by gamma2$^{+/-}$ were reversed by ketamine (mPFC, hippocampus)
Rosa *et al.*, 2016	Female Swiss mice	Ketamine 0.1 mg/kg, i.p. (1h prior testing)	- Decreased immobility (TST)	

References	Species (rats or mice) and strain	Ketamine dose and route of administration	Behavioral and neurochemical changes	Molecular/cellular changes, brain region studied
		+ Muscimol 0.1 mg/kg, i.p. (30 min after ketamine injection)		
		Ketamine 1 mg/kg, i.p. (30 min prior testing) + Baclofen 1 mg/kg, i.p. (30 min before ketamine injection)	- Ketamine 1 mg/kg alone was sufficient to decrease immobility (TST), which was blocked by Baclofen	
Chowdhury *et al.*, 2017	Sprague–Dawley rats	Ketamine 3, 10 and 30 mg/kg, i.p. (30 min and 24h prior testing)	- Increased GABA content only at 30 min post-injection, not at 24h (mPFC) - Reduced immobility duration (FST, only at dose 30 mg/kg)	
Donegan & Lodge, 2017	Sprague–Dawley rats treated with chondroitinase to degrade PV+ neurons	Ketamine 10 mg/kg, i.p. (30 min and 1 week prior testing)	- Ketamine alone decreased immobility (FST), blocked by PV+ neurons degradation	
Pham *et al.*, 2017a	BALBc/J mice	Ketamine 10 mg/kg, i.p., (24h prior testing)	- Increased $GABA_{ext}$ (mPFC) - Increased swimming duration (FST)	
Ma & Leung, 2018	Long-Evans hooded rats	Ketamine 3 mg/kg, s.c. (acutely) + muscimol 0.5 µg/ 0.5 µL/side (intra-hippocampus, 15 min prior to ketamine)		- Ketamine alone induced gamma wave increase (posterior cingulate cortex (PCC) and hippocampus), blocked by muscimol intra-hippocampus (only in hippocampus)
		Ketamine 0.4 µg/ 0.4µL/side (intra-PCC, acutely) + Muscimol at same dose (15 min prior to ketamine)	- Ketamine induced hyperlocomotion, normalized by muscimol	- Ketamine disrupted prepulse inhibition, blocked by muscimol

$GABA_{ext}$: extracellular level of GABA. PV+: parvalbumin positive. FST: forced swim test. EPM: elevated plus maze. TST: tail suspension test. NSF: novelty suppressed feeding. i.p.: intraperitoneal injection. s.c.: sub-cutaneous injection. mPFC: medial prefrontal cortex. PFC: prefrontal cortex. PCC: posterior cingulate cortex. ^{1}H-MRS: proton magnetic resonance spectroscopy. CUS: chronic unpredictable stress.

Table 3: Ketamine antidepressant-like activity involved 5-HTergic neurotransmission in preclinical studies (rats and mice).

References	Species (rats or mice) and strain	Ketamine dose and route of administration	Microdialysis and 5-HT content in brain extracts	Behavioral changes	Molecular/cellular, neuronal firing acitivity changes
I) Ketamine altered 5-HT levels in the mPFC, the DRN and the ventral hippocampus measured by microdialysis					
Lorrain *et al.*, 2003b	Sprague–Dawley rats	Ketamine 25 mg/kg, s.c. (acutely)	- Increased 5-HT_{ext} (ventral hippocampus)		
Amargos-Bosch *et al.*, 2006	Wistar rats	Ketamine 25 mg/kg, s.c. (acutely)	- Increased 5-HT_{ext} (mPFC)		
		Ketamine 100, 300 and 1000 µM perfusion intra-mPFC	- No changes was seen on 5-HT_{ext} (mPFC)		
Lopez-Gil *et al.*, 2012	Wistar rats	Ketamine 25 mg/kg, s.c. (acutely)	- Increased 5-HT_{ext} (mPFC), blocked by tetrotodoxin intra-mPFC perfusion (1 µM)	- Only systemic injection increased hyperlocomotion and stereotypies, not blocked by TTX	
		Ketamine 3 mM intra-mPFC perfusion (acutely)	- Only bilateral (but not monolateral perfusion) increased 5-HT_{ext} (mPFC)		
Nishitani *et al.*, 2014	Wistar rats	Ketamine 5 and 25 mg/kg, s.c. (acutely) + NBQX 30 nmol intra-DRN (10 min prior to ketamine injection)	- Ketamine dose-dependently increased 5-HT_{ext} (mPFC and DRN). - The increase of 5-HT_{ext} in the DRN was blocked by NBQX		
		Ketamine 36.5 nmol intra-DRN (acutely)	- No change was seen on 5-HT_{ext} (DRN)		
	Rat organotypic DRN slice	Ketamine 100 µM	- Decreased 5-HT_{ext}		
Pham *et al.*, 2017b	BALBc/J mice	Ketamine 10 mg/kg, i.p. (24h prior testing)	- Increased 5-HT_{ext} (only in the mPFC, not in the DRN)	- Increased swimming duration (FST) - Blocked by pretreatment of pCPA	- Reduced 5-HT neuronal firing (DRN)
		Ketamine 2 nmol intra-mPFC (24h prior testing) + NBQX 0.1 µg intra-DRN (30 min prior to ketamine injection)	- Increased 5-HT_{ext} (mPFC), blocked by NBQX	- Increased swimming duration (FST) in the same mice (correlated positively with mPFC 5-HT_{ext}), blocked by NBQX	

References	Species (rats or mice) and strain	Ketamine dose and route of administration	Microdialysis and 5-HT content in brain extracts	Behavioral changes	Molecular/cellular, neuronal firing acitivity changes
Pham *et al.*, 2017a	BALBc/J mice	Ketamine 10 mg/kg, i.p. (24h prior testing)	- Increased 5-HT_{ext} (mPFC)	- Increased swimming duration (FST) in the same mice	
		Ketamine 2 nmol intra-mPFC (24h prior testing)	- Increased 5-HT_{ext} (mPFC)		
II) Ketamine altered 5-HT contents in brain extracts					
Kari *et al.*, 1978	Sprague-Dawley rats	Ketamine 50 mg/kg, i.p. (acutely)	- Increased 5-HT level (last for 12 hours)		
Chatterjee *et al.*, 2012	Swiss albino mice	Ketamine 100 mg/kg, i.p. (acutely)	- No change in 5-HT level (cortex, striatum and hippocampus) - Increased 5-HIAA level (striatum)		
		Ketamine 100 mg/kg, i.p. x 10 days (sacrificed on the 11th day)	- Increased 5-HT level (only striatum) - Increased 5-HIAA level (cortex, striatum and hippocampus)		
		Ketamine 100 mg/kg, i.p. x 10 days (sacrificed on the 21th day for withdrawal protocol)	- Increased 5-HT level (only cortex) - No change in 5-HIAA level		
Gigliucci *et al.*, 2013	Sprague-Dawley rats	Ketamine 25 mg/kg, i.p. (1h or 24h prior testing) + pCPA pretreatment	- pCPA depleted cortical 5-HT content	- Ketamine reduced immobility duration (FST) - pCPA blocked ketamine (24h prior FST) effect, but not the 1h one.	
Rivera-Garcia *et al.*, 2015	Wistar rats	Ketamine 3 and 10 mg/kg, i.p. (acutely)	- Ketamine (only at 10 mg/kg) increased 5-HT tissue content (hippocampus, striatum and PFC)		
III) Ketamine altered only behavioral and molecular/cellular, neuronal firing activity changes					
Tso *et al.*, 2004	Wistar rats forebrain slices	(S)- and (R)-Ketamine 100 µM (20 min prior testing)			- Increased 5-HT efflux (up to 80%) and 5-HT uptake (up to 200%)
McCardle & Gartside, 2012	Rats DRN slices	Ketamine 100 and 300 µM (acutely)			- Decreased 5-HT neuronal firing rate and enhanced responses to 5-HT (DRN)

References	Species (rats or mice) and strain	Ketamine dose and route of administration	Microdialysis and 5-HT content in brain extracts	Behavioral changes	Molecular/cellular, neuronal firing acitivity changes
Fukumoto *et al.*, 2014	C57BL/6J mice	Ketamine 30 mg/kg, i.p. (30 min prior testing) + pCPA pretreatment		- pCPA blocked ketamine effects in the NSF	
El Iskandrani *et al.*, 2015	Sprague–Dawley rats	Acute: Ketamine 10 and 25 mg/kg i.p. (30min prior to electrophysiology) Chronic: Ketamine 10 mg/kg/day x 3 days			- No change in 5-HT neuronal firing rate (DRN)
Fukumoto *et al.*, 2016	C57BL/6J mice	Ketamine 3, 10 and 30 mg/kg, i.p. or 0.3 and 3 nmol/side intra-mPFC (30min or 24h prior testing) + pCPA pretreatment. Mice were sacrificed at 90 min post-injection of ketamine for the c-Fos colocalization		- Ketamine (only at 30 mg/kg or 0.3 nmol intra-mPFC, at both time points) decreased immobility (FST), blocked by pCPA	- Ketamine (only at 30 mg/kg or 0.3 nmol intra-mPFC) increased c-Fos expression on 5-HT neurons (DRN)
IV) Ketamine interacted with 5-HT receptors					
Kim *et al.*, 1999	ICR mice	Ketamine 10 and 20 mg/kg, i.p. Cyproheptadine 1 and 3 mg/kg, i.p. (30 min prior to ketamine)		- Ketamine increased head-movements number (HTR test), while cyproheptadine decreased this parameter	
Mansbach *et al.*, 2001	Wistar rats	Ketamine 10 mg/kg, s.c. (15 min prior testing) + Ziprasidone 17.8 mg/kg orally (3h prior testing) Clozapine 3.2 and 5.6 mg/kg, s.c. (30 min prior testing)			- Ketamine disrupted PPI (startle response session), blocked by ziprasidone and clozapine
Amargos-Bosch *et al.*, 2006	Wistar rats	Ketamine 25 mg/kg, s.c. (acutely) + Ritanserin 5.0 mg/kg, i.p. Clozapine 1.0 mg/kg, s.c. Olanzapine 1.0 mg/kg, s.c. (15 min prior to ketamine injection)	- Ketamine alone increased 5-HT_{ext} (mPFC) - Only Olanzapine and Clozapine, but not Ritanserin, blocked this effect of ketamine		

References	Species (rats or mice) and strain	Ketamine dose and route of administration	Microdialysis and 5-HT content in brain extracts	Behavioral changes	Molecular/cellular, neuronal firing acitivity changes
Kos *et al.*, 2006	Sprague–Dawley rats	Ketamine 15 mg/kg, i.p. (acutely) + MDL72222 0.3, 1 and 3 mg/kg, s.c. (30 min prior testing)		- MDL72222 did not alter ketamine-induced deficit in PPI or ketamine's discriminative effects	
	C57BL/6J mice	Ketamine alone 12.5 – 66 mg/kg, i.p. (30 min prior testing) OR Combination of: Ketamine 12.5 mg/kg, i.p. (5 min prior testing) + MDL72222 1 mg/kg, s.c. (25 min before ketamine)		- Ketamine alone (at 50 and 66 mg/kg) induced decrease of immobility (TST) - MDL72222 potentiated ketamine's effect in this test from 12.5 mg/kg of ketamine.	
Galici *et al.*, 2008	C57BL6/J mice	Ketamine 30 mg/kg, s.c. + SB-269970 3, 10 and 30 mg/kg, i.p. (30 min prior to ketamine injection)		- SB-269970 reversed ketamine-induced hyperactivity but not the PPI deficit	
Nikiforuk *et al.*, 2013a	Sprague–Dawley rats	EMD 386088 2.5 and 5 mg/kg, i.p.		- EMD 386088 reversed ketamine-induced cognition and memory deficit, but not the deficit in PPI	
Nikiforuk *et al.*, 2013b	Sprague–Dawley rats	Ketamine 20 mg/kg, i.p. (30 min prior testing) + SB-269970 1 mg/kg, i.p. (30 min prior ketamine injection)		- SB-269970 ameliorated ketamine-induced cognition and memory deficit, but not the deficit of PPI	
Yoshizawa *et al.*, 2013	Fischer rats	Ketamine 1.25-5 mg/kg, i.p. (10 min prior testing) + Clozapine 1 mg/kg, s.c. Ketanserin 0.3 mg/kg, s.c. (30 min prior testing)		- Ketamine induced discriminative stimulus effect, blocked by clozapine and ketanserin	
Fukumoto *et al.*, 2014	C57BL/6J mice	Ketamine 30 mg/kg, i.p. (30 min prior testing) + WAY100635 0.3, 1 and 3 mg/kg, s.c. (60 min prior testing)		- WAY100635 (only at 3 mg/kg) blocked ketamine effects in the NSF	

References	Species (rats or mice) and strain	Ketamine dose and route of administration	Microdialysis and 5-HT content in brain extracts	Behavioral changes	Molecular/cellular, neuronal firing acitivity changes
		Ketamine 30 mg/kg, i.p. (30 min prior testing) + Ritanserin 0.5 mg/kg, i.p. (60 min prior testing)		- Ritanserin blocked ketamine effects in the NSF	
Yamanaka *et al.*, 2014	Rhesus monkeys	Ketamine 30 mg/kg, i.v. bolus (100 min prior to PET scan) + 7.5 mg/kg/h i.v. continuous + NBQX 1 mg/kg, i.v. (15 min prior to PET scan)			- Increased 5-HT_{1B} binding and decreased SERT binding (nucleus accumbens and ventral pallidum), blocked by NBQX
Holuj *et al.*, 2015	Sprague–Dawley rats	Ketamine 20 mg/kg, i.p. (30 min prior testing) + SB-269970 1 mg/kg, i.p. (30 min prior ketamine injection)		- SB-269970 reversed ketamine-induced social withdrawal	
Rivera-Garcia *et al.*, 2015	Wistar rats	Ketamine 3, 10 and 20 mg/kg, i.p. (20 min prior testing) + WAY100635 1 mg/kg, i.p. (20 min prior to ketamine injection)		- Ketamine alone induced increases on head-movements number (a 5-HT-dependent parameter). WAY100635 does not affect this effect	

5-HT_{ext}: extracellular level of glutamate, measured by microdialysis. FST: forced swim test. NSF: novelty suppressed feeding. HTR: head-twitch response. mPFC: medial prefrontal cortex. PFC: prefrontal cortex. DRN: dorsal raphe nucleus. i.p.: intraperitoneal injection. s.c.: sub-cutaneous injection. pCPA: para-chlorophenylalanine. TTX: tetrodotoxin. PPI: prepulse inhibition.

CONFICT OF INTEREST

The authors declare no conflict of interest.

ACKNOWLEDGEMENTS

We would like to thank Denis J. David and Jean-Philippe Guilloux for helpful discussions on the manuscript.

REFERENCES

[1] Krystal, J.H.; Karper, L.P.; Seibyl, J.P.; Freeman, G.K.; Delaney, R.; Bremner, J.D.; Heninger, G.R.; Bowers, M.B., Jr., and Charney, D.S. Subanesthetic effects of the noncompetitive NMDA antagonist, ketamine, in humans. Psychotomimetic, perceptual, cognitive, and neuroendocrine responses. *Arch Gen Psychiatry*, **1994**, *51*(3), 199-214.

[2] Berman, R.M.; Cappiello, A.; Anand, A.; Oren, D.A.; Heninger, G.R.; Charney, D.S., and Krystal, J.H. Antidepressant effects of ketamine in depressed patients. *Biol Psychiatry*, **2000**, *47*(4), 351-4.

[3] Zarate, C.A., Jr.; Singh, J.B.; Carlson, P.J.; Brutsche, N.E.; Ameli, R.; Luckenbaugh, D.A.; Charney, D.S., and Manji, H.K. A randomized trial of an N-methyl-D-aspartate antagonist in treatment-resistant major depression. *Arch Gen Psychiatry*, **2006**, *63*(8), 856-64.

[4] Ruhe, H.G.; van Rooijen, G.; Spijker, J.; Peeters, F.P., and Schene, A.H. Staging methods for treatment resistant depression. A systematic review. *J Affect Disord*, **2012**, *137*(1-3), 35-45.

[5] McIntyre, R.S.; Filteau, M.J.; Martin, L.; Patry, S.; Carvalho, A.; Cha, D.S.; Barakat, M., and Miguelez, M. Treatment-resistant depression: definitions, review of the evidence, and algorithmic approach. *J Affect Disord*, **2014**, *156*, 1-7.

[6] Thomas, L.; Kessler, D.; Campbell, J.; Morrison, J.; Peters, T.J.; Williams, C.; Lewis, G., and Wiles, N. Prevalence of treatment-resistant depression in primary care: cross-sectional data. *Br J Gen Pract*, **2013**, *63*(617), e852-8.

[7] Duman, R.S. and Aghajanian, G.K. Synaptic dysfunction in depression: potential therapeutic targets. *Science*, **2012**, *338*(6103), 68-72.

[8] Kim, Y.K. and Na, K.S. Role of glutamate receptors and glial cells in the pathophysiology of treatment-resistant depression. *Prog Neuropsychopharmacol Biol Psychiatry*, **2016**, *70*, 117-26.

[9] Caddy, C.; Giaroli, G.; White, T.P.; Shergill, S.S., and Tracy, D.K. Ketamine as the prototype glutamatergic antidepressant: pharmacodynamic actions, and a systematic review and meta-analysis of efficacy. *Ther Adv Psychopharmacol*, **2014**, *4*(2), 75-99.

[10] Fond, G.; Loundou, A.; Rabu, C.; Macgregor, A.; Lancon, C.; Brittner, M.; Micoulaud-Franchi, J.A.; Richieri, R.; Courtet, P.; Abbar, M.; Roger, M.; Leboyer, M., and Boyer, L. Ketamine administration in depressive disorders: a systematic review and meta-analysis. *Psychopharmacology (Berl)*, **2014**, *231*(18), 3663-76.

[11] Xu, Y.; Hackett, M.; Carter, G.; Loo, C.; Galvez, V.; Glozier, N.; Glue, P.; Lapidus, K.; McGirr, A.; Somogyi, A.A.; Mitchell, P.B., and Rodgers, A. Effects of Low-Dose and Very Low-Dose Ketamine among Patients with Major Depression: a Systematic Review and Meta-Analysis. *Int J Neuropsychopharmacol*, **2016**, *19*(4).

[12] Newport, D.J.; Carpenter, L.L.; McDonald, W.M.; Potash, J.B.; Tohen, M.; Nemeroff, C.B.; Biomarkers, A.P.A.C.o.R.T.F.o.N., and Treatments. Ketamine and Other NMDA Antagonists: Early Clinical Trials and Possible Mechanisms in Depression. *Am J Psychiatry*, **2015**, *172*(10), 950-66.

[13] Romeo, B.; Choucha, W.; Fossati, P., and Rotge, J.Y. Meta-analysis of short- and mid-term efficacy of ketamine in unipolar and bipolar depression. *Psychiatry Res*, **2015**, *230*(2), 682-8.

[14] Sanacora, G.; Zarate, C.A.; Krystal, J.H., and Manji, H.K. Targeting the glutamatergic system to develop novel, improved therapeutics for mood disorders. *Nat Rev Drug Discov*, **2008**, *7*(5), 426-37.

[15] WHO. Depression: A Global Crisis. *World Health Organisation - World Federation for Mental Health*, **2012**.

[16] Murray, C.J. and Lopez, A.D. Evidence-based health policy--lessons from the Global Burden of Disease Study. *Science*, **1996**, *274*(5288), 740-3.

[17] Nautiyal, K.M. and Hen, R. Serotonin receptors in depression: from A to B. *F1000Res*, **2017**, *6*, 123.

[18] Mrazek, D.A.; Hornberger, J.C.; Altar, C.A., and Degtiar, I. A review of the clinical, economic, and societal burden of treatment-resistant depression: 1996-2013. *Psychiatr Serv*, **2014**, *65*(8), 977-87.

[19] Browne, C.A. and Lucki, I. Antidepressant effects of ketamine: mechanisms underlying fast-acting novel antidepressants. *Front Pharmacol*, **2013**, *4*, 161.

[20] Pham, T.H.; Defaix, C.; Xu, X.; Deng, S.-X.; Fabresse, N.; Alvarez, J.-C.; Landry, D.W.; Brachman, R.A.; Denny, C.A., and Gardier, A.M. Common neurotransmission recruited in (R,S)-ketamine and (2R,6R)-hydroxynorketamine-induced sustained antidepressant-like effects. *Biological Psychiatry*, **2017**.

[21] Pham, T.H.; Mendez-David, I.; Defaix, C.; Guiard, B.P.; Tritschler, L.; David, D.J., and Gardier, A.M. Ketamine treatment involves medial prefrontal cortex serotonin to induce a rapid antidepressant-like activity in BALB/cJ mice. *Neuropharmacology*, **2017**, *112*, 198-209.

[22] Caddy, C.; Amit, B.H.; McCloud, T.L.; Rendell, J.M.; Furukawa, T.A.; McShane, R.; Hawton, K., and Cipriani, A. Ketamine and other glutamate receptor modulators for depression in adults. *Cochrane Database Syst Rev*, **2015**, (9), CD011612.

[23] Papadimitropoulou, K.; Vossen, C.; Karabis, A.; Donatti, C., and Kubitz, N. Comparative efficacy and tolerability of pharmacological and somatic interventions in adult patients with treatment-resistant depression: a systematic review and network meta-analysis. *Curr Med Res Opin*, **2017**, *33*(4), 701-711.

[24] Kokkinou, M.; Ashok, A.H., and Howes, O.D. The effects of ketamine on dopaminergic function: meta-analysis and review of the implications for neuropsychiatric disorders. *Mol Psychiatry*, **2018**, *23*(1), 59-69.

[25] Romeo, B.; Choucha, W.; Fossati, P., and Rotge, J.Y. [Clinical and biological predictors of ketamine response in treatment-resistant major depression: Review]. *Encephale*, **2017**, *43*(4), 354-362.

[26] Li, N.; Lee, B.; Liu, R.J.; Banasr, M.; Dwyer, J.M.; Iwata, M.; Li, X.Y.; Aghajanian, G., and Duman, R.S. mTOR-dependent synapse formation underlies the rapid antidepressant effects of NMDA antagonists. *Science*, **2010**, *329*(5994), 959-64.

[27] Duman, R.S.; Aghajanian, G.K.; Sanacora, G., and Krystal, J.H. Synaptic plasticity and depression: new insights from stress and rapid-acting antidepressants. *Nat Med*, **2016**, *22*(3), 238-49.

[28] Can, A.; Zanos, P.; Moaddel, R.; Kang, H.J.; Dossou, K.S.; Wainer, I.W.; Cheer, J.F.; Frost, D.O.; Huang, X.P., and Gould, T.D. Effects of Ketamine and Ketamine Metabolites on Evoked Striatal Dopamine Release, Dopamine Receptors, and Monoamine Transporters. *J Pharmacol Exp Ther*, **2016**, *359*(1), 159-70.

[29] Zanos, P.; Moaddel, R.; Morris, P.J.; Georgiou, P.; Fischell, J.; Elmer, G.I.; Alkondon, M.; Yuan, P.; Pribut, H.J.; Singh, N.S.; Dossou, K.S.; Fang, Y.; Huang, X.P.; Mayo, C.L.; Wainer, I.W.; Albuquerque, E.X.; Thompson, S.M.; Thomas, C.J.; Zarate, C.A., Jr., and Gould, T.D. NMDAR inhibition-independent antidepressant actions of ketamine metabolites. *Nature*, **2016**, *533*(7604), 481-6.

[30] Amargos-Bosch, M.; Lopez-Gil, X.; Artigas, F., and Adell, A. Clozapine and olanzapine, but not haloperidol, suppress serotonin efflux in the medial prefrontal cortex elicited by phencyclidine and ketamine. *Int J Neuropsychopharmacol*, **2006**, *9*(5), 565-73.

[31] Razoux, F.; Garcia, R., and Lena, I. Ketamine, at a dose that disrupts motor behavior and latent inhibition, enhances prefrontal cortex synaptic efficacy and glutamate release in the nucleus accumbens. *Neuropsychopharmacology*, **2007**, *32*(3), 719-27.

[32] Farahmandfar, M.; Akbarabadi, A.; Bakhtazad, A., and Zarrindast, M.R. Recovery from ketamine-induced amnesia by blockade of GABA-A receptor in the medial prefrontal cortex of mice. *Neuroscience*, **2017**, *344*, 48-55.

[33] Nestler, E.J.; Gould, E.; Manji, H.; Buncan, M.; Duman, R.S.; Greshenfeld, H.K.; Hen, R.; Koester, S.; Lederhendler, I.; Meaney, M.; Robbins, T.; Winsky, L., and Zalcman, S. Preclinical models: status of basic research in depression. *Biol Psychiatry*, **2002**, *52*(6), 503-28.

[34] Miller, O.H.; Moran, J.T., and Hall, B.J. Two cellular hypotheses explaining the initiation of ketamine's antidepressant actions: Direct inhibition and disinhibition. *Neuropharmacology*, **2016**, *100*, 17-26.

[35] Lord, B.; Wintmolders, C.; Langlois, X.; Nguyen, L.; Lovenberg, T., and Bonaventure, P. Comparison of the ex vivo receptor occupancy profile of ketamine to several NMDA receptor antagonists in mouse hippocampus. *Eur J Pharmacol*, **2013**, *715*(1-3), 21-5.

[36] Murray, F.; Kennedy, J.; Hutson, P.H.; Elliot, J.; Huscroft, I.; Mohnen, K.; Russell, M.G., and Grimwood, S. Modulation of [3H]MK-801 binding to NMDA receptors in vivo and in vitro. *Eur J Pharmacol*, **2000**, *397*(2-3), 263-70.

[37] Gideons, E.S.; Kavalali, E.T., and Monteggia, L.M. Mechanisms underlying differential effectiveness of memantine and ketamine in rapid antidepressant responses. *Proc Natl Acad Sci U S A*, **2014**, *111*(23), 8649-54.

[38] Domino, E.F. Taming the ketamine tiger. 1965. *Anesthesiology*, **2010**, *113*(3), 678-84.

[39] Muller, J.; Pentyala, S.; Dilger, J., and Pentyala, S. Ketamine enantiomers in the rapid and sustained antidepressant effects. *Ther Adv Psychopharmacol*, **2016**, *6*(3), 185-92.

[40] Maxwell, C.R.; Ehrlichman, R.S.; Liang, Y.; Trief, D.; Kanes, S.J.; Karp, J., and Siegel, S.J. Ketamine produces lasting disruptions in encoding of sensory stimuli. *J Pharmacol Exp Ther*, **2006**, *316*(1), 315-24.

[41] Morris, P.J.; Moaddel, R.; Zanos, P.; Moore, C.E.; Gould, T.; Zarate, C.A., Jr., and Thomas, C.J. Synthesis and N-Methyl-d-aspartate (NMDA) Receptor Activity of Ketamine Metabolites. *Org Lett*, **2017**, *19*(17), 4572-4575.

[42] Fukumoto, K.; Iijima, M., and Chaki, S. The Antidepressant Effects of an mGlu2/3 Receptor Antagonist and Ketamine Require AMPA Receptor Stimulation in the mPFC and Subsequent Activation of the 5-HT Neurons in the DRN. *Neuropsychopharmacology*, **2016**, *41*(4), 1046-56.

[43] Moghaddam, B.; Adams, B.; Verma, A., and Daly, D. Activation of glutamatergic neurotransmission by ketamine: a novel step in the pathway from NMDA receptor blockade to dopaminergic and cognitive disruptions associated with the prefrontal cortex. *J Neurosci*, **1997**, *17*(8), 2921-7.

[44] Li, N.; Liu, R.J.; Dwyer, J.M.; Banasr, M.; Lee, B.; Son, H.; Li, X.Y.; Aghajanian, G., and Duman, R.S. Glutamate N-methyl-D-aspartate receptor antagonists rapidly reverse behavioral and synaptic deficits caused by chronic stress exposure. *Biol Psychiatry*, **2011**, *69*(8), 754-61.

[45] Liu, R.J.; Fuchikami, M.; Dwyer, J.M.; Lepack, A.E.; Duman, R.S., and Aghajanian, G.K. GSK-3 inhibition potentiates the synaptogenic and antidepressant-like effects of subthreshold doses of ketamine. *Neuropsychopharmacology*, **2013**, *38*(11), 2268-77.

[46] Rantamaki, T. and Yalcin, I. Antidepressant drug action--From rapid changes on network function to network rewiring. *Prog Neuropsychopharmacol Biol Psychiatry*, **2016**, *64*, 285-92.

[47] Autry, A.E.; Adachi, M.; Nosyreva, E.; Na, E.S.; Los, M.F.; Cheng, P.F.; Kavalali, E.T., and Monteggia, L.M. NMDA receptor blockade at rest triggers rapid behavioural antidepressant responses. *Nature*, **2011**, *475*(7354), 91-5.

[48] Nosyreva, E.; Szabla, K.; Autry, A.E.; Ryazanov, A.G.; Monteggia, L.M., and Kavalali, E.T. Acute suppression of spontaneous neurotransmission drives synaptic potentiation. *J Neurosci*, **2013**, *33*(16), 6990-7002.

[49] Lindholm, J.S.; Autio, H.; Vesa, L.; Antila, H.; Lindemann, L.; Hoener, M.C.; Skolnick, P.; Rantamaki, T., and Castren, E. The antidepressant-like effects of glutamatergic drugs ketamine and AMPA receptor potentiator LY 451646 are preserved in bdnf(+)/(-) heterozygous null mice. *Neuropharmacology*, **2012**, *62*(1), 391-7.

[50] Liu, R.J.; Lee, F.S.; Li, X.Y.; Bambico, F.; Duman, R.S., and Aghajanian, G.K. Brain-derived neurotrophic factor Val66Met allele impairs basal and ketamine-stimulated synaptogenesis in prefrontal cortex. *Biol Psychiatry*, **2012**, *71*(11), 996-1005.

[51] Laje, G.; Lally, N.; Mathews, D.; Brutsche, N.; Chemerinski, A.; Akula, N.; Kelmendi, B.; Simen, A.; McMahon, F.J.; Sanacora, G., and Zarate, C., Jr. Brain-derived neurotrophic factor Val66Met polymorphism and antidepressant efficacy of ketamine in depressed patients. *Biol Psychiatry*, **2012**, *72*(11), e27-8.

[52] Huang, B.S. and Liston, C. Cortex-wide optical imaging and network analysis of antidepressant effects. *Brain*, **2017**, *140*(8), 2074-2078.

[53] Yang, C.; Qu, Y.; Abe, M.; Nozawa, D.; Chaki, S., and Hashimoto, K. (R)-ketamine shows greater potency and longer lasting antidepressant effects than its metabolite (2R,6R)-hydroxynorketamine. *Biological Psychiatry*, **2016**.

[54] Zhang, J.C.; Li, S.X., and Hashimoto, K. R (-)-ketamine shows greater potency and longer lasting antidepressant effects than S (+)-ketamine. *Pharmacol Biochem Behav*, **2014**, *116*, 137-41.

[55] Shirayama, Y. and Hashimoto, K. Effects of a single bilateral infusion of R-ketamine in the rat brain regions of a learned helplessness model of depression. *Eur Arch Psychiatry Clin Neurosci*, **2017**, *267*(2), 177-182.

[56] Yang, C.; Han, M.; Zhang, J.C.; Ren, Q., and Hashimoto, K. Loss of parvalbumin-immunoreactivity in mouse brain regions after repeated intermittent administration of esketamine, but not R-ketamine. *Psychiatry Res*, **2016**, *239*, 281-3.

[57] Krystal, J.H.; Sanacora, G.; Blumberg, H.; Anand, A.; Charney, D.S.; Marek, G.; Epperson, C.N.; Goddard, A., and Mason, G.F. Glutamate and GABA systems as targets for novel antidepressant and mood-stabilizing treatments. *Mol Psychiatry*, **2002**, *7 Suppl 1*, S71-80.

[58] Douglas, R.J. and Martin, K.A. Mapping the matrix: the ways of neocortex. *Neuron*, **2007**, *56*(2), 226-38.

[59] Lodge, D. The history of the pharmacology and cloning of ionotropic glutamate receptors and the development of idiosyncratic nomenclature. *Neuropharmacology*, **2009**, *56*(1), 6-21.

[60] Choi, D.W.; Maulucci-Gedde, M., and Kriegstein, A.R. Glutamate neurotoxicity in cortical cell culture. *J Neurosci*, **1987**, *7*(2), 357-68.

[61] Balazs, R. Trophic effect of glutamate. *Curr Top Med Chem*, **2006**, *6*(10), 961-8.

[62] Petroff, O.A. GABA and glutamate in the human brain. *Neuroscientist*, **2002**, *8*(6), 562-73.

[63] Hartmann, J.; Dedic, N.; Pohlmann, M.L.; Hausl, A.; Karst, H.; Engelhardt, C.; Westerholz, S.; Wagner, K.V.; Labermaier, C.; Hoeijmakers, L.; Kertokarijo, M.; Chen, A.; Joels, M.; Deussing, J.M., and Schmidt, M.V. Forebrain glutamatergic, but not GABAergic, neurons mediate anxiogenic effects of the glucocorticoid receptor. *Mol Psychiatry*, **2017**, *22*(3), 466-475.

[64] Lener, M.S.; Niciu, M.J.; Ballard, E.D.; Park, M.; Park, L.T.; Nugent, A.C., and Zarate, C.A., Jr. Glutamate and Gamma-Aminobutyric Acid Systems in the Pathophysiology of Major Depression and Antidepressant Response to Ketamine. *Biol Psychiatry*, **2017**, *81*(10), 886-897.

[65] Ren, Z.; Pribiag, H.; Jefferson, S.J.; Shorey, M.; Fuchs, T.; Stellwagen, D., and Luscher, B. Bidirectional Homeostatic Regulation of a Depression-Related Brain State by Gamma-Aminobutyric Acidergic Deficits and Ketamine Treatment. *Biol Psychiatry*, **2016**, *80*(6), 457-68.

[66] Sanacora, G.; Treccani, G., and Popoli, M. Towards a glutamate hypothesis of depression: an emerging frontier of neuropsychopharmacology for mood disorders. *Neuropharmacology*, **2012**, *62*(1), 63-77.

[67] Baker, K.G.; Halliday, G.M.; Hornung, J.P.; Geffen, L.B.; Cotton, R.G., and Tork, I. Distribution, morphology and number of monoamine-synthesizing and substance P-containing neurons in the human dorsal raphe nucleus. *Neuroscience*, **1991**, *42*(3), 757-75.

[68] Herculano-Houzel, S. The human brain in numbers: a linearly scaled-up primate brain. *Front Hum Neurosci*, **2009**, *3*, 31.

[69] Heresco-Levy, U.; Gelfin, G.; Bloch, B.; Levin, R.; Edelman, S.; Javitt, D.C., and Kremer, I. A randomized add-on trial of high-dose D-cycloserine for treatment-resistant depression. *Int J Neuropsychopharmacol*, **2013**, *16*(3), 501-6.

[70] Ishimura, K.; Takeuchi, Y.; Fujiwara, K.; Tominaga, M.; Yoshioka, H., and Sawada, T. Quantitative analysis of the distribution of serotonin-immunoreactive cell bodies in the mouse brain. *Neurosci Lett*, **1988**, *91*(3), 265-70.

[71] Hardingham, G.E. and Bading, H. Synaptic versus extrasynaptic NMDA receptor signalling: implications for neurodegenerative disorders. *Nat Rev Neurosci*, **2010**, *11*(10), 682-96.

[72] Magistretti, P.J. Neuron-glia metabolic coupling and plasticity. *J Exp Biol*, **2006**, *209*(Pt 12), 2304-11.

[73] Perez-Alvarez, A. and Araque, A. Astrocyte-neuron interaction at tripartite synapses. *Curr Drug Targets*, **2013**, *14*(11), 1220-4.

[74] Gunduz-Bruce, H. The acute effects of NMDA antagonism: from the rodent to the human brain. *Brain Res Rev*, **2009**, *60*(2), 279-86.

[75] Rothstein, J.D.; Dykes-Hoberg, M.; Pardo, C.A.; Bristol, L.A.; Jin, L.; Kuncl, R.W.; Kanai, Y.; Hediger, M.A.; Wang, Y.; Schielke, J.P., and Welty, D.F. Knockout of glutamate transporters reveals a major role for astroglial transport in excitotoxicity and clearance of glutamate. *Neuron*, **1996**, *16*(3), 675-86.

[76] Zheng, K.; Scimemi, A., and Rusakov, D.A. Receptor actions of synaptically released glutamate: the role of transporters on the scale from nanometers to microns. *Biophys J*, **2008**, *95*(10), 4584-96.

[77] Verkhratsky, A.; Rodriguez, J.J., and Steardo, L. Astrogliopathology: a central element of neuropsychiatric diseases? *Neuroscientist*, **2014**, *20*(6), 576-88.

[78] Kim, J.S.; Schmid-Burgk, W.; Claus, D., and Kornhuber, H.H. Increased serum glutamate in depressed patients. *Arch Psychiatr Nervenkr (1970)*, **1982**, *232*(4), 299-304.
[79] Altamura, C.A.; Mauri, M.C.; Ferrara, A.; Moro, A.R.; D'Andrea, G., and Zamberlan, F. Plasma and platelet excitatory amino acids in psychiatric disorders. *Am J Psychiatry*, **1993**, *150*(11), 1731-3.
[80] Mauri, M.C.; Ferrara, A.; Boscati, L.; Bravin, S.; Zamberlan, F.; Alecci, M., and Invernizzi, G. Plasma and platelet amino acid concentrations in patients affected by major depression and under fluvoxamine treatment. *Neuropsychobiology*, **1998**, *37*(3), 124-9.
[81] Mitani, H.; Shirayama, Y.; Yamada, T.; Maeda, K.; Ashby, C.R., Jr., and Kawahara, R. Correlation between plasma levels of glutamate, alanine and serine with severity of depression. *Prog Neuropsychopharmacol Biol Psychiatry*, **2006**, *30*(6), 1155-8.
[82] Levine, J.; Panchalingam, K.; Rapoport, A.; Gershon, S.; McClure, R.J., and Pettegrew, J.W. Increased cerebrospinal fluid glutamine levels in depressed patients. *Biol Psychiatry*, **2000**, *47*(7), 586-93.
[83] Maes, M.; Verkerk, R.; Vandoolaeghe, E.; Lin, A., and Scharpe, S. Serum levels of excitatory amino acids, serine, glycine, histidine, threonine, taurine, alanine and arginine in treatment-resistant depression: modulation by treatment with antidepressants and prediction of clinical responsivity. *Acta Psychiatr Scand*, **1998**, *97*(4), 302-8.
[84] Kucukibrahimoglu, E.; Saygin, M.Z.; Caliskan, M.; Kaplan, O.K.; Unsal, C., and Goren, M.Z. The change in plasma GABA, glutamine and glutamate levels in fluoxetine- or S-citalopram-treated female patients with major depression. *Eur J Clin Pharmacol*, **2009**, *65*(6), 571-7.
[85] Auer, D.P.; Putz, B.; Kraft, E.; Lipinski, B.; Schill, J., and Holsboer, F. Reduced glutamate in the anterior cingulate cortex in depression: an in vivo proton magnetic resonance spectroscopy study. *Biol Psychiatry*, **2000**, *47*(4), 305-13.
[86] Mirza, Y.; Tang, J.; Russell, A.; Banerjee, S.P.; Bhandari, R.; Ivey, J.; Rose, M.; Moore, G.J., and Rosenberg, D.R. Reduced anterior cingulate cortex glutamatergic concentrations in childhood major depression. *J Am Acad Child Adolesc Psychiatry*, **2004**, *43*(3), 341-8.
[87] Pfleiderer, B.; Michael, N.; Erfurth, A.; Ohrmann, P.; Hohmann, U.; Wolgast, M.; Fiebich, M.; Arolt, V., and Heindel, W. Effective electroconvulsive therapy reverses glutamate/glutamine deficit in the left anterior cingulum of unipolar depressed patients. *Psychiatry Res*, **2003**, *122*(3), 185-92.
[88] Michael, N.; Erfurth, A.; Ohrmann, P.; Arolt, V.; Heindel, W., and Pfleiderer, B. Metabolic changes within the left dorsolateral prefrontal cortex occurring with electroconvulsive therapy in patients with treatment resistant unipolar depression. *Psychol Med*, **2003**, *33*(7), 1277-84.
[89] Hasler, G.; van der Veen, J.W.; Tumonis, T.; Meyers, N.; Shen, J., and Drevets, W.C. Reduced prefrontal glutamate/glutamine and gamma-aminobutyric acid levels in major depression determined using proton magnetic resonance spectroscopy. *Arch Gen Psychiatry*, **2007**, *64*(2), 193-200.
[90] Hashimoto, K. The role of glutamate on the action of antidepressants. *Prog Neuropsychopharmacol Biol Psychiatry*, **2011**, *35*(7), 1558-68.
[91] Bhagwagar, Z.; Wylezinska, M.; Jezzard, P.; Evans, J.; Ashworth, F.; Sule, A.; Matthews, P.M., and Cowen, P.J. Reduction in occipital cortex gamma-aminobutyric acid concentrations in medication-free recovered unipolar depressed and bipolar subjects. *Biol Psychiatry*, **2007**, *61*(6), 806-12.
[92] Sapolsky, R.M. The possibility of neurotoxicity in the hippocampus in major depression: a primer on neuron death. *Biol Psychiatry*, **2000**, *48*(8), 755-65.
[93] Moghaddam, B. Stress preferentially increases extraneuronal levels of excitatory amino acids in the prefrontal cortex: comparison to hippocampus and basal ganglia. *J Neurochem*, **1993**, *60*(5), 1650-7.
[94] Musazzi, L.; Milanese, M.; Farisello, P.; Zappettini, S.; Tardito, D.; Barbiero, V.S.; Bonifacino, T.; Mallei, A.; Baldelli, P.; Racagni, G.; Raiteri, M.; Benfenati, F.; Bonanno, G., and Popoli, M. Acute stress increases depolarization-evoked glutamate release in the rat prefrontal/frontal cortex: the dampening action of antidepressants. *PLoS One*, **2010**, *5*(1), e8566.
[95] Popoli, M.; Yan, Z.; McEwen, B.S., and Sanacora, G. The stressed synapse: the impact of stress and glucocorticoids on glutamate transmission. *Nat Rev Neurosci*, **2011**, *13*(1), 22-37.
[96] Bagley, J. and Moghaddam, B. Temporal dynamics of glutamate efflux in the prefrontal cortex and in the hippocampus following repeated stress: effects of pretreatment with saline or diazepam. *Neuroscience*, **1997**, *77*(1), 65-73.
[97] Lowy, M.T.; Wittenberg, L., and Yamamoto, B.K. Effect of acute stress on hippocampal glutamate levels and spectrin proteolysis in young and aged rats. *J Neurochem*, **1995**, *65*(1), 268-74.
[98] Reznikov, L.R.; Grillo, C.A.; Piroli, G.G.; Pasumarthi, R.K.; Reagan, L.P., and Fadel, J. Acute stress-mediated increases in extracellular glutamate levels in the rat amygdala: differential effects of antidepressant treatment. *Eur J Neurosci*, **2007**, *25*(10), 3109-14.
[99] Bonanno, G.; Giambelli, R.; Raiteri, L.; Tiraboschi, E.; Zappettini, S.; Musazzi, L.; Raiteri, M.; Racagni, G., and Popoli, M. Chronic antidepressants reduce depolarization-evoked glutamate release and protein interactions favoring formation of SNARE complex in hippocampus. *J Neurosci*, **2005**, *25*(13), 3270-9.
[100] Michael-Titus, A.T.; Bains, S.; Jeetle, J., and Whelpton, R. Imipramine and phenelzine decrease glutamate overflow in the prefrontal cortex--a possible mechanism of neuroprotection in major depression? *Neuroscience*, **2000**, *100*(4), 681-4.
[101] Tokarski, K.; Bobula, B.; Wabno, J., and Hess, G. Repeated administration of imipramine attenuates glutamatergic transmission in rat frontal cortex. *Neuroscience*, **2008**, *153*(3), 789-95.
[102] Li, C.X.; Wang, Y.; Gao, H.; Pan, W.J.; Xiang, Y.; Huang, M., and Lei, H. Cerebral metabolic changes in a depression-like rat model of chronic forced swimming studied by ex vivo high resolution 1H magnetic resonance spectroscopy. *Neurochem Res*, **2008**, *33*(11), 2342-9.
[103] Wang, W.; Guo, H.; Zhang, S.X.; Li, J.; Cheng, K.; Bai, S.J.; Yang, D.Y.; Wang, H.Y.; Liang, Z.H.; Liao, L.; Sun, L., and Xie, P. Targeted Metabolomic Pathway Analysis and Validation Revealed Glutamatergic Disorder in the Prefrontal Cortex among the Chronic Social Defeat Stress Mice Model of Depression. *J Proteome Res*, **2016**, *15*(10), 3784-3792.
[104] Jett, J.D.; Bulin, S.E.; Hatherall, L.C.; McCartney, C.M., and Morilak, D.A. Deficits in cognitive flexibility induced by chronic unpredictable stress are associated with impaired glutamate neurotransmission in the rat medial prefrontal cortex. *Neuroscience*, **2017**, *346*, 284-297.
[105] Ding, X.F.; Li, Y.H.; Chen, J.X.; Sun, L.J.; Jiao, H.Y.; Wang, X.X., and Zhou, Y. Involvement of the glutamate/glutamine cycle and glutamate transporter GLT-1 in antidepressant-like effects of Xiao Yao san on chronically stressed mice. *BMC Complement Altern Med*, **2017**, *17*(1), 326.
[106] Rubio-Casillas, A. and Fernandez-Guasti, A. The dose makes the poison: from glutamate-mediated neurogenesis to neuronal atrophy and depression. *Rev Neurosci*, **2016**, *27*(6), 599-622.
[107] Jett, J.D.; Boley, A.M.; Girotti, M.; Shah, A.; Lodge, D.J., and Morilak, D.A. Antidepressant-like cognitive and behavioral effects of acute ketamine administration associated with plasticity in the ventral hippocampus to medial prefrontal cortex pathway. *Psychopharmacology (Berl)*, **2015**, *232*(17), 3123-33.
[108] Murrough, J.W.; Abdallah, C.G., and Mathew, S.J. Targeting glutamate signalling in depression: progress and prospects. *Nat Rev Drug Discov*, **2017**.
[109] Shepard, R. and Coutellier, L. Changes in the Prefrontal Glutamatergic and Parvalbumin Systems of Mice Exposed to Unpredictable Chronic Stress. *Mol Neurobiol*, **2017**.
[110] Barnes, J.; Mondelli, V., and Pariante, C.M. Genetic Contributions of Inflammation to Depression. *Neuropsychopharmacology*, **2017**, *42*(1), 81-98.
[111] Miller, A.H. and Raison, C.L. The role of inflammation in depression: from evolutionary imperative to modern treatment target. *Nat Rev Immunol*, **2016**, *16*(1), 22-34.
[112] Haroon, E. and Miller, A.H. Inflammation Effects on Brain Glutamate in Depression: Mechanistic Considerations and Treatment Implications. *Curr Top Behav Neurosci*, **2017**, *31*, 173-198.
[113] Haroon, E.; Fleischer, C.C.; Felger, J.C.; Chen, X.; Woolwine, B.J.; Patel, T.; Hu, X.P., and Miller, A.H. Conceptual convergence: increased inflammation is associated with increased basal ganglia glutamate in patients with major depression. *Mol Psychiatry*, **2016**, *21*(10), 1351-7.
[114] Haroon, E.; Miller, A.H., and Sanacora, G. Inflammation, Glutamate, and Glia: A Trio of Trouble in Mood Disorders. *Neuropsychopharmacology*, **2017**, *42*(1), 193-215.
[115] Cornwell, B.R.; Salvadore, G.; Furey, M.; Marquardt, C.A.; Brutsche, N.E.; Grillon, C., and Zarate, C.A., Jr. Synaptic potentiation is critical

for rapid antidepressant response to ketamine in treatment-resistant major depression. *Biol Psychiatry*, **2012**, *72*(7), 555-61.
[116] Milak, M.S.; Proper, C.J.; Mulhern, S.T.; Parter, A.L.; Kegeles, L.S.; Ogden, R.T.; Mao, X.; Rodriguez, C.I.; Oquendo, M.A.; Suckow, R.F.; Cooper, T.B.; Keilp, J.G.; Shungu, D.C., and Mann, J.J. A pilot in vivo proton magnetic resonance spectroscopy study of amino acid neurotransmitter response to ketamine treatment of major depressive disorder. *Mol Psychiatry*, **2016**, *21*(3), 320-7.
[117] Rotroff, D.M.; Corum, D.G.; Motsinger-Reif, A.; Fiehn, O.; Bottrel, N.; Drevets, W.C.; Singh, J.; Salvadore, G., and Kaddurah-Daouk, R. Metabolomic signatures of drug response phenotypes for ketamine and esketamine in subjects with refractory major depressive disorder: new mechanistic insights for rapid acting antidepressants. *Transl Psychiatry*, **2016**, *6*(9), e894.
[118] Chowdhury, G.M.; Zhang, J.; Thomas, M.; Banasr, M.; Ma, X.; Pittman, B.; Bristow, L.; Schaeffer, E.; Duman, R.S.; Rothman, D.L.; Behar, K.L., and Sanacora, G. Transiently increased glutamate cycling in rat PFC is associated with rapid onset of antidepressant-like effects. *Mol Psychiatry*, **2017**, *22*(1), 120-126.
[119] Melo, A.; Kokras, N.; Dalla, C.; Ferreira, C.; Ventura-Silva, A.P.; Sousa, N., and Pego, J.M. The positive effect on ketamine as a priming adjuvant in antidepressant treatment. *Transl Psychiatry*, **2015**, *5*, e573.
[120] Gardier, A.M. Antidepressant activity: contribution of brain microdialysis in knock-out mice to the understanding of BDNF/5-HT transporter/5-HT autoreceptor interactions. *Front Pharmacol*, **2013**, *4*, 98.
[121] Lorrain, D.S.; Baccei, C.S.; Bristow, L.J.; Anderson, J.J., and Varney, M.A. Effects of ketamine and N-methyl-D-aspartate on glutamate and dopamine release in the rat prefrontal cortex: modulation by a group II selective metabotropic glutamate receptor agonist LY379268. *Neuroscience*, **2003**, *117*(3), 697-706.
[122] Zhu, X.; Ye, G.; Wang, Z.; Luo, J., and Hao, X. Sub-anesthetic doses of ketamine exert antidepressant-like effects and upregulate the expression of glutamate transporters in the hippocampus of rats. *Neurosci Lett*, **2017**, *639*, 132-137.
[123] Gladding, C.M. and Raymond, L.A. Mechanisms underlying NMDA receptor synaptic/extrasynaptic distribution and function. *Mol Cell Neurosci*, **2011**, *48*(4), 308-20.
[124] Traynelis, S.F.; Wollmuth, L.P.; McBain, C.J.; Menniti, F.S.; Vance, K.M.; Ogden, K.K.; Hansen, K.B.; Yuan, H.; Myers, S.J., and Dingledine, R. Glutamate receptor ion channels: structure, regulation, and function. *Pharmacol Rev*, **2010**, *62*(3), 405-96.
[125] Nikolaev, M.V.; Magazanik, L.G., and Tikhonov, D.B. Influence of external magnesium ions on the NMDA receptor channel block by different types of organic cations. *Neuropharmacology*, **2012**, *62*(5-6), 2078-85.
[126] Pozzi, L.; Pollak Dorocic, I.; Wang, X.; Carlen, M., and Meletis, K. Mice lacking NMDA receptors in parvalbumin neurons display normal depression-related behavior and response to antidepressant action of NMDAR antagonists. *PLoS One*, **2014**, *9*(1), e83879.
[127] Miller, O.H.; Yang, L.; Wang, C.C.; Hargroder, E.A.; Zhang, Y.; Delpire, E., and Hall, B.J. GluN2B-containing NMDA receptors regulate depression-like behavior and are critical for the rapid antidepressant actions of ketamine. *Elife*, **2014**, *3*, e03581.
[128] Boyer, P.A.; Skolnick, P., and Fossom, L.H. Chronic administration of imipramine and citalopram alters the expression of NMDA receptor subunit mRNAs in mouse brain. A quantitative in situ hybridization study. *J Mol Neurosci*, **1998**, *10*(3), 219-33.
[129] Lee, Y.A. and Goto, Y. Chronic stress modulation of prefrontal cortical NMDA receptor expression disrupts limbic structure-prefrontal cortex interaction. *Eur J Neurosci*, **2011**, *34*(3), 426-36.
[130] Pittaluga, A.; Raiteri, L.; Longordo, F.; Luccini, E.; Barbiero, V.S.; Racagni, G.; Popoli, M., and Raiteri, M. Antidepressant treatments and function of glutamate ionotropic receptors mediating amine release in hippocampus. *Neuropharmacology*, **2007**, *53*(1), 27-36.
[131] Barbon, A.; Popoli, M.; La Via, L.; Moraschi, S.; Vallini, I.; Tardito, D.; Tiraboschi, E.; Musazzi, L.; Giambelli, R.; Gennarelli, M.; Racagni, G., and Barlati, S. Regulation of editing and expression of glutamate alpha-amino-propionic-acid (AMPA)/kainate receptors by antidepressant drugs. *Biol Psychiatry*, **2006**, *59*(8), 713-20.
[132] Groc, L.; Bard, L., and Choquet, D. Surface trafficking of N-methyl-D-aspartate receptors: physiological and pathological perspectives. *Neuroscience*, **2009**, *158*(1), 4-18.
[133] Deutschenbaur, L.; Beck, J.; Kiyhankhadiv, A.; Muhlhauser, M.; Borgwardt, S.; Walter, M.; Hasler, G.; Sollberger, D., and Lang, U.E. Role of calcium, glutamate and NMDA in major depression and therapeutic application. *Prog Neuropsychopharmacol Biol Psychiatry*, **2015**, *4*(64), 325-33.
[134] Paoletti, P.; Bellone, C., and Zhou, Q. NMDA receptor subunit diversity: impact on receptor properties, synaptic plasticity and disease. *Nat Rev Neurosci*, **2013**, *14*(6), 383-400.
[135] Marsden, W.N. Stressor-induced NMDAR dysfunction as a unifying hypothesis for the aetiology, pathogenesis and comorbidity of clinical depression. *Med Hypotheses*, **2011**, *77*(4), 508-28.
[136] Stanika, R.I.; Pivovarova, N.B.; Brantner, C.A.; Watts, C.A.; Winters, C.A., and Andrews, S.B. Coupling diverse routes of calcium entry to mitochondrial dysfunction and glutamate excitotoxicity. *Proc Natl Acad Sci U S A*, **2009**, *106*(24), 9854-9.
[137] Skolnick, P.; Popik, P., and Trullas, R. Glutamate-based antidepressants: 20 years on. *Trends Pharmacol Sci*, **2009**, *30*(11), 563-9.
[138] Pilc, A.; Wieronska, J.M., and Skolnick, P. Glutamate-based antidepressants: preclinical psychopharmacology. *Biol Psychiatry*, **2013**, *73*(12), 1125-32.
[139] Kiselycznyk, C.; Jury, N.J.; Halladay, L.R.; Nakazawa, K.; Mishina, M.; Sprengel, R.; Grant, S.G.; Svenningsson, P., and Holmes, A. NMDA receptor subunits and associated signaling molecules mediating antidepressant-related effects of NMDA-GluN2B antagonism. *Behav Brain Res*, **2015**, *287*, 89-95.
[140] Layer, R.T.; Popik, P.; Olds, T., and Skolnick, P. Antidepressant-like actions of the polyamine site NMDA antagonist, eliprodil (SL-82.0715). *Pharmacol Biochem Behav*, **1995**, *52*(3), 621-7.
[141] Bagot, R.C.; Tse, Y.C.; Nguyen, H.B.; Wong, A.S.; Meaney, M.J., and Wong, T.P. Maternal care influences hippocampal N-methyl-D-aspartate receptor function and dynamic regulation by corticosterone in adulthood. *Biol Psychiatry*, **2012**, *72*(6), 491-8.
[142] Johnson, J.W.; Glasgow, N.G., and Povysheva, N.V. Recent insights into the mode of action of memantine and ketamine. *Curr Opin Pharmacol*, **2015**, *20*, 54-63.
[143] Lenze, E.J.; Skidmore, E.R.; Begley, A.E.; Newcomer, J.W.; Butters, M.A., and Whyte, E.M. Memantine for late-life depression and apathy after a disabling medical event: a 12-week, double-blind placebo-controlled pilot study. *Int J Geriatr Psychiatry*, **2012**, *27*(9), 974-80.
[144] Zarate, C.A., Jr.; Singh, J.B.; Quiroz, J.A.; De Jesus, G.; Denicoff, K.K.; Luckenbaugh, D.A.; Manji, H.K., and Charney, D.S. A double-blind, placebo-controlled study of memantine in the treatment of major depression. *Am J Psychiatry*, **2006**, *163*(1), 153-5.
[145] Jimenez-Sanchez, L.; Campa, L.; Auberson, Y.P., and Adell, A. The role of GluN2A and GluN2B subunits on the effects of NMDA receptor antagonists in modeling schizophrenia and treating refractory depression. *Neuropsychopharmacology*, **2014**, *39*(11), 2673-80.
[146] Lu, W.; Shi, Y.; Jackson, A.C.; Bjorgan, K.; During, M.J.; Sprengel, R.; Seeburg, P.H., and Nicoll, R.A. Subunit composition of synaptic AMPA receptors revealed by a single-cell genetic approach. *Neuron*, **2009**, *62*(2), 254-68.
[147] Jensen, V.; Kaiser, K.M.; Borchardt, T.; Adelmann, G.; Rozov, A.; Burnashev, N.; Brix, C.; Frotscher, M.; Andersen, P.; Hvalby, O.; Sakmann, B.; Seeburg, P.H., and Sprengel, R. A juvenile form of postsynaptic hippocampal long-term potentiation in mice deficient for the AMPA receptor subunit GluR-A. *J Physiol*, **2003**, *553*(Pt 3), 843-56.
[148] Hayashi, T.; Umemori, H.; Mishina, M., and Yamamoto, T. The AMPA receptor interacts with and signals through the protein tyrosine kinase Lyn. *Nature*, **1999**, *397*(6714), 72-6.
[149] Anggono, V. and Huganir, R.L. Regulation of AMPA receptor trafficking and synaptic plasticity. *Curr Opin Neurobiol*, **2012**, *22*(3), 461-9.
[150] Shi, S.; Hayashi, Y.; Esteban, J.A., and Malinow, R. Subunit-specific rules governing AMPA receptor trafficking to synapses in hippocampal pyramidal neurons. *Cell*, **2001**, *105*(3), 331-43.
[151] Hayashi, Y.; Shi, S.H.; Esteban, J.A.; Piccini, A.; Poncer, J.C., and Malinow, R. Driving AMPA receptors into synapses by LTP and CaMKII: requirement for GluR1 and PDZ domain interaction. *Science*, **2000**, *287*(5461), 2262-7.
[152] Kasai, H.; Fukuda, M.; Watanabe, S.; Hayashi-Takagi, A., and Noguchi, J. Structural dynamics of dendritic spines in memory and cognition. *Trends Neurosci*, **2010**, *33*(3), 121-9.
[153] Marsden, W.N. Synaptic plasticity in depression: molecular, cellular and functional correlates. *Prog Neuropsychopharmacol Biol Psychiatry*, **2013**, *43*, 168-84.

[154] Andrasfalvy, B.K.; Smith, M.A.; Borchardt, T.; Sprengel, R., and Magee, J.C. Impaired regulation of synaptic strength in hippocampal neurons from GluR1-deficient mice. *J Physiol*, **2003**, *552*(Pt 1), 35-45.

[155] Zamanillo, D.; Sprengel, R.; Hvalby, O.; Jensen, V.; Burnashev, N.; Rozov, A.; Kaiser, K.M.; Koster, H.J.; Borchardt, T.; Worley, P.; Lubke, J.; Frotscher, M.; Kelly, P.H.; Sommer, B.; Andersen, P.; Seeburg, P.H., and Sakmann, B. Importance of AMPA receptors for hippocampal synaptic plasticity but not for spatial learning. *Science*, **1999**, *284*(5421), 1805-11.

[156] Rosa, M.L.; Guimaraes, F.S.; Pearson, R.C., and Del Bel, E.A. Effects of single or repeated restraint stress on GluR1 and GluR2 flip and flop mRNA expression in the hippocampal formation. *Brain Res Bull*, **2002**, *59*(2), 117-24.

[157] Schwendt, M. and Jezova, D. Gene expression of two glutamate receptor subunits in response to repeated stress exposure in rat hippocampus. *Cell Mol Neurobiol*, **2000**, *20*(3), 319-29.

[158] Duric, V.; Banasr, M.; Stockmeier, C.A.; Simen, A.A.; Newton, S.S.; Overholser, J.C.; Jurjus, G.J.; Dieter, L., and Duman, R.S. Altered expression of synapse and glutamate related genes in post-mortem hippocampus of depressed subjects. *Int J Neuropsychopharmacol*, **2013**, *16*(1), 69-82.

[159] Kallarackal, A.J.; Kvarta, M.D.; Cammarata, E.; Jaberi, L.; Cai, X.; Bailey, A.M., and Thompson, S.M. Chronic stress induces a selective decrease in AMPA receptor-mediated synaptic excitation at hippocampal temporoammonic-CA1 synapses. *J Neurosci*, **2013**, *33*(40), 15669-74.

[160] Toth, E.; Gersner, R.; Wilf-Yarkoni, A.; Raizel, H.; Dar, D.E.; Richter-Levin, G.; Levit, O., and Zangen, A. Age-dependent effects of chronic stress on brain plasticity and depressive behavior. *J Neurochem*, **2008**, *107*(2), 522-32.

[161] Naylor, P.; Stewart, C.A.; Wright, S.R.; Pearson, R.C., and Reid, I.C. Repeated ECS induces GluR1 mRNA but not NMDAR1A-G mRNA in the rat hippocampus. *Brain Res Mol Brain Res*, **1996**, *35*(1-2), 349-53.

[162] Wong, M.L.; Smith, M.A.; Licinio, J.; Doi, S.Q.; Weiss, S.R.; Post, R.M., and Gold, P.W. Differential effects of kindled and electrically induced seizures on a glutamate receptor (GluR1) gene expression. *Epilepsy Res*, **1993**, *14*(3), 221-7.

[163] Barbon, A.; Caracciolo, L.; Orlandi, C.; Musazzi, L.; Mallei, A.; La Via, L.; Bonini, D.; Mora, C.; Tardito, D.; Gennarelli, M.; Racagni, G.; Popoli, M., and Barlati, S. Chronic antidepressant treatments induce a time-dependent up-regulation of AMPA receptor subunit protein levels. *Neurochem Int*, **2011**, *59*(6), 896-905.

[164] Ampuero, E.; Rubio, F.J.; Falcon, R.; Sandoval, M.; Diaz-Veliz, G.; Gonzalez, R.E.; Earle, N.; Dagnino-Subiabre, A.; Aboitiz, F.; Orrego, F., and Wyneken, U. Chronic fluoxetine treatment induces structural plasticity and selective changes in glutamate receptor subunits in the rat cerebral cortex. *Neuroscience*, **2010**, *169*(1), 98-108.

[165] Gibbons, A.S.; Brooks, L.; Scarr, E., and Dean, B. AMPA receptor expression is increased post-mortem samples of the anterior cingulate from subjects with major depressive disorder. *J Affect Disord*, **2012**, *136*(3), 1232-7.

[166] Freudenberg, F.; Celikel, T., and Reif, A. The role of alpha-amino-3-hydroxy-5-methyl-4-isoxazolepropionic acid (AMPA) receptors in depression: central mediators of pathophysiology and antidepressant activity? *Neurosci Biobehav Rev*, **2015**, *52*, 193-206.

[167] Martinez-Turrillas, R.; Frechilla, D., and Del Rio, J. Chronic antidepressant treatment increases the membrane expression of AMPA receptors in rat hippocampus. *Neuropharmacology*, **2002**, *43*(8), 1230-7.

[168] Chourbaji, S.; Vogt, M.A.; Fumagalli, F.; Sohr, R.; Frasca, A.; Brandwein, C.; Hortnagl, H.; Riva, M.A.; Sprengel, R., and Gass, P. AMPA receptor subunit 1 (GluR-A) knockout mice model the glutamate hypothesis of depression. *FASEB J*, **2008**, *22*(9), 3129-34.

[169] Ferreira, J.S.; Schmidt, J.; Rio, P.; Aguas, R.; Rooyakkers, A.; Li, K.W.; Smit, A.B.; Craig, A.M., and Carvalho, A.L. GluN2B-Containing NMDA Receptors Regulate AMPA Receptor Traffic through Anchoring of the Synaptic Proteasome. *J Neurosci*, **2015**, *35*(22), 8462-79.

[170] Maeng, S.; Zarate, C.A., Jr.; Du, J.; Schloesser, R.J.; McCammon, J.; Chen, G., and Manji, H.K. Cellular mechanisms underlying the antidepressant effects of ketamine: role of alpha-amino-3-hydroxy-5-methylisoxazole-4-propionic acid receptors. *Biol Psychiatry*, **2008**, *63*(4), 349-52.

[171] Koike, H.; Iijima, M., and Chaki, S. Involvement of AMPA receptor in both the rapid and sustained antidepressant-like effects of ketamine in animal models of depression. *Behav Brain Res*, **2011**, *224*(1), 107-11.

[172] Koike, H. and Chaki, S. Requirement of AMPA receptor stimulation for the sustained antidepressant activity of ketamine and LY341495 during the forced swim test in rats. *Behav Brain Res*, **2014**, *271*, 111-5.

[173] Beurel, E.; Grieco, S.F.; Amadei, C.; Downey, K., and Jope, R.S. Ketamine-induced inhibition of glycogen synthase kinase-3 contributes to the augmentation of alpha-amino-3-hydroxy-5-methylisoxazole-4-propionic acid (AMPA) receptor signaling. *Bipolar Disord*, **2016**, *18*(6), 473-480.

[174] Zhang, J.C.; Yao, W.; Dong, C.; Yang, C.; Ren, Q.; Ma, M.; Han, M., and Hashimoto, K. Comparison of ketamine, 7,8-dihydroxyflavone, and ANA-12 antidepressant effects in the social defeat stress model of depression. *Psychopharmacology (Berl)*, **2015**, *232*(23), 4325-35.

[175] Farley, S.; Apazoglou, K.; Witkin, J.M.; Giros, B., and Tzavara, E.T. Antidepressant-like effects of an AMPA receptor potentiator under a chronic mild stress paradigm. *Int J Neuropsychopharmacol*, **2010**, *13*(9), 1207-18.

[176] Martinez-Turrillas, R.; Del Rio, J., and Frechilla, D. Sequential changes in BDNF mRNA expression and synaptic levels of AMPA receptor subunits in rat hippocampus after chronic antidepressant treatment. *Neuropharmacology*, **2005**, *49*(8), 1178-88.

[177] Tan, C.H.; He, X.; Yang, J., and Ong, W.Y. Changes in AMPA subunit expression in the mouse brain after chronic treatment with the antidepressant maprotiline: a link between noradrenergic and glutamatergic function? *Exp Brain Res*, **2006**, *170*(4), 448-56.

[178] El Iskandrani, K.S.; Oosterhof, C.A.; El Mansari, M., and Blier, P. Impact of subanesthetic doses of ketamine on AMPA-mediated responses in rats: An in vivo electrophysiological study on monoaminergic and glutamatergic neurons. *J Psychopharmacol*, **2015**, *35*(3), 334-336.

[179] Abdallah, C.G.; Sanacora, G.; Duman, R.S., and Krystal, J.H. Ketamine and rapid-acting antidepressants: a window into a new neurobiology for mood disorder therapeutics. *Annu Rev Med*, **2015**, *66*, 509-23.

[180] Homayoun, H. and Moghaddam, B. NMDA receptor hypofunction produces opposite effects on prefrontal cortex interneurons and pyramidal neurons. *J Neurosci*, **2007**, *27*(43), 11496-500.

[181] Bretin, S.; Louis, C.; Seguin, L.; Wagner, S.; Thomas, J.Y.; Challal, S.; Rogez, N.; Albinet, K.; Iop, F.; Villain, N.; Bertrand, S.; Krazem, A.; Berachochea, D.; Billiald, S.; Tordjman, C.; Cordi, A.; Bertrand, D.; Lestage, P., and Danober, L. Pharmacological characterisation of S 47445, a novel positive allosteric modulator of AMPA receptors. *PLoS One*, **2017**, *12*(9), e0184429.

[182] Baumbarger, P.; Muhlhauser, M.; Yang, C.R., and Nisenbaum, E.S. LY392098, a novel AMPA receptor potentiator: electrophysiological studies in prefrontal cortical neurons. *Neuropharmacology*, **2001**, *40*(8), 992-1002.

[183] Li, X.; Tizzano, J.P.; Griffey, K.; Clay, M.; Lindstrom, T., and Skolnick, P. Antidepressant-like actions of an AMPA receptor potentiator (LY392098). *Neuropharmacology*, **2001**, *40*(8), 1028-33.

[184] Li, X.; Witkin, J.M.; Need, A.B., and Skolnick, P. Enhancement of antidepressant potency by a potentiator of AMPA receptors. *Cell Mol Neurobiol*, **2003**, *23*(3), 419-30.

[185] Vandenberg, R.J. and Ryan, R.M. Mechanisms of glutamate transport. *Physiol Rev*, **2013**, *93*(4), 1621-57.

[186] El Mestikawy, S.; Wallen-Mackenzie, A.; Fortin, G.M.; Descarries, L., and Trudeau, L.E. From glutamate co-release to vesicular synergy: vesicular glutamate transporters. *Nat Rev Neurosci*, **2011**, *12*(4), 204-16.

[187] Wojcik, S.M.; Rhee, J.S.; Herzog, E.; Sigler, A.; Jahn, R.; Takamori, S.; Brose, N., and Rosenmund, C. An essential role for vesicular glutamate transporter 1 (VGLUT1) in postnatal development and control of quantal size. *Proc Natl Acad Sci U S A*, **2004**, *101*(18), 7158-63.

[188] Montana, V.; Ni, Y.; Sunjara, V.; Hua, X., and Parpura, V. Vesicular glutamate transporter-dependent glutamate release from astrocytes. *J Neurosci*, **2004**, *24*(11), 2633-42.

[189] Uezato, A.; Meador-Woodruff, J.H., and McCullumsmith, R.E. Vesicular glutamate transporter mRNA expression in the medial temporal lobe in major depressive disorder, bipolar disorder, and schizophrenia. *Bipolar Disord*, **2009**, *11*(7), 711-25.

[190] Brancato, A.; Bregman, D.; Ahn, H.F.; Pfau, M.L.; Menard, C.; Cannizzaro, C.; Russo, S.J., and Hodes, G.E. Sub-chronic variable stress

induces sex-specific effects on glutamatergic synapses in the nucleus accumbens. *Neuroscience*, **2017**, *350*, 180-189.
[191] Gegelashvili, G.; Dehnes, Y.; Danbolt, N.C., and Schousboe, A. The high-affinity glutamate transporters GLT1, GLAST, and EAAT4 are regulated via different signalling mechanisms. *Neurochem Int*, **2000**, *37*(2-3), 163-70.
[192] Gegelashvili, G. and Schousboe, A. Cellular distribution and kinetic properties of high-affinity glutamate transporters. *Brain Res Bull*, **1998**, *45*(3), 233-8.
[193] Choudary, P.V.; Molnar, M.; Evans, S.J.; Tomita, H.; Li, J.Z.; Vawter, M.P.; Myers, R.M.; Bunney, W.E., Jr.; Akil, H.; Watson, S.J., and Jones, E.G. Altered cortical glutamatergic and GABAergic signal transmission with glial involvement in depression. *Proc Natl Acad Sci U S A*, **2005**, *102*(43), 15653-8.
[194] Cryan, J.F. and Kaupmann, K. Don't worry 'B' happy!: a role for GABA(B) receptors in anxiety and depression. *Trends Pharmacol Sci*, **2005**, *26*(1), 36-43.
[195] John, C.S.; Smith, K.L.; Van't Veer, A.; Gompf, H.S.; Carlezon, W.A., Jr.; Cohen, B.M.; Ongur, D., and Bechtholt-Gompf, A.J. Blockade of astrocytic glutamate uptake in the prefrontal cortex induces anhedonia. *Neuropsychopharmacology*, **2012**, *37*(11), 2467-75.
[196] Liu, W.X.; Wang, J.; Xie, Z.M.; Xu, N.; Zhang, G.F.; Jia, M.; Zhou, Z.Q.; Hashimoto, K., and Yang, J.J. Regulation of glutamate transporter 1 via BDNF-TrkB signaling plays a role in the anti-apoptotic and antidepressant effects of ketamine in chronic unpredictable stress model of depression. *Psychopharmacology (Berl)*, **2016**, *233*(3), 405-15.
[197] Gasull-Camos, J.; Tarres-Gatius, M.; Artigas, F., and Castane, A. Glial GLT-1 blockade in infralimbic cortex as a new strategy to evoke rapid antidepressant-like effects in rats. *Transl Psychiatry*, **2017**, *7*(2), e1038.
[198] Doble, A. The pharmacology and mechanism of action of riluzole. *Neurology*, **1996**, *47*(6 Suppl 4), S233-41.
[199] Frizzo, M.E.; Dall'Onder, L.P.; Dalcin, K.B., and Souza, D.O. Riluzole enhances glutamate uptake in rat astrocyte cultures. *Cell Mol Neurobiol*, **2004**, *24*(1), 123-8.
[200] Zarate, C.A., Jr.; Machado-Vieira, R.; Henter, I.; Ibrahim, L.; Diazgranados, N., and Salvadore, G. Glutamatergic modulators: the future of treating mood disorders? *Harv Rev Psychiatry*, **2010**, *18*(5), 293-303.
[201] Mathew, S.J.; Gueorguieva, R.; Brandt, C.; Fava, M., and Sanacora, G. A Randomized, Double-Blind, Placebo-Controlled, Sequential Parallel Comparison Design Trial of Adjunctive Riluzole for Treatment-Resistant Major Depressive Disorder. *Neuropsychopharmacology*, **2017**, *42*(13), 2567-2574.
[202] Ibrahim, L.; Diazgranados, N.; Franco-Chaves, J.; Brutsche, N.; Henter, I.D.; Kronstein, P.; Moaddel, R.; Wainer, I.; Luckenbaugh, D.A.; Manji, H.K., and Zarate, C.A., Jr. Course of improvement in depressive symptoms to a single intravenous infusion of ketamine vs add-on riluzole: results from a 4-week, double-blind, placebo-controlled study. *Neuropsychopharmacology*, **2012**, *37*(6), 1526-33.
[203] Luscher, B.; Shen, Q., and Sahir, N. The GABAergic deficit hypothesis of major depressive disorder. *Mol Psychiatry*, **2011**, *16*(4), 383-406.
[204] Pinard, A.; Seddik, R., and Bettler, B. GABAB receptors: physiological functions and mechanisms of diversity. *Adv Pharmacol*, **2010**, *58*, 231-55.
[205] Bowery, N.G.; Bettler, B.; Froestl, W.; Gallagher, J.P.; Marshall, F.; Raiteri, M.; Bonner, T.I., and Enna, S.J. International Union of Pharmacology. XXXIII. Mammalian gamma-aminobutyric acid(B) receptors: structure and function. *Pharmacol Rev*, **2002**, *54*(2), 247-64.
[206] DeFelipe, J.; Lopez-Cruz, P.L.; Benavides-Piccione, R.; Bielza, C.; Larranaga, P.; Anderson, S.; Burkhalter, A.; Cauli, B.; Fairen, A.; Feldmeyer, D.; Fishell, G.; Fitzpatrick, D.; Freund, T.F.; Gonzalez-Burgos, G.; Hestrin, S.; Hill, S.; Hof, P.R.; Huang, J.; Jones, E.G.; Kawaguchi, Y.; Kisvarday, Z.; Kubota, Y.; Lewis, D.A.; Marin, O.; Markram, H.; McBain, C.J.; Meyer, H.S.; Monyer, H.; Nelson, S.B.; Rockland, K.; Rossier, J.; Rubenstein, J.L.; Rudy, B.; Scanziani, M.; Shepherd, G.M.; Sherwood, C.C.; Staiger, J.F.; Tamas, G.; Thomson, A.; Wang, Y.; Yuste, R., and Ascoli, G.A. New insights into the classification and nomenclature of cortical GABAergic interneurons. *Nat Rev Neurosci*, **2013**, *14*(3), 202-16.
[207] Rudy, B.; Fishell, G.; Lee, S., and Hjerling-Leffler, J. Three groups of interneurons account for nearly 100% of neocortical GABAergic neurons. *Dev Neurobiol*, **2011**, *71*(1), 45-61.
[208] Povysheva, N.V.; Gonzalez-Burgos, G.; Zaitsev, A.V.; Kroner, S.; Barrionuevo, G.; Lewis, D.A., and Krimer, L.S. Properties of excitatory synaptic responses in fast-spiking interneurons and pyramidal cells from monkey and rat prefrontal cortex. *Cereb Cortex*, **2006**, *16*(4), 541-52.
[209] Demars, M.P. and Morishita, H. Cortical parvalbumin and somatostatin GABA neurons express distinct endogenous modulators of nicotinic acetylcholine receptors. *Mol Brain*, **2014**, *7*, 75.
[210] Petty, F. and Schlesser, M.A. Plasma GABA in affective illness. A preliminary investigation. *J Affect Disord*, **1981**, *3*(4), 339-43.
[211] Petty, F. and Sherman, A.D. Plasma GABA levels in psychiatric illness. *J Affect Disord*, **1984**, *6*(2), 131-8.
[212] Gerner, R.H. and Hare, T.A. CSF GABA in normal subjects and patients with depression, schizophrenia, mania, and anorexia nervosa. *Am J Psychiatry*, **1981**, *138*(8), 1098-101.
[213] Sanacora, G.; Mason, G.F.; Rothman, D.L.; Behar, K.L.; Hyder, F.; Petroff, O.A.; Berman, R.M.; Charney, D.S., and Krystal, J.H. Reduced cortical gamma-aminobutyric acid levels in depressed patients determined by proton magnetic resonance spectroscopy. *Arch Gen Psychiatry*, **1999**, *56*(11), 1043-7.
[214] Sanacora, G.; Gueorguieva, R.; Epperson, C.N.; Wu, Y.T.; Appel, M.; Rothman, D.L.; Krystal, J.H., and Mason, G.F. Subtype-specific alterations of gamma-aminobutyric acid and glutamate in patients with major depression. *Arch Gen Psychiatry*, **2004**, *61*(7), 705-13.
[215] Price, R.B.; Shungu, D.C.; Mao, X.; Nestadt, P.; Kelly, C.; Collins, K.A.; Murrough, J.W.; Charney, D.S., and Mathew, S.J. Amino acid neurotransmitters assessed by proton magnetic resonance spectroscopy: relationship to treatment resistance in major depressive disorder. *Biol Psychiatry*, **2009**, *65*(9), 792-800.
[216] Maciag, D.; Hughes, J.; O'Dwyer, G.; Pride, Y.; Stockmeier, C.A.; Sanacora, G., and Rajkowska, G. Reduced density of calbindin immunoreactive GABAergic neurons in the occipital cortex in major depression: relevance to neuroimaging studies. *Biol Psychiatry*, **2010**, *67*(5), 465-70.
[217] Rajkowska, G.; O'Dwyer, G.; Teleki, Z.; Stockmeier, C.A., and Miguel-Hidalgo, J.J. GABAergic neurons immunoreactive for calcium binding proteins are reduced in the prefrontal cortex in major depression. *Neuropsychopharmacology*, **2007**, *32*(2), 471-82.
[218] Xu, A.; Cui, S., and Wang, J.H. Incoordination among Subcellular Compartments Is Associated with Depression-Like Behavior Induced by Chronic Mild Stress. *Int J Neuropsychopharmacol*, **2016**, *19*(5).
[219] Scifo, E.; Pabba, M.; Kapadia, F.; Ma, T.; Lewis, D.A.; Tseng, G.C., and Sibille, E. Sustained Molecular Pathology Across Episodes and Remission in Major Depressive Disorder. *Biol Psychiatry*, **2018**, *83*(1), 81-89.
[220] Ma, K.; Xu, A.; Cui, S.; Sun, M.R.; Xue, Y.C., and Wang, J.H. Impaired GABA synthesis, uptake and release are associated with depression-like behaviors induced by chronic mild stress. *Transl Psychiatry*, **2016**, *6*(10), e910.
[221] Fuchs, T.; Jefferson, S.J.; Hooper, A.; Yee, P.H.; Maguire, J., and Luscher, B. Disinhibition of somatostatin-positive GABAergic interneurons results in an anxiolytic and antidepressant-like brain state. *Mol Psychiatry*, **2017**, *22*(6), 920-930.
[222] Shen, Q.; Lal, R.; Luellen, B.A.; Earnheart, J.C.; Andrews, A.M., and Luscher, B. gamma-Aminobutyric acid-type A receptor deficits cause hypothalamic-pituitary-adrenal axis hyperactivity and antidepressant drug sensitivity reminiscent of melancholic forms of depression. *Biol Psychiatry*, **2010**, *68*(6), 512-20.
[223] Earnheart, J.C.; Schweizer, C.; Crestani, F.; Iwasato, T.; Itohara, S.; Mohler, H., and Luscher, B. GABAergic control of adult hippocampal neurogenesis in relation to behavior indicative of trait anxiety and depression states. *J Neurosci*, **2007**, *27*(14), 3845-54.
[224] Verkuyl, J.M.; Hemby, S.E., and Joels, M. Chronic stress attenuates GABAergic inhibition and alters gene expression of parvocellular neurons in rat hypothalamus. *Eur J Neurosci*, **2004**, *20*(6), 1665-73.
[225] Fischell, J.; Van Dyke, A.M.; Kvarta, M.D.; LeGates, T.A., and Thompson, S.M. Rapid Antidepressant Action and Restoration of Excitatory Synaptic Strength After Chronic Stress by Negative Modulators of Alpha5-Containing GABAA Receptors. *Neuropsychopharmacology*, **2015**, *40*(11), 2499-509.
[226] Zanos, P.; Nelson, M.E.; Highland, J.N.; Krimmel, S.R.; Georgiou, P.; Gould, T.D., and Thompson, S.M. A Negative Allosteric Modulator for alpha5 Subunit-Containing GABA Receptors Exerts a Rapid and

Persistent Antidepressant-Like Action without the Side Effects of the NMDA Receptor Antagonist Ketamine in Mice. *eNeuro*, **2017**, *4*(1).

[227] Mombereau, C.; Kaupmann, K.; Gassmann, M.; Bettler, B.; van der Putten, H., and Cryan, J.F. Altered anxiety and depression-related behaviour in mice lacking GABAB(2) receptor subunits. *Neuroreport*, **2005**, *16*(3), 307-10.

[228] Mombereau, C.; Kaupmann, K.; Froestl, W.; Sansig, G.; van der Putten, H., and Cryan, J.F. Genetic and pharmacological evidence of a role for GABA(B) receptors in the modulation of anxiety- and antidepressant-like behavior. *Neuropsychopharmacology*, **2004**, *29*(6), 1050-62.

[229] Felice, D.; O'Leary, O.F.; Pizzo, R.C., and Cryan, J.F. Blockade of the GABA(B) receptor increases neurogenesis in the ventral but not dorsal adult hippocampus: relevance to antidepressant action. *Neuropharmacology*, **2012**, *63*(8), 1380-8.

[230] Nowak, G.; Partyka, A.; Palucha, A.; Szewczyk, B.; Wieronska, J.M.; Dybala, M.; Metz, M.; Librowski, T.; Froestl, W.; Papp, M., and Pilc, A. Antidepressant-like activity of CGP 36742 and CGP 51176, selective GABAB receptor antagonists, in rodents. *Br J Pharmacol*, **2006**, *149*(5), 581-90.

[231] Hu, W.; Zhang, M.; Czeh, B.; Flugge, G., and Zhang, W. Stress impairs GABAergic network function in the hippocampus by activating nongenomic glucocorticoid receptors and affecting the integrity of the parvalbumin-expressing neuronal network. *Neuropsychopharmacology*, **2010**, *35*(8), 1693-707.

[232] Esel, E.; Kose, K.; Hacimusalar, Y.; Ozsoy, S.; Kula, M.; Candan, Z., and Turan, T. The effects of electroconvulsive therapy on GABAergic function in major depressive patients. *J ECT*, **2008**, *24*(3), 224-8.

[233] Dubin, M.J.; Mao, X.; Banerjee, S.; Goodman, Z.; Lapidus, K.A.; Kang, G.; Liston, C., and Shungu, D.C. Elevated prefrontal cortex GABA in patients with major depressive disorder after TMS treatment measured with proton magnetic resonance spectroscopy. *J Psychiatry Neurosci*, **2016**, *41*(3), E37-45.

[234] Sanacora, G.; Mason, G.F.; Rothman, D.L., and Krystal, J.H. Increased occipital cortex GABA concentrations in depressed patients after therapy with selective serotonin reuptake inhibitors. *Am J Psychiatry*, **2002**, *159*(4), 663-5.

[235] Sanacora, G.; Mason, G.F.; Rothman, D.L.; Hyder, F.; Ciarcia, J.J.; Ostroff, R.B.; Berman, R.M., and Krystal, J.H. Increased cortical GABA concentrations in depressed patients receiving ECT. *Am J Psychiatry*, **2003**, *160*(3), 577-9.

[236] Bhagwagar, Z.; Wylezinska, M.; Taylor, M.; Jezzard, P.; Matthews, P.M., and Cowen, P.J. Increased brain GABA concentrations following acute administration of a selective serotonin reuptake inhibitor. *Am J Psychiatry*, **2004**, *161*(2), 368-70.

[237] Feger, J. and Robledo, P. The Effects of Activation or Inhibition of the Subthalamic Nucleus on the Metabolic and Electrophysiological Activities Within the Pallidal Complex and Substantia Nigra in the Rat. *Eur J Neurosci*, **1991**, *3*(10), 947-952.

[238] Littlewood, C.L.; Jones, N.; O'Neill, M.J.; Mitchell, S.N.; Tricklebank, M., and Williams, S.C. Mapping the central effects of ketamine in the rat using pharmacological MRI. *Psychopharmacology (Berl)*, **2006**, *186*(1), 64-81.

[239] Perrine, S.A.; Ghoddoussi, F.; Michaels, M.S.; Sheikh, I.S.; McKelvey, G., and Galloway, M.P. Ketamine reverses stress-induced depression-like behavior and increased GABA levels in the anterior cingulate: an 11.7 T 1H-MRS study in rats. *Prog Neuropsychopharmacol Biol Psychiatry*, **2014**, *51*, 9-15.

[240] Rosa, P.B.; Neis, V.B.; Ribeiro, C.M.; Moretti, M., and Rodrigues, A.L. Antidepressant-like effects of ascorbic acid and ketamine involve modulation of GABAA and GABAB receptors. *Pharmacol Rep*, **2016**, *68*(5), 996-1001.

[241] Irifune, M.; Sato, T.; Kamata, Y.; Nishikawa, T.; Dohi, T., and Kawahara, M. Evidence for GABA(A) receptor agonistic properties of ketamine: convulsive and anesthetic behavioral models in mice. *Anesth Analg*, **2000**, *91*(1), 230-6.

[242] Herrero, M.T.; Oset-Gasque, M.J.; Lopez, E.; Vicente, S., and Gonzalez, M.P. Mechanism by which GABA, through its GABA(A) receptor, modulates glutamate release from rat cortical neurons in culture. *Neurochem Int*, **1999**, *34*(2), 141-8.

[243] Horne, A.L.; Harrison, N.L.; Turner, J.P., and Simmonds, M.A. Spontaneous paroxysmal activity induced by zero magnesium and bicuculline: suppression by NMDA antagonists and GABA mimetics. *Eur J Pharmacol*, **1986**, *122*(2), 231-8.

[244] Solati, J.; Hajikhani, R., and Golub, Y. Activation of GABAA receptors in the medial prefrontal cortex produces an anxiolytic-like response. *Acta Neuropsychiatr*, **2013**, *25*(4), 221-6.

[245] Schneider, P.G. and Rodriguez de Lores Arnaiz, G. Ketamine prevents seizures and reverses changes in muscarinic receptor induced by bicuculline in rats. *Neurochem Int*, **2013**, *62*(3), 258-64.

[246] Wakasugi, M.; Hirota, K.; Roth, S.H., and Ito, Y. The effects of general anesthetics on excitatory and inhibitory synaptic transmission in area CA1 of the rat hippocampus in vitro. *Anesth Analg*, **1999**, *88*(3), 676-80.

[247] Nakao, S.; Nagata, A.; Miyamoto, E.; Masuzawa, M.; Murayama, T., and Shingu, K. Inhibitory effect of propofol on ketamine-induced c-Fos expression in the rat posterior cingulate and retrosplenial cortices is mediated by GABAA receptor activation. *Acta Anaesthesiol Scand*, **2003**, *47*(3), 284-90.

[248] Khanegheini, A.; Nasehi, M., and Zarrindast, M.R. The modulatory effect of CA1 GABAb receptors on ketamine-induced spatial and non-spatial novelty detection deficits with respect to Ca(2+). *Neuroscience*, **2015**, *305*, 157-68.

[249] Ma, J. and Leung, L.S. Involvement of posterior cingulate cortex in ketamine-induced psychosis relevant behaviors in rats. *Behav Brain Res*, **2018**, *338*, 17-27.

[250] Behrens, M.M.; Ali, S.S.; Dao, D.N.; Lucero, J.; Shekhtman, G.; Quick, K.L., and Dugan, L.L. Ketamine-induced loss of phenotype of fast-spiking interneurons is mediated by NADPH-oxidase. *Science*, **2007**, *318*(5856), 1645-7.

[251] Abbasi, J. Ketamine Minus the Trip: New Hope for Treatment-Resistant Depression. *JAMA*, **2017**, *318*(20), 1964-1966.

[252] Sabbagh, J.J.; Murtishaw, A.S.; Bolton, M.M.; Heaney, C.F.; Langhardt, M., and Kinney, J.W. Chronic ketamine produces altered distribution of parvalbumin-positive cells in the hippocampus of adult rats. *Neurosci Lett*, **2013**, *550*, 69-74.

[253] Jeevakumar, V.; Driskill, C.; Paine, A.; Sobhanian, M.; Vakil, H.; Morris, B.; Ramos, J., and Kroener, S. Ketamine administration during the second postnatal week induces enduring schizophrenia-like behavioral symptoms and reduces parvalbumin expression in the medial prefrontal cortex of adult mice. *Behav Brain Res*, **2015**, *282*, 165-75.

[254] Brown, J.A.; Ramikie, T.S.; Schmidt, M.J.; Baldi, R.; Garbett, K.; Everheart, M.G.; Warren, L.E.; Gellert, L.; Horvath, S.; Patel, S., and Mirnics, K. Inhibition of parvalbumin-expressing interneurons results in complex behavioral changes. *Mol Psychiatry*, **2015**, *20*(12), 1499-507.

[255] Wang, N.; Zhang, G.F.; Liu, X.Y.; Sun, H.L.; Wang, X.M.; Qiu, L.L.; Yang, C., and Yang, J.J. Downregulation of neuregulin 1-ErbB4 signaling in parvalbumin interneurons in the rat brain may contribute to the antidepressant properties of ketamine. *J Mol Neurosci*, **2014**, *54*(2), 211-8.

[256] Zhou, Z.; Zhang, G.; Li, X.; Liu, X.; Wang, N.; Qiu, L.; Liu, W.; Zuo, Z., and Yang, J. Loss of phenotype of parvalbumin interneurons in rat prefrontal cortex is involved in antidepressant- and propsychotic-like behaviors following acute and repeated ketamine administration. *Mol Neurobiol*, **2015**, *51*(2), 808-19.

[257] McGarry, L.M. and Carter, A.G. Inhibitory Gating of Basolateral Amygdala Inputs to the Prefrontal Cortex. *J Neurosci*, **2016**, *36*(36), 9391-406.

[258] Yang, C.; Shirayama, Y.; Zhang, J.C.; Ren, Q.; Yao, W.; Ma, M.; Dong, C., and Hashimoto, K. R-ketamine: a rapid-onset and sustained antidepressant without psychotomimetic side effects. *Transl Psychiatry*, **2015**, *5*, e632.

[259] Kinney, J.W.; Davis, C.N.; Tabarean, I.; Conti, B.; Bartfai, T., and Behrens, M.M. A specific role for NR2A-containing NMDA receptors in the maintenance of parvalbumin and GAD67 immunoreactivity in cultured interneurons. *J Neurosci*, **2006**, *26*(5), 1604-15.

[260] Donegan, J.J. and Lodge, D.J. Hippocampal Perineuronal Nets Are Required for the Sustained Antidepressant Effect of Ketamine. *Int J Neuropsychopharmacol*, **2017**, *20*(4), 354-358.

[261] Carlen, M.; Meletis, K.; Siegle, J.H.; Cardin, J.A.; Futai, K.; Vierling-Claassen, D.; Ruhlmann, C.; Jones, S.R.; Deisseroth, K.; Sheng, M.; Moore, C.I., and Tsai, L.H. A critical role for NMDA receptors in parvalbumin interneurons for gamma rhythm induction and behavior. *Mol Psychiatry*, **2012**, *17*(5), 537-48.

[262] Lazarewicz, M.T.; Ehrlichman, R.S.; Maxwell, C.R.; Gandal, M.J.; Finkel, L.H., and Siegel, S.J. Ketamine modulates theta and gamma oscillations. *J Cogn Neurosci*, **2010**, *22*(7), 1452-64.

[263] Hong, L.E.; Summerfelt, A.; Buchanan, R.W.; O'Donnell, P.; Thaker, G.K.; Weiler, M.A., and Lahti, A.C. Gamma and delta neural oscillations and association with clinical symptoms under subanesthetic ketamine. *Neuropsychopharmacology*, **2010**, *35*(3), 632-40.
[264] Pinault, D. N-methyl d-aspartate receptor antagonists ketamine and MK-801 induce wake-related aberrant gamma oscillations in the rat neocortex. *Biol Psychiatry*, **2008**, *63*(8), 730-5.
[265] Xue, J.G.; Masuoka, T.; Gong, X.D.; Chen, K.S.; Yanagawa, Y.; Law, S.K., and Konishi, S. NMDA receptor activation enhances inhibitory GABAergic transmission onto hippocampal pyramidal neurons via presynaptic and postsynaptic mechanisms. *J Neurophysiol*, **2011**, *105*(6), 2897-906.
[266] Artigas, F. Serotonin receptors involved in antidepressant effects. *Pharmacol Ther*, **2013**, *137*(1), 119-31.
[267] Martin, C.B.; Gassmann, M.; Chevarin, C.; Hamon, M.; Rudolph, U.; Bettler, B.; Lanfumey, L., and Mongeau, R. Effect of genetic and pharmacological blockade of GABA receptors on the 5-HT2C receptor function during stress. *J Neurochem*, **2014**, *131*(5), 566-72.
[268] Jacobs, B.L. and Azmitia, E.C. Structure and function of the brain serotonin system. *Physiol Rev*, **1992**, *72*(1), 165-229.
[269] Sodhi, M.S. and Sanders-Bush, E. Serotonin and brain development. *Int Rev Neurobiol*, **2004**, *59*, 111-74.
[270] Hamon, M. and Blier, P. Monoamine neurocircuitry in depression and strategies for new treatments. *Prog Neuropsychopharmacol Biol Psychiatry*, **2013**, *45*, 54-63.
[271] Delgado, P.L.; Price, L.H.; Miller, H.L.; Salomon, R.M.; Aghajanian, G.K.; Heninger, G.R., and Charney, D.S. Serotonin and the neurobiology of depression. Effects of tryptophan depletion in drug-free depressed patients. *Arch Gen Psychiatry*, **1994**, *51*(11), 865-74.
[272] Hoyer, D.; Clarke, D.E.; Fozard, J.R.; Hartig, P.R.; Martin, G.R.; Mylecharane, E.J.; Saxena, P.R., and Humphrey, P.P. International Union of Pharmacology classification of receptors for 5-hydroxytryptamine (Serotonin). *Pharmacol Rev*, **1994**, *46*(2), 157-203.
[273] Pehrson, A.L. and Sanchez, C. Serotonergic modulation of glutamate neurotransmission as a strategy for treating depression and cognitive dysfunction. *CNS Spectr*, **2014**, *19*(2), 121-33.
[274] du Jardin, K.G.; Muller, H.K.; Elfving, B.; Dale, E.; Wegener, G., and Sanchez, C. Potential involvement of serotonergic signaling in ketamine's antidepressant actions: A critical review. *Prog Neuropsychopharmacol Biol Psychiatry*, **2016**, *71*, 27-38.
[275] Meunier, C.N.; Amar, M.; Lanfumey, L.; Hamon, M., and Fossier, P. 5-HT(1A) receptors direct the orientation of plasticity in layer 5 pyramidal neurons of the mouse prefrontal cortex. *Neuropharmacology*, **2013**, *71*, 37-45.
[276] Fernandez, S.P.; Cauli, B.; Cabezas, C.; Muzerelle, A.; Poncer, J.C., and Gaspar, P. Multiscale single-cell analysis reveals unique phenotypes of raphe 5-HT neurons projecting to the forebrain. *Brain Struct Funct*, **2016**, *221*(8), 4007-4025.
[277] Woolley, D.W. and Shaw, E. Some neurophysiological aspects of serotonin. *Br Med J*, **1954**, *2*(4880), 122-6.
[278] Placidi, G.P.; Oquendo, M.A.; Malone, K.M.; Huang, Y.Y.; Ellis, S.P., and Mann, J.J. Aggressivity, suicide attempts, and depression: relationship to cerebrospinal fluid monoamine metabolite levels. *Biol Psychiatry*, **2001**, *50*(10), 783-91.
[279] Saldanha, D.; Kumar, N.; Ryali, V.; Srivastava, K., and Pawar, A.A. Serum Serotonin Abnormality in Depression. *Med J Armed Forces India*, **2009**, *65*(2), 108-12.
[280] Roy, A.; De Jong, J., and Linnoila, M. Cerebrospinal fluid monoamine metabolites and suicidal behavior in depressed patients. A 5-year follow-up study. *Arch Gen Psychiatry*, **1989**, *46*(7), 609-12.
[281] Stockmeier, C.A. Neurobiology of serotonin in depression and suicide. *Ann N Y Acad Sci*, **1997**, *836*, 220-32.
[282] Hagan, C.E.; McDevitt, R.A.; Liu, Y.; Furay, A.R., and Neumaier, J.F. 5-HT(1B) autoreceptor regulation of serotonin transporter activity in synaptosomes. *Synapse*, **2012**, *66*(12), 1024-34.
[283] Kambeitz, J.P. and Howes, O.D. The serotonin transporter in depression: Meta-analysis of in vivo and post mortem findings and implications for understanding and treating depression. *J Affect Disord*, **2015**, *186*, 358-66.
[284] Romero, L.; Hervas, I., and Artigas, F. The 5-HT1A antagonist WAY-100635 selectively potentiates the presynaptic effects of serotonergic antidepressants in rat brain. *Neurosci Lett*, **1996**, *219*(2), 123-6.
[285] Artigas, F.; Adell, A., and Celada, P. Pindolol augmentation of antidepressant response. *Curr Drug Targets*, **2006**, *7*(2), 139-47.
[286] Artigas, F.; Romero, L.; de Montigny, C., and Blier, P. Acceleration of the effect of selected antidepressant drugs in major depression by 5-HT1A antagonists. *Trends Neurosci*, **1996**, *19*(9), 378-83.
[287] Fabre, V.; Beaufour, C.; Evrard, A.; Rioux, A.; Hanoun, N.; Lesch, K.P.; Murphy, D.L.; Lanfumey, L.; Hamon, M., and Martres, M.P. Altered expression and functions of serotonin 5-HT1A and 5-HT1B receptors in knock-out mice lacking the 5-HT transporter. *Eur J Neurosci*, **2000**, *12*(7), 2299-310.
[288] Le Poul, E.; Boni, C.; Hanoun, N.; Laporte, A.M.; Laaris, N.; Chauveau, J.; Hamon, M., and Lanfumey, L. Differential adaptation of brain 5-HT1A and 5-HT1B receptors and 5-HT transporter in rats treated chronically with fluoxetine. *Neuropharmacology*, **2000**, *39*(1), 110-22.
[289] Malagie, I.; Trillat, A.C.; Bourin, M.; Jacquot, C.; Hen, R., and Gardier, A.M. 5-HT1B Autoreceptors limit the effects of selective serotonin re-uptake inhibitors in mouse hippocampus and frontal cortex. *J Neurochem*, **2001**, *76*(3), 865-71.
[290] Riad, M.; Zimmer, L.; Rbah, L.; Watkins, K.C.; Hamon, M., and Descarries, L. Acute treatment with the antidepressant fluoxetine internalizes 5-HT1A autoreceptors and reduces the in vivo binding of the PET radioligand [18F]MPPF in the nucleus raphe dorsalis of rat. *J Neurosci*, **2004**, *24*(23), 5420-6.
[291] Guilloux, J.P.; David, D.J.; Guiard, B.P.; Chenu, F.; Reperant, C.; Toth, M.; Bourin, M., and Gardier, A.M. Blockade of 5-HT1A receptors by (+/-)-pindolol potentiates cortical 5-HT outflow, but not antidepressant-like activity of paroxetine: microdialysis and behavioral approaches in 5-HT1A receptor knockout mice. *Neuropsychopharmacology*, **2006**, *31*(10), 2162-72.
[292] Furczyk, K.; Schutova, B.; Michel, T.M.; Thome, J., and Buttner, A. The neurobiology of suicide - A Review of post-mortem studies. *J Mol Psychiatry*, **2013**, *1*(1), 2.
[293] Lopez-Gil, X.; Jimenez-Sanchez, L.; Romon, T.; Campa, L.; Artigas, F., and Adell, A. Importance of inter-hemispheric prefrontal connection in the effects of non-competitive NMDA receptor antagonists. *Int J Neuropsychopharmacol*, **2012**, *15*(7), 945-56.
[294] Lorrain, D.S.; Schaffhauser, H.; Campbell, U.C.; Baccei, C.S.; Correa, L.D.; Rowe, B.; Rodriguez, D.E.; Anderson, J.J.; Varney, M.A.; Pinkerton, A.B.; Vernier, J.M., and Bristow, L.J. Group II mGlu receptor activation suppresses norepinephrine release in the ventral hippocampus and locomotor responses to acute ketamine challenge. *Neuropsychopharmacology*, **2003**, *28*(9), 1622-32.
[295] Nishitani, N.; Nagayasu, K.; Asaoka, N.; Yamashiro, M.; Shirakawa, H.; Nakagawa, T., and Kaneko, S. Raphe AMPA receptors and nicotinic acetylcholine receptors mediate ketamine-induced serotonin release in the rat prefrontal cortex. *Int J Neuropsychopharmacol*, **2014**, *17*(8), 1321-6.
[296] Gigliucci, V.; O'Dowd, G.; Casey, S.; Egan, D.; Gibney, S., and Harkin, A. Ketamine elicits sustained antidepressant-like activity via a serotonin-dependent mechanism. *Psychopharmacology (Berl)*, **2013**, *228*(1), 157-66.
[297] Rivera-Garcia, M.T.; Lopez-Rubalcava, C., and Cruz, S.L. Preclinical characterization of toluene as a non-classical hallucinogen drug in rats: participation of 5-HT, dopamine and glutamate systems. *Psychopharmacology (Berl)*, **2015**, *232*(20), 3797-808.
[298] Fuchikami, M.; Thomas, A.; Liu, R.; Wohleb, E.S.; Land, B.B.; DiLeone, R.J.; Aghajanian, G.K., and Duman, R.S. Optogenetic stimulation of infralimbic PFC reproduces ketamine's rapid and sustained antidepressant actions. *Proc Natl Acad Sci U S A*, **2015**, *112*(26), 8106-11.
[299] Carreno, F.R.; Donegan, J.J.; Boley, A.M.; Shah, A.; DeGuzman, M.; Frazer, A., and Lodge, D.J. Activation of a ventral hippocampus-medial prefrontal cortex pathway is both necessary and sufficient for an antidepressant response to ketamine. *Mol Psychiatry*, **2016**, *21*(9), 1298-308.
[300] Covington, H.E.; Lobo, M.K.; Maze, I.; Vialou, V.; Hyman, J.M.; Zaman, S.; LaPlant, Q.; Mouzon, E.; Ghose, S.; Tamminga, C.A.; Neve, R.L.; Deisseroth, K., and Nestler, E.J. Antidepressant effect of optogenetic stimulation of the medial prefrontal cortex. *J Neurosci*, **2010**, *30*(48), 16082-90.
[301] Warden, M.R.; Selimbeyoglu, A.; Mirzabekov, J.J.; Lo, M.; Thompson, K.R.; Kim, S.Y.; Adhikari, A.; Tye, K.M.; Frank, L.M., and Deisseroth, K. A prefrontal cortex-brainstem neuronal projection that controls response to behavioural challenge. *Nature*, **2012**, *492*(7429), 428-32.

[302] Aghajanian, G.K. and Marek, G.J. Serotonin induces excitatory postsynaptic potentials in apical dendrites of neocortical pyramidal cells. *Neuropharmacology*, **1997**, *36*(4-5), 589-99.
[303] Hajos, M.; Richards, C.D.; Szekely, A.D., and Sharp, T. An electrophysiological and neuroanatomical study of the medial prefrontal cortical projection to the midbrain raphe nuclei in the rat. *Neuroscience*, **1998**, *87*(1), 95-108.
[304] Peyron, C.; Petit, J.M.; Rampon, C.; Jouvet, M., and Luppi, P.H. Forebrain afferents to the rat dorsal raphe nucleus demonstrated by retrograde and anterograde tracing methods. *Neuroscience*, **1998**, *82*(2), 443-68.
[305] Varga, V.; Szekely, A.D.; Csillag, A.; Sharp, T., and Hajos, M. Evidence for a role of GABA interneurones in the cortical modulation of midbrain 5-hydroxytryptamine neurones. *Neuroscience*, **2001**, *106*(4), 783-92.
[306] Harandi, M.; Aguera, M.; Gamrani, H.; Didier, M.; Maitre, M.; Calas, A., and Belin, M.F. gamma-Aminobutyric acid and 5-hydroxytryptamine interrelationship in the rat nucleus raphe dorsalis: combination of radioautographic and immunocytochemical techniques at light and electron microscopy levels. *Neuroscience*, **1987**, *21*(1), 237-51.
[307] Wang, Q.P.; Ochiai, H., and Nakai, Y. GABAergic innervation of serotonergic neurons in the dorsal raphe nucleus of the rat studied by electron microscopy double immunostaining. *Brain Res Bull*, **1992**, *29*(6), 943-8.
[308] Challis, C.; Beck, S.G., and Berton, O. Optogenetic modulation of descending prefrontocortical inputs to the dorsal raphe bidirectionally bias socioaffective choices after social defeat. *Front Behav Neurosci*, **2014**, *8*, 43.
[309] Celada, P.; Puig, M.V.; Casanovas, J.M.; Guillazo, G., and Artigas, F. Control of dorsal raphe serotonergic neurons by the medial prefrontal cortex: Involvement of serotonin-1A, GABA(A), and glutamate receptors. *J Neurosci*, **2001**, *21*(24), 9917-29.
[310] Jankowski, M.P. and Sesack, S.R. Prefrontal cortical projections to the rat dorsal raphe nucleus: ultrastructural features and associations with serotonin and gamma-aminobutyric acid neurons. *J Comp Neurol*, **2004**, *468*(4), 518-29.
[311] Varga, V.; Kocsis, B., and Sharp, T. Electrophysiological evidence for convergence of inputs from the medial prefrontal cortex and lateral habenula on single neurons in the dorsal raphe nucleus. *Eur J Neurosci*, **2003**, *17*(2), 280-6.
[312] Pollak Dorocic, I.; Furth, D.; Xuan, Y.; Johansson, Y.; Pozzi, L.; Silberberg, G.; Carlen, M., and Meletis, K. A whole-brain atlas of inputs to serotonergic neurons of the dorsal and median raphe nuclei. *Neuron*, **2014**, *83*(3), 663-78.
[313] Russo, S.J. and Nestler, E.J. The brain reward circuitry in mood disorders. *Nat Rev Neurosci*, **2013**, *14*(9), 609-25.
[314] Ishikawa, A. and Nakamura, S. Ventral hippocampal neurons project axons simultaneously to the medial prefrontal cortex and amygdala in the rat. *J Neurophysiol*, **2006**, *96*(4), 2134-8.
[315] Hamani, C. and Nobrega, J.N. Deep brain stimulation in clinical trials and animal models of depression. *Eur J Neurosci*, **2010**, *32*(7), 1109-17.
[316] McCardle, C.E. and Gartside, S.E. Effects of general anaesthetics on 5-HT neuronal activity in the dorsal raphe nucleus. *Neuropharmacology*, **2012**, *62*(4), 1787-96.
[317] Tso, M.M.; Blatchford, K.L.; Callado, L.F.; McLaughlin, D.P., and Stamford, J.A. Stereoselective effects of ketamine on dopamine, serotonin and noradrenaline release and uptake in rat brain slices. *Neurochem Int*, **2004**, *44*(1), 1-7.
[318] Gartside, S.E.; Cole, A.J.; Williams, A.P.; McQuade, R., and Judge, S.J. AMPA and NMDA receptor regulation of firing activity in 5-HT neurons of the dorsal and median raphe nuclei. *Eur J Neurosci*, **2007**, *25*(10), 3001-8.
[319] Pallotta, M.; Segieth, J.; Sadideen, F., and Whitton, P.S. Repeated but not acute clomipramine decreases the effect of N-methyl-D-aspartate receptor activation on serotonergic transmission between the raphe nuclei and frontal cortex. *Neuropharmacology*, **2001**, *41*(3), 294-300.
[320] Pallotta, M.; Segieth, J., and Whitton, P.S. N-methyl-d-aspartate receptors regulate 5-HT release in the raphe nuclei and frontal cortex of freely moving rats: differential role of 5-HT1A autoreceptors. *Brain Res*, **1998**, *783*(2), 173-8.
[321] Smith, J.C. and Whitton, P.S. Nitric oxide modulates N-methyl-D-aspartate-evoked serotonin release in the raphe nuclei and frontal cortex of the freely moving rat. *Neurosci Lett*, **2000**, *291*(1), 5-8.
[322] Martin, D.C.; Introna, R.P., and Aronstam, R.S. Inhibition of neuronal 5-HT uptake by ketamine, but not halothane, involves disruption of substrate recognition by the transporter. *Neurosci Lett*, **1990**, *112*(1), 99-103.
[323] Yamanaka, H.; Yokoyama, C.; Mizuma, H.; Kurai, S.; Finnema, S.J.; Halldin, C.; Doi, H., and Onoe, H. A possible mechanism of the nucleus accumbens and ventral pallidum 5-HT1B receptors underlying the antidepressant action of ketamine: a PET study with macaques. *Transl Psychiatry*, **2014**, *4*, e342.
[324] Zhao, Y. and Sun, L. Antidepressants modulate the in vitro inhibitory effects of propofol and ketamine on norepinephrine and serotonin transporter function. *J Clin Neurosci*, **2008**, *15*(11), 1264-9.
[325] Roth, B.L.; Gibbons, S.; Arunotayanun, W.; Huang, X.P.; Setola, V.; Treble, R., and Iversen, L. The ketamine analogue methoxetamine and 3- and 4-methoxy analogues of phencyclidine are high affinity and selective ligands for the glutamate NMDA receptor. *PLoS One*, **2013**, *8*(3), e59334.
[326] Manchia, M.; Carpiniello, B.; Valtorta, F., and Comai, S. Serotonin Dysfunction, Aggressive Behavior, and Mental Illness: Exploring the Link Using a Dimensional Approach. *ACS Chem Neurosci*, **2017**, *8*(5), 961-972.
[327] Owens, M.J.; Knight, D.L., and Nemeroff, C.B. Second-generation SSRIs: human monoamine transporter binding profile of escitalopram and R-fluoxetine. *Biol Psychiatry*, **2001**, *50*(5), 345-50.
[328] Nguyen, H.T.; Guiard, B.P.; Bacq, A.; David, D.J.; David, I.; Quesseveur, G.; Gautron, S.; Sanchez, C., and Gardier, A.M. Blockade of the high-affinity noradrenaline transporter (NET) by the selective 5-HT reuptake inhibitor escitalopram: an in vivo microdialysis study in mice. *Br J Pharmacol*, **2013**, *168*(1), 103-16.
[329] Gardier, A.M.; Malagie, I.; Trillat, A.C.; Jacquot, C., and Artigas, F. Role of 5-HT1A autoreceptors in the mechanism of action of serotoninergic antidepressant drugs: recent findings from in vivo microdialysis studies. *Fundam Clin Pharmacol*, **1996**, *10*(1), 16-27.
[330] David, D.J.; Bourin, M.; Jego, G.; Przybylski, C.; Jolliet, P., and Gardier, A.M. Effects of acute treatment with paroxetine, citalopram and venlafaxine in vivo on noradrenaline and serotonin outflow: a microdialysis study in Swiss mice. *Br J Pharmacol*, **2003**, *140*(6), 1128-36.
[331] Stassen, H.H.; Angst, J., and Delini-Stula, A. Onset of action under antidepressant treatment. *Eur Psychiatry*, **1997**, *12*(4), 163-5.
[332] David, D.J.; Samuels, B.A.; Rainer, Q.; Wang, J.W.; Marsteller, D.; Mendez, I.; Drew, M.; Craig, D.A.; Guiard, B.P.; Guilloux, J.P.; Artymyshyn, R.P.; Gardier, A.M.; Gerald, C.; Antonijevic, I.A.; Leonardo, E.D., and Hen, R. Neurogenesis-dependent and -independent effects of fluoxetine in an animal model of anxiety/depression. *Neuron*, **2009**, *62*(4), 479-93.
[333] Trillat, A.C.; Malagie, I.; Mathe-Allainmat, M.; Anmella, M.C.; Jacquot, C.; Langlois, M., and Gardier, A.M. Synergistic neurochemical and behavioral effects of fluoxetine and 5-HT1A receptor antagonists. *Eur J Pharmacol*, **1998**, *357*(2-3), 179-84.
[334] Guiard, B.P.; Guilloux, J.P.; Reperant, C.; Hunt, S.P.; Toth, M., and Gardier, A.M. Substance P neurokinin 1 receptor activation within the dorsal raphe nucleus controls serotonin release in the mouse frontal cortex. *Mol Pharmacol*, **2007**, *72*(6), 1411-8.
[335] Riad, M.; Watkins, K.C.; Doucet, E.; Hamon, M., and Descarries, L. Agonist-induced internalization of serotonin-1a receptors in the dorsal raphe nucleus (autoreceptors) but not hippocampus (heteroreceptors). *J Neurosci*, **2001**, *21*(21), 8378-86.
[336] Mannoury la Cour, C.; El Mestikawy, S.; Hanoun, N.; Hamon, M., and Lanfumey, L. Regional differences in the coupling of 5-hydroxytryptamine-1A receptors to G proteins in the rat brain. *Mol Pharmacol*, **2006**, *70*(3), 1013-21.
[337] Mongeau, R.; Welner, S.A.; Quirion, R., and Suranyi-Cadotte, B.E. Further evidence for differential affinity states of the serotonin1A receptor in rat hippocampus. *Brain Res*, **1992**, *590*(1-2), 229-38.
[338] Fukumoto, K.; Iijima, M., and Chaki, S. Serotonin-1A receptor stimulation mediates effects of a metabotropic glutamate 2/3 receptor antagonist, 2S-2-amino-2-(1S,2S-2-carboxycycloprop-1-yl)-3-(xanth-9-yl)propanoic acid (LY341495), and an N-methyl-D-aspartate receptor antagonist, ketamine, in the novelty-suppressed feeding test. *Psychopharmacology (Berl)*, **2014**, *231*(11), 2291-8.
[339] Forster, E.A.; Cliffe, I.A.; Bill, D.J.; Dover, G.M.; Jones, D.; Reilly, Y., and Fletcher, A. A pharmacological profile of the selective silent

5-HT1A receptor antagonist, WAY-100635. *Eur J Pharmacol*, **1995**, *281*(1), 81-8.
[340] Martel, J.C.; Leduc, N.; Ormiere, A.M.; Faucillon, V.; Danty, N.; Culie, C.; Cussac, D., and Newman-Tancredi, A. WAY-100635 has high selectivity for serotonin 5-HT(1A) versus dopamine D(4) receptors. *Eur J Pharmacol*, **2007**, *574*(1), 15-9.
[341] Gothert, M.; Schlicker, E.; Fink, K., and Classen, K. Effects of RU 24969 on serotonin release in rat brain cortex: further support for the identity of serotonin autoreceptors with 5-HT1B sites. *Arch Int Pharmacodyn Ther*, **1987**, *288*(1), 31-42.
[342] Hoyer, D. and Middlemiss, D.N. Species differences in the pharmacology of terminal 5-HT autoreceptors in mammalian brain. *Trends Pharmacol Sci*, **1989**, *10*(4), 130-2.
[343] Langlois, X.; Gerard, C.; Darmon, M.; Chauveau, J.; Hamon, M., and el Mestikawy, S. Immunolabeling of central serotonin 5-HT1D beta receptors in the rat, mouse, and guinea pig with a specific anti-peptide antiserum. *J Neurochem*, **1995**, *65*(6), 2671-81.
[344] Guilloux, J.P.; David, D.J.; Xia, L.; Nguyen, H.T.; Rainer, Q.; Guiard, B.P.; Reperant, C.; Deltheil, T.; Toth, M.; Hen, R., and Gardier, A.M. Characterization of 5-HT(1A/1B)-/- mice: an animal model sensitive to anxiolytic treatments. *Neuropharmacology*, **2011**, *61*(3), 478-88.
[345] Naughton, M.; Mulrooney, J.B., and Leonard, B.E. A review of the role of serotonin receptors in psychiatric disorders. *Hum Psychopharmacol*, **2000**, *15*(6), 397-415.
[346] Kusumi, I.; Boku, S., and Takahashi, Y. Psychopharmacology of atypical antipsychotic drugs: From the receptor binding profile to neuroprotection and neurogenesis. *Psychiatry Clin Neurosci*, **2015**, *69*(5), 243-58.
[347] Bristow, L.J.; O'Connor, D.; Watts, R.; Duxon, M.S., and Hutson, P.H. Evidence for accelerated desensitisation of 5-HT(2C) receptors following combined treatment with fluoxetine and the 5-HT(1A) receptor antagonist, WAY 100,635, in the rat. *Neuropharmacology*, **2000**, *39*(7), 1222-36.
[348] Boothman, L.; Raley, J.; Denk, F.; Hirani, E., and Sharp, T. In vivo evidence that 5-HT(2C) receptors inhibit 5-HT neuronal activity via a GABAergic mechanism. *Br J Pharmacol*, **2006**, *149*(7), 861-9.
[349] Mongeau, R.; Martin, C.B.; Chevarin, C.; Maldonado, R.; Hamon, M.; Robledo, P., and Lanfumey, L. 5-HT2C receptor activation prevents stress-induced enhancement of brain 5-HT turnover and extracellular levels in the mouse brain: modulation by chronic paroxetine treatment. *J Neurochem*, **2010**, *115*(2), 438-49.
[350] Kim, H.S.; Park, I.S.; Lim, H.K., and Choi, H.S. NMDA receptor antagonists enhance 5-HT2 receptor-mediated behavior, head-twitch response, in PCPA-treated mice. *Arch Pharm Res*, **1999**, *22*(2), 113-8.
[351] Mansbach, R.S.; Carver, J., and Zorn, S.H. Blockade of drug-induced deficits in prepulse inhibition of acoustic startle by ziprasidone. *Pharmacol Biochem Behav*, **2001**, *69*(3-4), 535-42.
[352] Yoshizawa, K.; Mori, T.; Ueno, T.; Nishiwaki, M.; Shibasaki, M.; Shimizu, N.; Narita, M., and Suzuki, T. Involvement of serotonin receptor mechanisms in the discriminative stimulus effects of ketamine in rats. *J Pharmacol Sci*, **2013**, *121*(3), 237-41.
[353] Maricq, A.V.; Peterson, A.S.; Brake, A.J.; Myers, R.M., and Julius, D. Primary structure and functional expression of the 5HT3 receptor, a serotonin-gated ion channel. *Science*, **1991**, *254*(5030), 432-7.
[354] Martin, P.; Gozlan, H., and Puech, A.J. 5-HT3 receptor antagonists reverse helpless behaviour in rats. *Eur J Pharmacol*, **1992**, *212*(1), 73-8.
[355] Nakagawa, Y.; Ishima, T., and Takashima, T. The 5-HT3 receptor agonist attenuates the action of antidepressants in the forced swim test in rats. *Brain Res*, **1998**, *786*(1-2), 189-93.
[356] Kos, T.; Popik, P.; Pietraszek, M.; Schafer, D.; Danysz, W.; Dravolina, O.; Blokhina, E.; Galankin, T., and Bespalov, A.Y. Effect of 5-HT3 receptor antagonist MDL 72222 on behaviors induced by ketamine in rats and mice. *Eur Neuropsychopharmacol*, **2006**, *16*(4), 297-310.
[357] Nikiforuk, A.; Fijal, K.; Potasiewicz, A.; Popik, P., and Kos, T. The 5-hydroxytryptamine (serotonin) receptor 6 agonist EMD 386088 ameliorates ketamine-induced deficits in attentional set shifting and novel object recognition, but not in the prepulse inhibition in rats. *J Psychopharmacol*, **2013**, *27*(5), 469-76.
[358] Galici, R.; Boggs, J.D.; Miller, K.L.; Bonaventure, P., and Atack, J.R. Effects of SB-269970, a 5-HT7 receptor antagonist, in mouse models predictive of antipsychotic-like activity. *Behav Pharmacol*, **2008**, *19*(2), 153-9.
[359] Nikiforuk, A.; Kos, T.; Fijal, K.; Holuj, M.; Rafa, D., and Popik, P. Effects of the selective 5-HT7 receptor antagonist SB-269970 and amisulpride on ketamine-induced schizophrenia-like deficits in rats. *PLoS One*, **2013**, *8*(6), e66695.
[360] Holuj, M.; Popik, P., and Nikiforuk, A. Improvement of ketamine-induced social withdrawal in rats: the role of 5-HT7 receptors. *Behav Pharmacol*, **2015**, *26*(8), 766-75.
[361] Lopez-Gil, X.; Babot, Z.; Amargos-Bosch, M.; Sunol, C.; Artigas, F., and Adell, A. Clozapine and haloperidol differently suppress the MK-801-increased glutamatergic and serotonergic transmission in the medial prefrontal cortex of the rat. *Neuropsychopharmacology*, **2007**, *32*(10), 2087-97.
[362] Shi, W.X. and Zhang, X.X. Dendritic glutamate-induced bursting in the prefrontal cortex: further characterization and effects of phencyclidine. *J Pharmacol Exp Ther*, **2003**, *305*(2), 680-7.
[363] Brachman, R.A.; McGowan, J.C.; Perusini, J.N.; Lim, S.C.; Pham, T.H.; Faye, C.; Gardier, A.M.; Mendez-David, I.; David, D.J.; Hen, R., and Denny, C.A. Ketamine as a Prophylactic Against Stress-Induced Depressive-like Behavior. *Biol Psychiatry*, **2016**, *79*(9), 776-86.
[364] Zhao, J.; Wang, Y., and Wang, D. The Effect of Ketamine Infusion in the Treatment of Complex Regional Pain Syndrome: a Systemic Review and Meta-analysis. *Curr Pain Headache Rep*, **2018**, *22*(2), 12.
[365] Lindefors, N.; Barati, S., and O'Connor, W.T. Differential effects of single and repeated ketamine administration on dopamine, serotonin and GABA transmission in rat medial prefrontal cortex. *Brain Res*, **1997**, *759*(2), 205-12.
[366] Riga, M.S.; Sanchez, C.; Celada, P., and Artigas, F. Involvement of 5-HT3 receptors in the action of vortioxetine in rat brain: Focus on glutamatergic and GABAergic neurotransmission. *Neuropharmacology*, **2016**, *108*, 73-81.
[367] Dale, E.; Grunnet, M.; Pehrson, A.L.; Frederiksen, K.; Larsen, P.H.; Nielsen, J.; Stensbol, T.B.; Ebert, B.; Yin, H.; Lu, D.; Liu, H.; Jensen, T.N.; Yang, C.R., and Sanchez, C. The multimodal antidepressant vortioxetine may facilitate pyramidal cell firing by inhibition of 5-HT3 receptor expressing interneurons: An in vitro study in rat hippocampus slices. *Brain Res*, **2017**.
[368] Lin, L.C. and Sibille, E. Somatostatin, neuronal vulnerability and behavioral emotionality. *Mol Psychiatry*, **2015**, *20*(3), 377-87.
[369] Duman, R.S. Neuronal damage and protection in the pathophysiology and treatment of psychiatric illness: stress and depression. *Dialogues Clin Neurosci*, **2009**, *11*(3), 239-55.
[370] Morales, I.; Sabate, M., and Rodriguez, M. Striatal glutamate induces retrograde excitotoxicity and neuronal degeneration of intralaminar thalamic nuclei: their potential relevance for Parkinson's disease. *Eur J Neurosci*, **2013**, *38*(1), 2172-82.
[371] Moussawi, K.; Riegel, A.; Nair, S., and Kalivas, P.W. Extracellular glutamate: functional compartments operate in different concentration ranges. *Front Syst Neurosci*, **2011**, *5*, 94.
[372] Caillard, O.; Moreno, H.; Schwaller, B.; Llano, I.; Celio, M.R., and Marty, A. Role of the calcium-binding protein parvalbumin in short-term synaptic plasticity. *Proc Natl Acad Sci U S A*, **2000**, *97*(24), 13372-7.
[373] Kuki, T.; Fujihara, K.; Miwa, H.; Tamamaki, N.; Yanagawa, Y., and Mushiake, H. Contribution of parvalbumin and somatostatin-expressing GABAergic neurons to slow oscillations and the balance in beta-gamma oscillations across cortical layers. *Front Neural Circuits*, **2015**, *9*, 6.
[374] Pongdhana, K.; Ogawa, N.; Hirose, Y.; Ono, T.; Kosaka, F., and Mori, A. Effects of ketamine on the cholecystokinin, somatostatin, substance P, and thyrotropin releasing hormone in discrete regions of rat brain. *Neurochem Res*, **1987**, *12*(1), 73-7.
[375] Cryan, J.F.; Markou, A., and Lucki, I. Assessing antidepressant activity in rodents: recent developments and future needs. *Trends Pharmacol Sci*, **2002**, *23*(5), 238-45.
[376] Blier, P.; Chaput, Y., and de Montigny, C. Long-term 5-HT reuptake blockade, but not monoamine oxidase inhibition, decreases the function of terminal 5-HT autoreceptors: an electrophysiological study in the rat brain. *Naunyn Schmiedebergs Arch Pharmacol*, **1988**, *337*(3), 246-54.
[377] Le Poul, E.; Laaris, N.; Doucet, E.; Laporte, A.M.; Hamon, M., and Lanfumey, L. Early desensitization of somato-dendritic 5-HT1A autoreceptors in rats treated with fluoxetine or paroxetine. *Naunyn Schmiedebergs Arch Pharmacol*, **1995**, *352*(2), 141-8.
[378] Chaput, Y.; de Montigny, C., and Blier, P. Effects of a selective 5-HT reuptake blocker, citalopram, on the sensitivity of 5-HT autoreceptors:

electrophysiological studies in the rat brain. *Naunyn Schmiedebergs Arch Pharmacol*, **1986**, *333*(4), 342-8.

[379] Hanoun, N.; Mocaer, E.; Boyer, P.A.; Hamon, M., and Lanfumey, L. Differential effects of the novel antidepressant agomelatine (S 20098) versus fluoxetine on 5-HT1A receptors in the rat brain. *Neuropharmacology*, **2004**, *47*(4), 515-26.

[380] Kotermanski, S.E. and Johnson, J.W. Mg2+ imparts NMDA receptor subtype selectivity to the Alzheimer's drug memantine. *J Neurosci*, **2009**, *29*(9), 2774-9.

[381] Mendez-David, I.; Boursier, C.; Domergue, V.; Colle, R.; Falissard, B.; Corruble, E.; Gardier, A.M.; Guilloux, J.P., and David, D.J. Differential Peripheral Proteomic Biosignature of Fluoxetine Response in a Mouse Model of Anxiety/Depression. *Front Cell Neurosci*, **2017**, *11*, 237.

[382] Mekiri, M.; Gardier, A.M.; David, D.J., and Guilloux, J.P. In: *Resistance to chronic antidepressant treatment: A behavioural and neurogenic study in a neuroendocrine-based mice model of anxiety/depression* In: 45th Annual Meeting of Neuroscience, Chicago, U.S.A., **November 2015**.

[383] Tritschler, L.; Kheirbek, M.A.; Dantec, Y.L.; Mendez-David, I.; Guilloux, J.P.; Faye, C.; Doan, J.; Pham, T.H.; Hen, R.; David, D.J., and Gardier, A.M. Optogenetic activation of granule cells in the dorsal dentate gyrus enhances dopaminergic neurotransmission in the Nucleus Accumbens. *Neurosci Res*, **2017**.

[384] Burgdorf, J.; Zhang, X.L.; Nicholson, K.L.; Balster, R.L.; Leander, J.D.; Stanton, P.K.; Gross, A.L.; Kroes, R.A., and Moskal, J.R. GLYX-13, a NMDA receptor glycine-site functional partial agonist, induces antidepressant-like effects without ketamine-like side effects. *Neuropsychopharmacology*, **2013**, *38*(5), 729-42.

Received: date Revised: date Accepted: date

Objectif de ma thèse

Les crises du trouble dépressif majeure (TDM), en particulier de la dépression résistante au traitement (TRD), ainsi que les problèmes des traitements classiques actuels (délai d'action retardé important, faibles taux d'efficacité) soulignent l'importance de trouver une solution plus efficace. La kétamine induit une réponse rapide et persistante à la dépression, pourtant ses effets indésirables en clinique (hallucinations, risque de dépendance) ainsi que ceux observés en préclinique (schizophrénie, hyperlocomotion, stéréotypies) limitent son application thérapeutique.

En comprenant ces défis, nous avons voulu à contribuer à la connaissance de son mécanisme d'action antidépresseur rapide, chez la souris. Notre étude est réalisée 24 heures après l'administration d'une seule dose faible (10 mg/kg, i.p. ou 2 nmol intra-mPFC) de kétamine pour étudier son effet "soutenu". C'est la condition la plus reconnue pour imiter l'effet antidépresseur de cette molécule chez l'homme. Nous utilisons, au cours de notre étude, des souris BALB/cJ, pour leur phénotype hyper-anxieux (Dulawa *et al.*, 2004). Selon les études moléculaires, le mPFC joue un rôle important dans l'effet antidépresseur de la kétamine, i.e., une augmentation de l'expression de mTOR et du BDNF qui induit la synaptogenèse des neurones corticaux chez les rongeurs (Duman *et al.*, 2016; Li *et al.*, 2010). Pourtant, les études neurochimiques, en particulier celles qui ont une relation proche du comportement, sont très limitées en nombre.

Le 1er objectif de ma thèse est d'**étudier l'interaction entre le système sérotoninergique du circuit mPFC – noyau du raphé dorsal** (NRD, une région dans laquelle se trouve une forte population des corps cellulaires sérotoninergiques) **dans l'effet de type antidépresseur rapide de la kétamine** (**Article 1**), en comparaison avec un traitement antidépresseur classique de référence (fluoxétine).

La kétamine ne peut pas être l'antidépresseur de demain, du fait de ses effets indésirables. Mais son métabolite pourrait être un antidépresseur prometteur. Le 2ème objectif, la suite de notre travail est d'**évaluer l'effet antidépresseur du métabolite principal de la racémique (*R,S*)-kétamine, le (2*R*,6*R*)-hydroxynorkétamine (HNK)**. Cette molécule posséderait une activité antidépressive potentielle comparable à celle de la kétamine (Zanos *et al.*, 2016), mais avec moins d'effets néfastes. Il a montré que contrairement à la (*R,S*)-kétamine qui agirait comme bloqueur du récepteur NMDA, le (2*R*,6*R*)-HNK activerait

directement le récepteur AMPA. Pourtant, Yang *et al.*, 2016 a réfuté cette hypothèse en montrant que seule la (*R*)-kétamine présente des effets de type antidépresseur chez les souris mâles C57BL/6j. De plus, aucune étude n'a montré l'effet neurochimique de (2R,6R)-HNK. Ce sujet d'actualité, malgré des résultats controversés, nous a inspiré (**Article 2**).

Nous avons d'abord évalué l'effet antidépresseur du (2*R*,6*R*)-HNK chez la souris, dans nos conditions expérimentales, en comparant avec sa molécule mère, la (*R,S*)-kétamine, dans le test de microdialyse *in vivo* couplé avec la nage forcée (forced swim test, FST). Nous étudions ainsi simultanément les effets comportementaux et neurochimiques (5-HT, glutamate, glutamine et GABA) de ces deux molécules pour mieux les comparer. Ensuite, nous avons vérifié leurs concentrations plasmatiques à 30 minutes et à 24 heures après l'administration. Ces données permettent de déterminer le taux du métabolisme de la (*R,S*)-kétamine vers le (2*R*,6*R*)-HNK, ainsi que les taux résiduels à 24 heures. En sachant que le (2*R*,6*R*)-HNK agirait directement sur le récepteur AMPA pour favoriser la décharge électrique neuronale, nous avons ensuite réalisé une étude de zéro-net-flux pour étudier la fonction des transporteurs glutamatergiques, afin de confirmer l'origine du glutamate extracellulaire trouvé dans les dialysats corticaux. Notre étude a fourni des informations précises et originales sur les modifications comportementales et neurochimiques chez la souris BALB/Cj induites par ces deux molécules.

Pour renforcer ces résultats, l'isomère "S" (2*S*,6*S*)-HNK, a été comparé au (2*R*,6*R*)-HNK (Résultats complémentaires).

Le 3ème objectif, après avoir confirmé une participation dynamique du glutamate, du GABA et de la 5-HT extracellulaires corticales dans l'effet antidépresseur "soutenu" de la kétamine, nous avons étudié plus en détail **le système glutamatergique et GABAergique du circuit mPFC-NRD à l'aide des agents pharmacologiques et de la technique d'optogénétique**. Dans cet article, le circuit mPFC-NRD est activé ou bloqué localement à l'aide d'antagonistes ou d'agonistes sélectifs du récepteur $GABA_A$ ou du récepteur AMPA, et à l'aide de l'outil optogénétique qui permet d'utiliser la lumière pour contrôler l'activité électrique d'une population de neurones sélectifs, ici dans notre étude, les neurones glutamatergiques pyramidaux du mPFC. De plus, nous avons utilisé l'acide dihydrokainique (DHK), un inhibiteur sélectif de transporteur GLT1 du glutamate, pour mieux comprendre comment ce transporteur limite les concentrations intra-synaptiques de glutamate libérées par la kétamine et intervient dans son activité antidépressive (comme déjà montrés chez le rat, Gasull-Camos *et al.*, 2017).

Ces résultats permettent d'approfondir les connaissances de ce circuit neuronal, ainsi que l'implication de différents types de récepteurs et de neurones dans les modifications neurochimiques induites par la kétamine (**Article 3**).

Après une partie consacrée aux méthodes utilisées pour réaliser ces travaux de thèse, les articles expérimentaux seront insérés "en anglais" dans leur format de publication, précédés d'un paragraphe en français précisant la question posée et introduisant l'étude, puis suivis de commentaires résumant les principaux effets découverts.

Matériels et méthodes

Mon projet de thèse se compose de 3 méthodes principales : la microdialyse *in vivo*, les tests comportementaux et l'optogénétique. Après avoir maîtrisé chaque technique individuelle, j'ai réussi à combiner la microdialyse *in vivo* avec les tests comportementaux (la nage forcée ou "forced swim test – FST" et le novelty suppressed feeding – NSF) et ultérieurement, la microdialyse *in vivo* couplée avec le FST et l'optogénétique. La combinaison de ces techniques permet d'avoir l'accès à des données profondes en corrélant les changements comportementaux avec les modifications des concentrations de neurotransmetteurs au niveau cérébral.

Les tests comportementaux ont été réalisés et filmés par moi-même, puis scorés et vérifiés par Pr. Denis DAVID.

La mise au point de l'optogénétique dans notre labo a été faite par Dr. Laurent TRITSCHLER. Sous ses instructions, je l'ai développée pour combiner l'optogénétique avec la microdialyse *in vivo* et le FST chez la même souris.

L'illustration de tous les tests se trouve dans Figure 4, Figure 11, Figure 12, Figure 13, Figure 14, Figure 20 et Figure 23.

1 Animaux

Les animaux ont été hébergés au sein du Service Commun Animalerie de la Faculté (SCA) dans des cages d'élevage standard sur un portoir ventilé, avec un accès libre à l'eau et à la nourriture (cycle jour/nuit : 12h/12h non inversé). La température des pièces était maintenue à un niveau constant de +22°C.

Les études de microdialyse et de comportements ont été réalisées chez des souris BALBc/J âgées de 9 à 12 semaines et pesant de 20 à 25g. Les animaux ont été logés par groupe de 4 par cage. Cette souche a été choisie pour leur phénotype hyper-anxieux (Dulawa *et al.*, 2004). Les animaux utilisés comme contrôles étaient issus des mêmes portées ("littermates").

2 Microdialyse intracérébrale *in vivo* chez la souris éveillée

2.1 Principe

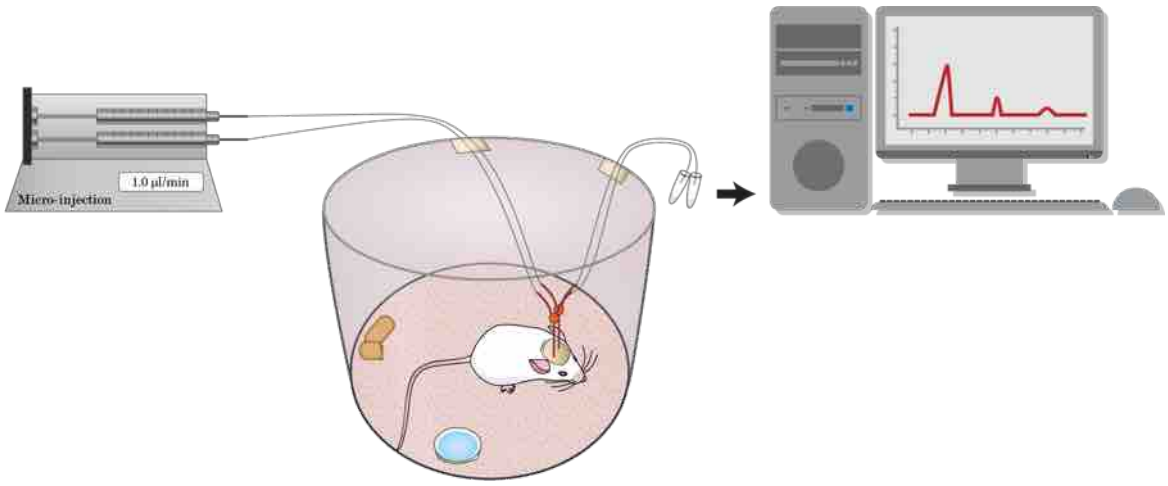

Figure 4. Installation de la microdialyse in vivo chez la souris éveillée

La technique de microdialyse *in vivo*, chez l'animal anesthésié ou éveillé, a été mise au point par le groupe de Delgado *et al.*, 1972, puis perfectionnée par Ungerstedt, 1991. Son principe repose sur la loi de diffusion passive de composés de faibles poids moléculaires à travers une membrane poreuse, du compartiment le plus concentré en neurotransmetteurs (l'espace extracellulaire synaptique) vers le compartiment le moins concentré (la sonde de dialyse perfusé avec une solution tampon à pH physiologique ne contenant pas de neurotransmetteurs). Cette technique (Figure 4), appliquée dans notre laboratoire chez la souris éveillée, libre de ses mouvements, permet le recueil d'échantillons (dialysats) toutes les 15 ou 30 minutes avec des débits de 0,5 à 1,5 µl/min selon le protocole expérimental et la région cérébrale dialysée. Dans ces échantillons, nous mesurons la sérotonine (5-HT), la noradrénaline (NA), la dopamine (DA) et leurs métabolites, ainsi que le glutamate (Glu), la glutamine (Gln) et le GABA. Ces molécules sont ensuite quantifiées par une méthode analytique de dosage impliquant une chromatographie liquide haute performance (HPLC) couplée à un détecteur électrochimique pour les monoamines et par la chromatographie en phase liquide couplée à la spectrométrie de masse (LC-MS, en coopération avec SAMM plateforme) pour Glu, Gln et GABA. Les concentrations de neurotransmetteurs mesurées reflètent l'équilibre physiologique entre le mécanisme de libération calcium-dépendant du neurotransmetteur et celui de sa recapture par le transporteur sélectif (par exemple, le transporteur neuronal SERT pour la sérotonine, et principalement le transporteur glial GLT-1

pour le glutamate). Une étude complète de microdialyse intracérébrale comporte 4 phases : (1) l'implantation chirurgicale de la sonde par stéréotaxie sous anesthésie, (2) le recueil des dialysats (valeur basale des concentrations extracellulaires du neurotransmetteur avant traitement, puis 2 à 3 heures après le traitement), (3) le prélèvement des cerveaux en vue de la vérification macroscopique précise du site d'implantation de la membrane de microdialyse et (4) l'analyse chromatographique des dialysats.

Les sondes de microdialyse sont composées d'un capillaire de d'entrée, et d'un capillaire de sortie et, au laboratoire, d'une membrane en cuprophane perméable, laissant passer les molécules de poids moléculaires inférieurs à 6000 Daltons (Geeraerts *et al.*, 2008) dont la 5-HT, le Glu, la Gln et le GABA dans notre étude (Figure 5).

Dans ce projet, le cortex médian préfrontal (mPFC) et le noyau du raphé dorsal (NRD) ont été étudiés pour déterminer l'effet de l'administration systémique et locale, intra-corticale de la kétamine (Figure 6).

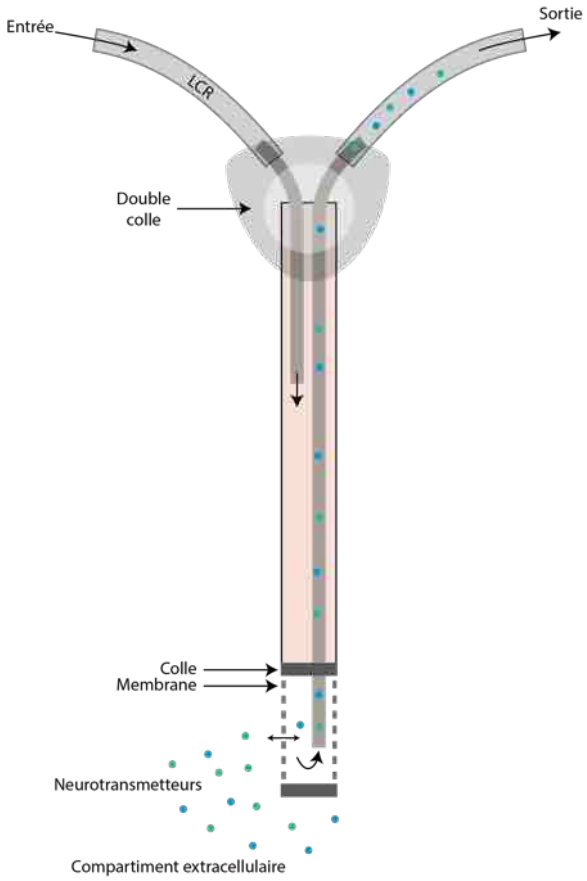

Figure 5. Composition d'une sonde de microdialyse conventionnée

2.2 Chirurgie de l'implantation des sondes de microdialyse

Les souris ont été anesthésiées à l'aide d'hydrate de chloral (400 mg/kg ; i.p.), puis placées sur un appareil stéréotaxique afin de les maintenir immobile grâce à des barres d'oreilles et un étau buccal fixant la mâchoire supérieure. L'appareil stéréotaxique permet le déplacement avec une grande précision d'un bras muni de vis micrométriques portant la sonde de dialyse dans les trois dimensions (Antéro-postérité, Latéralité et Ventralité). Après

l'incision longitudinale de la peau du crâne, celle-ci est écartée et l'os crânien nettoyé avec de l'eau oxygénée (10 volumes). Le bregma, point d'intersection des lignes de suture des os du crâne est alors visible et sert de point de référence (point "zéro") antéro-postérité et latéral (Figure 6). Avant chaque implantation la position horizontale de la tête de l'animal est vérifiée en s'assurant que la différence de hauteur entre le bregma et le lambda ne dépasse pas 35 µm.

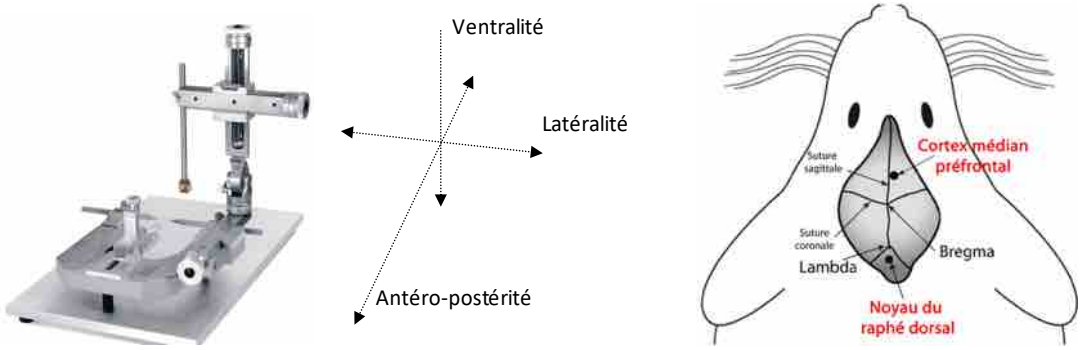

Figure 6. Régions cérébrales d'intérêts du projet de recherche chez la souris

A partir de ce point et grâce aux coordonnées données par l'atlas stéréotaxique de la souris (Tableau 3), l'os du crâne est percé manuellement à l'aide d'une aiguille Terumo (gauge 23G), en deux points symétriquement opposés pour le cortex frontal (région symétrique, présente dans chaque hémisphère) ou en un seul point pour le NRD. La surface de la dure mère constitue le point de coordonnée "zéro" de l'axe dorso-ventral. La sonde est descendue manuellement et très lentement à raison d'un millimètre (mm) par minute pour limiter les conséquences de la destruction tissulaire, puis collée à l'os crânien avec du ciment dentaire (GACD, Paris, France). Après cette étape de chirurgie, les souris sont placées isolément dans des cages cylindriques en plexiglas dans lesquelles elles sont libres de leurs mouvements et ont un accès ad libitum à l'eau et à la nourriture. Environ 20 heures après la chirurgie, les animaux sont prêts à être utilisés pour les expériences de microdialyse.

	Antéro-postérité	**Latéralité**	**Ventralité**
mPFC	+2,2 mm	± 0,5 mm	- 3,4 mm
NRD (avec un angle de 15°)	- 4,5 mm	+ 1,2 mm	- 4,8 mm

Tableau 3. Coordonnées des 2 régions étudiées par l'atlas stéréotaxique de la souris Paxinos et Franklin (2007)

2.3 Microdialyse intracérébrale

2.3.1 Microdialyse conventionnelle

L'ensemble de la procédure et son principe sont rappelés dans la Figure 4. Le jour de la dialyse, l'entrée des sondes est reliée à un perfuseur automatique (CMA 100, Phymep, Paris) délivrant du LCR artificiel de composition suivante :

Composants	Concentration (en mM)
NaCl	147
KCl	3,5
CaCl2	2,26
NaHCO3	1
NaH2PO4	1
pH	7,4 ± 0,2

Tableau 4. Composition du liquide céphalo-rachidien (LCR) artificiel

Cette solution tampon artificielle est donc délivrée de manière continue et diffuse à travers la membrane de dialyse (Figure 5). Après 1 à 2 heures de stabilisation, les 4 à 6 premiers échantillons sont recueillis par le capillaire de sortie, de manière à établir la moyenne des concentrations extracellulaires basales de 5-HT (5-HT_{ext}), de glutamate (Glu_{ext}), de glutamine (Gln_{ext}) et de GABA ($GABA_{ext}$) pour chaque souris. Les effets des substances pharmacologiques à étudier (kétamine ou fluoxétine) par voies intra-péritonéale (i.p.) sous un volume de 0,1 ml/10 g de poids corporel sont comparés aux effets de leur solvant administré comme contrôle.

A la fin de la séance de microdialyse, les souris sont euthanasiées par une injection létale d'hydrate de chloral. Les cerveaux sont prélevés, puis conservés dans une solution de PFA 4% (paraformaldéhyde) à +4°C dans un réfrigérateur avant leur analyse histologique.

2.3.2 Perfusion locale dans une région cérébrale donnée ("reverse dialysis")

Chacune des substances étudiées sera dissoute dans une solution tampon mimant le LCR et la concentration de la solution est adaptée en fonction du volume injecté. D'abord, la solution normale de LCR (sans substances) est délivrée de manière continue et diffuse à travers la membrane de dialyse. Après 1 à 2 heures de stabilisation, les 4 à 6 premiers échantillons sont recueillis comme ci-dessus pour calculer la moyenne des concentrations extracellulaires

basales des neurotransmetteurs pour chaque souris. La seringue et le cathéter sont ensuite remplis de la solution tampon artificielle contenant la molécule à étudier à concentrations variables. Les effets de ces substances pharmacologiques sur les neurotransmetteurs sont calculés en pourcentage de variations des concentrations basales de neurotransmetteurs.

2.3.3 Injection locale dans une région cérébrale donnée

Différente de la perfusion locale limitée par le rendement de la membrane de microdialyse, cette technique permet que les substances étudiées soient délivrées à travers une capillaire indépendant, accolé à la membrane pour que les substances soient injectées directement dans la région d'intérêt avec un rendement de 100%.

La longueur du capillaire d'injection est en fait plus courte que celle du capillaire de sortie pour ne pas limiter le recueil des dialysats dans la zone de microdialyse (Figure 7).

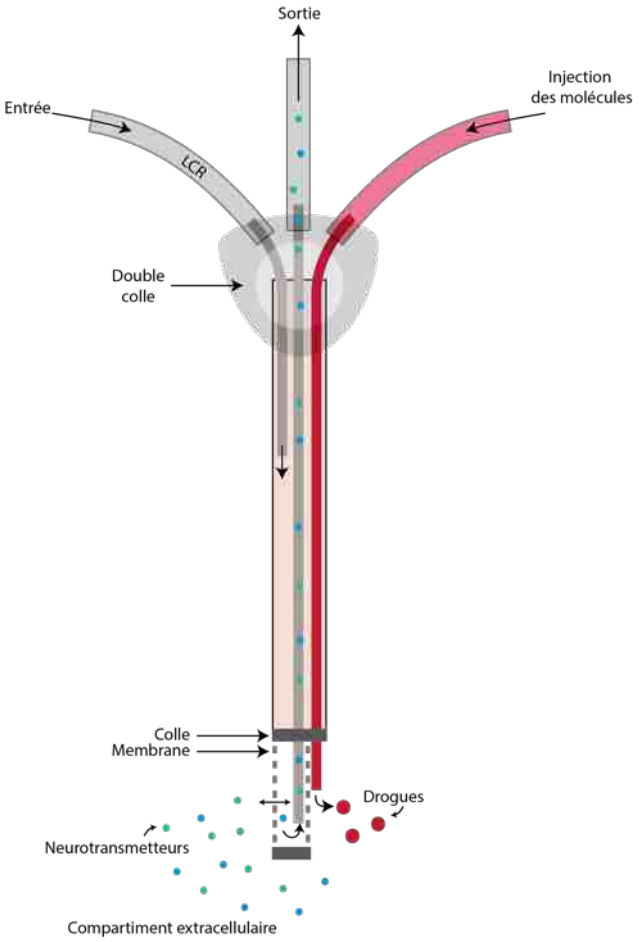

Figure 7. Schéma d'une sonde de microdialyse "modifiée" pour l'injection locale

2.4 Vérification du rôle de la recapture du glutamate par les transporters glutamatergiques par la technique "no-net-flux", une méthode de microdialyse quantitative

Que mesurons-nous *in vivo* dans les dialysats ? les concentrations extracellulaires d'un neurotransmetteur. Mais il s'agit du reflet d'un équilibre entre la libération de ce

neurotransmetteur (“release”), et sa recapture (“reuptake” par les transporteurs glutamatergiques neuronaux et gliaux). La technique “no-net-flux”, ou “zero-net-flux”, ou microdialyse quantitative *in vivo* a été développée par Lonnroth *et al.*, 1987 dans le but de répondre à cette question. Cela permet aussi de vérifier l’origine neuronale de Glu_{ext}. Ceci est particulièrement important pour le glutamate pour lequel les astrocytes et la glutamine jouent un rôle important dans la Glu_{ext} dans les dialysats (Bonvento *et al.*, 2017). Concrètement, des concentrations croissantes d’une substance connue (ex : le glutamate) sont perfusées à travers la sonde de microdialyse placée dans le mPFC dans notre étude. Le sens du gradient de concentrations entre la solution tampon perfusée et l’espace extracellulaire synaptique favorise la diffusion du glutamate dans le mPFC. Quand la concentration de la substance dans le compartiment extracellulaire (C_{out}) est égale à celle du milieu tampon perfusée (C_{in}), nous le nommons “no-net-flux à l’équilibre” qui est calculé par différence entre (C_{out} - C_{in} = 0). En reliant la différence entre ces 2 compartiments, la concentration de la substance dans le compartiment extracellulaire peut alors être déduite.

Dans mon projet, cette technique a été appliquée pour mesurer quelle est la part de la recapture de glutamate par rapport à sa libération dans les dialysats en réponse à la kétamine . Trois concentrations différentes, de la moins à la plus concentrée, de glutamate ont été perfusées à travers la sonde de microdialyse chez des souris BALB/Cj. Entre chaque concentration de glutamate, le milieu tampon normal sans glutamate, est perfusée pour permettre de retrouver la ligne de base avant de perfuser la concentration suivante (Figure 8). La différence entre la quantité de glutamate perfusée dans le milieu tampon (C_{in}) et celle récupérée à la sortie de la sonde de microdialyse (C_{out}) définie la ligne de no-net-flux (consulter l’Article 2 page 153 – Pham *et al.*, 2017, Biol Psy, dans la partie Résultats pour plus d’information). Nous comparons la valeur du no-net-flux entre des souris contrôles ayant un fonctionnement normal des transporteurs glutamatergiques *versus* des souris ayant reçu les molécules d’intérêt (la kétamine et le (2R,6R)-HNK) 24h avant l’expérimentation. La déclivité de la pente de no-net-flux reflète ce fonctionnement: une diminution de cette pente montre une réduction de la fonction des transporters glutamatergiques par la kétamine ou le (2R,6R)-HNK) et une augmentation de cette pente présente l’inverse.

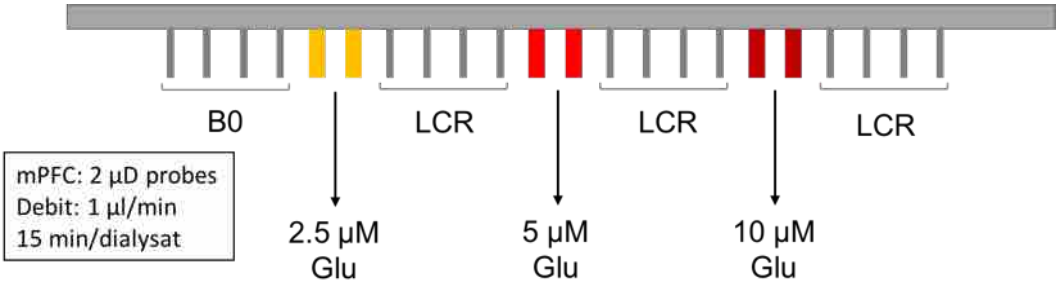

Figure 8. Protocole de no-net-flux

2.5 La vérification histologique de l'implantation de sondes microdialyse

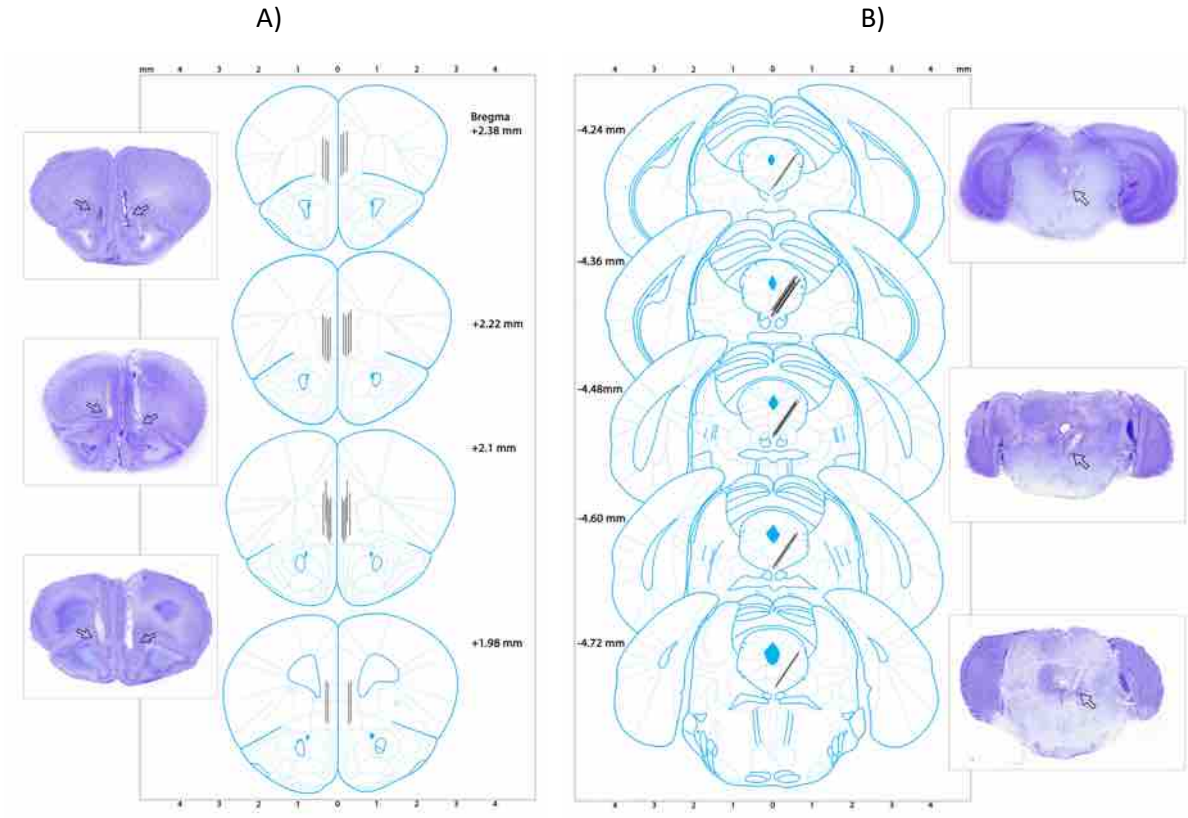

Figure 9. Vérification de l'emplacement des sondes de microdialyse sur des coupes de cerveaux de mPFC (A) et de NRD (B) selon l'Atlas du cerveau de souris de Paxinos et Franklin (2007).

À la fin des expériences de microdialyse, les animaux sont sacrifiés et leurs cerveaux sont prélevés. Ces cerveaux sont ensuite coupés en tranches de 20 µm d'épaisseur à l'aide d'un cryostat, puis les coupes sont colorées avec le crésyl violet. Seuls les résultats du dosage des neurotransmetteurs chez les souris correctement implantées dans les régions d'intérêt (mPFC,

NRD) ont été pris en compte dans nos études. La Figure 9 présente un exemple de résultats obtenus sur des coupes de cerveaux représentant les régions de microdialyse dans le mPFC (A) et le NRD (B) selon l'Atlas du cerveau de souris de Paxinos et Franklin (2007).

Box 1. Les applications de la microdialyse intracérébrale *in vivo* en étudiant des agents pharmacologiques

1) PRINCIPE DE LA MICRODIALYSE

Son principe repose sur la loi de diffusion passive de composés de faibles poids moléculaires à travers une membrane poreuse, du compartiment le plus concentré aux neurotransmetteurs (l'espace extracellulaire synaptique) vers le compartiment le moins concentré (la sonde de dialyse perfusée avec une solution tampon à pH physiologique (ex LCR artificiel) ne contenant pas de neurotransmetteurs).

2) L'APPLICATION CONVENTIONNELLE DE LA MICRODIALYSE

La sonde de microdialyse est composée d'un capillaire d'entrée, et d'un capillaire de sortie et d'une membrane en cuprophane perméable, laissant passer les molécules de poids moléculaires inférieurs à 6000 Daltons dont des neurotransmetteurs centraux.

3) LA MICRODIALYSE "INVERSE"

Les molécules d'intérêt peuvent être dissoutes dans le LCR artificiel et diffusent dans le cerveau à travers la membrane de la microdialyse selon le principe décrit ci-dessus. La diffusion des molécules dépendent du rendement de la membrane.

4) L'INJECTION LOCALE A TRAVERS LA SONDE DE MICRODIALYSE

Les molécules d'intérêt sont injectées directement dans le cerveau à l'aide d'une cathéter collée à la sonde de microdialyse. La diffusion des molécules est alors indépendante du rendement de la membrane de dialyse.

5) LE NO-NET-FLUX ou microdialyse quantitative

Cette technique est appliquée pour l'étude de la fonctionnalité de la recapture des neurotransmetteurs et connaître la part de ce qui est libéré (release) *versus* recapté (reuptake) dans les concentrations d'un neurotransmetteur mesurées dans les dialysats. En général, des concentrations différentes d'une substance connue (le glutamate dans notre étude) sont perfusées à travers la sonde de microdialyse. Le moment où la concentration de la substance du compartiment extracellulaire (C_{out}) est égale à celle du milieu tampon perfusée (C_{in}), est appelé le no-net-flux à l'équilibre et calculé par différence ($C_{out} - C_{in} = 0$). En reliant cette différence entre ces 2 compartiments, la concentration de la substance au compartiment extracellulaire peut être définie. L'administration unique ou répétée d'un médicament peut influer sur cette différence.

2.6 L'analyse chromatographique

La quantification de la 5-HT, contenue dans les échantillons de microdialyse, a été réalisé par chromatographie liquide à haute performance (HPLC) couplée à un détecteur ampérométrique (1049A, Hewlett-Packard, Les Ulis, France) (Figure 10). Une colonne XL-ODS de 4,6 x 7,0 mm (taille des particules de 3 µm; Beckman) est utilisée pour la séparation. La phase mobile est composée de : $NaH_2PO_4.2H_2O$ (107 mM) ; EDTA (0,14 mM) ; acide octanosulfonique ($C_8H_{17}NaO_3S$, 0,77 mM) ; méthanol 350 ml ; l'eau ultrapure 2000 ml ; pH 4,1 (ajustée avec l'acide orthophosphorique à 85 %). La limite de sensibilité pour la 5-HT est de ≈ 0,5 fmol/ échantillon (signal-to-noise ratio = 2). Le temps de rétention de la 5-HT est de 13 à 14 minutes.

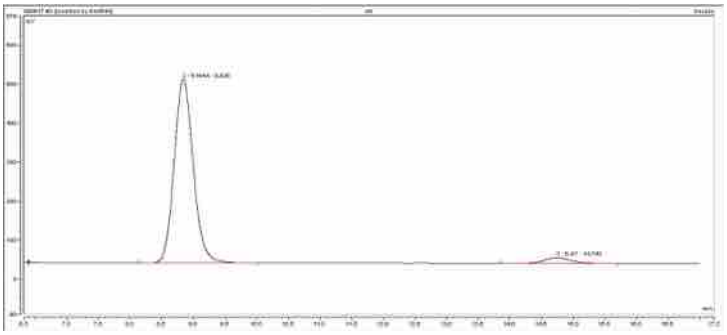

Figure 10. Exemple de la chromatographie de la 5-HT par HPLC

Le glutamate, la glutamine et le GABA ont été quantifié par HPLC couplée à la spectrométrie de masse en tandem (LC-MS/MS). Les étapes de la mise au point et la validation de la méthode sont détaillées dans l'article de **C. Defaix *et al*., 2018, Journal of Pharmaceutical and Bioanalytical Analysis** (voir page 121).

D'une manière simplifiée, une gamme étalon, avec des concentrations connues des différents composés, est réalisée avant l'analyse des échantillons récupérés chez l'animal par microdialyse. Deux standards internes (Glu-d5 et GABA-d6) ont été utilisés afin de pouvoir quantifier les concentrations des composés. Ils sont ajoutés dans la gamme étalon et dans tous les dialysats. La séparation des composés est réalisée par une colonne Nucleoshell HILIC, EC 100/2 ; 2,7 µm (Macherey-Nagel, Hoerdt, France) en utilisant un gradient d'élution avec une phase mobile composée d'une phase aqueuse (25 mM de formate d'ammonium, pH 3,5) et d'une phase organique (acétonitrile). La détection simultanée des composés est effectuée par spectrométrie de masse. Cette méthode analytique, largement répandue, est sensible, sélective et bien adaptée à la quantification des composés dans les dialysats. Une fois élués, les composés sont détectés à 13,9 min pour le glutamate, 13,8 pour la glutamine et 12,6 pour le GABA. La limite de quantification est ≈ 0,63 ng/ml pour GABA, 1,25 ng/ml pour Glu et 3,15 ng/ml pour Gln (signal-to-noise ratio = 10).

2.7 Principaux avantages et inconvénients de la technique de microdialyse chez les Rongeurs

Avantages	Inconvénients
• Outil d'étude préclinique du neurotransmetteurs centraux. • Permet également d'apporter in situ des molécules exogènes, avec des dégâts minimes au tissu cérébral, puisqu'il n'y pas d'échanges de liquide au niveau de la sonde. • Chez une même souris, il est possible d'implanter plusieurs sondes : Ex : une sonde dans le NRD (corps cellulaires), et 2 sondes dans une région terminale (hippocampe, cortex frontal), donc d'étudier un circuit neuronal. • L'animal utilisé peut être dialysé pendant deux jours consécutifs. Chaque animal peut être utilisé comme son propre témoin suite par exemple à un traitement pharmacologique. • Nombre d'animaux (5-6 par groupe) peut être moins important que dans les études comportementaux (10-12 par groupe). • Animaux vigils et libres de leurs mouvements pendant l'expérimentation pharmacologique. • Corrélation possible avec le comportement.	• Coût des sondes commerciales et difficulté d'en fabriquer "artisanalement". • Contrôle de la qualité de l'implantation a posteriori. • Important diamètre de la sonde (0.3 mm) ne permettant pas de distinguer chez la souris le cortex infra-limbique du cortex pré-limbique comme c'est le cas chez le rat (Gasull-Camos *et al.*, 2017). • Implantation assez approximative de la membrane (il faut surtout vérifier l'emplacement de l'extrémité de la membrane). • Résolution temporelle faible (10-15 minutes entre chaque échantillon). • En lien avec le débit de perfusion du tampon extracellulaire (1 µl/min) avec un dialysat toutes les 15-20 minutes. • 1 souris par jour pour 1 expérimentateur. Il faut beaucoup d'entraînement pour pouvoir s'occuper de plus de souris. • Expérience longue (3 à 6 mois) pour évaluer les effets de plusieurs doses d'un ligand par rapport à un groupe contrôle (souris traitées avec le véhicule ; souris "wild-type" (WT) versus souris "knockout" KO. • En ce qui concernent les antidépresseurs, peu d'intérêt de mesurer les concentrations extracellulaires des métabolites comme le 5-HIAA.

	• Effet du stress, délicate manipulation des animaux, ce qui nécessite un expérimentateur chevronné pour obtenir des résultats fiables.

Tableau 5. Des avantages et inconvénients de la technique de microdialyse

3 Tests comportementaux prédictifs d'un phénotype ou d'une activité de type antidépresseur/anxiolytique

Une résumé des tests comportementaux prédictifs des activités de type antidépresseur/anxiolytique est présentée dans **Box 2**. Au-dessous, seuls les tests impliqués dans ce projet sont décrits en détail.

3.1 Test de nage forcée (Forced Swim Test, FST) : test prédictif d'une activité antidépressive

La souris est placée dans un récipient en plastique transparent de 19 cm de diamètre et 23 cm de profondeur remplis aux 2/3 avec de l'eau à 23-25°C et la durée de son immobilité/mobilité est mesurée pendant 6 minutes. Seuls les 4 dernières minutes sont prises en compte (Porsolt *et al.*, 1977). Les experts savent dissocier la durée de mobilité dans le FST en deux éléments : le temps de nage (swimming) qui représente l'activation de la neurotransmission sérotoninergique centrale et le temps d'escalade (climbing) qui représente l'activation de la neurotransmission noradrénergique centrale (Cryan *et al.*, 2002b) (Figure 11).

Figure 11. Test de la nage forcée (FST)

3.2 Test d'alimentation supprimée par la nouveauté ou novelty suppressed feeding : test prédictif d'un phénotype ou d'une activité anxiolytique/antidépressive

Ce test induit une situation de motivations conflictuelles chez l'animal, entre celle dirigée vers la nourriture et la peur de s'aventurer au centre de l'enceinte fortement éclairée. Ce test a montré son aptitude à mettre en évidence des changements dans le comportement des rongeurs comme le Rat et la Souris, après un traitement anxiolytiques (traitement aigu) et antidépresseurs (traitement chronique) (Santarelli *et al.*, 2003). L'animal à jeun depuis 24 heures est placé dans une cage rectangulaire de 2500 cm (50x40x20 cm). Au centre de cette cage est disposé un cercle blanc éclairé dans lequel sont déposés 2 granulés de nourriture. L'animal est alors placé dans un coin du dispositif la tête face à la paroi, puis un chronomètre est immédiatement lancé. La latence pour mordre manifestement le granulé (croquer dans le granulé en utilisant ses pattes avant) est enregistrée. Les animaux sont testés individuellement pendant une période de 10 minutes (David *et al.*, 2009; Santarelli *et al.*, 2003). Nous mesurons le temps de latence mis par l'animal pour aller se nourrir (Figure 12). À la suite de ce test, l'animal est replacé dans sa cage et nous mesurons sa consommation de nourriture pour vérifier que les variations du temps de latence entre des animaux traités et des animaux non traités sont dues à l'activité anxiolytique/antidépresseur des molécules étudiées et non à un appétit moindre.

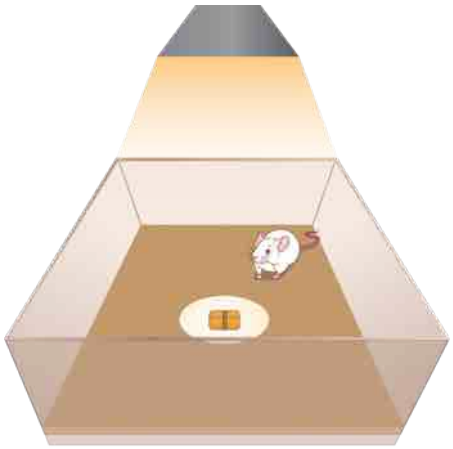

Figure 12. Test Novelty Suppressed Feeding (NSF)

Box 2. Les tests prédictifs d'un phénotype ou d'une activité anxiolytique/antidépressive chez les rongeurs

1) LA DEPRESSION :

FST – Forced swim test ou test de nage forcée

La souris est placée dans un récipient en plastique transparent remplis aux 2/3 avec de l'eau à 23-25°C et la durée de son immobilité/mobilité est mesurée pendant 6 minutes. Seules les 4 dernières minutes sont prises en compte (Porsolt *et al.*, 1977).

Le splash test

Une solution de sucrose à 10% est vaporisée sur le cou de l'animal. Cette solution est non seulement collante, ce qui doit initier un toilettage chez le rongeur, mais également appétissante. Plusieurs paramètres sont mesurés : la latence à initier un toilettage, le temps total et la fréquence des toilettages (sur une période de 5 minutes) (David *et al.*, 2009).

TST – Tail suspension test ou test de suspension caudale

L'animal est suspendu par le bout de la queue à l'aide d'un scotch doux à un crochet pendant 6 minutes. La durée de l'immobilité ainsi que la puissance des mouvements de l'animal sont mesurées (Porsolt *et al.*, 1987).

2) LA DEPRESSION/ANXIETE :

NSF - novelty suppressed feeding

Ce test induit une situation de motivations conflictuelles chez l'animal, entre celle dirigée vers la nourriture et la peur de s'aventurer au centre de l'enceinte fortement éclairée. L'animal à jeun depuis 24 heures est placé dans une cage rectangulaire, au centre de laquelle est disposé un cercle blanc éclairé dans lequel sont déposés 2 granulés de nourriture. La latence mis par l'animal pour aller se nourrir est mesurée. Plus celle-ci est longue, plus l'animal est considéré comme dépressif /anxieux (Bodnoff *et al.*, 1988; David *et al.*, 2009).

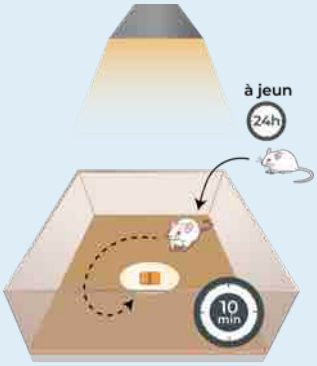

3) L'ANXIETE :

L'Open field ou le test du champ ouvert

L'animal est placé dans un angle d'une cage ouverte pendant 30 minutes. En général, les animaux évitent l'aire centrale par rapport à la périphérie. Le nombre d'entrées et le temps passé dans cette aire centrale reflète l'état anxieux de l'animal (Gentsch *et al.*, 1981).

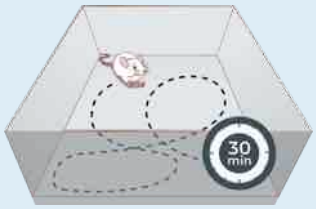

EPM – elevated plus maze ou le labyrinthe en croix surélevé

Le labyrinthe est composé de 2 bras ouverts et 2 bras fermés reliés par une plateforme centrale. Le nombre total d'entrées dans les 4 bras est mesuré pendant 5 minutes. Un phénotype anxieux se caractérise par une diminution du temps passé dans les bras ouverts par rapport au temps passé dans les bras fermés (Pellow & File, 1986).

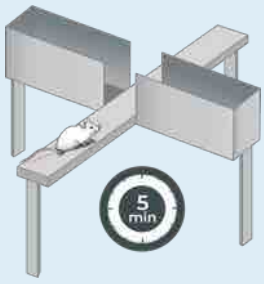

4 Combinaison de la microdialyse et des tests comportementaux

4.1 La microdialyse couplée avec la nage forcée (FST) chez les mêmes souris

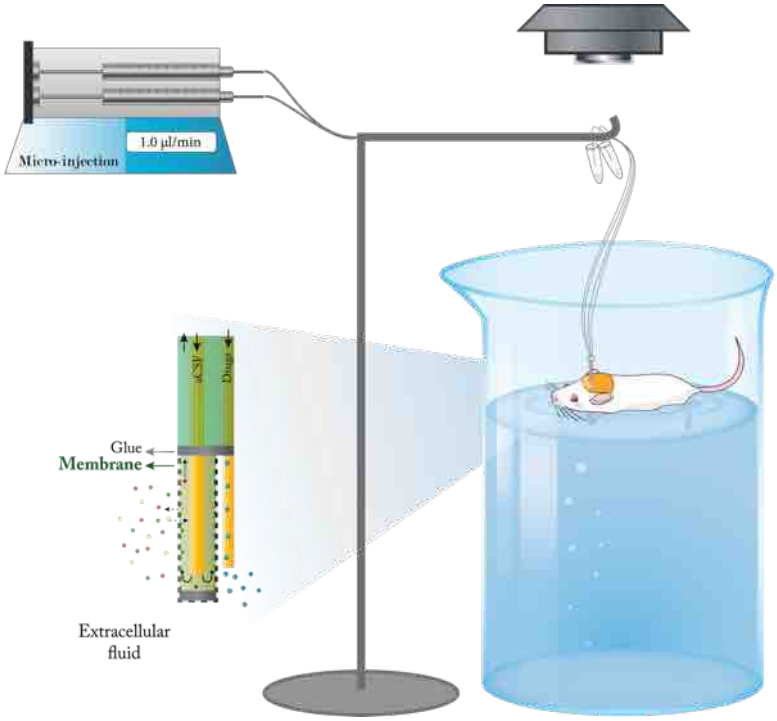

Figure 13. La microdialyse couplée avec le FST chez la même souris

La combinaison de la microdialyse *in vivo* chez la souris éveillée et le FST permet de mesurer des changements parallèles de comportement et des concentrations extracellulaires cérébrales de neurotransmetteurs chez la même souris (Figure 13). La chirurgie pour implanter les sondes de microdialyse dans les régions étudiées est réalisée 24h avant les tests comportementaux. Après environ 20h pour récupérer de l'anesthésie, la procédure de microdialyse est opérationnelle, et sa durée varie selon les protocoles, de 2 à 3 hrs. Pendant cette procédure de microdialyse, le FST sera réalisé en 6 mins et les dialysats sont collectés en parallèle. En quantifiant ces dialysats, nous prenons connaissance de l'effet du stress de la nage forcée, ainsi que l'effet de l'injection d'une substance (par voie i.p. par exemple), en mesurant les valeurs de bases et celles du groupe contrôle (positive et négative).

Les capillaires doivent être assez longs pour tenir sur le support et ne pas perturber les mouvements de la souris.

4.2 La microdialyse couplée avec le NSF chez la même souris

Le NSF permet de prédire des activités de type anxiolytique et d'antidépresseur chez la souris. Nous nous intéressons donc aux effets du NSF combiné avec la microdialyse. La veille de l'expérience, les sondes de microdialyse sont implantées chez la souris en même temps qu'elle est mise à jeun. Après 24h, la procédure de microdialyse couplée avec le NSF est réalisée. Pendant les 120 min de microdialyse, la souris passera environ 10 minutes dans le centre de l'enceinte, où elle présente des motivations conflictuelles, entre celle de se nourrir et la peur de s'aventurer au centre de l'enceinte fortement éclairée (Figure 14).

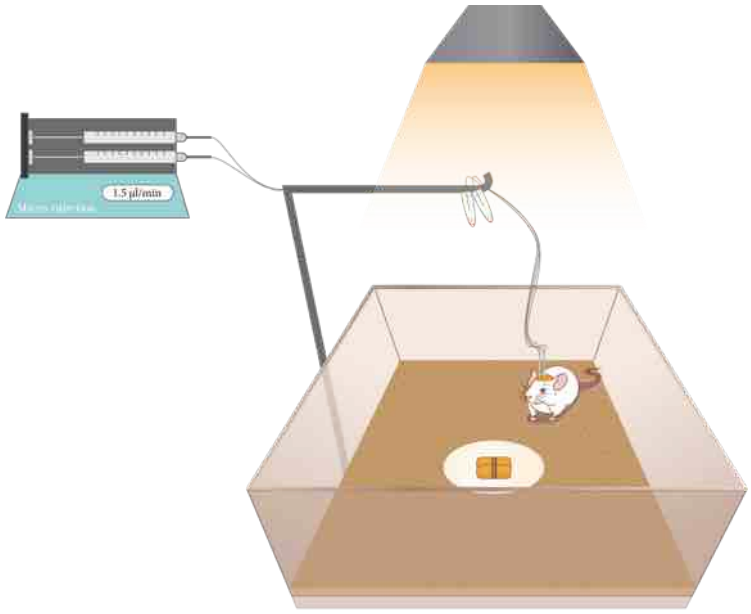

Figure 14. La microdialyse couplée avec le NSF chez la même souris

4.3 Principaux avantages et inconvénients de la technique de microdialyse couplée avec les tests de comportements

En dehors des avantages et inconvénients de la microdialyse elle-même déjà analysé ci-dessus (Tableau 5), le couplage de la microdialyse avec un test comportemental présente quelques particularités :

Avantages	Inconvénients
• Permet de récupérer des données neurochimiques et comportementales chez le même animal. • Possible de corréler ces données pour trouver quel neurotransmetteur assume quelle tâche de comportement. • Utile pour étudier l'effet pharmacologique des antidépresseurs, ainsi que l'influence de l'effet de stress sur le comportement (toujours comparés à des souris témoins).	• L'expérimentateur doit maîtriser les deux techniques pour pouvoir les combiner. • Au moins 3 animaux par jour : un contrôle négatif, un contrôle positif et une souris ayant reçu la molécule étudiée : ce qui exige un(e) expérimentateur expérimenté(e) • Effet du stress peut perturber les concentrations basales de neurotransmetteurs et par exemple la valeur d'immobilité basale dans le FST. • Les cathéters de microdialyse peuvent perturber les mouvements des animaux : à surveiller. • 1 seul expérimentateur dans la salle • Le test de NSF est plus difficile à réaliser car l'implantation de la sonde de microdialyse et la mise à jeun de l'animal se font en même temps, c'est-à-dire à t24h dans notre étude. L'effet de la faim devient alors plus important et sévère. L'effet de l'implantation des sondes de microdialyse perturbe aussi la latence de la souris à se nourrir (normalement maximum 10 mins) jusqu'à 20 mins.

Tableau 6. Avantages et inconvénients de la technique de microdialyse couplée à un test comportemental

5 Optogénétique

5.1 Principe

Pour définir les relations neuro-anatomiques et fonctionnelles entre le cerveau et le comportement, les neurosciences ont traditionnellement reposé sur la lésion / ablation, la stimulation électrique et l'activation / l'inactivation pharmacologiques. Bien qu'elles restent essentielles, ces techniques présentent des limites notamment vis à vis de précision de la structure cellulaire étudier (Stuber & Mason, 2013). Comprendre comment le cerveau génère des comportements dépend non seulement de la région étudiée, mais aussi du type de neurone qui la compose et enfin des circuits neuronaux qui s'y connectent. Les circuits neuronaux sont constitués d'une grande diversité de types de neurones, dont chacun a un type de connexion qui lui est propre. Il est ainsi essentiel de pouvoir analyser comment ces différents types de neurones fonctionnent ensemble.

Francis Crick (Crick, 1999) a imaginé la possibilité d'utiliser des outils moléculaires capables d'émettre de la 'lumière' pour activer et désactiver l'activité d'un ou plusieurs types de neurones, ce qui nous permet d'étudier un type neuronal spécifique ainsi qu'un circuit dans lequel ils envoient le signal. Cette utilisation de la 'lumière' nécessite de ce fait des types de cellules sensibles à la lumière, autrement dit, photoactivés. Il a anticipé ainsi la naissance de la discipline connue aujourd'hui sous le nom de "optogénétique".

Le terme "optogénétique" a été inventé ultérieurement par Ed Boyden et Karl Deisseroth à Stanford (Deisseroth *et al.*, 2006). Ce terme désigne aujourd'hui l'utilisation d'outils moléculaires qui peuvent être génétiquement ciblés pour l'observation et la manipulation de structures ou fonctions cellulaires spécifiques à l'aide de la lumière (Dugue *et al.*, 2012), donc une combinaison de techniques d'optique et de génétique. L'optogénétique permet donc de contrôler l'activité électrique d'une population de neurones spécifiques par simple illumination laser, *in vitro* sur des coupes de cerveaux, ou *in vivo* chez l'animal en situation comportementale. Cette technique possède des propriétés supérieures aux méthodes conventionnelles, y compris (i) – la spécificité de type de cellule, (ii) – la spécificité temporale (en milliseconde) et (iii) – la spécificité de la voie dans laquelle les synapses fonctionnent, autrement dit, du circuit neuronal impliqué. Elle est ainsi considérée par les neurobiologistes comme une révolution technologique majeure (Dugue & Tricoire, 2015).

Les réactifs clés utilisés en optogénétique sont des protéines sensibles à la lumière. Le contrôle neuronal est réalisé en utilisant des protéines photosensibles, appelées activateurs optogénétiques comme la channel-rhodopsine (ChR2, découverte par Nagel *et al.*, 2002), ou inhibiteurs optogénétiques comme l'halo-rhodopsine (NpHR, découverte par Matsuno-Yagi & Mukohata, 1977) et l'archéo-rhodopsine (Arch, découverte par Sugiyama *et al.*, 1989) – des photorécepteurs sensoriels trouvés dans des algues vertes ou des micro-organismes unicellulaires (Figure 15). L'obtention des animaux génétiquement modifiés pour exprimer ces protéines sensibles à la lumière est faite dans notre laboratoire par 2 méthodes différentes : (i) – modèle mutant chez la souris, de façon inductive ou (ii) – à l'aide d'un vecteur viral qui cible sélectivement une population de neurones d'intérêt (i.e., des neurones pyramidaux glutamatergiques) uniquement dans la région étudiée. Dans ce cas, le virus est administré 8 semaines avant de réaliser les expériences chez des souris sauvages adultes. La méthode qui utilise un virus est souvent privilégiée principalement par le fait qu'elle s'affranchi du maintien d'une lignée de souris transgénique. Cette méthode permet donc de disposer rapidement d'un nombre d'animaux suffisant.

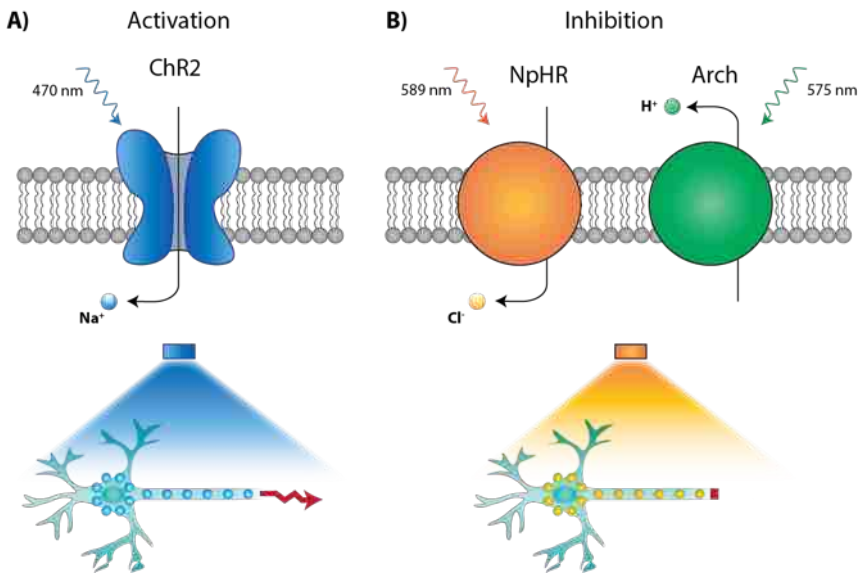

Figure 15. Réponse des photorécepteurs sensoriels sous l'effet de la lumière par l'optogénétique.

A) Activation des neurones en activant ChR2

B) Inhibition des neurones en activant NpHR ou Arch.

(illustrée d'après Deisseroth, 2011; Pastrana, 2010; M. B. Schneider *et al.*, 2008)

Le couplage de l'optogénétique avec d'autres techniques présente de nombreux avantages pour évaluer les propriétés de voies neuronales complexes dans situation physiologique, pathologique ou suite à un traitement pharmacologique. Dans ce dernier cas les propriétés pharmacologiques d'une molécule pourront donc être affinées jusqu'au niveaux de voies de projection très fines dans le système nerveux.

Dans mon projet, je me suis intéressée à la combinaison de 3 techniques différentes : l'optogénétique – pour contrôler (soit activer, soit inhiber) les neurones glutamatergiques pyramidaux du mPFC, la microdialyse – pour suivre les modifications des concentrations extracellulaires de différents neurotransmetteurs, et le FST – pour suivre les changements comportementaux prédictifs de l'activité antidépressive de la kétamine suite à l'activation/inhibition de cette population neuronale par optogénétique. Ce protocole est divisé en 5 étapes :

Étape 1 : injecter des virus dans la région étudiée, le mPFC, et attendre au moins 8 semaines pour que l'infection virale se propage aux neurones glutamatergique du mPFC et que les virus migrent (et donc que les opsines soient exprimées) tant au niveau des corps cellulaires des neurones pyramidaux qu'au niveau des terminaisons de ces neurones notamment situées dans le NRD. Nous nous intéressons donc au rôle des neurones glutamatergique de la voie mPFC-NRD.

Étape 2 : implanter des sondes optogénétiques et de microdialyse au moins 24h avant l'expérience afin que les souris puissent se rétablir.

Étape 3 : effectuer la microdialyse, la stimulation optogénétique et le FST en même temps.

Étape 4 : dosage des neurotransmetteurs.

Étape 5 : vérifier l'expression de l'opsine dans la région étudiée par immunohistochimie sur des coupes de cerveaux.

5.2 Fabrication des optrodes

La fabrication des sondes d'optogénétique - "optrodes" est faite en 5 étapes (d'après Sparta *et al.*, 2011) (Figure 16):

1. Couper la fibre optique (200 µm de diamètre, 0,37 aperture numérique de fibre multimode) à la longueur appropriée. Chaque fibre optique coupée se compose de 2 extrémités (T1 et T2).
2. Vérifier qu'au moins une extrémité est parfaitement circulaire et que la coupure soit régulière et puisse avoir l'aspect d'un miroir à l'observation microscopique, aucune rayure n'est donc permise. La coupure correcte est alors identifiée comme T1 et l'autre extrémité de la fibre est alors identifiée comme T2. Les fibres optiques ne présentant aucune coupures correctes sont éliminées.

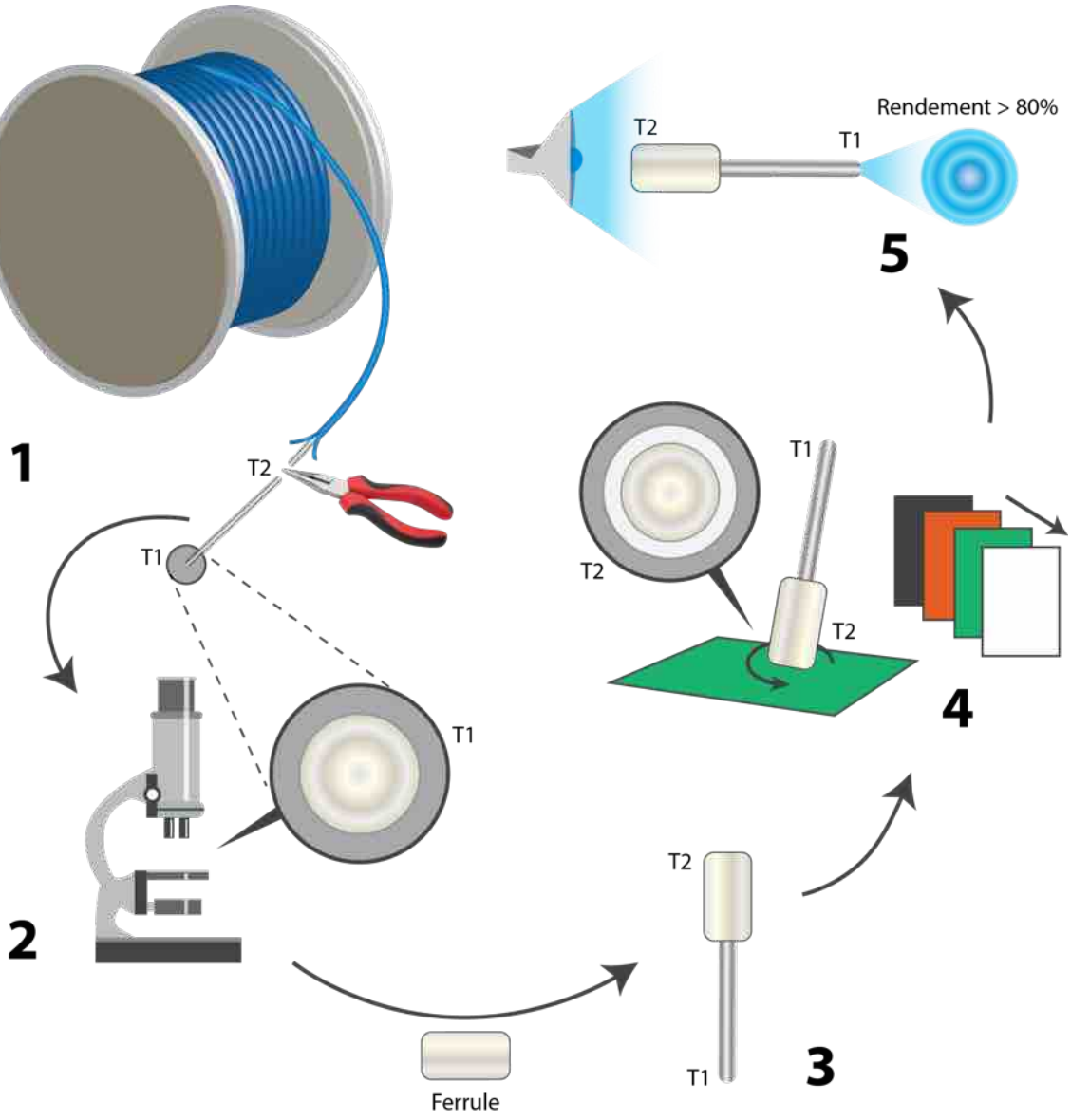

Figure 16. Les étapes de fabrication des sondes d'optogénétique.
1. Couper la fibre optique. 2. Vérifier l'extrémité T1. 3. Coller la fibre optique avec la ferrule. 4. Polir l'extrémité T2. 5. Vérifier le rendement de la lumière.

3. Insérer la fibre optique par son extrémité T2 dans la ferrule céramique (diamètre interne ∅230 µm) et la coller.
4. Polir l'extrémité T2 qui a été collé dans la ferrule sur des feuilles papier abrasif. Quatre granularités différentes sont utilisées allant vers le grain le plus fin (5 µm de carbure de silicium, 3 et 1 µm d'oxyde d'aluminium et 0.3 µm d'alumine calcinée grès, ThorLabs). A l'issue du polissage, l'extrémité T2 doit avoir une forme de disque régulier et avoir une surface parfaitement lisse.
5. Le rendement de l'optrode est alors mesuré à l'aide d'un Wattmètre (PM20, ThorLabs). Ce rendement consiste en le rapport entre la puissance délivré par le laser et celle émise par l'optrode connecté à ce même laser. Un rendement supérieur à 80% est nécessaire pour que l'optrode puisse être utilisée.

Une fois que ces étapes ont été réalisées, l'optrode est prête pour fabriquer des sondes mixtes d'optogénétique-microdialyse (Figure 17).

5.3 Chirurgie pour injecter le virus et implanter des sondes d'optogénétique

Deux virus différents ont été utilisés dans mon projet :

- AAV5-CamKII-**ChR2**-YFP (AAV Vectors – 6,2x10^{12} vg/ml – Dr. Karl Deisseroth) : a pour objectif de faire exprimer la protéine channel-rhodopsine 2 (ChR2). Il s'agit d'un canal ionique de la membrane plasmique perméable aux ions Na^+. Cette protéine-canal est sensible à une lumière bleue de longueur d'onde de 473 nm (système laser d'OEM). L'activation par la lumière va ouvrir le canal ionique ce qui va permettre l'entrée des ions Na^+ dans la cellule pour faire entrer les ions Na^+, et ainsi dépolariser la membrane neuronale et donc stimuler les neurones. Avec ce virus, le promoteur CamKII est choisi pour cibler l'expression des canaux ChR2 sélectivement sur des neurones pyramidaux glutamatergiques. Une population importante des corps cellulaires de ces neurones se trouve dans le mPFC, dont leurs projections aboutissent à plusieurs régions y inclus le NRD. Enfin, dans cette construction virale le rapporteur YFP (yellow fluorescent protein) est ajouter : il permet de faire exprimer cette protéine fluorescente de la même manière que l'opsine. Ce rapporteur permet, *post-mortem*, de visualiser indirectement l'expression de l'opsine.

- AAV5-CamKII-**Arch**-GFP (AAV Vectors – 7,5x10^{12} vg/ml – Dr. Ed Boyden) : a pour objectif de faire exprimer la protéine archeo-rhodopsine (Arch). Il s'agit d'un canal ionique de la membrane plasmique perméable aux ions Cl^- et sensible à la lumière dans la gamme vert-jaune de longueur d'onde de 575 nm (système laser d'OEM). L'activation de ce canal par la lumière va permettre l'entrée d'ions Cl^- dans le neurone et donc de l'hyperpolariser : ce phénomène va ainsi l'inhiber. Dans ce cas encore l'rhodopsine sera exprimée sélectivement dans le neurones pyramidaux grâce au promoteur CamKII et son expression sera révélée par la protéine fluorescente GFP (green fluorescent protein).

Enfin, à titre de contrôle, le AAV5-CamKII-GFP (AAV Vectors – 5,3x10^{12} vg/ml – Dr. Ed Boyden) est utilisé. Malgré une construction similaire aux deux autres virus, il n'induit pas l'expression d'opsine. Il est injecté dans les souris "littermates" de groupe contrôle comme référence pour une comparaison optimale avec les souris ayant reçu ChR2 et Arch.

L'injection de virus est faite dans une cohorte de souris BALBc/J. Le volume d'injection est 0,4 µL/ côté (les charges virales sont marquées en-dessus), de manière bilatérale intra-mPFC (Figure 20A). Après 8 semaines d'infection pour que le virus soit bien transféré vers les terminaisons neuronales dans le NRD, la combinaison des sondes de microdialyse et de la fibre optique (pour introduire la lumière de façon intracérébrale) (Figure 17) sont implantées dans ces 2 régions cérébrales (Figure 20B). La puissance de la lumière délivrée à travers cette fibre optique sera modulée en fonction du rendement obtenu pour chaque optrode de façon à délivrer la même puissance à chaque animal.

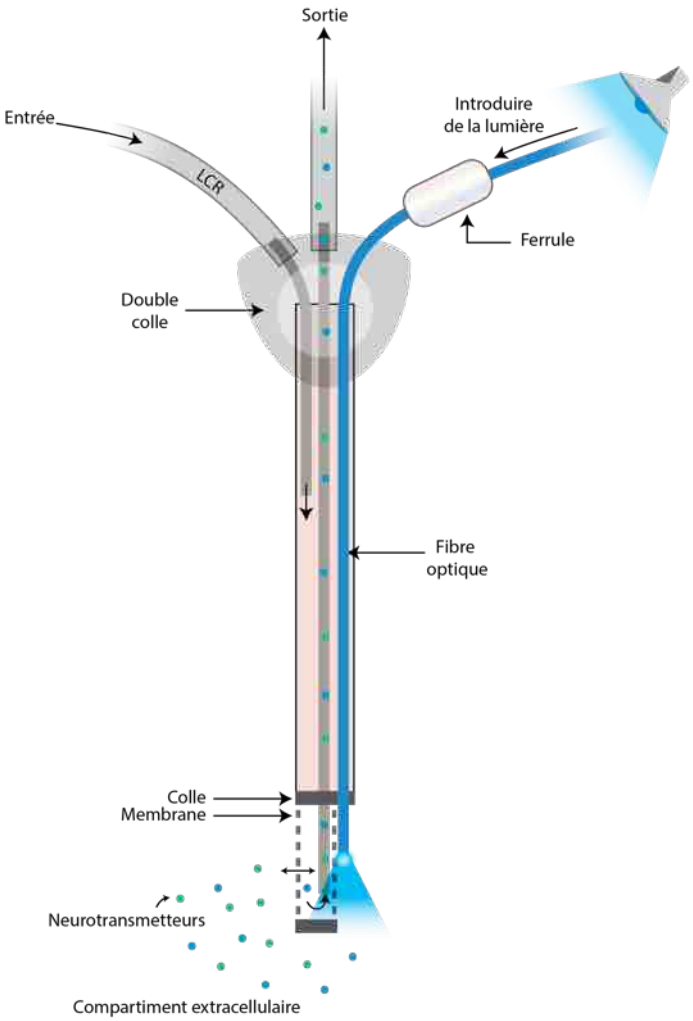

Figure 17. Composition une sonde microdialyse – optogénétique

5.4 Vérification de l'expression de l'opsine par immunohistochimie

Les souris ont été perfusées avec du paraformaldéhyde (PFA) 4% immédiatement à la fin de l'expérience. Leurs cerveaux ont ensuite été prélevés et conservés dans du PFA à 4°C pendant 24 heures. Le PFA a ensuite été remplacé par du sucrose 10% + azide 0.1% qui a été changé tous les jours pendant 3 jours consécutifs. Ces cerveaux ont ensuite été coupés en tranches de 35 µm d'épaisseur à l'aide d'un cryostat. Les coupes ont été récoltées par série de 6 puis réparties une à une dans une plaque en plastique de 24 puits remplis de PBS + azide 0.1% (pour prévenir le développement de champignons) de manière à obtenir 6 copies d'un cerveau par souris. Cette plaque a été conservée à 4°C jusqu'à la réalisation de l'immunohistochimie.

Les coupes de cerveaux ont été triées afin de sélectionner les régions d'intérêt puis lavées dans du PBS 1X. Seules les coupes de mPFC et de DRN ont été prises en compte. Les étapes suivantes ont ensuite été réalisées :

1. Laver avec du PBST 1X (PBS + Triton) durant 10 minutes. Répéter le lavage 3 fois.
2. Fixer les protéines avec du 0,5% Triton + 5% NDS dans du PBS pendant 2h à température ambiante.
3. Ajouter l'anticorps primaire: anti-GFP de lapin (Invitrogen) à 0,2% + 0,5% Triton + 5% NDS dans du PBS, à 4°C toute la nuit.
4. Laver à nouveau avec du PBS 1X durant 10 minutes. Répéter le lavage 3 fois.
5. Ajouter l'anticorps secondaire : anti-Cy3 de lapin à 0,4% obtenu chez l'âne (Jackson Immuno-Research) + 10% NDS dans du PBS, à température ambiante pendant 2h.
6. Laver de nouveau avec du 1X PBS durant 10 minutes. Répéter le lavage 3 fois.
7. Monter les coupes sur lames et laisser sécher pendant environ 20 minutes en protégeant de la lumière.
8. Ajouter une à deux gouttes de fluoromount (Sigma) avant de mettre la lamelle et regarder au microscope pour vérifier l'expression de virus.

L'expression de virus est montrée ci-dessous dans Figure 18.

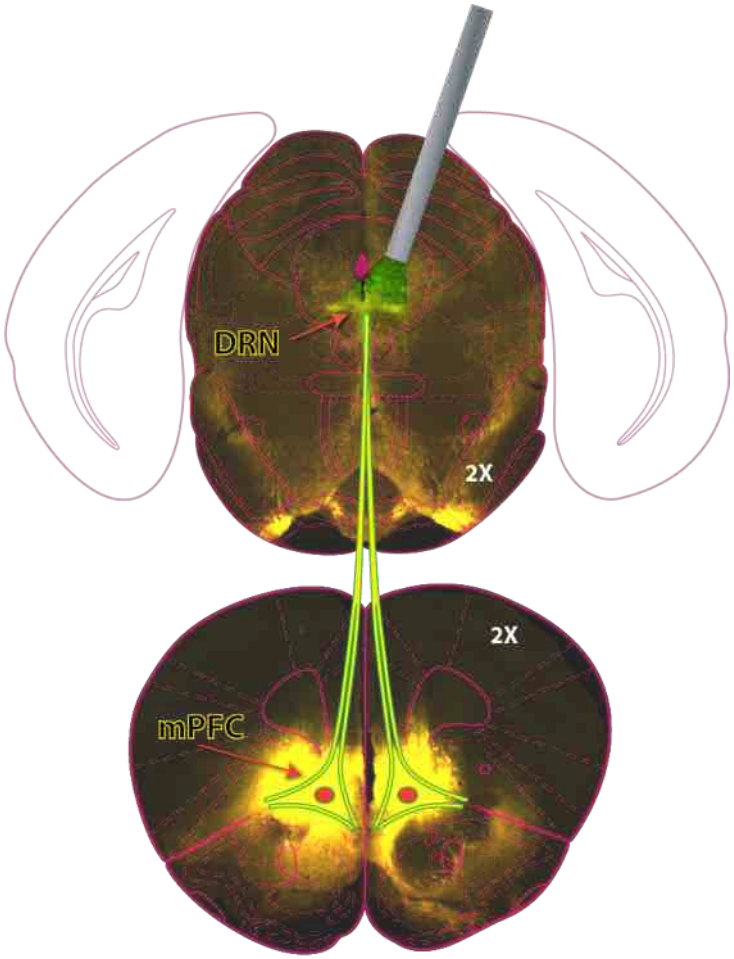

Figure 18. Vérification de l'expression de l'opsine par immunohistochimie

5.5 La combinaison "Optogénétique – Microdialyse – FST" chez la même souris

Mon projet se concentre sur 2 parties :

1) Examiner l'effet de la stimulation de système glutamatergique sur le comportement et la neurochimie chez la souris (Figure 19 et Figure 20) : Le mPFC est très impliqué dans l'effet antidépresseur de la kétamine à 24h après l'administration (Duman & Aghajanian, 2012). Pour évaluer le rôle potentiel de la projection glutamatergique mPFC-NRD dans l'effet antidépresseur de la kétamine, nous évaluerons si la stimulation optogénétique de cette voie serait capable de mimer l'effet de la kétamine. Le virus AAV5-CamKII-**ChR2**-YFP est injecté à 8 semaines avant d'implantation de sondes microdialyse-optogénétique. Les souris sont alors implantées avec 2 sondes qui couplent microdialyse et optogénétique dans le mPFC et une troisième sonde microdialyse simple est implantée dans le NRD, afin d'étudier l'effet de la stimulation au corps cellulaire (mPFC) sur les terminaisons neuronales (NRD). Au jour 1, donc le lendemain de l'implantation des sondes, l'expérience de microdialyse est réalisée. Dix dialysats sont ainsi collectés par chaque sonde de microdialyse (couplé ou non à

l'optogénétique). Après les 4 premières collectes, la stimulation optogénétique est réalisée (8 mW, 10 Hz en lumière pulsée, 1 minute ON puis 1 minute OFF pendant 1 heure pour imiter la fréquence de décharge électrique en condition physiologique), ceci a une durée qui s'étale sur la collecte de deux dialysats. Enfin suite à la stimulation, 4 nouveaux dialysats sont collectés. Au jour 2, donc 24h après la stimulation, la souris est passée de nouveau le processus de microdialyse, au milieu duquel le FST est exécuté chez le même animal (Figure 19).

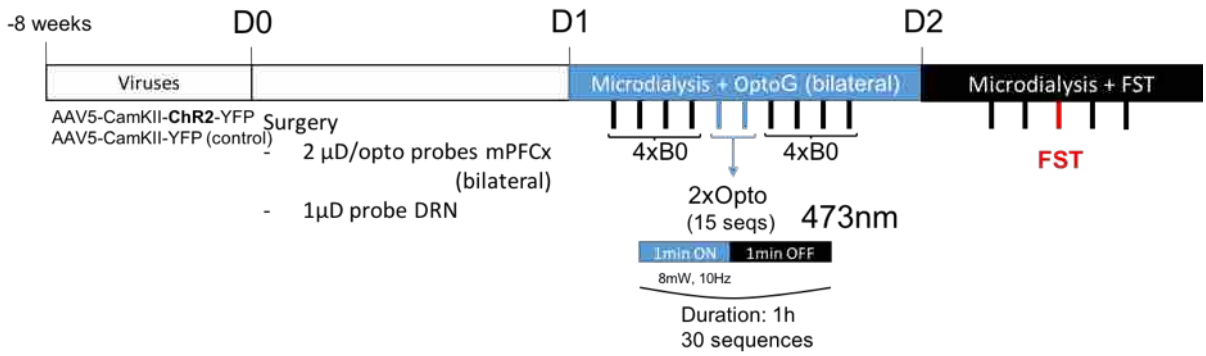

Figure 19. Protocole d'optogénetique avec la combinaison d'une sonde de microdialyse et d'une fibre optique lors de l'évaluation de la mobilité de la souris dans le FST

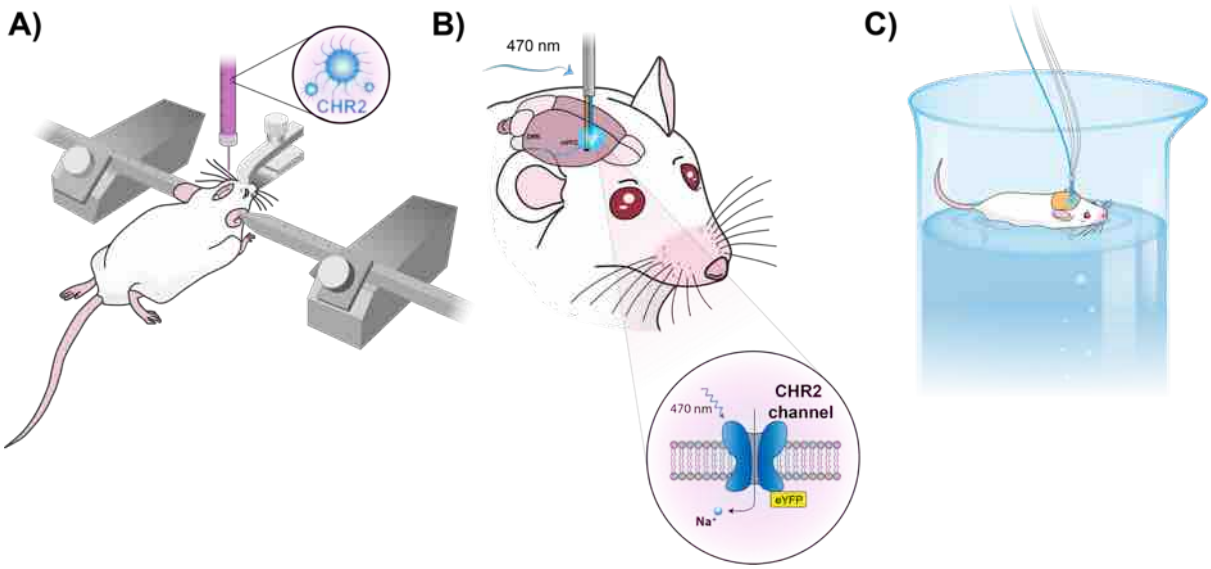

Figure 20. Processus d'optogénétique.

A) Injection intracérébrale du virus. B) Implantation d'une sonde de microdialyse combinée avec la fibre optique. C) Mesure de l'effet de la stimulation optogénétique des neurones sur le comportement et les concentrations extracellulaires cérébrales de neurotransmetteurs.

2) Étude de l'implication du circuit mPFC-NRD sur les activités de type antidépresseur de la kétamine chez la souris (Figure 21 et Figure 22) : après vérifier que la stimulation de mPFC peut induire une réponse antidépressive comparable à celle de la kétamine, l'implication réelle du circuit mPFC-NRD dans ces effets est abordée de manière plus directe. L'objectif est d'inhiber les projections du mPFC qui arrivent dans le NRD et d'évaluer si nous pouvons ainsi bloquer tout ou partie des effets de la kétamine. Ainsi, le virus AAV5-CamKII-**Arch**-GFP est administré de façon bilatérale dans le mPFC. Le virus diffuse jusqu'au NRD : en 8 semaines, l'expression du gène est alors considérée comme stable dans la population neuronale cible. Grâce à ce protocole, **seuls les neurones impliqués dans ce circuit mPFC-NRD sont inhibés par le laser**. La sonde de microdialyse couplée à la fibre d'optogénétique est ensuite implantée dans le NRD. Au jour 1, donc le lendemain de l'implantation des sondes, la kétamine (10 mg/kg) est injectée par voie intrapéritonéale (i.p.). Au jour 2, donc 24h après cette injection, la lumière de longueur d'onde de 575 nm (15 mW en continue) est appliquée dans le NRD pour activer les canaux Arch ce qui inhibe immédiatement les neurones glutamatergiques du circuit mPFC-NRD. Nous mesurons en parallèle les changements de comportement (e.g., inhibition de la mobilité dans le FST) et de neurochimie (5-HT) pour savoir quel est le pourcentage d'implication de ce circuit dans les activités de type antidépresseur de la kétamine.

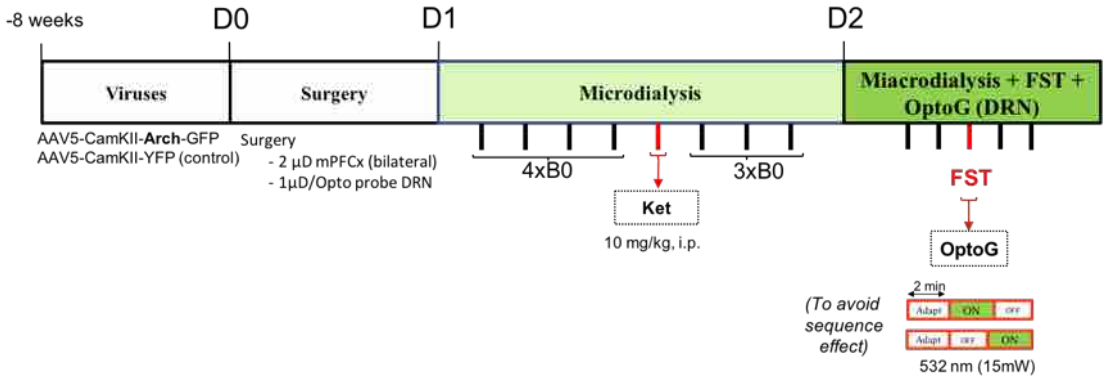

Figure 21. Protocole d'inhibition du circuit neuronal mPFC-NRD par optogénétique

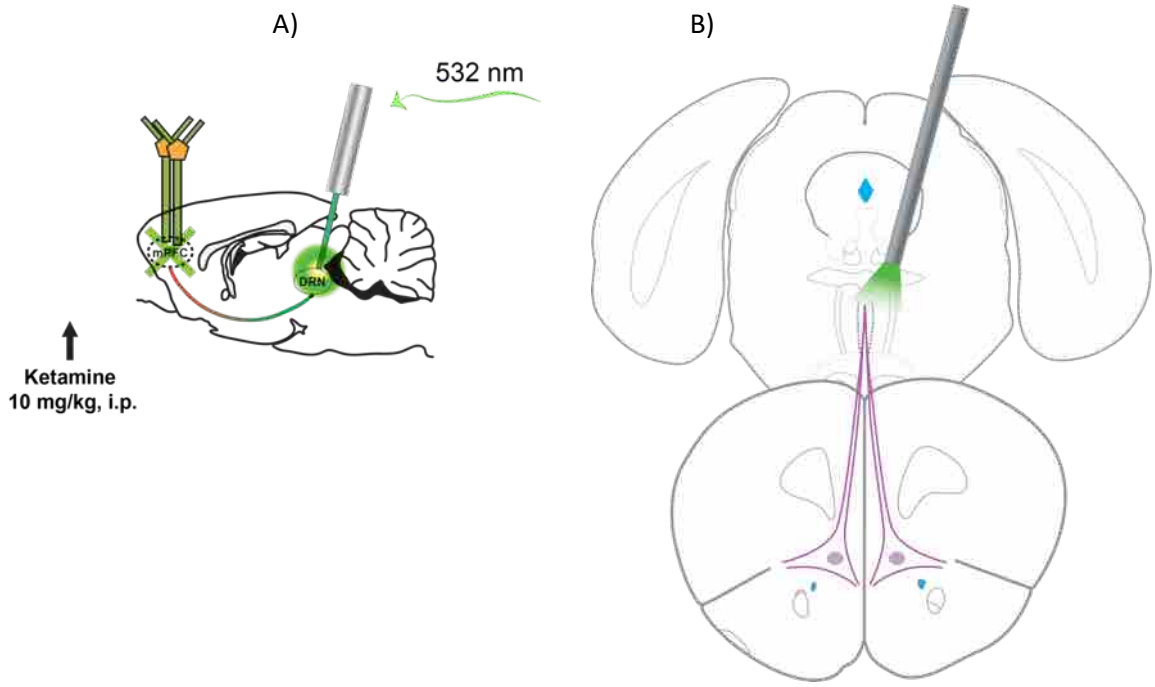

Figure 22. Circuit mPFC-NRD inhibé par l'optogénétique

La combinaison de microdialyse-optogénétique couplée au FST constitue un modèle original présenté Figure 23. L'animal, ayant reçu la kétamine 24h avant, est placé dans un bécher contenant de l'eau à une température de 23-25°C pendant 6 minutes. Cette période de FST est divisée en 3 parties : 0-2 min, 2-4 min et 4-6 min (Figure 21). Les 2 premières minutes permettent l'adaptation de l'animal dans l'environnement aqueux. La 2ème partie (2 à 4 minutes) est mesurée sans la lumière laser (OFF), pour connaître le comportement de la souris à l'état basal. Ici seul l'effet de la kétamine sur la durée de la nage est évalué. La 3ème partie (4 à 6 minutes) du test est mesurée avec la lumière (ON), pour évaluer l'effet de l'inhibition du circuit mPFC-NRD sur la durée de la nage. Ceci permet d'évaluer si l'inhibition de la voie mPFC-NRD empêche l'effet antidépresseur de la kétamine. Pour éviter l'effet de la séquence d'inhibition, l'application de la lumière a lieu dans le créneau 4-6 mins comme décrit ou dans le créneau 2-4 mins. Pour résumer, les 6 minutes du test sont séparées en 3 parties de deux minutes chacune et deux types de séquences sont appliquées à savoir (OFF/ON/OFF) et (OFF/OFF/ON) (Figure 21).

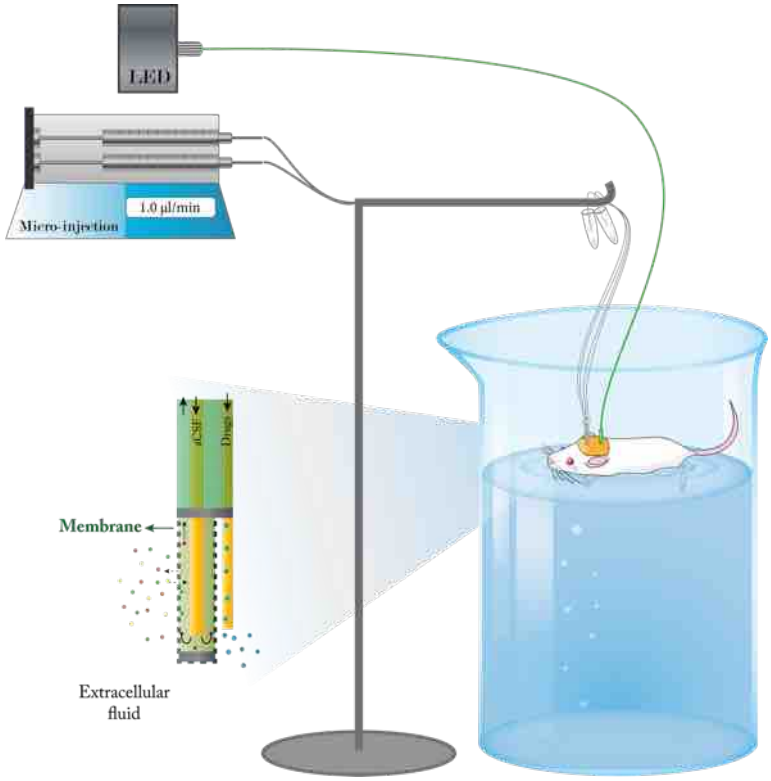

Figure 23. Installation de système Optogénétique – Microdialyse – FST chez la souris

Les dialysats sont collectés pendant ce temps. Puisqu'il faut un volume de dialysats suffisant pour pouvoir doser les neurotransmetteurs 5-HT, glutamate et GABA, les tubes collectés incluent les données de l'ensemble de la nage, donc avant et après l'inhibition. Les résultats reflètent ainsi l'effet global de la kétamine sur le temps de nage comme référence et comprends l'influence de l'inhibition.

5.6 Principaux avantages et inconvénients du couplage "Optogénétique - microdialyse – FST" chez la souris

Le couplage "optogénétique – microdialyse – FST" présente des propriétés particulières :

Avantages	Inconvénients
• Contrôler une population spécifique de neurones avec une haute sélectivité : seuls les neurones exprimant le gène codant pour les récepteurs photosensoriels peuvent répondre à la stimulation lumineuse. • Contrôler de façon temporelle ces neurones : les neurones ne sont activés ou inhibés que lorsque la lumière laser est appliquée. • Outil puissant pour étudier le rôle fonctionnel de circuits neuronaux. • Permet de générer des données neurochimiques et comportementales concomitantes chez le même animal. • Évaluation de l'implication d'un neurotransmetteur particulier dans une tâche comportementale. • Utile pour étudier le mécanisme d'action des molécules tels que des antidépresseurs.	• La stimulation des neurones par l'optogénétique engendre une activation synchrone de tous les neurones qui expriment l'opsine : ce n'est pas le cas dans des conditions physiologiques. • L'expérimentateur doit maîtriser les 3 techniques pour pouvoir les combiner. • Vis à vis des test comportementaux non combinés : il est difficile de travailler sur des groupes d'animaux de grande ampleur. Un effet comportemental modéré est donc compliqué à mettre en évidence.

Tableau 7. Avantages et inconvénients de la technique couplant "optogénétique – microdialyse – FST" chez la souris

6 Article de la méthodologie du dosage de glutamate, glutamine et GABA par HPLC couplée à la spectrométrie de masse en tandem (LC-MS/MS)

Titre de l'article : Rapid analysis of glutamate, glutamine and GABA in mice frontal cortex microdialysis samples using HPLC coupled to electrospray tandem mass spectrometry

C. Defaix, A. Solgadi, **T.H. Pham**, A.M. Gardier, P. Chaminade, L. Tritschler.

Publiée en Journal of Pharmaceutical and Biomedical Analysis, 2018, 152:31-38

doi.org/10.1016/j.jpba.2018.01.039

Question posée :

La mise au point d'une méthode simple de LC-MS/MS pour quantifier le glutamate, la glutamine et le GABA dans les échantillons de microdialyse in vivo recueillis chez la souris.

Résumé de l'étude :

La mesure *in vivo* de plusieurs neurotransmetteurs est très intéressante mais reste difficile dans le domaine des neurosciences. Le GABA et l'acide L-glutamique sont respectivement les principaux neurotransmetteurs inhibiteurs et excitateurs du système nerveux central et leurs modifications sont liées à diverses maladies telles que l'anxiété et le trouble dépressif majeur. Cette étude a décrit une méthode simple permettant la quantification simultanée LC-MS / MS de l'acide L-glutamique, de la glutamine et du GABA. Les dialysats ont été acquis à partir d'échantillons du cortex médian préfrontal par la microdialyse chez des souris en liberté de mouvement. La séparation chromatographique a été effectuée par la chromatographie liquide à interaction hydrophile (HILIC) avec une colonne de silice modifiée à base d'ammonium-acide sulfonique cœur-enveloppe en utilisant une élution en gradient avec des phases mobiles constituées d'un tampon formiate d'ammonium 25 mM pH 3,5 et d'acétonitrile. La détection de l'acide L-glutamique, de la glutamine et du GABA, ainsi que les étalons internes [d6]-GABA et [d5]-glutamate a été réalisée sur un spectromètre de masse triple quadrupolaire en ionisation électrospray positive et mode de surveillance multi-réactions. La limite de quantification était de 0,63 ng/ml pour le GABA, de 1,25 ng/ml pour l'acide L-glutamique et de 3,15 ng/ml pour la glutamine, et l'exactitude et la précision intra-jour et inter-jour ont été évaluées pour les trois dialysats. Par conséquent, la

pertinence physiologique de la méthode a été appliquée avec succès pour la détermination des niveaux extracellulaires basaux et la libération provoquée par le potassium de ces substances neuroactives dans le cortex médian préfrontal chez des souris adultes C57BL/6 éveillées.

Contribution personnelle :

Au cours de ce travail :

- J'ai fait la mise au point de la microdialyse *in vivo* chez ces animaux avec Dr. Céline Defaix et je lui ai fourni des échantillons à doser en spectrométrie
- J'ai réalisé le suivi des animaux
- J'ai participé à l'analyse des résultats et à la rédaction de l'article

Journal of Pharmaceutical and Biomedical Analysis 152 (2018) 31–38

Contents lists available at ScienceDirect

Journal of Pharmaceutical and Biomedical Analysis

journal homepage: www.elsevier.com/locate/jpba

Rapid analysis of glutamate, glutamine and GABA in mice frontal cortex microdialysis samples using HPLC coupled to electrospray tandem mass spectrometry

Celine Defaix[a], Audrey Solgadi[b], Thu Ha Pham[a], Alain M. Gardier[a], Pierre Chaminade[b,c], Laurent Tritschler[a,*]

[a] CESP/UMR-S 1178, Univ. Paris-Sud, Fac. Pharmacie, INSERM, Université Paris-Saclay, Chatenay Malabry, 92290, France
[b] SAMM, Institut Paris-Saclay d'Innovation Thérapeutique, UMS IPSIT UPSud – US 31 Inserm – UMS 3679 CNRS, Fac. Pharmacie, Université Paris-Saclay, Chatenay Malabry, 92290, France
[c] Lip(Sys)^2 – EA7357, Chimie Analytique Pharmaceutique, Université Paris-Sud, Université Paris-Saclay, Chatenay Malabry, 92290, France

ARTICLE INFO

Article history:
Received 10 November 2017
Received in revised form 17 January 2018
Accepted 18 January 2018
Available online 31 January 2018

Keys words:
Glutamate
Glutamine
GABA
Microdialysis
LC–MS/MS
Mouse brain

ABSTRACT

In vivo measurement of multiple neurotransmitters is highly interesting but remains challenging in the field of neuroscience. GABA and L-glutamic acid are the major inhibitory and excitatory neurotransmitters, respectively, in the central nervous system, and their changes are related to a variety of diseases such as anxiety and major depressive disorder. This study described a simple method allowing the simultaneous LC–MS/MS quantification of L-glutamic acid, glutamine and GABA. Analytes were acquired from samples of the prefrontal cortex by microdialysis technique in freely moving mice. The chromatographic separation was performed by hydrophilic interaction liquid chromatography (HILIC) with a core-shell ammonium-sulfonic acid modified silica column using a gradient elution with mobile phases consisting of a 25 mM pH 3.5 ammonium formate buffer and acetonitrile. The detection of L-glutamic acid, glutamine and GABA, as well as the internal standards [d6]-GABA and [d5]-glutamate was performed on a triple quadrupole mass spectrometer in positive electrospray ionization and multiple reaction monitoring mode. The limit of quantification was 0.63 ng/ml for GABA, 1.25 ng/ml for L-glutamic acid and 3.15 ng/ml for glutamine, and the intra-day and inter-day accuracy and precision have been assessed for the three analytes. Therefore, the physiological relevance of the method was successfully applied for the determination of basal extracellular levels and potassium-evoked release of these neuroactive substances in the prefrontal cortex in adult awake C57BL/6 mice.

1. Introduction

In mammals, L-glutamic acid (glutamate, Glu) and γ-aminobutyric acid (GABA) are the main amino acid excitatory and inhibitory neurotransmitters in the brain, respectively. Both are involved in many aspects of normal brain functioning including behavior as well as the physiological homeostasis of the whole organism. Both neurotransmitters create an opposite excitatory/inhibitory balance in the brain. Therefore, the physiological equilibrium between Glu and GABA has a great impact on the brain function, in healthy conditions, but also in cerebral pathologies: epilepsy is probably the best example in which the disequilibrium between excitatory and inhibitory neurotransmission leads to induce seizures [1]. At the cellular level, more particularly at the synapse, the Glu and GABA are mainly uptaken by astrocytes. Neuron-astrocyte signaling is a classical example of cell–cell communication *via* the Glu/GABA and glutamine (Gln) cycle. Astrocytes support neuronal metabolism and prevent extracellular accumulation of neurotransmitters and excitotoxicity, especially for Glu. The activity of astrocytes is reflected at least in part, by the Gln synthesis. This amino acid is the metabolic link between astrocytes and neurons in the "tripartite synapse" functional organization encompassing the presynaptic neuron, the postsynaptic neuron and the astrocytes [2]. It is then informative to have the quantification of these three analytes in the same time, in order to have the whole picture of the tripartite synapse. Thus, the ratios of extracellular Gln/Glu levels and extracellular Glu/GABA

* Corresponding author.
E-mail address: laurent.tritschler@u-psud.fr (L. Tritschler).

https://doi.org/10.1016/j.jpba.2018.01.039
0731-7085/

levels reflect the astrocyte/neuronal cycling and the balance excitation/inhibition, respectively, in a particular brain region [3].

To obtain samples containing these amino acid neurotransmitters with the minimal effects on the brain function, the microdialysis technique was chosen. This technique is based on the implantation of a probe with semi-permeable membrane into a specific brain area. The implanted probe is then perfused with an artificial cerebrospinal fluid (aCSF) with the same osmolarity as the interstitial space avoiding water flux. The pores of the membrane allow the crossing of small molecules (cut-off 20,000), such as amino acid neurotransmitters. It permits continuous collection of samples with small molecular weight molecules [4]. Interestingly, microdialysis is performed in awake, freely moving rodents reflecting as near as possible their physiological state. Although this technique was developed decades ago, it is still one of the gold standards for the *in vivo* evaluation of the brain neurotransmissions (release, reuptake), with a special interest in mouse, knockout of this species being widely used for genetic manipulations as animal models of psychiatric diseases [5]. Furthermore, we can draw a correlation between responses to behavioral tests and changes in extracellular levels of neurotransmitters when both parameters are measured in the same mouse [6].

The separation and quantification of the analytes in microdialysates need a sensitive and selective analytical method. To date, several methods have been used for the quantification of amino acid neurotransmitters in tissues or biological fluids using a wide range of reagents, additives, derivatization procedures, equipments and detectors. Thus, high performance liquid chromatography (HPLC) can be combine with various detection systems such as ultra-violet detection (LC-UV), fluorescent detection (LC-FD) [7], electrochemical detection (LC-EC) [8] or mass spectrometry (LC–MS) (see [9] for a review). Among these methods, HPLC coupled to tandem mass spectrometry (LC–MS/MS) is commonly used for multi-analyte detection; an analyte can be identified by its retention time, molecular weight and characteristic fragmentation ions. Thus, it has proven to be a reliable method to detect a vast variety of analytes in different biological matrices. Plasma, serum, urine and native CSF are substrates, obtained in clinic, where LC–MS/MS was used to perform multiple amino acids assay, including Glu and Gln. In such studies, the samples needed to be processed (deproteination, precipitation, desiccation, suspension) [10–12]. By contrast, in the present study, the use of a dialysis membrane allows avoiding any pretreatment of dialysate samples to measure extracellular brain neurotransmitters levels in rodents.

Few microdialysis studies previously reported the simultaneous determination of amino acid neurotransmitters levels by LC–MS/MS or LC-FD in various rat brain areas (Table 1). Thus, Buck et al. [13] investigated changes in extracellular Glu and GABA concentrations in the globus pallidus by using LC–MS/MS method. Otherwise, another study described the simultaneous LC-FD quantification of multiple D- and L-amino acids, among them extracellular levels of GABA ($GABA_{ext}$) and Glu (Glu_{ext}) in frontocortical dialysates in freely moving rats ([7]; see Table 1). In the same way, multi-analyte approach for the measurement of neuromediators was develop from rat hippocampus microdialysates [14] or cerebrospinal fluid [15]. However, most of the studies quantified amino acid neurotransmitters in rat [16–18] or in post-mortem homogenates of mouse brain tissues ([19–21]; see Table 2). More recently, the UHPLC–MS/MS method was set up for simultaneous determination of dopamine, serotonin and their metabolites, as well as Glu and GABA in rodent brain tissue and extracellular fluid [22]. To validate this method, the authors measured extracellular levels of these neurotransmitters in rat nucleus accumbens and ventral tegmental area (VTA).

Such studies being rare in freely moving mice, the present study describes a simple method using sensitive method HPLC coupled to a triple quadrupole tandem mass spectrometry dedicated to quantify simultaneously Glu_{ext}, Gln_{ext} and $GABA_{ext}$ in mice dialysate samples. This method was applied in the medial prefrontal cortex (mPFC) to study the excitatory neurotransmitter Glu, the inhibitory one, GABA as well as the intermediate metabolite Gln. The small volume of dialysate analyzed (5 μl) permits a high temporal resolution, which is compatible with pharmacological studies. As a proof of concept, we chose as mood relevant brain area, the mPFC, which is mainly involved in the antidepressant-like activity of selective serotonin reuptake inhibitors (SSRI). Moreover, neuronal depolarization with a high potassium concentration (120 mM) was performed to induce neurotransmitters' release [23]. KCl-evoked neurotransmitter release is one of the tests used to verify the neuronal origin of extracellular neurotransmitter levels measured in dialysate samples. The time course of modifications of Glu_{ext}, Gln_{ext} and $GABA_{ext}$ in dialysates was then successfully measured with the method developed here.

2. Materials and methods

2.1. Animals

Adult male C57BL/6 mice were purchased from Taconic Farms (Lille Skensved, Denmark). All mice were 7–8 weeks old, weighed 23–25 g at the beginning of the experiment, and were maintained on a 12 l:12 D schedule (lights on at 06:00 h). They were housed in groups of five. Food and water were provided *ad libitum*. All the experiments in animals were performed on compliance with the European Ethical Guidelines (86/609/EEC), as well as with the French National laws (project approval of the Ethical Committee, number APAFIS#5489-2016052717037691 v2).

2.2. In vivo *microdialysis procedure*

Each mouse (n = 17) was anesthetized with chloral hydrate (400 mg kg^{-1}, i.p.) and implanted with two microdialysis probes (CMA7 model, Carnegie Medicine, Stockholm, Sweden) located in the right and left mPFC. Stereotaxic coordinates in mm from bregma: A = +2.2, L = ±0.5, V = −3.4 (A, anterior; L, lateral; and V, ventral) [6]. On the next day, the probes were continuously perfused with an artificial cerebrospinal fluid (aCSF, composition in mM: NaCl 147, KCl 3.5, $CaCl_2$ 1.26, $MgCl_2$ 1, NaH_2PO_4 1.0, $NaHCO_3$ 25, pH 7.4 ± 0.02) at a flow rate of 1.0 μl/min through the mPFC using CMA/100 pump (Carnegie Medicine, Stockholm, Sweden), while animals were awake and freely moving in their cage. Dialysate samples were collected every 15 min for 120 min. Basal Glu_{ext}, Gln_{ext} and $GABA_{ext}$ were determined one hour after the onset of aCSF perfusion, corresponding to a stabilization period. These basal levels, determined from fractions 1–3 (15–45 min), were used to establish the reference values B0 defined as 100% for each compound. To activate the neurotransmission, a high concentration of potassium (KCl 120 mM) was added to the aCSF during fraction 4 (45–60 min). Samples were then collected up to the fraction 8, with the same conditions described for the fractions 1–3. The correct location of the probes was controlled macroscopically at the end of the dialysis experiment. Only mice correctly implanted with the probes were included in the data analysis.

2.3. Analytical standards and reagents

γ-aminobutyric acid (GABA), L-glutamic acid (Glu), glutamine (Gln), DL-glutamic acid-2,3,3,4,4-d5 (Glu-d5), 4-aminobutyric acid-2,2,3,3,4,4-d6 (GABA-d6), acetonitrile, ammonium formate, formic acid and all compound used to aCSF were purchased from Sigma-Aldrich (L'isle d'Abeau Chesnes, France).

Table 1
Determination of extracellular Glu and GABA concentrations in rat brain microdialysis studies in the literature.

Brain areas	Glu_{ext} concentrations (ng/ml)	$GABA_{ext}$ concentrations (ng/ml)	Methods	References
Globus pallidus	27.8	1.312	HPLC–MS/MS	[13]
Prefrontal cortex	48.6	1030	HPLC-FD	[7]
Hippocampus	544.8	605.9	UHPLC–MS/MS	[14]
Ventral tegmental area	64.6	3.81	UHPLC–MS/MS	[22]
Nucleus accumbens	735	9590	UHPLC–MS/MS	[22]

Table 2
Summary of recent findings on simultaneous quantification of amino acid neurotransmitters levels in various brain tissues in mice post-mortem homogenates.

Analytes	Methods	Matrices	References
Glu, Gln, GABA	LC–MS/MS	Whole brain extracts	[19]
Glu, GABA, EP,5-HT, 5-HIAA, DA, NE	LC–MS/MS	Hippocampus tissues	[20]
Glu, GABA, DA, BH4, 5-HT, NE, EP	LC–MS/MS	Brain tissues (9 regions)	[21]
Glu, GABA, 5-HT, 5-HIAA, DA, HVA, 3-MT, NE, ACh	UHPLC–MS/MS	Prefrontal cortex and striatum tissues	[22]

DA, Dopamine; DA metabolites: HVA, homovanillic and 3-MT, 3-methoxytyramine; 5-HT, serotonin; 5-HIAA, 5-hydroxyindoleacetic acid; BH4, tetrahydrobiopterin; NE, norepinephrine; EP, epinephrine; Ach, acetylcholine

2.4. Preparation of standard solutions and calibration curves

The stock standard solutions of Glu, Gln and GABA were dissolved separately in aCSF at the concentration of 1, 20 and 0.5 mg/ml, respectively and stored at 4 °C. A series of solutions mixtures of desired concentrations were prepared by suitable dilutions of the stock solutions. As internal standards (IS), Glu-d5 and GABA-d6 were used. The IS stock solutions were prepared in water at the concentration of 1 mg/ml for Glu-d5 and 0.25 mg/ml for GABA-d6. IS, at a final concentration of 60 μg/ml for Glu-d5 and 15 μg/ml for GABA-d6, were added either into the 10 μl of the microdialysis samples, or into the 25 μl of the standard samples.

Calibration standards samples were freshly prepared from the original stock solution in each experiment. The calibration curves were built within the following range for the analytes: 2.5–2000 ng/ml for Glu; 62.5–50,000 ng/ml for Gln; and 0.63–500 ng/ml for GABA. The calibration samples, which contained the three analytes, were analyzed at the beginning and at the end of each day. A quality control standard (in ng/ml: 80, 5000 and 8 for Glu, Gln and GABA, respectively) was injected after 20 injections to ensure the validity of the calibration curve. The predicted value expected to not exceed ± 15% of the theoretical value.

2.5. Method validation

The performances of the method developed herein were assessed in terms of specificity, linearity, precision and accuracy (intra and inter-day variation), limits of detection (LODs) and quantification (LOQs), according to the Food and Drug Administration (FDA) guideline on bioanalytical method validation [24]. The specificity of the method was determined by comparing the blank chromatograms with those corresponding to dialysate samples. Blank samples were aCSF without adding any component to the matrix.

The linearity of the calibration curve was evaluated by analyzing compounds standard solutions at different concentrations. It is defined by the intercept of the calibration curve, slope and determination coefficient (R^2). All analytes showed good linearity with $R^2 \geq 0.999$. Calibration curves for each analyte were obtained by linear regression analysis, and plotting the peak area ratio of analytes to the IS *versus* the theoretical concentration of analytes. The obtained results were used to calculate overall linearity as well as accuracy and precision at each concentration level.

To evaluate the precision and accuracy of the method, the intra-day and inter-day variations were assessed using three quality control (QC) points for each calibration curve that consists of three levels low, mid and high. The concentrations of QC points were 4, 80 and 800 ng/ml for Glu; 100, 5000 and 20,000 ng/ml for Gln; and 0.8, 8 and 100 ng/ml for GABA. Five replicates at each QC samples were analyzed on the single day in order to evaluate intra-day variability and were repeated for 4 days to determine inter-day variability. Precision was expressed as relative standard deviation (%RSD) for replicate measurements and the value of accuracy was expressed as a relative error (%RE) by deviation between theoretical and calculated concentrations.

A series of decreasing concentrations of QC solution was analyzed to determine the LOD and LOQ. LOD is the minimum amount of analytes detectable in the sample, while the LOQ is the minimum amount that can be quantified by the method. These parameters were calculated from the signal-to-noise ratio (LODs signal-to-noise = 3, LOQ signal-to-noise = 10).

2.6. Liquid chromatographic and mass spectrometric conditions

Mobile phase A consisted of ammonium formate (25 mM) in distilled water, pH 3.5 adjusted with formic acid and mobile phase B comprised of acetonitrile (ACN). The chromatographic separation was performed with a hydrophilic interaction liquid chromatography (HILIC) column (Nucleoshell HILIC, EC 100/2, 2.7 μm, Macherey-Nagel, Hoerdt, France) equipped with a column protection system (Nucleoshell HILIC, EC 4/2, 2.7 μm, Macherey-Nagel, Hoerdt, France). The analytes (Glu, Gln and GABA), in standards solutions and samples dialysates, were separated using a gradient elution starting at 95% of eluent B, keeping this composition constant for 1 min and then decreased linearly to 85% in 3 min. This composition was held for 8 min before decreasing to 50% for 3 min, then returning to the initial conditions for 0.1 min, followed by a re-equilibration time of 2 min for a total run time of 21.1 min. Flow rate was 300 μl/min and the injection volume was 5 μl. The column temperature was set at 23 ± 1 °C and the sample temperature at 5 ± 1 °C.

Chromatographic analyses were performed on a Dionex Ultimate-3000 HPLC (DGP-3600 M) equipped with a Dionex WPS-3000PL injector. The column switching valve was set at 0.00 min to the waste and at 2.00 min to the mass spectrometer and at 21.1 min to the waste again. HPLC was connected on-line to a triple quadrupole mass spectrometer detector (TQD) with electrospray ionization (ESI) interface (Quattro Ultima, Waters, Guyancourt, France). Detection was performed in positive multiple reaction monitoring (MRM) mode. ESI parameters were set as follow-

Table 3
MRM transitions and MS parameters for the Glu, Gln, GABA and internal standards.

Compounds	Precursor ion (*m*/*z*)	Collision energy (eV)	Production ion (*m*/*z*)	Retention time (min)	Dwell time (s)
Glu	148.1	15	84	13.9	0.02
Gln	147.1	20	84	13.8	0.02
GABA	104.1	10	87.1	12.6	0.02
Glu-d5	153.1	15	134.9	13.9	0.02
GABA-d6	110	10	93	12.6	0.02

ing: capillary voltage 4 kV, cone voltage 35 V, source temperature 120 °C and desolvation temperature 350 °C, with a nitrogen flow of 500 l/hr. Collision-induced dissociation was performed using argon as the collision gas. The MRM transitions and the collision energies are shown in Table 3. The HPLC and MS system were controlled by Chromeleon 6.8 (Thermo Fisher Scientific, Illkirch, France) and MassLynx 4.1 software (Waters, Guyancourt, France), respectively.

3. Results and discussion

3.1. Optimization of LC–MS/MS conditions

Initial experiments were realized to achieve an appropriate separation between analytes (Glu, Gln and GABA) together with suitable peak shapes and stable retention time. We selected a core-shell ammonium-sulfonic acid modified silica column HILIC column, which is suitable for the retention and separation of very polar and hydrophilic compounds [25]. To optimize the chromatographic separation and the intensity of the three analytes, different mobile phase compositions were investigated. ACN and methanol were compared to select the constitution of organic phase. The best results were obtained with the ACN as organic solvent. During the method development, we also found that the salt content and pH value in the buffer solution had a great impact on the retention time and MS signal of the analytes. Three ammonium formate concentrations were tested: 50, 25 and 10 mM. Formic acid was used as modifier to adjust the pH, from 2.7 to 4.2, of the aquaeous solution of ammonium formate. To summarize, the aqueous phase consisted of a buffer solution containing 25 mM ammonium formate and pH of 3.5 using a gradient program (see the section "Liquid chromatographic and mass spectrometric conditions") that started at 95% ACN for separation of the targeted analytes. These conditions have been established in order to allow a satisfying separation of Glu and Gln considering the common ions of their isotopic profiles. In addition, the conditions described here allowed using a moderate salt level of the aqueous phase, which limits the salt accumulation on the ESI capillary. Fig. 2 shows chromatograms of a standard mixture of Glu (50 ng/ml); Gln (1250 ng/ml) and GABA (1.25 ng/ml) and IS. The analytes and internal standards were eluted from the HILIC column and detected at 13.9 min for Glu, 13.8 min for Gln and 12.6 min for GABA (Table 3 and Fig. 2). No interferences were seen for blank injections of the matrix for analytes and IS and no additives were evaluated to improve the analytical signal and the resolution of the chromatographic peaks. At the end of the experiment, the column was washed with 50/50 water-ACN for 30 min. The procedure is intended to protect the column from endogenous substances and extend its life.

Based on the experience of previous works in the literatures, the positive ion mode and ESI source was selected because it showed higher sensitivity for all compounds of interest ([14–22] and [26] for a review). The optimal conditions for MS/MS detection were set up by direct infusion of the standard solutions into the mass spectrometer. The protonated molecules [M+H$^+$], *m*/*z* 148.1, 147.1, 104.1, 153.1 and 110 for Glu, Gln, GABA, Glu-d5 and GABA-d6, respectively, were selected as precursor ions (Table 3). The MRM

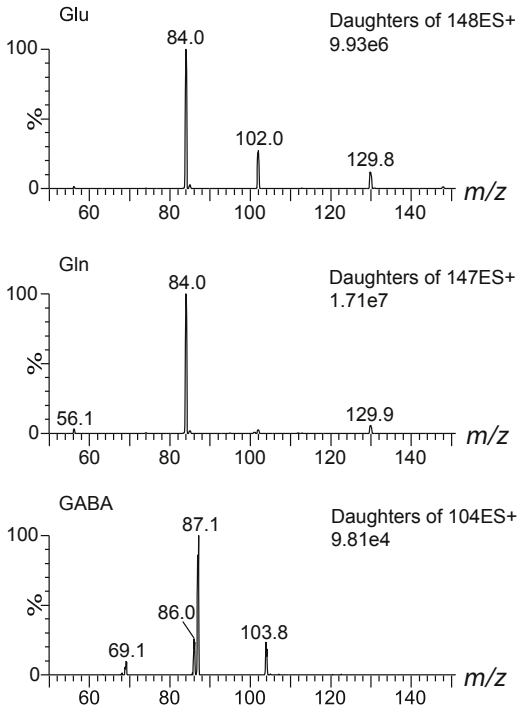

Fig. 1. ESI–MS/MS positive ion scanning spectra for Glu, Gln and GABA.

transitions, collision energies, retention times and dwell times used for the measurement of the compounds and the IS are provided in Table 3. Using the MRM mode, several fragment ions were generated and the full-scan product ion spectrums are shown as Fig. 1. The most abundant transition ion was selected to obtain maximum sensitivity. To improve the sensitivity of the method, we evaluated the possibility of increasing the injection volumes. Two injection volumes, 5 and 10 μl, were studied. While an extra broadening of the peaks was observed for the 10 μl injection, the volume of 5 μl was selected. In these conditions, the partial loop was chosen as injection mode. Due to the high amount of salts in microdialysis samples and to prevent a possible clogging of the source capillary, a switching valve was used for 2 min to avoid delivering of salts into the mass spectrometer and thus to increase the sensitivity of the analysis.

3.2. Method validation

Two IS were selected to quantify the concentration of Glu, Gln and GABA. Glu-d5 was selected as the IS of Glu and Gln. The reliability and reproducibility of this method was evaluated by determining the inter-day and intra-day accuracy and precision using 3 QC concentrations (five determinations per concentration) distributed throughout the dynamic range for each analyte (see the section "Preparation of standard solutions and calibration curves"). The results for inter-day and intra-day accuracy and precision of the method for all analytes were summarized in Table 4. The intra- and inter-day precisions (%RSD) ranged from 1.3% to 13.3% and 4.2% to

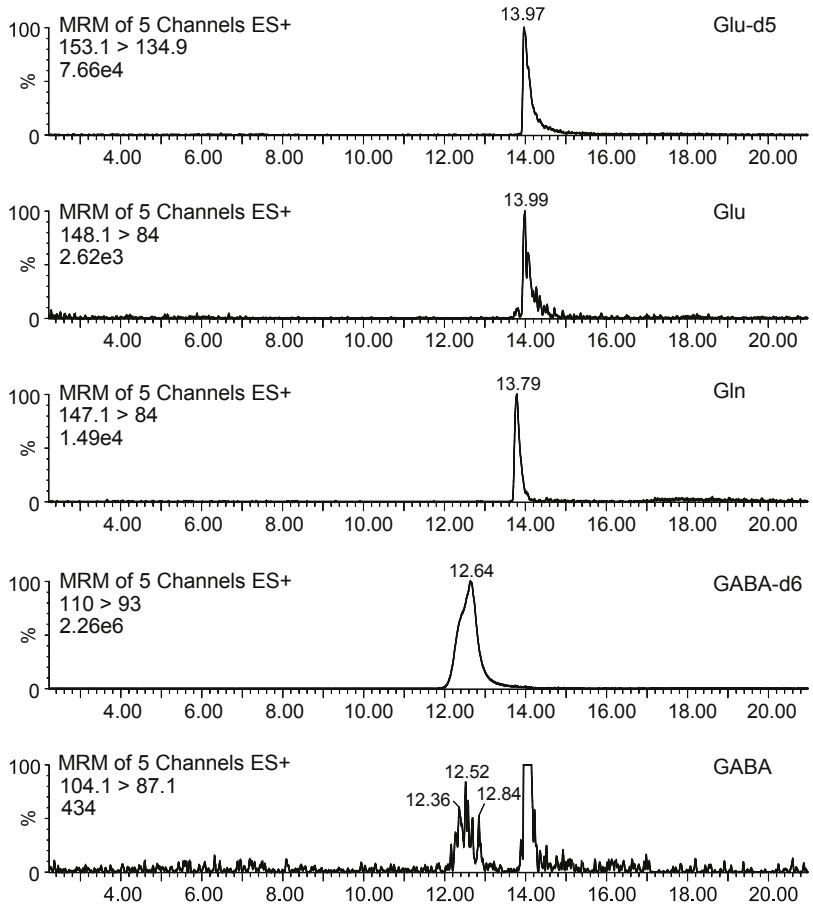

Fig. 2. Representative chromatograms of a standard sample: Glu (50 ng/ml); Gln (1250 ng/ml) and GABA (1.25 ng/ml). Internal standards Glu-d5 and GABA-d6 were used at 60 μg/ml and 15 μg/ml respectively.

Table 4
Intraday and interday precision and accuracy of the HPLC–MS/MS method for determination of Glu, Gln and GABA concentrations in standard solutions.

Compounds	Concentrations (ng/ml)	Intraday		Interday	
		Precision(%RSD)	Accuracy(%RE)	Precision(%RSD)	Accuracy(%RE)
Glu	4	13.3	8.8	41.9	63.4
	80	2.7	−6.9	23.2	5.36
	800	1.3	−0.5	8.3	1.9
Gln	100	7.2	−52.7	31.8	−27
	5000	8.2	4.6	7.9	5.0
	20000	2.9	3.8	4.2	3.4
GABA	0.8	6.9	4.9	37.9	107.9
	8	10.6	−12.4	23.6	16.6
	100	6.7	5.9	18.1	4.4

Table 5
Calibration parameters for the measurement of Glu, Gln and GABA concentrations in standard solutions by HPLC–MS/MS.

Compounds	LOD (ng/ml)	LOQ (ng/ml)	Linear range	Correlation coefficient (R^2)
Glu	0.25	1.25	2.5–2000 ng/ml	0.9999
Gln	1.6	3.15	62.5–50000 ng/ml	0.9999
GABA	0.45	0.63	0.63–500 ng/ml	0.9997

Table 6
Extracellular levels of Glu, Gln, GABA, Gln_{ext}/Glu_{ext} and $Glu_{ext}/GABA_{ext}$ ratios as measured at baseline (n = 17) and after KCl perfusion (at t = 60 min, n = 5) in the mPFC by using microdialysis in C57Bl/6 mice. Values are reported as mean ± SEM.

Conditions	Glu_{ext}	Gln_{ext}	$GABA_{ext}$	Gln_{ext}/Glu_{ext} ratio	$Glu_{ext}/GABA_{ext}$ ratio
Basal extracellular levels in ng/ml (pmol/sample)	80.8 ± 1.8 (2.8 ± 0.1)	4734 ± 66 (161.9 ± 2.3)	7.9 ± 0.1 (0.38 ± 0.01)	58.6	10.2
Effects of KCl-induced release on neurotransmitters levels in ng/ml (pmol/sample)	344 ± 151 (11.7 ± 2.6)	3836 ± 579 (131.2 ± 19.8)	57.9 ± 14.1 (2.8 ± 0.7)	11.1	5.9

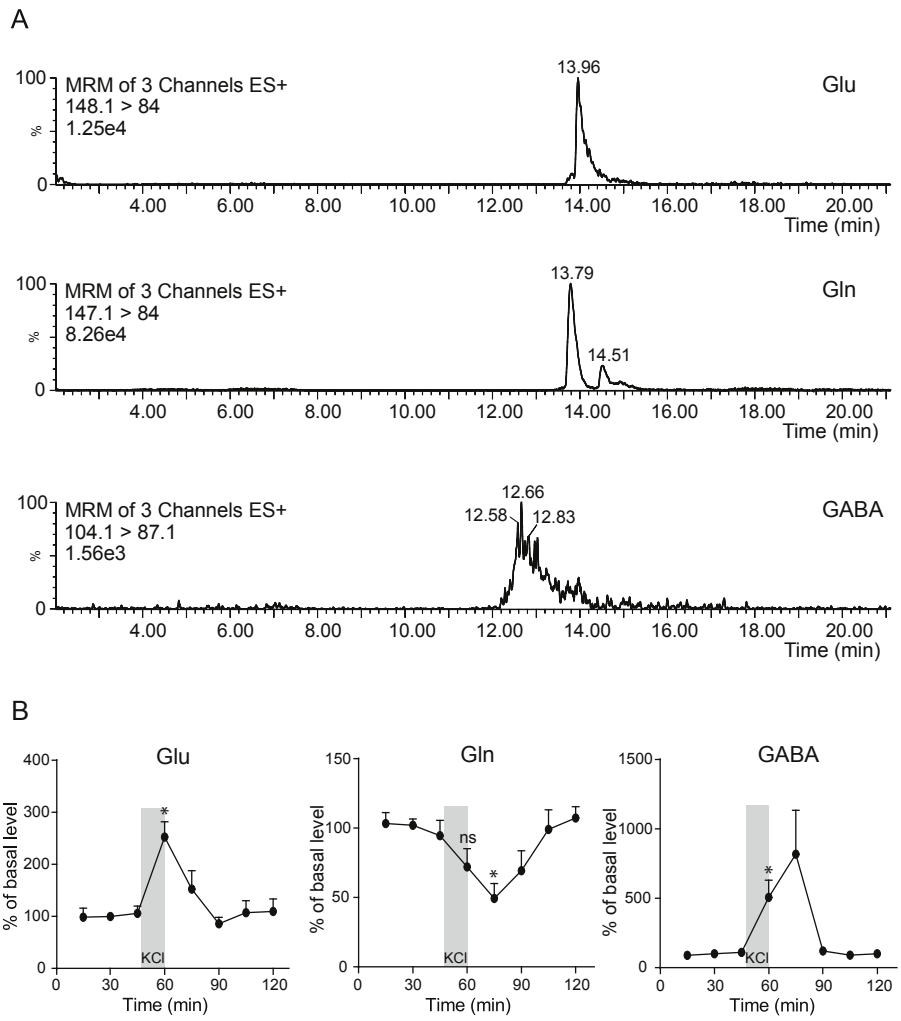

Fig. 3. (A) Representative chromatograms of microdialysis samples from the mPFC with high dose of KCl (120 mM, at t = 60 min, n = 5). (B) Time course of potassium-evoked Glu, Gln and GABA release in the mPFC. From time point 45 min, the aCSF was switched to the KCl-enriched aCSF (120 mM for 15 min, gray bars) to induce the release (membrane depolarization) of these analytes in mouse mPFC. Data are expressed as% of basal release (mean of samples 15, 30 and 45 min as basal reference) and are represented as mean ± SEM. One-way ANOVA $F_{(7,32)} = 6.1$; 3.6; 5.1 respectively for Glu, Gln and GABA followed by Bonferroni *post-hoc* test, each * represents $p < 0.05$ *vs* time 45 min.

41.9%, respectively, while the accuracy (%RE) ranged from −52.7% to 8.8% and −27% to 107.9%, respectively, for all the QC levels. The QC mid is particularly of interest: it was defined according to the basal values for each analytes measured preliminarily in mPFC of mice (data not shown). Indeed, precision and accuracy intra- and inter-day of the QC mid values range from −12% to 23% were within the acceptable range, allowing relevant assays under physiological conditions. Linearity was given in the tested range of 2.5–2000 ng/ml for Glu, 0.63–500 ng/ml for GABA and 62.5–50000 ng/ml for Gln. Based on our preliminary observations the lowest values used for the calibration have been determined in order to obtain the basal analytes levels in the mPFC of mice around the middle of the calibration curves, taking also into consideration to have the lowest value superior of the LOQ. Similarly, the highest values were in accordance to the analytes concentrations variations observed following KCl perfusion. The calibration curves for each analytes were obtained by linear regression analysis. The values obtained for R^2 was above 0.999 for all analytes. This indicated a good linearity within the stated ranges. Concerning the sensitivity, the calculated LODs are in range from 0.25 ng/ml for Glu, 0.45 ng/ml for GABA to 1.6 ng/ml for Gln. The corresponding LOQs ranged from 0.63 ng/ml for GABA, 1.25 ng/ml for Glu to 3.15 ng/ml for Gln. The values obtained are shown in Table 5.

3.3. Application of the method to monitor extracellular GABA, glutamate and glutamine levels in cortical dialysate samples in mice

To demonstrate the feasibility of the present LC–MS/MS method, Glu_{ext}, Gln_{ext} and $GABA_{ext}$ levels were monitored using intracortical *in vivo* microdialysis technique in freely moving mice. The basal values of Glu_{ext}, Gln_{ext} and $GABA_{ext}$ in mPFC dialysates (Table 6) were in a range making them compatible with the LOQs determined in this study, i.e., they were (in ng/ml): 80.8 ± 1.8, 4734 ± 66 and 7.9 ± 0.1 respectively (n = 17). It is difficult to compare these values with the ones available in the literature. Indeed, GABA, Glu and Gln concentrations in the mouse brain were often measured in brain tissue homogenates ([20–22]; see Table 2), which reflect both intra- and extra-cellular neurotransmitters' concentrations. By contrast, intracerebral microdialysis specifically measures the extracellular levels of neurotransmitters and their metabolites. However, the ranges of the values measured here in mice agree with microdialysis studies performed in various rat brain areas (Table 1). For example, Buck et al. [13] in the globus pallidus and Bergh et al. [22] in the VTA obtained similar values that the ones found in the present study for GABA and Glu. Interestingly, in the same study [22], $GABA_{ext}$ in the nucleus accumbens was more than a thou-

sand time higher that in the VTA or than the ones we obtained in the mouse mPFC. Another study found also high levels of $GABA_{ext}$ and Glu_{ext} in the hippocampus compared to those we obtained here (Table 1). However, little is known about the regulation of synaptic excitatory/inhibitory balance in the brain and concomitant changes in Glu/GABA neurotransmission, respectively, following drugs' administration in rodents.

We then applied this analytical method to measure the effects of a local KCl perfusion in 5 animals (120 mM for 15 min), thus inducing a neuronal depolarization and GABA and Glu release [27]. Such a KCl-induced depolarization increased extracellular levels neurotransmitters in mPFC dialysates as expected (Fig. 3A). Glu_{ext} and $GABA_{ext}$ increased by about 300% and 1000%, respectively, 15 min after the perfusion of a high dose of KCl and progressively returned to baseline values over the next 30 min. These results agree with another microdialysis study, in which, a perfusion of 100 mM KCl was performed in the rat globus pallidus inducing a 14- and 8-fold increase in $GABA_{ext}$ and Glu_{ext}, respectively [13]. By contrast, Gln_{ext} decreased by about 50% of the baseline concentration 30 min after KCl perfusion, and returned to the baseline level over the ensuing 1 h (Fig. 3B). The decrease in Gln_{ext} correlates with the Glu_{ext} increase. This observation makes sense, considering that Gln is the intermediate metabolite used by the neurons for the Glu synthesis. It makes us to consider that the methodology presented here can reflect astrocyte-neuron interaction at tripartite synapse [2] and its modification induced by external factors (e.g., the KCl concentration). Thus, we also measured the Gln/Glu turnover as an index of astroglial/neuronal Glu turnover in the mPFC (Table 6). Indeed, a decrease in the ratio of Gln/Glu levels was reported in the CSF of depressed patients suggesting abnormalities in the astrocyte-neuron communication in the brains of these subjects [28]. We found a ratio of 58.6 in the mPFC under basal conditions, and a decrease in Gln_{ext}/Glu_{ext} ratio (11.1) following KCl perfusion (Table 6), due to an increase in mPFC Glu_{ext} and a concomitant decrease in Gln_{ext}. It suggests that KCl-evoked release of Glu in the mPFC modified the astroglial/neuronal turnover. These changes in glutamine levels may be indicative of changes in the cycling of Gln/Glu, which has a central role in energy homeostasis between astrocytes and neurons [29]. Similarly, we also measured the $Glu_{ext}/GABA_{ext}$ ratio in the mPFC (Table 6). We found a ratio of 10.2 in the mPFC under basal conditions, and a decrease in this ratio following KCl perfusion (Glu/GABA = 5.9), suggesting a modification of the excitatory/inhibitory neurotransmitters balance in the mPFC induced by a neuronal depolarization. Such a modification in the Glu/GABA ratio was also observed following an acute restraint stress in the rat [3] as well as in stress-based depression model in mice [30].

Altogether, the present study describes a simple method applied here to the mouse mPFC, which can be easily adaptable to study $Glu/Gln/GABA_{ext}$ changes in various brain regions in mice. Thus, it can be useful to characterize astrocyte-neuron metabolic interactions, as well as the Glu (excitatory)/GABA (inhibitory) balance in brain regions of rodents.

4. Conclusion

A fast and sensitive method requiring a small volume of samples to quantify simultaneously extracellular levels of Glu, GABA and Gln in small brain regions in freely moving mice has been developed and validated. The main objective of this work was to set up a LC–MS/MS method to separate simultaneously Glu, Gln and GABA, then to validate this method by quantifying these compounds using intracerebral microdialysis in awake mice. This method is of interest especially to evaluate the effect of a treatment selectively in a restricted brain area: as an example the high concentration KCl used here affected the astrocyte-neuron metabolic interactions in the mPFC. The present method has shown acceptable precision and adequate sensitivity in quantifying the basal extracellular Glu, Gln and GABA levels in freely moving mice mPFC. The LC–MS/MS method was rapid with an analysis time of 21 min and the preparation of dialysate samples remains fast and easy.

The simplicity of this method makes possible to perform *in vivo* studies of changes in Glu/Gln/GABA release/reuptake in various brain areas. Moreover, changes in Gln/Glu and Glu/GABA ratio could be an asset in the characterization of model of complex psychiatric diseases, especially following a pharmacological treatment. Such microdialysis studies are rare in freely moving "knock-out" mice, for example, but they are nevertheless necessary for exploring the effects of psychotropic drugs, and for characterizing animal models of CNS disorders, such as anxiety/depression. Such a method can also help to depict neuronal circuits involved in the mechanism of action of antidepressants.

Conflict of interest

None regarding this work.

Acknowledgements

This work was supported by the technical assistance of Valerie Dupont-Domergue and the staff of the animal care facility of the SFR-UMS Institut Paris-Saclay Innovation Thérapeutique.

References

[1] M. Barker-Haliski, H.S. White, Glutamatergic mechanisms associated with seizures and epilepsy, Cold Spring Harbor Perspect. Med. 5 (2015) a022863.
[2] A. Perez-Alvarez, A. Araque, Astrocyte-neuron interaction at tripartite synapses, Curr. Drug Targets 14 (2013) 1220–1224.
[3] J.B. Drouet, F. Fauvelle, S. Maunoir-Regimbal, N. Fidier, R. Maury, A. Peinnequin, J. Denis, A. Buguet, F. Canini, Differences in prefrontal cortex Gaba/glutamate ratio after acute restraint stress in rats are associated with specific behavioral and neurobiological patterns, Neuroscience 285 (2015) 155–165.
[4] A.M. Gardier, I. Malagie, A.C. Trillat, C. Jacquot, F. Artigas, Role of 5-HT1A autoreceptors in the mechanism of action of serotoninergic antidepressant drugs: recent findings from in vivo microdialysis studies, Fundam. Clin. Pharmacol. 10 (1996) 16–27.
[5] K.M. Nautiyal, L. Tritschler, S.E. Ahmari, D.J. David, A.M. Gardier, R. Hen, A lack of serotonin 1 B autoreceptors results in decreased anxiety and depression-related behaviors, Neuropsychopharmacology 41 (2016) 2941–2950.
[6] T.H. Pham, C. Defaix, X. Xu, S.X. Deng, N. Fabresse, J.C. Alvarez, D.W. Landry, R.A. Brachman, C.A. Denny, A.M. Gardier, Common neurotransmission recruited in (R,S)-ketamine and (2R,6R)-hydroxynorketamine-Induced sustained antidepressant-like effects, Biol. Psychiatry (2017).
[7] A. Gobert, J.M. Rivet, R. Billiras, F. Parsons, M.J. Millan, Simultaneous quantification of D- vs. L-serine, taurine, kynurenate, phosphoethanolamine and diverse amino acids in frontocortical dialysates of freely-moving rats: differential modulation by N-methyl-D-aspartate (NMDA) and other pharmacological agents, J. Neurosci. Methods 202 (2011) 143–157.
[8] A. Zapata, V.I. Chefer, T.S. Shippenberg, L. Denoroy, Detection and quantification of neurotransmitters in dialysates, Curr. Protoc. Neurosci. (2013) (Unit 7.4).
[9] M. Perry, Q. Li, R.T. Kennedy, Review of recent advances in analytical techniques for the determination of neurotransmitters, Anal. Chim. Acta 653 (2009) 1–22.
[10] M. Piraud, C. Vianey-Saban, K. Petritis, C. Elfakir, J.-P. Steghens, D. Bouchu, Ion-pairing reversed-phase liquid chromatography/electrospray ionization mass spectrometric analysis of 76 underivatized amino acids of biological interest: a new tool for the diagnosis of inherited disorders of amino acid metabolism, Rapid Commun. Mass Spectrom.: RCM 19 (2005) 1587–1602.
[11] D.J. Dietzen, A.L. Weindel, M.O. Carayannopoulos, M. Landt, E.T. Normansell, T.E. Reimschisel, C.H. Smith, Rapid comprehensive amino acid analysis by liquid chromatography/tandem mass spectrometry: comparison to cation exchange with post-column ninhydrin detection, Rapid Commun. Mass Spectrom.:RCM 22 (2008) 3481–3488.
[12] A. Le, A. Ng, T. Kwan, K. Cusmano-Ozog, T.M. Cowan, A rapid, sensitive method for quantitative analysis of underivatized amino acids by liquid chromatography-tandem mass spectrometry (LC–MS/MS), J. Chromatogr. B Anal. Technol. Biomed. Life Sci. 944 (2014) 166–174.

[13] K. Buck, P. Voehringer, B. Ferger, Rapid analysis of GABA and glutamate in microdialysis samples using high performance liquid chromatography and tandem mass spectrometry, J. Neurosci. Methods 182 (2009) 78–84.
[14] A. Santos-Fandila, A. Zafra-Gomez, A. Barranco, A. Navalon, R. Rueda, M. Ramirez, Quantitative determination of neurotransmitters, metabolites and derivates in microdialysates by UHPLC-tandem mass spectrometry, Talanta 114 (2013) 79–89.
[15] J.A. Eckstein, G.M. Ammerman, J.M. Reveles, B.L. Ackermann, Analysis of glutamine, glutamate, pyroglutamate, and GABA in cerebrospinal fluid using ion pairing HPLC with positive electrospray LC/MS/MS, J. Neurosci. Methods 171 (2008) 190–196.
[16] R.R. Gonzalez, R.F. Fernandez, J.L.M. Vidal, A.G. Frenich, M.L.G. Perez, Development and validation of an ultra-high performance liquid chromatography-tandem mass-spectrometry (UHPLC-MS/MS) method for the simultaneous determination of neurotransmitters in rat brain samples, J. Neurosci. Methods 198 (2011) 187–194.
[17] K.Y. Zhu, Q.A. Fu, K.W. Leung, Z.C.F. Wong, R.C.Y. Choi, K.W.K. Tsim, The establishment of a sensitive method in determining different neurotransmitters simultaneously in rat brains by using liquid chromatography-electrospray tandem mass spectrometry, J. Chromatogr. B-Anal. Technol. Biomed. Life Sci. 879 (2011) 737–742.
[18] B.S. He, K.S. Bi, Y. Jia, J.H. Wang, C.X. Lv, R. Liu, L.S. Zhao, H.R. Xu, X.H. Chen, Q. Li, Rapid analysis of neurotransmitters in rat brain using ultra-fast liquid chromatography and tandem mass spectrometry: application to a comparative study in normal and insomnic rats, J. Mass Spectrom. 48 (2013) 969–978.
[19] S.P. Bathena, J.G. Huang, A.A. Epstein, H.E. Gendelman, M.D. Boska, Y. Alnouti, Rapid and reliable quantitation of amino acids and myo-inositol in mouse brain by high performance liquid chromatography and tandem mass spectrometry, J. Chromatogr. B-Anal. Technol. Biomed. Life Sci. 893 (2012) 15–20.
[20] F. Huang, J. Li, H.L. Shi, T.T. Wang, W. Muhtar, M. Du, B.B. Zhang, H. Wu, L. Yang, Z.B. Hu, X.J. Wu, Simultaneous quantification of seven hippocampal neurotransmitters in depression mice by LC–MS/MS, J. Neurosci. Methods 229 (2014) 8–14.
[21] T.H. Kim, J. Choi, H.G. Kim, H.R. Kim, Quantification of neurotransmitters in mouse brain tissue by using liquid chromatography coupled electrospray tandem mass spectrometry, J. Anal. Methods Chem. 2014 (2014) 506870.
[22] M.S.S. Bergh, I.L. Bogen, E. Lundanes, A.M.L. Oiestad, Validated methods for determination of neurotransmitters and metabolites in rodent brain tissue and extracellular fluid by reversed phase UHPLC–MS/MS, J. Chromatogr. B-Anal. Technol. Biomed. Life Sci. 1028 (2016) 120–129.
[23] A.M. Gardier, R.J. Wurtman, Persistent blockade of potassium-evoked serotonin release from rat frontocortical terminals after fluoxetine administration, Brain Res. 540 (1991) 325–330.
[24] FDA, Guidance for industry, bioanalytical method validation., US Department of Health and Human Services Food and Drug Administration, Center for Drug Evaluation and Research (CDER). (2001) Available at www.fda.gov/downloads/Drugs/GuidanceComplianceRegulatoryInformation/Guidances/UCM070107.pdf.
[25] W. Naidong, Bioanalytical liquid chromatography tandem mass spectrometry methods on underivatized silica columns with aqueous/organic mobile phases, J. Chromatogr. B Analyt. Technol. Biomed. Life Sci. 796 (2003) 209–224.
[26] N.B. Cech, C.G. Enke, Practical implications of some recent studies in electrospray ionization fundamentals, Mass Spectrom. Rev. 20 (2001) 362–387.
[27] W. Timmerman, B.H.C. Westerink, Brain microdialysis of GABA and glutamate: what does it signify? Synapse 27 (1997) 242–261.
[28] K. Hashimoto, D. Bruno, J. Nierenberg, C.R. Marmar, H. Zetterberg, K. Blennow, N. Pomara, Abnormality in glutamine-glutamate cycle in the cerebrospinal fluid of cognitively intact elderly individuals with major depressive disorder: a 3-year follow-up study, Transl. Psychiatry 6 (2016) e744.
[29] G. Bonvento, J. Valette, J. Flament, F. Mochel, E. Brouillet, Imaging and spectroscopic approaches to probe brain energy metabolism dysregulation in neurodegenerative diseases, J. Cereb. Blood Flow and Metab. 37 (2017) 1927–1943.
[30] E. Venzala, A.L. Garcia-Garcia, N. Elizalde, R.M. Tordera, Social vs. environmental stress models of depression from a behavioural and neurochemical approach, Eur. Neuropsychopharmacol. 23 (2013) 697–708.

Résultats expérimentaux

Article 1

« Ketamine treatment involves medial prefrontal cortex serotonin to induce a rapid antidepressant-like activity in BALB/cJ mice »

Pham *et al*., Neuropharmacology, 2017 Jan;112:198-209.

doi: 10.1016/j.neuropharm.2016.05.010. Epub 2016

Article 2

« Common neurotransmission recruited in (*R,S*)-ketamine and (2*R*,6*R*)-hydroxynorketamine-induced sustained antidepressant-like effects »

Pham *et al*., Biol Psychiatry. 2017 Oct 26. pii: S0006-3223(17)32130-3.

doi: 10.1016/j.biopsych.2017.10.020

Article 3

« Role of cortical and raphe $GABA_A$ and AMPA receptors in ketamine-induced fast antidepressant-like activity »

Pham *et al*., 2018

En préparation

Résultats complémentaires

1. Comparer l'effet antidépresseur du (2*R*,6*R*)-hydroxynorkétamine avec celui de son isomère (2*S*,6*S*)-hyrdoxynorkétamine
2. La microdialyse couplée avec le NSF chez la même souris

ARTICLE 1 : Ketamine treatment involves medial prefrontal cortex serotonin to induce a rapid antidepressant-like activity in BALB/cJ mice

T.H. Pham, I. Mendez-David, C. Defaix, B.P. Guiard, L. Tritschler, D.J. David, A.M. Gardier

Publié en Neuropharmacology, Janvier 2017, 112: 198-209,
doi.org/10.1016/j.neuropharm.2016.05.010

Question posée :

Est-ce que la kétamine, antagoniste non-compétitive de récepteur NMDA de L-glutamate, exerce son activité de type antidépresseur en interagissant avec le système sérotoninergique du circuit cortex médian préfrontal – noyau du raphé dorsal ?

Résumé de l'étude :

Contrairement aux antidépresseurs sérotoninergiques classiques, la kétamine, un antagoniste des récepteurs NMDA, présente une activité antidépressive (AD) rapide et persistante, à des doses sous-anesthésiques chez des patients déprimés résistants aux traitements classiques et lors d'études précliniques chez les rongeurs. Le mécanisme médiateur de cette activité n'est pas bien compris.

Méthodes : Ici, nous avons évalué le rôle du système sérotoninergique du cerveau dans l'activité de type AD d'une dose sous-anesthésique aiguë de kétamine. Nous avons comparé les réponses à la kétamine et à la fluoxétine dans plusieurs tests comportementaux actuellement utilisés pour prédire le potentiel anxiolytique / antidépresseur chez les rongeurs. Nous avons également mesuré leurs effets sur les niveaux de sérotonine extracellulaire 5-HT_{ext} dans le cortex médian préfrontal (mPFC) et le noyau du raphé dorsal (NRD), un noyau sérotoninergique impliqué dans le comportement émotionnel, et sur l'activité électrique "firing" des cellules de 5-HT dans le NRD chez des souris BALB/cJ de phénotype très anxieux.

Résultats : La kétamine (10 mg/kg, i.p.) n'avait pas d'effet anxiolytique, mais présentait une activité de type AD durable, c'est-à-dire 24 heures après l'administration, comparée à la fluoxétine (18 mg/kg, i.p.). La kétamine (144%) et la fluoxétine (171%) ont augmenté la 5-HT_{ext} du mPFC par rapport au véhicule. L'effet de type AD induit par la kétamine a été aboli par un inhibiteur de la tryptophane hydroxylase, la para-chlorophénylalanine (pCPA), soulignant le

rôle du système sérotoninergique dans son activité comportementale. De façon intéressante, l'augmentation de 5-HT_{ext} corticale après injection bilatérale intra-mPFC de kétamine (0,25 µg/côté) a été corrélée avec son activité AD comme mesuré sur la durée de nage dans le FST chez les mêmes souris. De plus, un prétraitement avec un antagoniste sélectif du récepteur AMPA (intra-NRD NBQX) a atténué les effets de la kétamine administrée intra-mPFC sur la durée de nage dans le FST et la 5-HT_{ext} du mPFC, suggérant que l'activité AD de la kétamine requiert des récepteurs AMPA du NRD et recrute le circuit neuronal du cortex préfrontal / tronc cérébral NRD chez les souris BALB/cJ.

Conclusion : Ces résultats confirment un rôle clé de la libération de 5-HT corticale dans l'activité de type AD de la kétamine après le blocage des récepteurs NMDA glutamatergiques. Des interactions étroites entre les systèmes glutamatergiques et sérotoninergiques du mPFC peuvent expliquer les différences dans cette activité entre la kétamine et la fluoxétine *in vivo*.

Contribution personnelle :

Au cours de travail :

- J'ai mené l'ensemble des tests comportementaux prédictifs des activités de type anxiolytique/antidépresseur chez la souris, avec la coopération du Pr. Denis David et du Dr. Indira Mendez-David
- J'ai réalisé le suivi des animaux incluant la préparation et l'administration du régime de pCPA
- J'ai mis au point et validé la technique de microdialyse-couplé avec le FST chez la même souris
- J'ai analysé les résultats et rédigé l'intégralité de l'article sous la supervision du Pr. Alain Gardier

Neuropharmacology 112 (2017) 198–209

Contents lists available at ScienceDirect

Neuropharmacology

journal homepage: www.elsevier.com/locate/neuropharm

Ketamine treatment involves medial prefrontal cortex serotonin to induce a rapid antidepressant-like activity in BALB/cJ mice

T.H. Pham [a, 1], I. Mendez-David [a, 1], C. Defaix [a], B.P. Guiard [b], L. Tritschler [a], D.J. David [a], A.M. Gardier [a, *]

[a] Université Paris-Saclay, Univ. Paris-Sud, Faculté de Pharmacie, INSERM UMR-S 1178, Chatenay Malabry, 92290, France
[b] UMR5169 CNRS "Centre de Recherches sur la Cognition Animale », Toulouse, 31062, France

ARTICLE INFO

Article history:
Received 26 January 2016
Received in revised form
9 May 2016
Accepted 15 May 2016
Available online 17 May 2016

Keywords:
Ketamine
Serotonin
Rapid antidepressant-like activity
Medial prefrontal cortex
Dorsal raphe nucleus
Antidepressant drug
Highly anxious BALB/cJ mice
Microdialysis

ABSTRACT

Unlike classic serotonergic antidepressant drugs, ketamine, an NMDA receptor antagonist, exhibits a rapid and persistent antidepressant (AD) activity, at sub-anaesthetic doses in treatment-resistant depressed patients and in preclinical studies in rodents. The mechanisms mediating this activity are unclear. Here, we assessed the role of the brain serotonergic system in the AD-like activity of an acute sub-anaesthetic ketamine dose. We compared ketamine and fluoxetine responses in several behavioral tests currently used to predict anxiolytic/antidepressant-like potential in rodents. We also measured their effects on extracellular serotonin levels $[5\text{-HT}]_{ext}$ in the medial prefrontal cortex (mPFCx) and brainstem dorsal raphe nucleus (DRN), a serotonergic nucleus involved in emotional behavior, and on 5-HT cell firing in the DRN in highly anxious BALB/cJ mice. Ketamine (10 mg/kg i.p.) had no anxiolytic-like effect, but displayed a long lasting AD-like activity, i.e., 24 h post-administration, compared to fluoxetine (18 mg/kg i.p.). Ketamine (144%) and fluoxetine (171%) increased mPFCx $[5\text{-HT}]_{ext}$ compared to vehicle. Ketamine-induced AD-like effect was abolished by a tryptophan hydroxylase inhibitor, *para*-chlorophenylalanine (PCPA) pointing out the role of the 5-HT system in its behavioral activity. Interestingly, increase in cortical $[5\text{-HT}]_{ext}$ following intra-mPFCx ketamine bilateral injection (0.25 μg/side) was correlated with its AD-like activity as measured on swimming duration in the FST in the same mice. Furthermore, pre-treatment with a selective AMPA receptor antagonist (intra-DRN NBQX) blunted the effects of intra-mPFCx ketamine on both the swimming duration in the FST and mPFCx $[5\text{-HT}]_{ext}$ suggesting that the AD-like activity of ketamine required activation of DRN AMPA receptors and recruited the prefrontal cortex/brainstem DRN neural circuit in BALB/c mice. These results confirm a key role of cortical 5-HT release in ketamine's AD-like activity following the blockade of glutamatergic NMDA receptors. Tight interactions between mPFCx glutamatergic and serotonergic systems may explain the differences in this activity between ketamine and fluoxetine *in vivo*.

This article is part of the Special Issue entitled 'Ionotropic glutamate receptors'.

1. Introduction

Ketamine, a non-competitive, glutamatergic *N*-methyl-D-aspartate receptor (NMDA-R) antagonist that binds to the phencyclidine site within this ionotropic Ca^{2+} channel, has been found to relieve symptoms within hours when administered at sub-anaesthetic doses in treatment-resistant depressed patients (Berman et al., 2000). Since this discovery, many studies have confirmed ketamine's efficacy in humans as well as in animals. However, the mechanism of action underpinning this rapid antidepressant response in animal models still remains largely unknown.

Preclinical studies with ketamine mainly focused on the glutamatergic system. Thus, ketamine was described as a powerful antagonist at NMDA receptors (elimination half-life < 1 h; *in vitro* $EC_{50} = 760$ nM; *in vivo* $ED_{50} = 4.4$ mg/kg) (Lord et al., 2013; Murray et al., 2000). Antagonism of NMDA-R could be the key pharmacological feature underlying the rapid antidepressant effect of a low dose of ketamine (Krystal et al., 2013). However, the neurochemical mechanisms underlying this response are likely to be more

* Corresponding author. Laboratoire de Neuropharmacologie, INSERM UMR-S 1178 "Depression, Plasticity and Resistance to Antidepressant Drugs", Univ. Paris-Sud, Fac. Pharmacie, 5 Rue J-B Clement, Tour D1, 2e etage, F-92296, Chatenay Malabry Cedex, France.
E-mail address: alain.gardier@u-psud.fr (A.M. Gardier).
[1] These authors contributed equally to this work.

http://dx.doi.org/10.1016/j.neuropharm.2016.05.010
0028-3908/

Abbreviations

$[5\text{-HT}]_{ext}$	extracellular serotonin level
5-HT	serotonin
8-OHDPAT	8-Hydroxy-*N*,*N*-dipropyl-2-aminotetralin
aCSF	artificial cerebrospinal fluid
BDNF	brain-derived neurotrophic factor
DA	dopamine
DRN	dorsal raphe nucleus
EPM	elevated plus maze
FST	forced swim test
i.p.	intraperitoneal
mPFCx	medial prefrontal cortex
MDD	major depressive disorder
mTOR	mammalian target of rapamycin
NBQX	2,3-dihydroxy-6-nitro-7-sulfamoyl-benzo[*f*] quinoxaline-2,3-dione
NSF	novelty suppressed feeding
OF	open field
PCP	phencyclidine
PCPA	*para*-chlorophenylalanine
TPH	tryptophan hydroxylase
SERT	serotonin transporter
SSRIs	selective serotonin reuptake inhibitors
NMDA-R	glutamatergic NMDA receptor
NMDR-2A/2B	glutamatergic NMDA receptor subunit 2A/2B
VTA	ventral tegmental area
WAY100635	*N*-[2-[4-(2-methoxyphenyl)-1-piperazinyl]ethyl]-*N*-(2-pyridyl)-cyclohexanecarboxamide

complex than a selective blockade of NMDA-R (Naughton et al., 2014). Its pharmacology has shown affinities (*and functional activity*) for PCP-site located on NMDA-R (0.5 μM; *antagonist*), NMDR-2A, NMDR-2B binding sites, but also for non-glutamatergic neurotransmitter receptors [sigma-1 receptor (*agonist*), muscarinic, μ opioid receptor, dopamine D_2 receptor (0.5 μM), 5-HT_2 receptor (*in vitro* 15 μM)] (Kapur and Seeman, 2002). Thus, the fast antidepressant effect of ketamine may involve non-selective multi-system changes, including the serotoninergic system, *via* direct and indirect effects (Kapur and Seeman, 2002). Indeed, recently, an *in vivo* microdialysis study performed in the prefrontal cortex of awake monkeys showed an increase in extracellular serotonin (5-HT) levels after acute ketamine injection (Yamamoto et al., 2013). Although functional interactions between glutamate and monoamines are well documented, surprisingly, an acute ketamine administration did not affect the firing activity of serotonin and dopamine neurons in rats (El Iskandrani et al., 2015).

Although ketamine antidepressant-like effects have been assessed, no study performed a behavioral characterization from the antidepressant-like effects to the anxiolytic-like effects.

The medial prefrontal cortex (mPFCx) plays a key role in ketamine's pharmacological effects, because NMDA-R, the main target with highest affinity to ketamine (Murray et al., 2000), is widely expressed in this brain region (Kamiyama et al., 2011; Sanz-Clemente et al., 2013). Artigas's group demonstrated that 5-HT release in the mPFCx depends on the excitatory glutamatergic transmission (Lopez-Gil et al., 2012). Moreover, it has been shown that mPFCx projections to the dorsal raphe nucleus (DRN) control stressful behavior (Amat et al., 2016). Indeed, a recent study demonstrated that the mPFCx is an important brain region in which deep brain stimulation produced the most profound antidepressant effects on a variety of depressive-like behavioral tests in rats (Lim et al., 2015). Thus, here, we hypothesized that serotonergic efflux in the mPFCx/DRN circuit can play a role, at least partially, in ketamine-induced rapid/long lasting antidepressant-like activity in rodents.

First, our study aimed to perform a behavioral characterization of putative long lasting anxiolytic/antidepressant-like effects ketamine (3 or 10 mg/kg, i.p., 24hr before testing), in comparison to fluoxetine (18 mg/kg, i.p, 24hr before testing) in male BALB/cJ mice using different behavioral paradigms predictive of anxiolytic- or antidepressant-like activity. Second, we investigated the role of the serotoninergic component in ketamine −induced changes in behavioral activity using *para*-chlorophenylalanine (PCPA)-induced serotonin depletion in the DRN and also following serotonin release as measured in the mPFCx using *in vivo* microdialysis under the same experimental conditions as behavioral tests. Finally, we challenged the effects of local intra-mPFCx ketamine administration in the microdialysis and the FST measured in the same animals, and then extending to a combination with intra-DRN administration of AMPA receptor antagonist NBQX to clarify the implication of mPFCx/DRN neural circuit. The present experimental strategy offers the possibility of linking ketamine's antidepressant/anxiolytic activity to the serotonergic system in regard to the behavioral and neurochemical levels, giving furthermore persuasive evidence for the implication of a serotonergic pathway in ketamine's antidepressant mechanism.

2. Materials and methods

2.1. Animals

Male BALB/cJ mice (7–8-weeks old) weighing 23–25 g at the beginning of the experiments were purchased from Janvier Labs (Le Genest-Saint-Isle). The BALB/cJ strain of mice was chosen for its baseline anxiety phenotype (Dulawa et al., 2004). They were housed in groups of five in a temperature (21 ± 1 °C) controlled room with a 12 h light: 12 h dark cycle (lights on at 06:00 h). Food and water were available *ad libitum* except during behavioral observations. Particular efforts were made to minimize the number of mice used in the experiments. Protocols were approved by the Institutional Animal Care and Use Committee in France (Council directive # 87–848, October 19, 1987, "Ministère de l'Agriculture et de la Forêt, Service Vétérinaire de la Santé et de la Protection Animale, permissions # 92–196" to A.M.G.) as well as with the European directive 2010/63/EU.

2.2. Drugs and treatments

Ketamine (3 or 10 mg/kg) purchased from Sigma-Aldrich (Saint-Quentin Fallavier, France) and fluoxetine hydrochloride (18 mg/kg) purchased from Anawa Trading (Zurich, Switzerland) were dissolved in vehicle (NaCl 0.9%) and administered 24 h prior to the behavioral tests. Drug doses and pre-treatment times were based on previous studies performed either in our laboratory for fluoxetine (David et al., 2009) or in the literature for ketamine (Li et al., 2010; Liu et al., 2012; Iijima et al., 2012; Koike et al., 2013; Zanos et al., 2015). Diazepam (1.5 mg/kg, i.p., 30 min before testing) was used as a positive control, in animal paradigm predictive of anxiolytic-like effects (David et al., 2007). *Para*-chlorophenylalanine methyl ester

Open Field

A

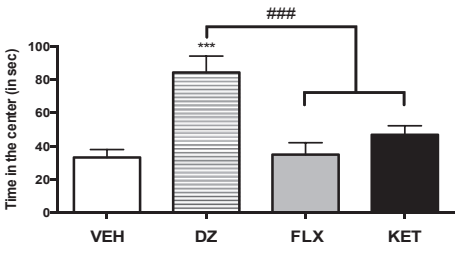

B

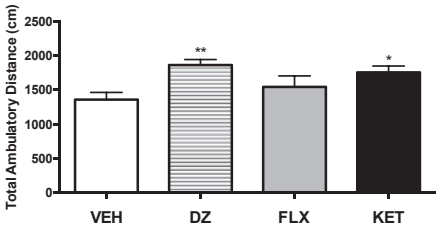

Elevated Plus Maze

C

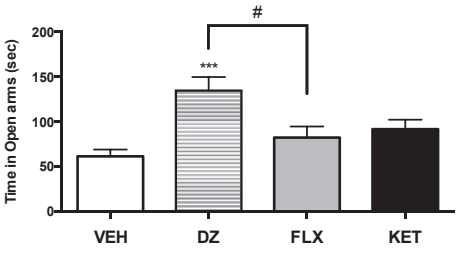

D

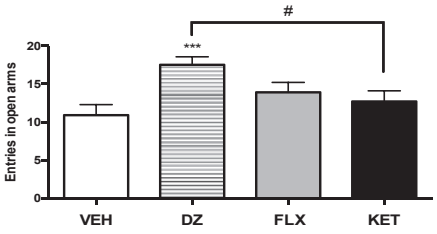

Novelty Suppressed Feeding

E

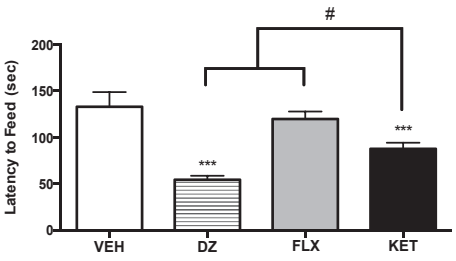

F

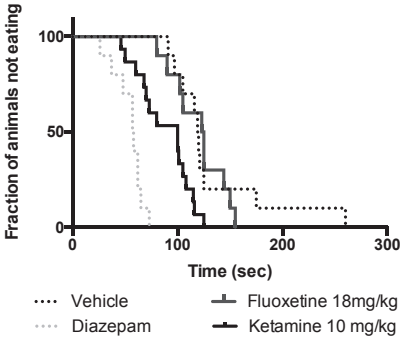

Splash Test

G

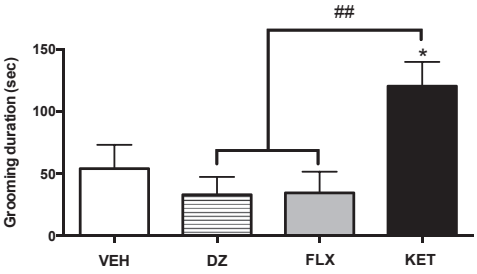

H

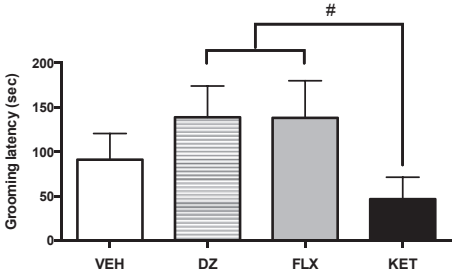

Forced Swim Test

I

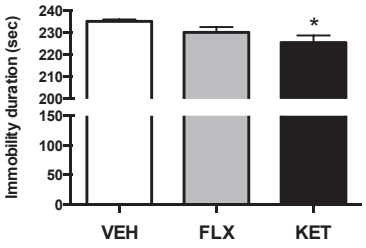

(PCPA, 150 mg/kg, i.p.) purchased from Sigma-Aldrich (Saint-Quentin Fallavier, France), was dissolved in Tween 1% solution and administered twice daily (at 9:00 and 17:00) for 3 consecutive days (Fukumoto and Chaki, 2015). Ketamine or fluoxetine were then administered 24 h after the final PCPA administration and behavioral tests occurred the following day. Immediately following these tests, the animals were sacrificed and the frontal cortex was dissected for 5-HT measurements to verify the depletion of tissue content induced by PCPA as previously described (Musumeci et al., 2015). Tissue content of 5-HT was determined using an ELISA kit from ImmuSmol (Pessac, France).

To study the mechanism underlying the serotonergic effects of ketamine, we tried to dissect the responsible neural circuits linking the mPFCx to the DRN. Thus, we performed an experiment using intra-DRN injection of NBQX, an AMPA receptor antagonist at 300 μM (NBQX disodium salt purchased from Tocris Bioscience, Lille, France) and measured two responses, FST and microdialysis in the same animal. This dose was chosen according to Lopez-Gil et al., 2007 and Fukumoto et al., 2016. NBQX was injected 30 min before a bilateral intra-mPFCx ketamine injection (0.5 μg). Then, dialysate samples were collected in the mPFCx 24 h after ketamine injection and the swimming duration in the FST was measured in these mice when dialysates were collected as in the protocol used in Fig. 4.

2.3. Behavioral assessment

For each behavioral tests of anxiolytic/antidepressant-like activity, a different cohort of BALB/cJ mice was tested. Behavioral testing occurred during the light phase between 07:00 and 19:00.

2.3.1. Open field (OF) test

OF was performed as described previously (Dulawa et al., 2004). Briefly, motor activity was quantified in four Plexiglas open field boxes 43 × 43 cm^2 (MED Associates, Georgia, VT). Two sets of 16 pulse-modulated infrared photobeams on opposite walls 2.5 cm apart, recorded x-y ambulatory movements. Activity chambers were computer interfaced for data sampling at 100 ms resolution. The computer defined grid lines dividing centre and surround regions, with the centre square consisting of four lines 11 cm from the wall. The animals were tested for 10 min to measure the total time spent and the numbers of entries into the centre and the distance travelled in the centre divided by total distance travelled.

2.3.2. Elevated plus maze (EPM) test

The elevated plus maze (EPM) is a widely used behavioral assay for rodents and it has been validated to assess the anti-anxiety effects of pharmacological agents (for review Walf and Frye, 2007). This test was performed as described by Mendez-David et al., 2014. The maze is a plus-cross-shaped apparatus, with two open arms and two arms closed by walls linked by a central platform 50 cm above the floor. Mice were individually put in the centre of the maze facing an open arm and were allowed to explore the maze during 5 min. The time spent in and the number of entries into the open arms were used as an anxiety index. All parameters were measured using a videotracker (EPM3C, Bioseb, Vitrolles, France).

2.3.3. Novelty suppressed feeding (NSF) paradigm

The NSF is a conflict test that elicits competing motivations: the drive to eat and the fear of venturing into the centre of a brightly lit arena. The latency to begin eating is used as an index of anxiety/depression-like behavior, because classical anxiolytic drugs as well as chronic antidepressants decrease this measure. The NSF test was carried out during a 10-min period as previously described David et al., 2009. Briefly, the testing apparatus consisted of a plastic box (50 × 50 × 20 cm), the floor of which was covered with approximately 2 cm of wooden bedding. Twenty-four hours prior to behavioral testing, all food was removed from the home cage. At the time of testing, a single pellet of food (regular chow) was placed on a white paper platform positioned in the centre of the box. Each animal was placed in a corner of the box, and a stopwatch was immediately started. The latency to eat (defined as the mouse sitting on its haunches and biting the pellet with the use of forepaws) was measured. Immediately afterwards, the animal was transferred to its home cage, and the amount of food consumed by the mouse in the subsequent 5 min was measured, serving as a control for change in appetite as a possible confounding factor.

2.3.4. Splash test (ST)

This test was performed as previously described to assess antidepressant-like activity (David et al., 2009; Mendez-David et al., 2014). This test consisted in squirting a 10% sucrose solution on the mouse's snout. The sucrose solution dirtied the coat and induced a grooming behavior as previously shown (Ducottet and Belzung, 2004; Rainer et al., 2012). The grooming duration and latency of different behaviours (face, paws, hindquarter and shoulders) were directly recorded over a 5 min period.

2.3.5. Forced swim test (FST)

The mouse forced swim test procedure (FST) is one of the most useful tools for antidepressants screening. Swimming, climbing and immobility behaviours were distinguished from each other according to the procedure previously described (Dulawa et al., 2004; Holick et al., 2008). Swimming behavior relies on the serotonergic system, and climbing behavior on the noradrenergic system in mouse (Holick et al., 2008). This was evidenced by the observation that desipramine, a noreinephrine reuptake inhibitor, reduces immobility duration increasing climbing behavior. In contrast, fluoxetine induced antidepressant-like effects by increasing the swimming behavior. Mice were placed individually into glass cylinders (height: 25 cm, diameter: 10 cm) containing 18 cm water, maintained at 23–25 °C for 6 min. The predominant behavior (swimming, immobility, or climbing: Holick et al., 2008) was scored for the last 4 min of the 6 min testing period using automated scoring was done using the automated X'PERT FST software (Bioseb, Vitrolles, France).

2.4. Intracerebral in vivo microdialysis

Each mouse was anesthetized with chloral hydrate (400 mg/kg, i.p.) and implanted with two microdialysis probes (CMA7 model, Carnegie Medicine, Stockholm, Sweden) located in the medial prefrontal cortex (mPFCx) and one microdialysis probe in the dorsal raphe nucleus (DRN). Stereotaxic coordinates in mm from bregma:

Fig. 1. Unlike fluoxetine, acute systemic administration of ketamine, 24 h before testing induced long lasting antidepressant-like activity but not anxiolytic-like effects. Anxiolytic/antidepressant-like activity of a single dose of ketamine (KET, 10 mg/kg, i.p.) compared to acute diazepam (DZ, 1.5 mg/kg, i.p.) or fluoxetine (FLX, 18 mg/kg, i.p.). Values plotted are mean ± S.E.M. (n = 10 per group). Effects of drugs on: (A, B) time in the centre and total ambulatory distance in the OF; (C, D) time and entries in open arms in the EPM; mean of latency to feed in seconds ± S.E.M. and (F) cumulative survival of mice that have not eaten over 10 min in the NSF; (G) grooming duration and (H) grooming latency in the ST; (I) immobility duration in the FST. Values plotted are mean ± S.E.M. (n = 10 per group). *p < 0.05; **p < 0.01; ***p < 0.001 significantly different from vehicle-treated group (VEH); #p < 0.05; ##p < 0.01; ###p < 0.001 significantly different from diazepam- or fluoxetine-treated group (One-way ANOVA).

mPFCx: A = +2.2, L = ±0.2, V = −3.4; DRN (with an angle of 15°): A = −4.5, L = +1.2, V = −4.7 (A, anterior; L, lateral; and V, ventral) (Calcagno and Invernizzi, 2010; Ferres-Coy et al., 2013; Nguyen et al., 2013). On the same day, after awakening, mice received an acute ketamine dose, or fluoxetine, or their vehicle i.p. On the next day, ≈24 h after ketamine administration, the probes were continuously perfused with an artificial cerebrospinal fluid (aCSF, composition in mmol/L: NaCl 147, KCl 3.5, $CaCl_2$ 2.26, NaH_2PO_4 1.0, pH 7.4 ± 0.2) at a flow rate of 1.0 μl/min through the mPFCx and 0.5 μl/min through the DRN using CMA/100 pump (Carnegie Medicine, Stockholm, Sweden), while animals were awake and freely moving in their cage. One hour after the start of aCSF perfusion stabilization period, four fractions were collected (one every 25 min) to measure the basal extracellular serotonin (5-hydroxytryptamine, $[5\text{-HT}]_{ext}$) levels in the mPFCx and DRN by using a high-performance liquid chromatography (HPLC) system (column Ultremex 3μ C18, 75 × 4.60 mm, particle size 3 μm, Phenomenex, Torrance, CA) coupled to an amperometric detector (VT03; Antec Leyden, The Netherlands). AUC values (% of baseline) were also calculated during the sample collections as previously described (Nguyen et al., 2013). The limit of sensitivity for 5-HT was ≈0.5 fmol/sample (signal-to-noise ratio = 2). At the end of the experiments, localization of microdialysis probes was verified histologically (Bert et al., 2004). To clarify the specific role of the mPFCx-DRN circuit, we also performed microdialysis and behavioral experiments in which ketamine (0.1 or 0.5 μg, i.e., ≈500 μM or 2.5 mM, respectively) or fluoxetine (0.5 μg) were dissolved in the aCSF and perfused locally at 0.2 μl/min into the mPFCx (bilateral) or DRN for 2 min *via* a silica catheter glued to the microdialysis probe 24 h prior to the tests. The concentration of ketamine was chosen according to Lopez-Gil et al., 2012, showing that a bilateral perfusion of ketamine 3 mM into the mPFCx produced a significant increase in local extracellular 5-HT levels in rats. The FST was performed when the microdialysis procedure still continued.

2.5. In vivo electrophysiological recordings

Twenty-four hours after a single administration of ketamine (10 mg/kg, i.p.) or fluoxetine (18 mg/kg, i.p.), mice were anesthetized with chloral hydrate (400 mg/kg, i.p.) and placed in a stereotaxic frame (using the David Kopf mouse adaptor) with the skull positioned horizontally. The extracellular recordings were performed using single glass micropipettes (R&D Scientific Glass, USA) for recordings in the DRN. Micropipettes were preloaded with fibreglass strands to promote capillary filling with a 2 M NaCl solution. Recording of DRN 5-HT neurons: Single glass micropipettes pulled on a pipette puller (Narishige, Japan) with impedances ranging from 2.5 to 5 mV, were positioned 0.2–0.5 mm posterior to the interaural line on the midline and lowered into the DRN, usually reached at a depth of 2.5–3.5 mm from the brain surface. Spontaneously active DRN 5-HT neurons were then identified according to the following criteria: a slow (0.5–2.5 Hz) and regular firing rate and a long-duration, positive action potential. Neurons were recorded for 2 min and data were expressed as the mean ± SEM of firing rate from all 5-HT neurons encountered during the different tracts. In Supplemental Fig. S1, we show an example of the electrophysiological effects of cumulative doses of ketamine (1–5 mg/kg, i.p.) in an anesthetized mouse on the spontaneous activity of 5-HT neurons as well as the effects of WAY 100635. After ensuring the stability of the recording, ketamine was injected, and the degree of change in firing was observed upon stabilization.

2.6. Statistics

All experimental results are given as the mean ± SEM. Data were analysed using Prism 6 software (GraphPad). The analyses of the behavioral data, the comparisons between groups were performed using one-way ANOVA followed by Fisher's PLSD *post hoc* analysis. In the NSF test, we used the Kaplan–Meier survival analysis owing to the lack of normal distribution of the data. Mantel–Cox log rank test was used to evaluate differences between experimental groups. A summary of statistical measures is included in Supplementary Table S2. Statistical significance was set at $p \leq 0.05$. A two-way ANOVA with pre-treatment (Vehicle vs NBQX) and treatment (Vehicle vs Ketamine) factors was also used followed by Fisher's PLSD *post hoc* test.

3. Results

3.1. Behavioral characterization of the anxiolytic/antidepressant-like activity of an acute ketamine dose in BALB/cJ mice

The anxiolytic-like responses elicited by ketamine administered 24 hrs before testing, were assessed in the Open Field (OF) and Elevated Plus Maze (EPM) tests. In both tests, diazepam (1.5 mg/kg, i.p.) had a marked effect on all anxiety parameters, resulting in an increased time spent in the centre, total ambulatory distance in the OF (Fig. 1A, B), time in open arms and entries into open arms in the EPM (Fig. 1C, D). Fluoxetine (18 mg/kg, i.p.) had no significant effects in both tests, while ketamine (10 mg/kg, i.p.) had only a significant effect on the total ambulatory distance (*$p < 0.05$, ANOVA one-way) in the OF (Fig. 1B, C). These data suggest that ketamine is devoid of long lasting anxiolytic-like activity in BALB/cJ mice.

We further examined the antidepressant-like activity of ketamine in these mice using the Novelty Suppressed Feeding (NSF) test, the Splash Test (ST) and the Forced Swim Test (FST). Unlike diazepam, the most effective drug decreasing the latency to feed in the NSF, unlike fluoxetine, ketamine significantly decreased the latency to feed (Fig. 1E, F). In the ST, ketamine induced a significant increase in grooming duration (Fig. 1G) and a decrease in grooming latency (Fig. 1H), compared to diazepam and fluoxetine, which had no effects. In the FST, ketamine significantly decreased the immobility duration, while fluoxetine did not (Fig. 1I). These results show that a systemic administration of a low dose of ketamine displays a long lasting antidepressant-like activity compared to fluoxetine in BALB/cJ mice.

3.2. Serotonergic parameters of response to ketamine: increases in the swimming duration in the FST after ketamine correlated with changes in extracellular 5-HT levels in the mPFCx and firing rate of DRN 5-HT neurons in mice

3.2.1. Swimming 5-HT behavior

Activation of the brain serotonergic system in rodents is known to mediate increases in swimming duration in the FST (Dulawa et al., 2004). In the FST, ketamine, but not fluoxetine, induced a significant increase in the swimming duration (Fig. 2A, B). According to Page et al., 1999, it suggests that the antidepressant-like activity of ketamine on FST-induced immobility at this time point requires endogenous 5-HT in BALB/cJ mice.

3.2.2. Dialysate 5-HT levels

To study the mechanism underlying this behavioral effect, changes induced by a systemic administration of ketamine (3 or 10 mg/kg) on $[5\text{-HT}]_{ext}$ in the mPFCx and DRN were evaluated by using intracerebral *in vivo* microdialysis. Since ketamine (3 mg/kg) did not change mPFCx and DRN $[5\text{-HT}]_{ext}$ (Table S1), we measured the serotonergic effects of the 10 mg/kg dose only. In the mPFCx (Fig. 2C, D), both drugs ketamine (144%) and fluoxetine (171%) increased mPFCx $[5\text{-HT}]_{ext}$ compared to vehicle. In the DRN (Fig. 2E,

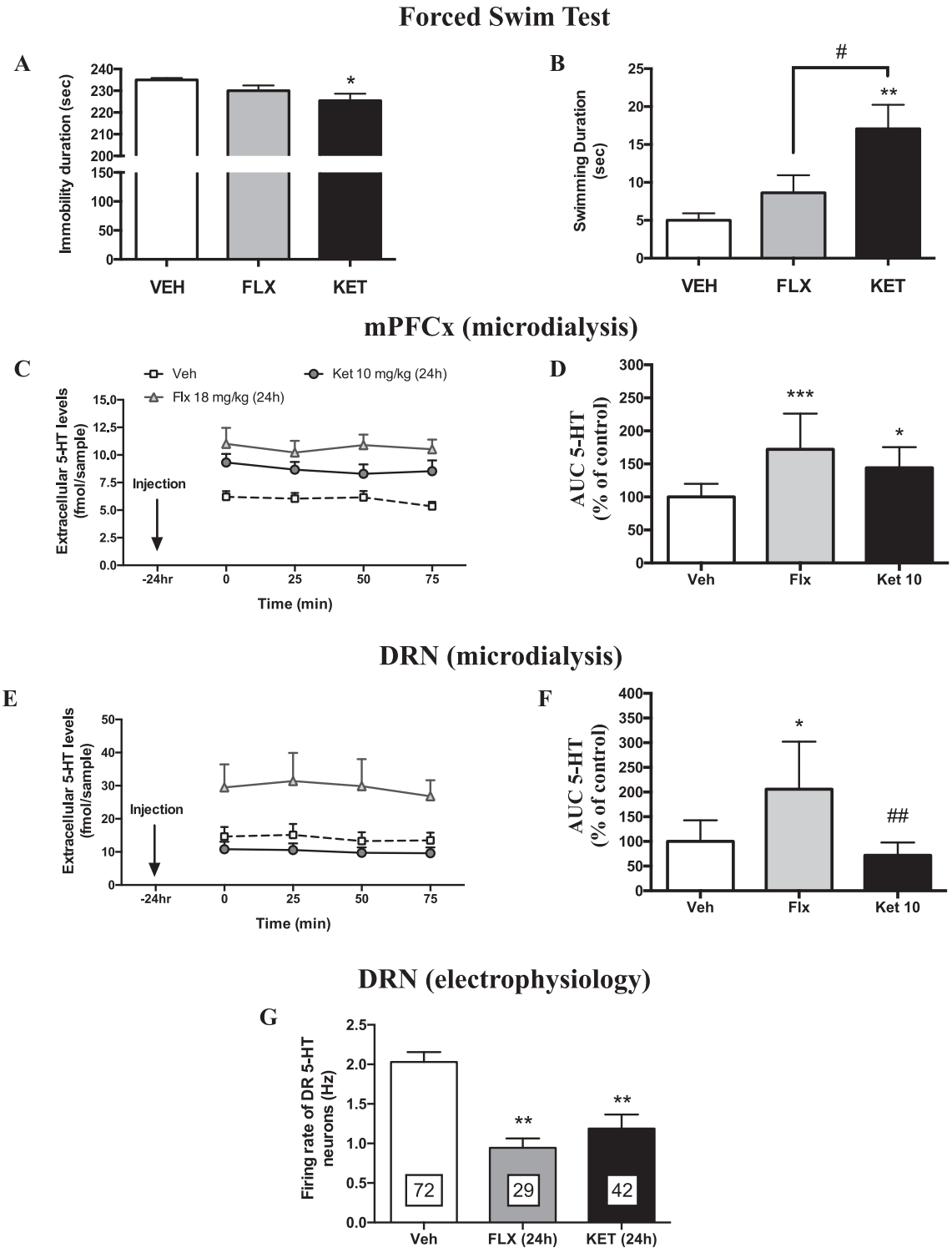

Fig. 2. Ketamine induced increase swimming behavior in the FST is related to enhanced extracellular 5-HT levels in the mPFCx in BALB/cJ mice. Antidepressant-like activity of ketamine (10 mg/kg, i.p.) on (A) the immobility and (B) swimming duration in the FST, compared with the vehicle- and fluoxetine (18 mg/kg, i.p.)-treated group (n = 10/group). (C, E) Time course. Values are mean ± S.E.M. of $[5\text{-HT}]_{ext}$ in the mPFCx and DRN expressed in fmol/sample following exposure to either vehicle, ketamine or fluoxetine. (D, F) Mean ± S.E.M. of AUC values were calculated for the amount of 5-HT outflow collected during 0–75 min, and expressed as percentages of vehicle. (G) Frequency (Hz) of 5-HT neurons recorded in the DRN of mice administered ketamine (10 mg/kg, i.p.) or fluoxetine (18 mg/kg, i.p.). The numbers within the histograms indicate the number of neurons recorded. All the values are expressed as mean ± S.E.M. *p < 0.05; **p < 0.01; ***p < 0.001 significantly different from vehicle-treated group (Veh). #p < 0.05; ##p < 0.01 significantly different from fluoxetine-treated group (Flx).

F), fluoxetine (205%), but not ketamine, increased $[5\text{-HT}]_{ext}$ compared to vehicle. These results indicate that the increased serotonergic activity induced by ketamine and fluoxetine are similar in the mPFCx, but their effects are different in the DRN in BALB/cJ mice.

3.2.3. Firing rate of DRN 5-HT neurons

To determine whether an acute administration of ketamine or fluoxetine can induce persistent changes in serotonergic activity, the firing rate of DRN 5-HT neurons was also measured (Fig. 2G). The DRN 5-HT neuronal activity was significantly reduced by 53% and 45% in fluoxetine and ketamine injected mice, respectively, compared to vehicle. Such decreases in DRN 5-HT cell firing suggest that, especially for ketamine, the antidepressant-like effect measured in the FST is not driven by an increased activity at the cell body level. The mPFCx contains different populations of serotonin neurons. Using whole-cell recordings in mPFCx slices, it was found that 5-HT dose-dependently increased the firing of fast spiking interneurons and decreased the firing of pyramidal neurons (Zhong and Yan, 2011). In addition, subanesthetic doses of ketamine selectively enhanced serotonergic neurotransmission in the mPFCx by inhibition of SERT activity (Yamamoto et al., 2013). Fluoxetine also induced a concentration-dependent increase in the excitability of interneurons, but had little effect on pyramidal neurons. These data suggest that the excitability of different neuronal populations in the mPFCx is tightly regulated by 5-HT. Thus, ketamine may also induce a global increase in the excitability of cortical neurons, but by a different mechanism of action than fluoxetine.

3.3. Effects of 5-HT depletion by PCPA on ketamine antidepressant-like activity in the FST

Depletion of serotonin by a pre-treatment with *p*-chlorophenylalanine (PCPA), a tryptophan hydroxylase (TPH) inhibitor, prevented SSRI-induced increases in swimming duration in the FST (Page et al., 1999). Pre-treatment with PCPA caused an average 79% decrease in the 5-HT content in the frontal cortex in mice, compared with a vehicle-treated group (Table S3). Ketamine significantly reduced the immobility time (Fig. 3A) and increased the swimming duration (Fig. 3B) in the FST in vehicle-pre-treated group (*$p < 0.05$ vs vehicle, ANOVA two-way). Changes in these parameters were blocked by pre-treatment with PCPA, while PCPA alone did not affect the immobility time, nor the swimming duration. These data again suggest that the antidepressant-like activity of ketamine requires an activation of the serotonergic neurotransmision in BALB/cJ mice.

3.4. Effects of local bilateral ketamine intra-mPFCx injection on extracellular 5-HT levels in the mPFCx and swimming behavior in the FST in the same BALB/cJ mice

To reveal the specific role of the mPFCx in the antidepressant-like activity of ketamine, we injected ketamine or fluoxetine (0.25 μg each side) dissolved in the aCSF bilaterally into the mPFCx. Then, 24 h after bilateral intra-mPFCx drugs injection, we measured the swimming duration for 6 min (at t60) in the FST while microdialysis samples were collected for 120 min. Ketamine 0.1 μg had no effect (data not shown). At 0.5 μg, it decreased the immobility duration due to an increase in swimming duration (Fig. 4A, B), and increased $[5\text{-HT}]_{ext}$ (AUC values by 157%) in the mPFCx compared to vehicle (Fig. 4C, D). By contrast, fluoxetine failed to alter both swimming duration and mPFCx $[5\text{-HT}]_{ext}$.

In addition, ketamine-induced increases in mPFCx $[5\text{-HT}]_{ext}$ correlated with its antidepressant-like activity, i.e., with increases in swimming duration in the FST (Fig. 4E). Although a correlation was found in the fluoxetine-treated group, the pattern of the correlation observed for both group are completely different: the range of values of swimming duration following intra-mPFCx fluoxetine injection is lower than that found in the ketamine-treated animals. This could be related to the absence of efficacy of local acute fluoxetine treatment in the FST parameters and in the mPFCx $[5\text{-HT}]_{ext}$.

Since a single intra-mPFC ketamine injection increased the swimming duration and mPFCx $[5\text{-HT}]_{ext}$ (Fig. 4), we tried to dissect the responsible neural circuit for this response by using an AMPA receptor antagonist locally injected into the DRN. We found that NBQX prevented the effects of intra-mPFCx ketamine injection on both the immobility (Fig. 5A) and swimming duration (Fig. 5B) in the FST, and blunted the effects of ketamine on $[5\text{-HT}]_{ext}$ in the same mice (Fig. 5C). AUC 5-HT values increased by only 31% in the

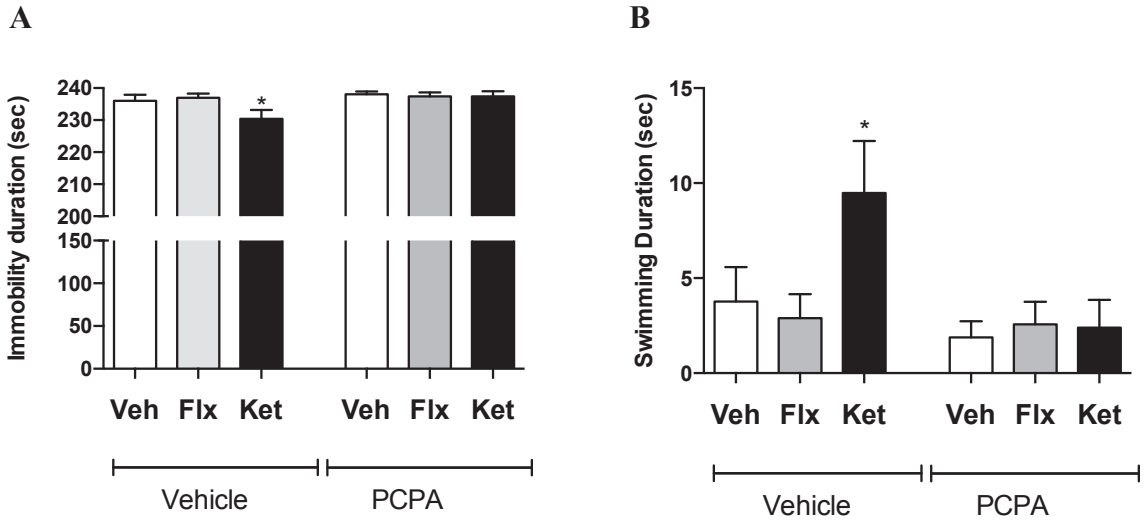

Fig. 3. Pre-treatment with PCPA abolished ketamine-induced antidepressant-like effect in the FST. Two groups of mice pre-treated with PCPA or vehicle prior to receiving ketamine (Ket, 10 mg/kg), fluoxetine (Flx, 18 mg/kg) or vehicle (Veh, NaCl 0.9%) were compared in the FST. In mice groups pre-treated with PCPA for 3 consecutive days, ketamine no longer exhibited its antidepressant-like effects, i.e., (A) decreases in the immobility duration and (B) increases in the swimming duration as it did in naïve groups pre-treated with the vehicle ($n = 6$ mice per group). *$p < 0.05$ different from Veh/Veh-treated group (two-way ANOVA).

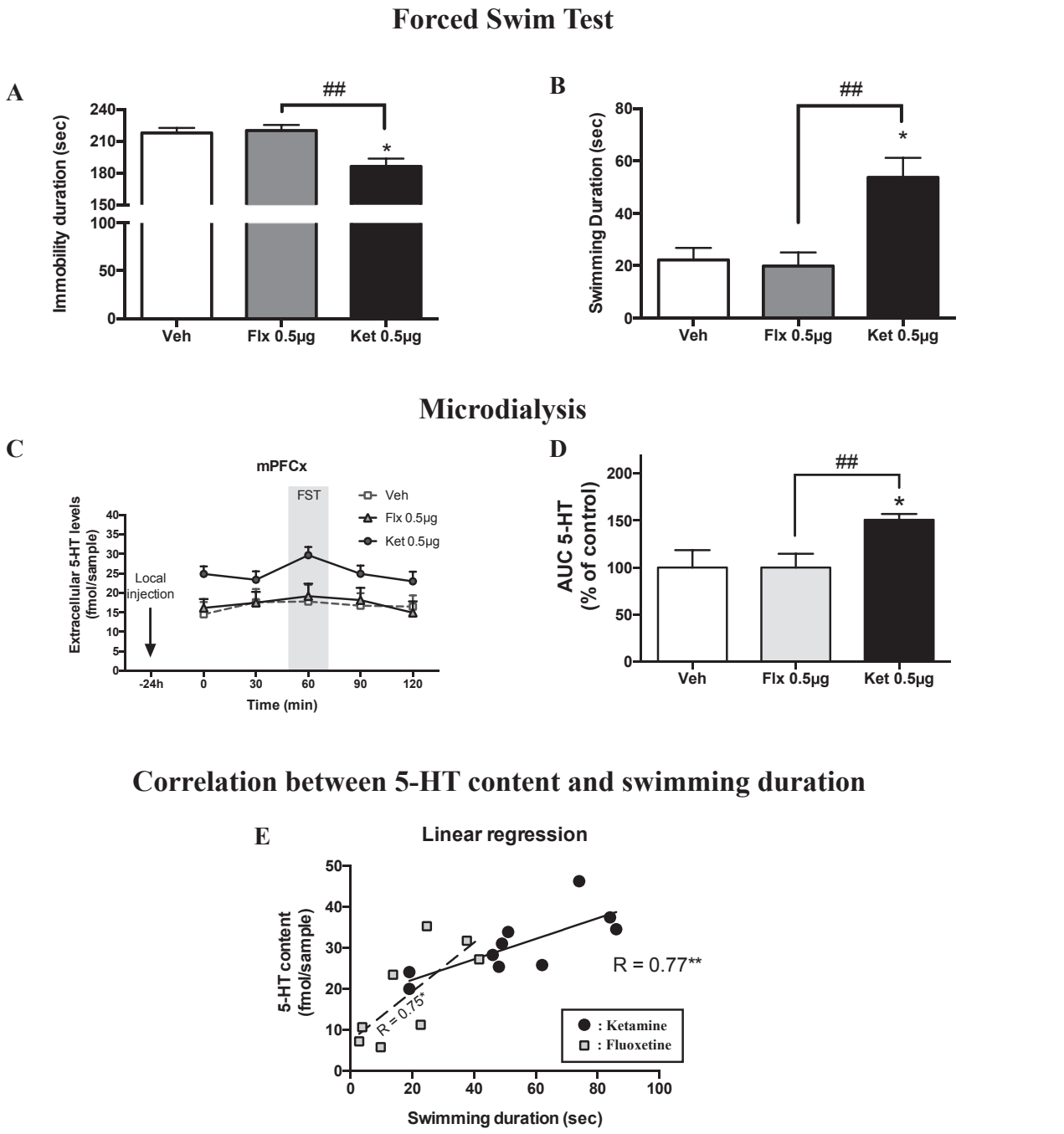

Fig. 4. Intra-mPFCx injection of ketamine-induced increase in swimming behavior in the FST, 24 h after drug injection, is correlated to increase in extracellular cortical 5-HT levels. Unlike fluoxetine (0.25 µg each side), bilateral intra-mPFCx ketamine (Ket) injection at dose 0.5 µg (0.25 µg each side) induced (A) a significant decrease in the immobility duration due to an increase in (B) the swimming duration, a serotonergic parameter in the FST. (C) A statistically significant increase in extracellular mPFCx 5-HT levels was observed in the same Ket-treated mice, but not in Flx-treated mice. The gray area indicates the duration of the FST (i.e., 6 min). (D) AUC values were calculated for the amount of 5-HT outflow collected during 0–120 min and expressed as percentages of baseline. (E) The correlation between extracellular mPFCx 5-HT levels at t60 min (i.e., during the FST) and the swimming duration is stronger in Ket-treated than in Flx-treated mice in regard to their respective *R* Pearson value. *p < 0.5 vs Vehicle (Veh). ##p < 0.01 vs Flx-treated group (one-way ANOVA).). *p < 0.05 and **p < 0.01 for the correlation of dialysate cortical 5-HT levels at t60 min with the swimming duration (n = 8–10 mice per group).

NBQX/Ketamine group compared with the NBQX/Veh group; Fig. 5D.

4. Discussion

In the present study, we performed a characterization of ketamine's anxiolytic/antidepressant-like effects in mice using five different behavioral tests in the highly anxious BALB/cJ strain of mice. We also conducted *in vivo* microdialysis after its systemic or intra-mPFCx administration to unveil putative associations between ketamine's behavioral activity and activation of the serotonergic neurotransmission. A dose of 10 mg/kg has been used in the present study and experiments were conducted 24 h after drugs' administration. It corresponds to conditions already described in other studies avoiding in particular hyperlocomotion observed with higher ketamine doses (Koike et al., 2013; Liu et al., 2012; Yang

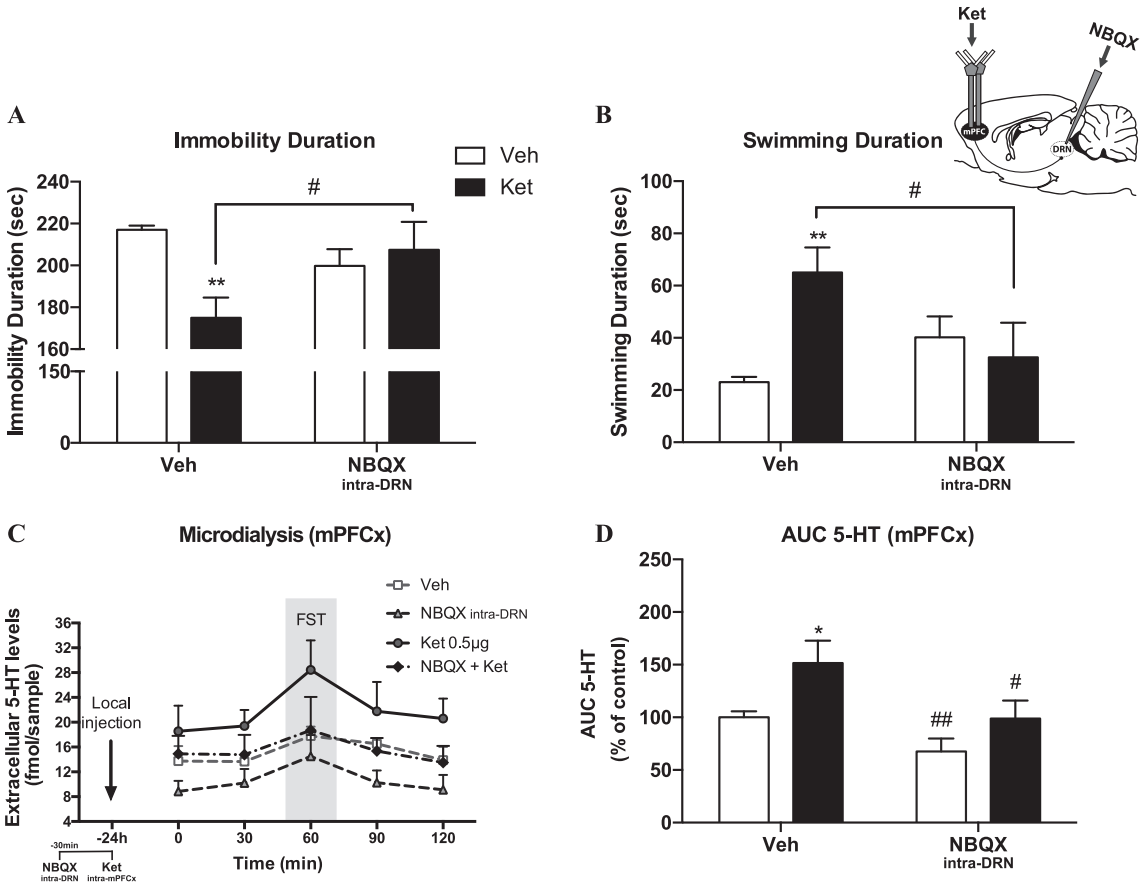

Fig. 5. Intra-DRN injection of NBQX, an AMPA receptor antagonist, abolished the effects of intra-mPFCx ketamine injection in both the FST and mPFCx [5-HT]$_{ext}$ as measured in the same mice. Intra-DRN NBQX injection at dose 0.1 µg blunted the effects of bilateral intra-mPFCx ketamine (Ket) injection at dose 0.5 µg (0.25 µg each side) on (A) the immobility duration due to an increase in (B) the swimming duration in the FST. This abolishment was also observed in (C) the time course and (D) AUC values of mPFCx [5-HT]$_{ext}$. Both the FST and microdialysis technique were performed in the same mice. The gray area in Fig. 5C indicates the duration of the FST (i.e., 6 min). *p < 0.5 and **p < 0.01 vs Vehicle/Vehicle (Veh). #p < 0.05 and ##p < 0.01 vs Veh/Ket (two-way ANOVA). n = 4–5 mice per group.

et al., 2012; Reus et al., 2011; Li et al., 2010) or when behavioral tests were performed immediately after its administration. By this time, ketamine no longer remained in the animals' circulatory system due to its short elimination half-life ($t_{1/2}$–13 min in mice: Maxwell et al., 2006), thus no more alteration in locomotor activity was observed beyond 30 min (Lindholm et al., 2012). More precisely, here, a single ketamine dose had no anxiolytic-like activity in the OF and EPM. In addition, at doses ≥20 mg/kg, changes in [5-HT]$_{ext}$ are not selective since ketamine induced an immediate increase in extracellular glutamate and dopamine (DA) levels (less than 140 min) in the rat nucleus accumbens and mPFCx (Moghaddam et al., 1997; Razoux et al., 2007).

By contrast, the three behavioral tests evaluating ketamine antidepressant-like activity yielded positive results. Ketamine effects in the NSF agree with the literature (Iijima et al., 2012), but here with a lower dose: 10 mg/kg *vs* 30 mg/kg. As expected, a single fluoxetine administration had no effects in the NSF and ST (David et al., 2009). In the FST, ketamine response on immobility time is mainly due to increases in swimming duration in BALB/cJ mice, a parameter likely reflecting activation of the brain serotonergic system (Page et al., 1999). Recently with a similar protocol (drug doses, time of study), Zanos and colleagues showed that, distinct from fluoxetine, ketamine administration resulted in rapid and persistent antidepressant-like effects following a single treatment in mice (Zanos et al., 2015). However, these authors did not measure the swimming duration in the FST. Here, the swimming/serotonergic parameter in the 24-h-FST gave new information compared to what was observed 30 min or several days after ketamine administration at similar doses (Koike et al., 2013). In the ST, ketamine increased grooming duration in BALB/cJ mice similarly to C57BL/6J mouse strain exposed to chronic mild stress (Franceschelli et al., 2015). Overall, such a behavioral characterization revealed that ketamine principally exerts an antidepressant-like activity, *via* an activation of serotonergic synaptic transmission.

Increase in swimming duration in the FST after a systemic ketamine administration suggests an activation of serotonergic synaptic transmission. Thus, we evaluated, the potential contribution of the serotonergic system to the antidepressant-like effect of ketamine in the FST using a pre-treatment with PCPA. PCPA-induced decrease in frontal cortex 5-HT levels in BALB/cJ mice (79%, see Supplementary Table S3) prevented the anti-immobility effects of ketamine, confirming a key role of the serotoninergic system in its antidepressant-like effect. Interestingly, a serotonergic-dependent mechanism of ketamine was already observed following TPH inhibition by PCPA pre-treatment in rats (Gigliucci et al., 2013). We then investigated the brain regions involved in this activity.

Using both routes of administration, we found that systemic or intra-mPFCx ketamine injection increased mPFCx/[5-HT]$_{ext}$, but not DRN/[5-HT]$_{ext}$. Microdialysis studies already reported ketamine-induced increases in cortical [5-HT]$_{ext}$, but over the first hours after its acute administration, and at higher doses (Amargos-Bosch et al., 2006; Lopez-Gil et al., 2012). Here, fluoxetine increased

mPFCx and DRN [5-HT]$_{ext}$ as it usually does after its immediate injection (David et al., 2003). Fluoxetine long $t_{1/2}$ (~5 h in rodents: Maxwell et al., 2006) may explain this persistent effect. At the electrophysiological level, acute fluoxetine still decreased discharge of 5-HT neurons confirming its ability to block SERT. Ketamine and fluoxetine can block the serotonin transporter, despite their differential inhibitory effects *in vitro* on SERT function (Ki = 160 μM *versus* 1 nM, respectively: Owens et al., 2001; Zhao and Sun, 2008). Their effects after systemic administration on mPFCx/[5-HT]$_{ext}$ are similar. By contrast, ketamine and fluoxetine had different effects on DRN/[5-HT]$_{ext}$. Autoradiographic studies indicated that the DRN contains a high number of SERT binding sites in rodents (Hrdina et al., 1990). Thus, unlike fluoxetine, ketamine effects on dialysate DRN/5-HT do not seem to involve a direct blocking effect on SERT (Malagie et al., 2002). However, a complex regulation of DRN/5-HT neurons by mPFCx afferents has been demonstrated: the stimulation of some DRN/5-HT neurons by descending excitatory fibers leads to 5-HT release (Celada et al., 2001). Thus, more experiments are required to understand the role of serotonin receptors, mPFCx-DRN circuit and signalling pathways in ketamine-induced antidepressant-like activity.

Interestingly, fluoxetine can bind to NMDA-R in rat cortex, but with a lower affinity than ketamine (Ki = 10.5 μM and Ki = 1.35 μM, respectively: Gilling et al., 2009; Szasz et al., 2007). Here, fluoxetine increased mPFCx/[5-HT]$_{ext}$ in the mPFCx and DRN, but only 24 h after its systemic administration and did not decrease immobility duration in the FST. These neurochemical effects were already reported in mice when assessed immediately after an acute SSRI i.p. injection and were linked to the selective inhibition of the serotonin transporter (Bortolozzi et al., 2004; Guiard et al., 2004).

A systemic administration of fluoxetine induced changes in [5-HT]$_{ext}$ in the mPFCx and DRN, but failed to trigger an antidepressant-like effect in the FST (Fig. 2). However, intra-mPFCx injection of fluoxetine did not alter both mPFCx [5-HT]$_{ext}$ and the antidepressant-like activity in the FST (Fig. 4). These different results may be due to the key difference between the protocol of Fig. 2 and that of Fig. 4: in the second one, mPFCx [5-HT]$_{ext}$ was measured under stressful conditions, i.e., the FST was performed when collecting dialysate samples in the same animal. In this case, the effects of increasing mPFCx [5-HT]$_{ext}$ are lost for fluoxetine, but not for ketamine, which still increased these cortical levels over 50%. It has been shown that, as a stressor, the FST did not modify [5-HT]$_{ext}$ in the frontal cortex, but increased its levels in the striatum and decreased them in the amygdala (Kirby et al., 1995). Thus, the FST modulates brain circuits involving the serotonergic system in a region-specific manner. It is likely that antidepressant drugs induced changes in these 5-HT circuits, so that fluoxetine has lost its ability to increase mPFCx [5-HT]$_{ext}$ at 24 h when microdialysis is performed during a stressful event as the FST, while ketamine has retained this ability. It is the increase in cortical [5-HT]$_{ext}$ during the FST that induces the antidepressant-like activity of ketamine. In this case, the measurement of mPFCx [5-HT]$_{ext}$ reflects this activity. By contrast, the increase in mPFCx [5-HT]$_{ext}$ induced by fluoxetine is not sufficient to induce a marked antidepressant-like effect under stress conditions. The correlation we draw between swimming duration and mPFCx [5-HT]$_{ext}$ when combining FST and microdialysis in the same mouse (Fig. 4) further confirms that there are clear differences between ketamine and fluoxetine-treated groups regarding their responses in both tests. Taken together, our data reveal that mPFCx plays a major role in promoting the [5-HT]$_{ext}$/FST responses to ketamine, and less for those of fluoxetine under stressful conditions.

To analyze these behavioral and neurochemical responses of ketamine possibly mobilizes neural circuits linking the mPFCx to the DRN, we studied the effects of an intra-DRN NBQX injection in BALB/c mice. The antidepressant-like effect of ketamine on the immobility duration due to an increase in the swimming duration was totally blocked by NBQX (Fig. 5A, B). This blockade was associated with a blunted effect of ketamine on mPFCx [5-HT]$_{ext}$ levels, which suggests that AMPA receptors located in mPFCx-DRN neural circuits. When given alone, intra-DRN NBQX decreased mPFCx [5-HT]$_{ext}$ levels in comparison to the corresponding control group (Fig. 5D). Taken together, these results suggest that DRN AMPA receptors exert a tonic control on mPFCx 5-HT release, and activation of mPFCx/DRN circuitry may underlie at least in part, ketamine's antidepressant-like activity. Although the functional relationship between the DRN and mPFCx is well documented (Lopez-Gil et al., 2007), further optogenetic experiments may help to confirm this hypothesis.

NMDA-R is widely expressed in the mPFCx (Kamiyama et al., 2011; Sanz-Clemente et al., 2013). Ketamine's rapid antidepressant-like response may require an increase in mammalian Target of Rapamycin (mTOR)-dependent expression of BDNF, ultimately leading to increased synaptogenesis in rat mPFCx (Li et al., 2010). Indeed, clinical evidence showed a direct relationship between prefrontal cortex activities, synaptic plasticity, plasma BNDF levels, and the rapid antidepressant effect of ketamine in treatment-resistant depression (Cornwell et al., 2012; Haile et al., 2014). Moreover, it is well known that the mTORC1 signaling pathway regulates protein translation following alterations in neuronal activity contributing to synaptic plasticity (Gerhard et al., 2016 for review). Previous studies showed that ketamine increased the proportion of large-diameter, mushroom-like spines in the prefrontal cortex *in vivo* 24 h after its administration (Li et al., 2010). In addition, expression of the synaptic markers synapsin I and postsynaptic density 95 (PSD95) remains increased 24 h after ketamine. Therefore, the effect of ketamine in modulating cortical glutamate signaling and the expression of neuroplasticity markers may explain its long lasting behavioral effect.

Local injection of a drug in a specific brain region provides useful information on its mechanism of action: intra-mPFCx ketamine increased cortical [5-HT]$_{ext}$ similarly to what was found after its systemic administration. It indicates that the NMDA-R responsible for serotonergic effects are located in the mPFCx. Our results stand out from those of the literature. For example, no changes in cortical [5-HT]$_{ext}$ occurred immediately after a local ketamine perfusion of 100–1000 μM in naïve rats (Amargos-Bosch et al., 2006). Thus, differential dosage of ketamine and time of observation might have divergent actions depending on the site of blockade of NMDA-R, either inside the mPFCx or outside, e.g., in the ventral hippocampus (Lopez-Gil et al., 2012; Brown et al., 2015). Our data agree with the work of Gigliucci et al., 2013, which has also demonstrated a role of 5-HT in mediating sustained antidepressant-like activity of ketamine in the FST. We added here a mechanistic approach showing in particular a sustained effect of ketamine on cortical [5-HT]$_{ext}$ after its local application.

Stimulation of the cortical serotonergic system may play, at least partially, a role in ketamine antidepressant-like activity here. However, this role may be either insufficient, or incomplete to explain this activity in the mPFCx because behavioral responses were different between ketamine and fluoxetine in the FST (swimming duration), ST and NSF, while they induced comparable increases in mPFCx/[5-HT]$_{ext}$ at this time point. To explain its fast antidepressant-like activity, it was hypothesized that ketamine directly blocks NMDA-R located on GABA interneurons. As a consequence, it decreases the inhibitory GABA-ergic tone, thus increases excitatory synapses and glutamate release in the mPFCx (Moghaddam et al., 1997). This cascade of events might explain the greater and persistent increase in mPFCx/[5-HT]$_{ext}$ induced by systemic and intra-mPFCx ketamine. In addition, ketamine may act

outside of the mPFCx to activate excitatory glutamatergic transmission, but within the mPFCx to release DA (Lorrain et al., 2003).

In conclusion, ketamine displays a more effective, a persistent more rapid antidepressant-like activity than fluoxetine in several behavioral tests. Unlike fluoxetine, acute ketamine reduced immobility duration at this time point in the FST by inducing a robust increase in swimming duration associated with mPFCx/$[5\text{-HT}]_{ext}$ increases. Moreover, the depletion of 5-HT synthesis by PCPA abolished ketamine effects in the FST. Thus, ketamine, a non 5-HT compound, surprisingly requires cortical 5-HT system to induce its antidepressant-like effects. Differences with fluoxetine in neural adaptation of mPFCx-DRN circuits are likely to mediate their serotonergic characteristics.

Conflict of interest

D.J.D. serves as a consultant for Lundbeck, Roche, and Servier. BPG serves as a consultant for Lundbeck and Phodé laboratoires. AMG serves as a consultant for Lundbeck and Servier.

Author's contribution

Thu Ha Pham, Denis J David and Alain M Gardier contributed to the conception and design of the study; Thu Ha Pham, Indira Mendez-David, Céline Defaix, Bruno Guiard, Laurent Tritschler and Denis J David contributed to the acquisition of data. Thu Ha Pham and Alain M Gardier wrote the manuscript. All the authors contributed to analysis of data, drafting the article for key intellectual content.

Acknowledgments

The authors would like to thank the animal care facility of SFR-UMRS Institut Paris Saclay d'Innovation Thérapeutique of University Paris-Sud for their technical assistance.

The laboratory was supported by the «Agence Nationale pour la Recherche» (ANR-12- SAMENTA-0007).

Appendix A. Supplementary data

Supplementary data related to this article can be found at http://dx.doi.org/10.1016/j.neuropharm.2016.05.010.

References

Amargos-Bosch, M., Lopez-Gil, X., Artigas, F., Adell, A., 2006. Clozapine and olanzapine, but not haloperidol, suppress serotonin efflux in the medial prefrontal cortex elicited by phencyclidine and ketamine. Int. J. Neuropsychopharmacol. 9, 565–573.

Amat, J., Dolzani, S.D., Tilden, S., Christianson, J.P., Kubala, K.H., Bartholomay, K., Sperr, K., Ciancio, N., Watkins, L.R., Maier, S.F., 2016. Previous ketamine produces an enduring blockade of neurochemical and behavioral effects of uncontrollable stress. J. Neurosci. 36, 153–161.

Berman, R.M., Cappiello, A., Anand, A., Oren, D.A., Heninger, G.R., Charney, D.S., Krystal, J.H., 2000. Antidepressant effects of ketamine in depressed patients. Biol. Psychiatry 47, 351–354.

Bert, L., Favale, D., Jego, G., Greve, P., Guilloux, J.P., Guiard, B.P., Gardier, A.M., Suaud-Chagny, M.F., Lestage, P., 2004. Rapid and precise method to locate microdialysis probe implantation in the rodent brain. J. Neurosci. Methods 140, 53–57.

Bortolozzi, A., Amargos-Bosch, M., Toth, M., Artigas, F., Adell, A., 2004. In vivo efflux of serotonin in the dorsal raphe nucleus of 5-HT1A receptor knockout mice. J. Neurochem. 88, 1373–1379.

Brown, K.M., Roy, K.K., Hockerman, G.H., Doerksen, R.J., Colby, D.A., 2015. Activation of the gamma-aminobutyric acid type B (GABA) receptor by agonists and positive allosteric modulators. J. Med. Chem. 58 (16), 6336–6347.

Calcagno, E., Invernizzi, R.W., 2010. Strain-dependent serotonin neuron feedback control: role of serotonin 2C receptors. J. Neurochem. 114, 1701–1710.

Celada, P., Puig, M.V., Casanovas, J.M., Guillazo, G., Artigas, F., 2001. Control of dorsal raphe serotonergic neurons by the medial prefrontal cortex: involvement of serotonin-1A, GABA(A), and glutamate receptors. J. Neurosci. 21, 9917–9929.

Cornwell, B.R., Salvadore, G., Furey, M., Marquardt, C.A., Brutsche, N.E., Grillon, C., Zarate Jr., C.A., 2012. Synaptic potentiation is critical for rapid antidepressant response to ketamine in treatment-resistant major depression. Biol. Psychiatry 72, 555–561.

David, D.J., Bourin, M., Jego, G., Przybylski, C., Jolliet, P., Gardier, A.M., 2003. Effects of acute treatment with paroxetine, citalopram and venlafaxine in vivo on noradrenaline and serotonin outflow: a microdialysis study in Swiss mice. Br. J. Pharmacol. 140, 1128–1136.

David, D.J., Klemenhagen, K.C., Holick, K.A., Saxe, M.D., Mendez, I., Santarelli, L., Craig, D.A., Zhong, H., Swanson, C.J., Hegde, L.G., Ping, X.I., Dong, D., Marzabadi, M.R., Gerald, C.P., Hen, R., 2007. Efficacy of the MCHR1 antagonist N-[3-(1-{[4-(3,4-difluorophenoxy)phenyl]methyl}(4-piperidyl))-4-methylphenyl]-2-m ethylpropanamide (SNAP 94847) in mouse models of anxiety and depression following acute and chronic administration is independent of hippocampal neurogenesis. J. Pharmacol. Exp. Ther. 321, 237–248.

David, D.J., Samuels, B.A., Rainer, Q., Wang, J.W., Marsteller, D., Mendez, I., Drew, M., Craig, D.A., Guiard, B.P., Guilloux, J.P., Artymyshyn, R.P., Gardier, A.M., Gerald, C., Antonijevic, I.A., Leonardo, E.D., Hen, R., 2009. Neurogenesis-dependent and -independent effects of fluoxetine in an animal model of anxiety/depression. Neuron 62, 479–493.

Ducottet, C., Belzung, C., 2004. Behaviour in the elevated plus-maze predicts coping after subchronic mild stress in mice. Physiol. Behav. 81, 417–426.

Dulawa, S.C., Holick, K.A., Gundersen, B., Hen, R., 2004. Effects of chronic fluoxetine in animal models of anxiety and depression. Neuropsychopharmacology 29, 1321–1330.

Ferres-Coy, A., Santana, N., Castane, A., Cortes, R., Carmona, M.C., Toth, M., Montefeltro, A., Artigas, F., Bortolozzi, A., 2013. Acute 5-HT(1)A autoreceptor knockdown increases antidepressant responses and serotonin release in stressful conditions. Psychopharmacol. Berl. 225, 61–74.

Franceschelli, A., Sens, J., Herchick, S., Thelen, C., Pitychoutis, P.M., 2015. Sex differences in the rapid and the sustained antidepressant-like effects of ketamine in stress-naive and "depressed" mice exposed to chronic mild stress. Neuroscience 290C, 49–60.

Fukumoto, K., Chaki, S., 2015. Involvement of serotonergic system in the effect of a metabotropic glutamate 5 receptor antagonist in the novelty-suppressed feeding test. J. Pharmacol. Sci. 127, 57–61.

Fukumoto, K., Iijima, M., Chaki, S., 2016. The antidepressant effects of an mGlu2/3 receptor antagonist and ketamine require AMPA receptor stimulation in the mPFC and subsequent activation of the 5-HT neurons in the DRN. Neuropsychopharmacology 41, 1046–1056.

Gerhard, D.M., Wohleb, E.S., Duman, R.S., 2016. Emerging treatment mechanisms for depression: focus on glutamate and synaptic plasticity. Drug Discov. Today 21, 454–464.

Gigliucci, V., O'Dowd, G., Casey, S., Egan, D., Gibney, S., Harkin, A., 2013. Ketamine elicits sustained antidepressant-like activity via a serotonin-dependent mechanism. Psychopharmacol. Berl. 228, 157–166.

Gilling, K.E., Jatzke, C., Hechenberger, M., Parsons, C.G., 2009. Potency, voltage-dependency, agonist concentration-dependency, blocking kinetics and partial untrapping of the uncompetitive N-methyl-D-aspartate (NMDA) channel blocker memantine at human NMDA (GluN1/GluN2A) receptors. Neuropharmacology 56, 866–875.

Guiard, B.P., Przybylski, C., Guilloux, J.P., Seif, I., Froger, N., De Felipe, C., Hunt, S.P., Lanfumey, L., Gardier, A.M., 2004. Blockade of substance P (neurokinin 1) receptors enhances extracellular serotonin when combined with a selective serotonin reuptake inhibitor: an in vivo microdialysis study in mice. J. Neurochem. 89, 54–63.

Haile, C.N., Murrough, J.W., Iosifescu, D.V., Chang, L.C., Al Jurdi, R.K., Foulkes, A., Iqbal, S., Mahoney 3rd, J.J., De La Garza 2nd, R., Charney, D.S., Newton, T.F., Mathew, S.J., 2014. Plasma brain derived neurotrophic factor (BDNF) and response to ketamine in treatment-resistant depression. Int. J. Neuropsychopharmacol. 17, 331–336.

Holick, K.A., Lee, D.C., Hen, R., Dulawa, S.C., 2008. Behavioral effects of chronic fluoxetine in BALB/cJ mice do not require adult hippocampal neurogenesis or the serotonin 1A receptor. Neuropsychopharmacology 33, 406–417.

Hrdina, P.D., Foy, B., Hepner, A., Summers, R.J., 1990. Antidepressant binding sites in brain: autoradiographic comparison of [3H]paroxetine and [3H]imipramine localization and relationship to serotonin transporter. J. Pharmacol. Exp. Ther. 252, 410–418.

Iijima, M., Fukumoto, K., Chaki, S., 2012. Acute and sustained effects of a metabotropic glutamate 5 receptor antagonist in the novelty-suppressed feeding test. Behav. Brain Res. 235, 287–292.

El Iskandrani, K.S., Oosterhof, C.A., El Mansari, M., Blier, P., 2015. Impact of subanesthetic doses of ketamine on AMPA-mediated responses in rats: an in vivo electrophysiological study on monoaminergic and glutamatergic neurons. J. Psychopharmacol. 35, 334–336.

Kamiyama, H., Matsumoto, M., Otani, S., Kimura, S.I., Shimamura, K.I., Ishikawa, S., Yanagawa, Y., Togashi, H., 2011. Mechanisms underlying ketamine-induced synaptic depression in rat hippocampus-medial prefrontal cortex pathway. Neuroscience 177, 159–169.

Kapur, S., Seeman, P., 2002. NMDA receptor antagonists ketamine and PCP have direct effects on the dopamine D(2) and serotonin 5-HT(2)receptors-implications for models of schizophrenia. Mol. Psychiatry 7, 837–844.

Kirby, L.G., Allen, A.R., Lucki, I., 1995. Regional differences in the effects of forced swimming on extracellular levels of 5-hydroxytryptamine and 5-hydroxyindoleacetic acid. Brain Res. 682, 189–196.

Koike, H., Iijima, M., Chaki, S., 2013. Effects of ketamine and LY341495 on the

depressive-like behavior of repeated corticosterone-injected rats. Pharmacol. Biochem. Behav. 107, 20–23.
Krystal, J.H., Sanacora, G., Duman, R.S., 2013. Rapid-acting glutamatergic antidepressants: the path to ketamine and beyond. Biol. Psychiatry 73, 1133–1141.
Li, N., Lee, B., Liu, R.J., Banasr, M., Dwyer, J.M., Iwata, M., Li, X.Y., Aghajanian, G., Duman, R.S., 2010. mTOR-dependent synapse formation underlies the rapid antidepressant effects of NMDA antagonists. Science 329, 959–964.
Lim, L.W., Janssen, M.L., Kocabicak, E., Temel, Y., 2015. The antidepressant effects of ventromedial prefrontal cortex stimulation is associated with neural activation in the medial part of the subthalamic nucleus. Behav. Brain Res. 279, 17–21.
Lindholm, J.S., Autio, H., Vesa, L., Antila, H., Lindemann, L., Hoener, M.C., Skolnick, P., Rantamaki, T., Castren, E., 2012. The antidepressant-like effects of glutamatergic drugs ketamine and AMPA receptor potentiator LY 451646 are preserved in bdnf(+)/(-) heterozygous null mice. Neuropharmacology 62, 391–397.
Liu, R.J., Lee, F.S., Li, X.Y., Bambico, F., Duman, R.S., Aghajanian, G.K., 2012. Brain-derived neurotrophic factor Val66Met allele impairs basal and ketamine-stimulated synaptogenesis in prefrontal cortex. Biol. Psychiatry 71, 996–1005.
Lopez-Gil, X., Babot, Z., Amargos-Bosch, M., Sunol, C., Artigas, F., Adell, A., 2007. Clozapine and haloperidol differently suppress the MK-801-increased glutamatergic and serotonergic transmission in the medial prefrontal cortex of the rat. Neuropsychopharmacology 32, 2087–2097.
Lopez-Gil, X., Jimenez-Sanchez, L., Romon, T., Campa, L., Artigas, F., Adell, A., 2012. Importance of inter-hemispheric prefrontal connection in the effects of non-competitive NMDA receptor antagonists. Int. J. Neuropsychopharmacol. 15, 945–956.
Lord, B., Wintmolders, C., Langlois, X., Nguyen, L., Lovenberg, T., Bonaventure, P., 2013. Comparison of the ex vivo receptor occupancy profile of ketamine to several NMDA receptor antagonists in mouse hippocampus. Eur. J. Pharmacol. 715, 21–25.
Lorrain, D.S., Baccei, C.S., Bristow, L.J., Anderson, J.J., Varney, M.A., 2003. Effects of ketamine and N-methyl-D-aspartate on glutamate and dopamine release in the rat prefrontal cortex: modulation by a group II selective metabotropic glutamate receptor agonist LY379268. Neuroscience 117, 697–706.
Malagie, I., David, D.J., Jolliet, P., Hen, R., Bourin, M., Gardier, A.M., 2002. Improved efficacy of fluoxetine in increasing hippocampal 5-hydroxytryptamine outflow in 5-HT(1B) receptor knock-out mice. Eur. J. Pharmacol. 443, 99–104.
Maxwell, C.R., Ehrlichman, R.S., Liang, Y., Trief, D., Kanes, S.J., Karp, J., Siegel, S.J., 2006. Ketamine produces lasting disruptions in encoding of sensory stimuli. J. Pharmacol. Exp. Ther. 316, 315–324.
Mendez-David, I., David, D.J., Darcet, F., Wu, M.V., Kerdine-Romer, S., Gardier, A.M., Hen, R., 2014. Rapid anxiolytic effects of a 5-HT(4) receptor agonist are mediated by a neurogenesis-independent mechanism. Neuropsychopharmacology 39, 1366–1378.
Moghaddam, B., Adams, B., Verma, A., Daly, D., 1997. Activation of glutamatergic neurotransmission by ketamine: a novel step in the pathway from NMDA receptor blockade to dopaminergic and cognitive disruptions associated with the prefrontal cortex. J. Neurosci. 17, 2921–2927.
Murray, F., Kennedy, J., Hutson, P.H., Elliot, J., Huscroft, I., Mohnen, K., Russell, M.G., Grimwood, S., 2000. Modulation of [3H]MK-801 binding to NMDA receptors in vivo and in vitro. Eur. J. Pharmacol. 397, 263–270.
Musumeci, G., Castrogiovanni, P., Castorina, S., Imbesi, R., Szychlinska, M.A., Scuderi, S., Loreto, C., Giunta, S., 2015. Changes in serotonin (5-HT) and brain-derived neurotrophic factor (BDFN) expression in frontal cortex and hippocampus of aged rat treated with high tryptophan diet. Brain Res. Bull. 119, 12–18.
Naughton, M., Clarke, G., O'Leary, O.F., Cryan, J.F., Dinan, T.G., 2014. A review of ketamine in affective disorders: current evidence of clinical efficacy, limitations of use and pre-clinical evidence on proposed mechanisms of action. J. Affect Disord. 156, 24–35.
Nguyen, H.T., Guiard, B.P., Bacq, A., David, D.J., David, I., Quesseveur, G., Gautron, S., Sanchez, C., Gardier, A.M., 2013. Blockade of the high-affinity noradrenaline transporter (NET) by the selective 5-HT reuptake inhibitor escitalopram: an in vivo microdialysis study in mice. Br. J. Pharmacol. 168, 103–116.
Owens, M.J., Knight, D.L., Nemeroff, C.B., 2001. Second-generation SSRIs: human monoamine transporter binding profile of escitalopram and R-fluoxetine. Biol. Psychiatry 50, 345–350.
Page, M.E., Detke, M.J., Dalvi, A., Kirby, L.G., Lucki, I., 1999. Serotonergic mediation of the effects of fluoxetine, but not desipramine, in the rat forced swimming test. Psychopharmacol. Berl. 147, 162–167.
Rainer, Q., Nguyen, H.T., Quesseveur, G., Gardier, A.M., David, D.J., Guiard, B.P., 2012. Functional status of somatodendritic serotonin 1A autoreceptor after long-term treatment with fluoxetine in a mouse model of anxiety/depression based on repeated corticosterone administration. Mol. Pharmacol. 81, 106–112.
Razoux, F., Garcia, R., Lena, I., 2007. Ketamine, at a dose that disrupts motor behavior and latent inhibition, enhances prefrontal cortex synaptic efficacy and glutamate release in the nucleus accumbens. Neuropsychopharmacology 32, 719–727.
Reus, G.Z., Stringari, R.B., Ribeiro, K.F., Ferraro, A.K., Vitto, M.F., Cesconetto, P., Souza, C.T., Quevedo, J., 2011. Ketamine plus imipramine treatment induces antidepressant-like behavior and increases CREB and BDNF protein levels and PKA and PKC phosphorylation in rat brain. Behav. Brain Res. 221, 166–171.
Sanz-Clemente, A., Nicoll, R.A., Roche, K.W., 2013. Diversity in NMDA receptor composition: many regulators, many consequences. Neuroscientist 19, 62–75.
Szasz, B.K., Mike, A., Karoly, R., Gerevich, Z., Illes, P., Vizi, E.S., Kiss, J.P., 2007. Direct inhibitory effect of fluoxetine on N-methyl-D-aspartate receptors in the central nervous system. Biol. Psychiatry 62, 1303–1309.
Walf, A.A., Frye, C.A., 2007. The use of the elevated plus maze as an assay of anxiety-related behavior in rodents. Nat. Protoc. 2, 322–328.
Yamamoto, S., Ohba, H., Nishiyama, S., Harada, N., Kakiuchi, T., Tsukada, H., Domino, E.F., 2013. Subanesthetic doses of ketamine transiently decrease serotonin transporter activity: a PET study in conscious monkeys. Neuropsychopharmacology 38, 2666–2674.
Yang, C., Li, X., Wang, N., Xu, S., Yang, J., Zhou, Z., 2012. Tramadol reinforces antidepressant effects of ketamine with increased levels of brain-derived neurotrophic factor and tropomyosin-related kinase B in rat hippocampus. Front. Med. 6, 411–415.
Zanos, P., Piantadosi, S.C., Wu, H.Q., Pribut, H.J., Dell, M.J., Can, A., Snodgrass, H.R., Zarate Jr., C.A., Schwarcz, R., Gould, T.D., 2015. The prodrug 4-Chlorokynurenine causes ketamine-like antidepressant effects, but not side effects, by NMDA/GlycineB-site inhibition. J. Pharmacol. Exp. Ther. 355, 76–85.
Zhao, Y., Sun, L., 2008. Antidepressants modulate the in vitro inhibitory effects of propofol and ketamine on norepinephrine and serotonin transporter function. J. Clin. Neurosci. 15, 1264–1269.
Zhong, P., Yan, Z., 2011. Differential regulation of the excitability of prefrontal cortical fast-spiking interneurons and pyramidal neurons by serotonin and fluoxetine. PLoS One 6, e16970.

Ketamine treatment involves medial prefrontal cortex serotonin to induce a rapid antidepressant-like activity in BALB/cJ mice

T. H. Pham[a], I. Mendez-David[a], C. Defaix[a], B. P. Guiard[b], L. Tritschler[a], D. J. David[a], A. M. Gardier[a*]

[a] Université Paris-Saclay, Univ. Paris-Sud, Faculté de Pharmacie, INSERM UMR-S 1178, Chatenay Malabry, 92290, France

[b] UMR5169 CNRS « Centre de Recherches sur la Cognition Animale », Toulouse, 31062, France

* Corresponding author

Received 26 January 2016, Revised 9 May 2016, Accepted 15 May 2016, Available online 17 May 2016.

Supplemental data

Supplemental Table 1 : Extracellular 5-HT levels in the mPFCx and DRN of mice receiving acute ketamine 3 mg/kg, i.p. 24 hours prior to the test.

$[5\text{-HT}]_{ext}$	**mPFCx** *(fmol/sample)*	**DRN** *(fmol/sample)*
Vehicle	5.75 ± 0.35	14.27 ± 2.50
Ketamine 3 mg/kg, i.p.	5.07 ± 0.65	10.04 ± 1.17

Data are means ± S.E.M. of extracellular 5-HT levels. n = 4 - 6 mice per group.

5-HT: serotonin; mPFCx: medial prefrontal cortex; DRN: dorsal raphe nucleus.

Supplementary Table 2 : Complete statistical summary analysis for behavioral, microdialysis and electrophysiology data

Tests	Measurement	Statistical Test	Comparison	Statistics	Degrees of freedom	p	Fig.
Open Field	Time in the center	1-way ANOVA		F=11.22	3, 36	<0.0001***	1A
		PLSD Post-hoc test	Vehicle vs. Diazepam			0.0001 ***	
			Diazepam vs. Fluoxetine 18mg/kg (24h)			< 0.0001 ***	
			Diazepam vs. Ketamine 10 mg/kg (24h)			0.0035 **	
	Ambulatory distance	1-way ANOVA		F=3.855	3, 36	0.0172 *	1B
		PLSD Post-hoc test	Vehicle vs. Diazepam			0.0036 **	
			Vehicle vs. Ketamine 10 mg/kg (24h)			0.0188 *	
Elevated Plus Maze	Time in Open arms	1-way ANOVA		F=6.854	3, 36	0.0009 ***	1C
		PLSD Post-hoc test	Vehicle vs. Diazepam			<0.0001 ***	
			Diazepam vs. Fluoxetine 18mg/kg (24h)			0.0033 **	
			Diazepam vs. Ketamine 10 mg/kg (24h)			0.014 *	
	Entries in Open arms	1-way ANOVA		F=4.643	3, 36	0.0076 **	1D
		PLSD Post-hoc test	Vehicle vs. Diazepam			0.0009 ***	
			Diazepam vs. Ketamine 10 mg/kg (24h)			0.013 *	
Novelty Suppressed Feeding	Latency to feed	Kaplan-Meier Survival analysis				< 0.001 ***	1E
		1-way ANOVA		F=13.06	3, 41	<0.0001 ***	
		PLSD Post-hoc test	Vehicle vs. Diazepam			<0.0001 ***	
			Vehicle vs. Ketamine 10 mg/kg (24h)			0.0009 ***	
			Diazepam vs. Fluoxetine 18 mg/kg (24h)			<0.0001 ***	
			Diazepam vs. Ketamine 10 mg/kg (24h)			0.012 *	
			Fluoxetine 18 mg/kg (24h) vs Ketamine 10 mg/kg (24h)			0.015 *	
Splash Test	Grooming Duration	1-way ANOVA		F=5.232	3, 35	0.004 **	1G
		PLSD Post-hoc test	Vehicle vs. Ketamine 10 mg/kg (24h)			0.01 *	
			Diazepam vs. Ketamine 10 mg/kg (24h)			0.0014 **	
			Fluoxetine 18 mg/kg (24h) vs Ketamine 10 mg/kg (24h)			0.0016 **	
	Grooming Latency	1-way ANOVA		F=1.914	3, 36	ns	1H
		PLSD Post-hoc test	Diazepam vs. Ketamine 10 mg/kg (24h)			0.047 *	
			Fluoxetine 18 mg/kg (24h) vs Ketamine 10 mg/kg (24h)			0.049 *	
Forced Swim Test (systemic)	Immobility Duration	1-way ANOVA		F=3.800	2, 22	0.038 *	1I
		PLSD Post-hoc test	Vehicle vs. Ketamine 10 mg/kg (24h)			0.011 *	
Forced Swim Test (systemic)	Swimming Duration	1-way ANOVA		F=7.027	2, 21	0.0046 **	2B
		PLSD Post-hoc test	Vehicle vs. Ketamine 10 mg/kg (24h)			0.002 **	
			Fluoxetine 18 mg/kg (24h) vs Ketamine 10 mg/kg (24h)			0.018 *	
Microdialysis (systemic adm.)	mPFCx AUC $[5\text{-HT}]_{ext}$	1-way ANOVA		F=9.821	3, 29	0.0001 ***	2D
		PLSD Post-hoc test	Vehicle vs. Fluoxetine 18 mg/kg (24h)			0.0008 ***	
			Vehicle vs. Ketamine 10 mg/kg (24h)			0.041 *	
			Fluoxetine 18 mg/kg vs Ketamine 3 mg/kg (24h)			0.0007 ***	
			Ketamine 3 mg/kg vs Ketamine 10 mg/kg (24h)			0.023 *	
	DRN AUC $[5\text{-HT}]_{ext}$	1-way ANOVA		F=6.776	3, 16	0.0037 **	2F
		PLSD Post-hoc test	Vehicle vs. Fluoxetine 18 mg/kg			0.031 *	
			Fluoxetine 18 mg/kg vs Ketamine 3			0.0098 **	

			mg/kg (24h)				
			Fluoxetine 18 mg/kg vs Ketamine 10 mg/kg (24h)			0.005 **	
Electro-physiology (systemic adm.)	Firing rate of DR 5-HT neurons (Hz)	1-way ANOVA		F=14.76	2, 13	0.0005 ***	**2G**
		PLSD Post-hoc test	Vehicle vs. Ketamine 10 mg/kg (24h)			0.003 **	
			Vehicle vs. Fluoxetine 18 mg/kg (24h)			0.0015 **	
Microdialysis (Intra-mPFCx injection)	mPFCx AUC $[5\text{-HT}]_{ext}$	1-way ANOVA		F=6.36	2, 39	0.011 *	**4D**
		PLSD Post-hoc test	Vehicle vs. Fluoxetine 0.5 µg (24h)			ns	
			Vehicle vs. Ketamine 0.5 µg (24h)			<0.05 *	
			Ketamine 0.5 µg vs Fluoxetine 0.5 µg (24h)			<0.01 **	
Forced Swim Test (local)	Immobility Duration	1-way ANOVA		F=8.93	2, 20	<0.01 **	**4A**
		PLSD Post-hoc test	Vehicle vs. Fluoxetine 0.5 µg (24h)			ns	
			Vehicle vs. Ketamine 0.5 µg (24h)			0.017 *	
			Ketamine 0.5 µg vs Fluoxetine 0.5 µg (24h)			0.003 **	
	Swimming Duration	1-way ANOVA		F=8.93	2, 20	<0.01 **	**4B**
		PLSD Post-hoc test	Vehicle vs. Fluoxetine 0.5 µg (24h)			ns	
			Vehicle vs. Ketamine 0.5 µg (24h)			0.017 *	
			Ketamine 0.5 µg vs Fluoxetine 0.5 µg (24h)			0.003 **	
Linear regression	5-HT content correlated swimming duration	Slope significant non-zero					**4E**
			Ketamine	F=5.28	10	<0.009 **	
			Fluoxetine	F=7.75	8	<0.03 *	
Microdialysis (Intra-mPFCx injection)	mPFCx AUC $[5\text{-HT}]_{ext}$	2-way ANOVA	Factor 1- Pre- treatment	F=6.336	1, 27	<0.05 *	**5D**
			Factor 2- Treatment	F=6.678	1, 27	<0.05 *	
			Interaction (F1 x F2)	F=0.377	1, 27	=0.5	
		PLSD Post-hoc test	Veh/Veh vs Veh/Ket			<0.05 *	
			Veh/Veh vs NBQX/Veh			ns	
			Veh/Veh vs NBQX/Ket			ns	
			Veh/Ket vs NBQX/Veh			<0.01 **	
			Veh/Ket vs NBQX/Ket			<0.05 *	
			NBQX/Veh vs NBQX/Ket			ns	
Forced Swim Test (local)	Immobility Duration	2-way ANOVA	Factor 1- Pre- treatment	F=3.517	1, 13	=0.08	**5A**
			Factor 2- Treatment	F=0.699	1, 13	=0.4	
			Interaction (F1 x F2)	F=7.384	1, 13	<0.05 *	
		PLSD Post-hoc test	Veh/Veh vs Veh/Ket			<0.01 **	
			Veh/Veh vs NBQX/Veh			ns	
			Veh/Veh vs NBQX/Ket			ns	
			Veh/Ket vs NBQX/Veh			ns	
			Veh/Ket vs NBQX/Ket			<0.05 *	
			NBQX/Veh vs NBQX/Ket			ns	
	Swimming Duration	2-way ANOVA	Factor 1- Pre- treatment	F=3.517	1, 13	=0.08	**5B**
			Factor 2- Treatment	F=0.699	1, 13	=0.4	
			Interaction (F1 x F2)	F=7.384	1, 13	<0.05 *	
		PLSD Post-hoc test	Veh/Veh vs Veh/Ket			<0.01 **	
			Veh/Veh vs NBQX/Veh			ns	
			Veh/Veh vs NBQX/Ket			ns	
			Veh/Ket vs NBQX/Veh			ns	
			Veh/Ket vs NBQX/Ket			<0.05 *	
			NBQX/Veh vs NBQX/Ket			ns	

Supplemental Table 3 : Pre-treatment with PCPA decrease cortical tissue level of serotonin.

	Vehicle	PCPA
5-HT level (ng/mg of protein)	46.99 ± 5.74	9.81 ± 1.55 ***

Data are mean ± S.E.M
n = 18 animals per group
*** p<0.001 vs group Vehicle (t-student test)

Supplemental Figure S1 : Effect of a single systemic injection of ketamine on the sensibility and function of autoreceptor 5-HT$_{1A}$ 24 hours prior to the test.

(A) Effect of an acute administration of ketamine (10 mg/kg, i.p.) on the sensibility of autoreceptor 5-HT$_{1A}$ in the 8-OHDPAT-induced hypothermia paradigm. No significant differences were seen between vehicle and ketamine. Data are means ± S.E.M. of body temperature reduction (in ^{o}C) mesured every 10 minutes, with 4 basal mesurements before injection of 8-OHDPAT (0.3 ; 0.5 and 1.0 mg/kg, s.c.). n = 5 mice per group.

(B) Effect of a single administration of ketamine on the firing activity of DRN 5-HT neurons. Integrated firing histogram showing the effects of cumulative doses of ketamine (1-5 mg/kg; i.p.) in an anesthetized mouse on the spontaneous activity of 5-HT neurons in the DRN. At the end of the recording, the reversal effects of the 5-HT$_{1A}$ receptor antagonist WAY100635 (0.5-1.5 mg/kg; i.p.) on ketamine-induced inhibition of serotonergic firing rate was also studied. The dose of WAY100635 used herein is three times higher than that requires to reverse 8-OHDPAT-induced inhibition of serotonergic firing rate in mice (Rainer et al., 2012). In this firing rate histogram, the arrows indicate the compounds administered and the time at which the injection of the specified dose was completed. WAY100635 did not reverse ketamine-induced decrease in firing rate of DRN 5-HT neurons.

Figure S1

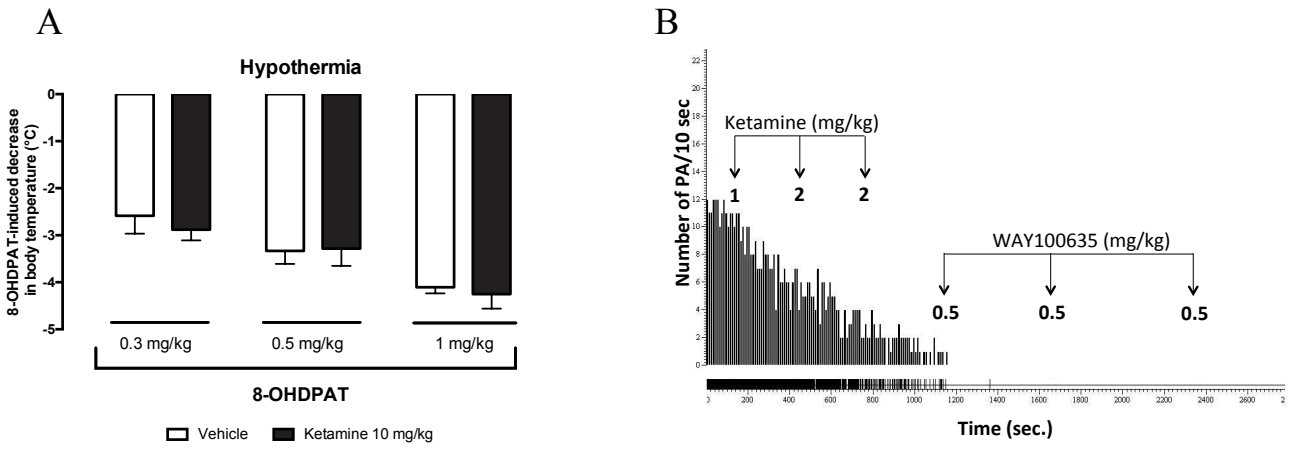

Commentaires sur l'Article 1 :

Cet article fournit une caractérisation complète des activités de type antidépresseur/anxiolytique de la kétamine chez des souris BALBc/J dans la condition expérimentale de notre laboratoire. Cette souche de souris avec son phénotype hyper-anxieux nous donne l'accès à des réponses comportementales et neurochimiques proches de celles d'un modèle de stress chez la souris.

La faible dose de 10 mg/kg, i.p. a été bien choisie d'après des études précédentes dans la littérature (Iijima *et al.*, 2012; Koike *et al.*, 2011; Li *et al.*, 2010; Zanos *et al.*, 2016). Notre travail donne un "plus" sur le sujet car toutes les expériences (la microdialyse et les tests comportementaux) ont été faites à 24 heures après l'administration aigue de la kétamine. En plus, la fluoxétine, un ISRS classique, était comparateur de la kétamine dans tous ces tests, donc nous donnant donc une vue plus précisée sur leur différence et leur similarité de mécanisme d'action. Le prétraitement de pCPA qui a déplété 80% de la 5-HT corticale, a aussi bloqué l'effet de la kétamine dans la nage forcée, soulignant une interaction entre le système sérotoninergique et sa réponse antidépressive.

Ici, nous sommes les premiers à mettre au point la combinaison de la microdialyse *in vivo* et la nage forcée chez la même souris. Ce couplage de deux techniques nous a permis de suivre les changements comportementaux de type antidépresseur et neurochimiques dans les deux régions étudiées (mPFC et NRD). De plus, nous avons réussi à trouver une corrélation positive entre ces deux paramètres sous l'effet de la kétamine, ce qui renforce notre hypothèse d'une interaction entre le système sérotoninergique et l'activité de type antidépresseur de la kétamine.

ARTICLE 2 : Common neurotransmission recruited in (*R,S*)-ketamine and (2*R*,6*R*)-hydroxynorketamine-induced sustained antidepressant-like effects

T.H. Pham, C. Defaix, X. Xu, S-X. Deng, D. Landry, R.A. Brachman, C.A. Denny, A.M. Gardier

Publié en Biological Psychiatry, 2017 Oct 26. pii: S0006-3223(17)32130-3.

doi: 10.1016/j.biopsych.2017.10.020

Schéma récapitulatif :

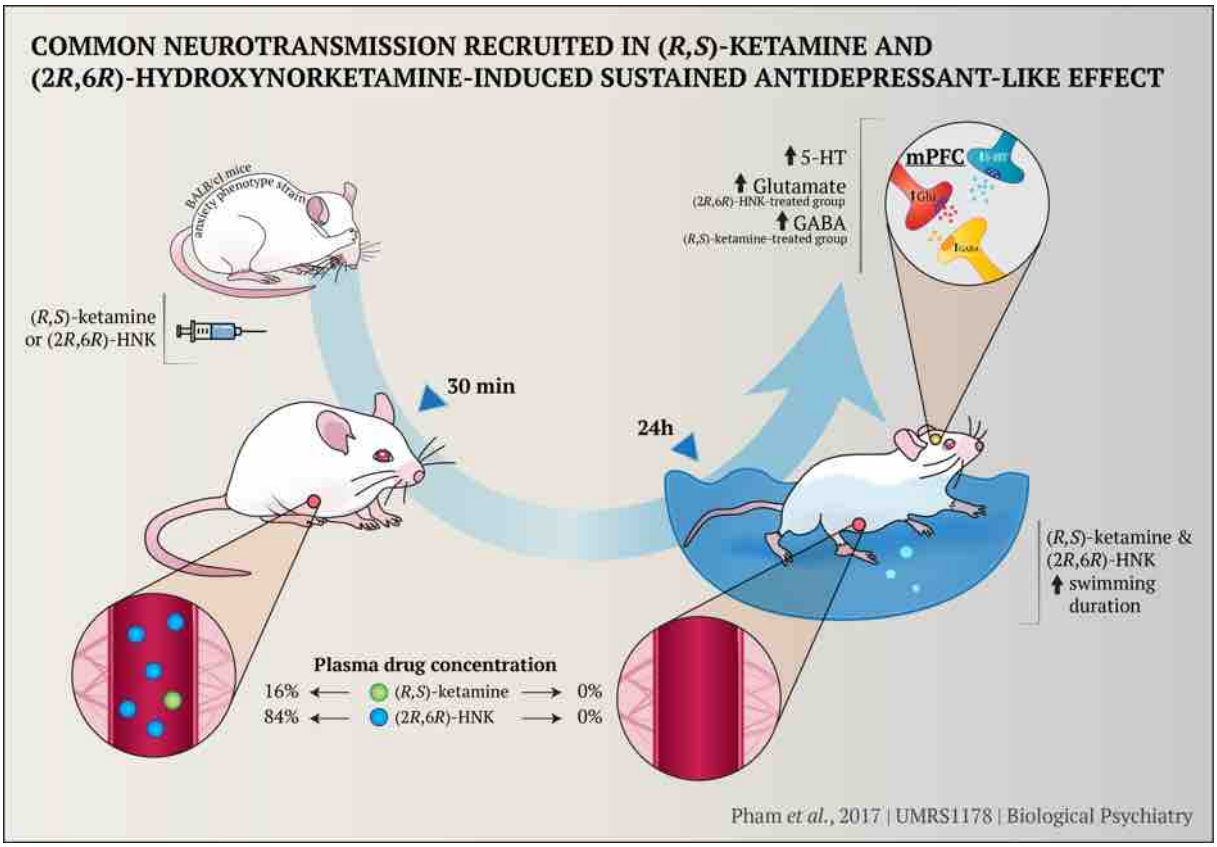

Question posée :

Est-ce que le (2*R*,6*R*)-hydroxynorkétamine, un des métabolites principaux du (*R,S*)-kétamine, possède un effet antidépresseur similaire à celui de sa molécule mère ?

Résumé de l'étude :

Racémique (*R,S*)-kétamine, un antagoniste du récepteur NMDA, présente une activité antidépressive rapide et persistante à des doses sous-anesthésiques chez les patients déprimés résistant aux traitements classiques et dans les études précliniques chez les rongeurs. Les mécanismes moléculaires et cellulaires impliqués dans ces activités sont inconnus. Nous avons précédemment rapporté que les augmentations induites par la (*R,S*)-kétamine de la libération présynaptique de la 5-HT dans le cortex préfrontal médian (mPFC) sont corrélées avec son activité antidépressive chez la souris. Cependant, la régulation de l'équilibre synaptique excitateur / inhibiteur et les modifications concomitantes de la neurotransmission du glutamate (Glu) / acide gamma-aminobutyrique (GABA) induites par la (*R,S*)-kétamine dans le mPFC des rongeurs ne sont pas claires.

Récemment, il a été montré que le métabolisme de la (*R,S*)-kétamine en (2*R*,6*R*)-hydroxynorkétamine (HNK) est essentiel pour son activité antidépressive, et implique une activation précoce de récepteur AMPA dans l'hippocampe et le mPFC de la souris. Cependant, la (*R*)-kétamine présente une plus grande puissance et des effets antidépresseurs plus durables que le (2*R*,6*R*)-HNK (Yang *et al.*, 2016).

Méthodes : Ici, nous avons comparé l'activité antidépressive soutenue et les changements de neurotransmetteurs entre la (*R,S*)-kétamine et le (2*R*,6*R*)-HNK chez les souris BALB/cJ, en utilisant le test de nage forcée (FST), prédictif des activités de type antidépresseur, couplé à la microdialyse *in vivo* chez les mêmes souris. Les niveaux extracellulaires corticaux de 5-HT, de GABA, de Glu et de glutamine ont été mesurés par HPLC couplée à un détecteur électrochimique ou à une spectrométrie de masse.

Résultats : Une dose unique de (*R,S*)-kétamine et de (2*R*,6*R*)-HNK (10 mg/kg, i.p., ou 1 nmol/côté, perfusée localement intra-mPFC) administrées 24 heures avant le test ont montré une activité antidépressive comparable dans le FST et les effets sérotoninergiques corticaux. De façon intéressante, le (2*R*,6*R*)-HNK a montré une activité plus glutamatergique que (*R,S*)-kétamine (+150% et +114 % vs véhicule, respectivement), tandis que la (*R,S*)-kétamine a augmenté plus de libération de GABA que le (2*R*,6*R*)-HNK (+63% et +35% vs véhicule, respectivement). Par ailleurs, la (*R,S*)-kétamine est métabolisée rapidement vers le (2*R*,6*R*)-HNK à 30 minutes post-injection et à 24 heures, les deux drogues n'existent plus dans le système.

En conclusion, nous avons trouvé que: (i) les deux drogues administrées à des doses équivalentes ont montré une activité antidépressive prolongée chez les souris et exercent indépendamment cette activité via le blocage de récepteur NMDA et l'activation de récepteur AMPA, respectivement; (ii) La libération corticale présynaptique de divers neurotransmetteurs excitateurs et inhibiteurs est nécessaire pour cette activité, ce qui peut avoir des conséquences durables; (iii) le (2*R*,6*R*)-HNK a augmenté la transmission synaptique excitatrice dans le mPFC en améliorant la libération présynaptique du Glu; et (iv) le (2*R*,6*R*)-HNK complète les effets neurochimiques de la (*R,S*)-kétamine dans le mPFC. Nous devons maintenant clarifier le mécanisme d'action de (*R,S*)-, (*R*)- ou (*S*)- kétamine et (2*R*,6*R*)-HNK en étudiant les événements cellulaires et moléculaires modulant leur activité dans le mPFC, et se concentrer sur les contrôles excitateurs / inhibiteurs descendants, par exemple, le circuit des mPFC / noyaux du raphé sur les neurones du mésencéphale. Par conséquent, il serait très intéressant de faire des comparaisons directes de ces composés dans de futures études cliniques chez des patients déprimés.

Contribution personnelle :

Au cours de travail :

- J'ai mené l'ensemble des tests de FST ainsi que le couplage de la microdialyse avec le FST chez les même souris. J'ai filmé toutes les vidéos de la nage puis le comptage du temps de nage a été validé par le Pr. Denis David.
- J'ai réalisé l'ensemble du zéro-net-flux, avec la participation du Dr. Céline Defaix pour le dosage de glutamate, GABA et glutamine.
- J'ai réalisé le suivi des animaux.
- J'ai analysé les résultats et rédigé l'intégralité de l'article sous la supervision du Pr. Alain Gardier.

Commentaires sur l'Article 2 :

Cet article donne des informations intéressantes sur le sujet d'actualité de la comparaison entre la (*R,S*)-kétamine et son métabolite (2*R*,6*R*)-HNK, à un moment où les résultats des études publiées, bien que très limités en nombre, sont controversés.

Ici, nous montrons pour la première fois des modifications neurochimiques de 5-HT, glutamate, GABA, glutamine et comportementale chez les même souris. Grâce à ces données, nous avons appris que le métabolite de (*R,S*)-kétamine est plus glutamatergique et moins GABAergique que sa molécule mère, même quand leurs effets sur la 5-HT sont comparables.

Notre étude est aussi la première à faire le zéro-net-flux pour étudier la fonction des transporteurs glutamatergiques chez la souris. Nous avons pu confirmer que l'augmentation de Glu_{ext} est due plus tôt à une stimulation de libération de glutamate qu'à une diminution de la recapture de glutamate par ces transporteurs.

Ces résultats confirment l'intérêt du (2*R*,6*R*)-HNK dans le domaine des traitements antidépresseurs et encouragent les études postérieures afin de mieux la comprendre.

Correspondence

Biological Psychiatry

Common Neurotransmission Recruited in (*R*,*S*)-Ketamine and (2*R*,6*R*)-Hydroxynorketamine–Induced Sustained Antidepressant-like Effects

To the Editor:

Racemic (*R*,*S*)-ketamine, an *N*-methyl-D-aspartate receptor (NMDAR) antagonist, exhibits a rapid and persistent antidepressant activity at subanesthetic doses in treatment-resistant depressed patients and in preclinical studies in rodents (1). (*R*,*S*)-ketamine also induces stress resilience (2). Molecular and cellular mechanisms mediating these activities are unknown. However, (*R*,*S*)-ketamine unlikely exerts its antidepressant-like activity solely via NMDAR blockade. We previously reported that (*R*,*S*)-ketamine-induced increases in presynaptic serotonin (5-hydroxytryptamine [5-HT]) release in the medial prefrontal cortex (mPFC) is correlated with its antidepressant-like activity in mice (3). The control exerted by the mPFC is important in regulating stress processing and in mediating antidepressant-like activity of both selective serotonin reuptake inhibitors and ketamine. However, regulation of synaptic excitatory/inhibitory balance and concomitant changes in glutamate (Glu)/gamma-aminobutyric acid (GABA) neurotransmission induced by (*R*,*S*)-ketamine in rodent mPFC are unclear (4).

Recently, Zanos *et al.* (5) reported that the metabolism of (*R*,*S*)-ketamine to (2*R*,6*R*)-hydroxynorketamine (HNK) is essential for the antidepressant-like activity and involves early activation of alpha-amino-3-hydroxy-5-methyl-4-isoxazole propionic acid receptor (AMPAR) in the mPFC and hippocampus. Conversely, Yang *et al.* (6) suggested that (*R*)-ketamine displays greater potency and longer-lasting antidepressant effects than (2*R*,6*R*)-HNK. However, brain regions and neurotransmitters supporting (2*R*,6*R*)-HNK effects are unknown. Here, we compared the sustained antidepressant-like activity and neurotransmitters' changes of (*R*,*S*)-ketamine and (2*R*,6*R*)-HNK in BALB/cJ mice (Janvier Labs, Le Genest-Saint-Isle, France) using the forced swim test (FST), a preclinical test to screen antidepressant-like activity of drugs (7), coupled to microdialysis. Cortical extracellular levels of 5-HT, GABA, Glu_{ext}, and glutamine (Gln_{ext}) were measured by high-pressure liquid chromatography coupled to either an electrochemical detector or mass spectrometry (3).

Male adult BALB/cJ mice, 9 to 12 weeks of age (body weight = 20 to 25 g; Janvier Labs, Le Genest-Saint-Isle, France) were used. This study was approved by the Institutional Animal Care and Use Committee in France (permission #92-196 to AMG). (*R*,*S*)-ketamine hydrochloride (Sigma-Aldrich, Saint-Quentin-Fallavier, France) and (2*R*,6*R*)-HNK hydrochloride (synthesized by the Organic Chemistry Collaborative Center, New York) were dissolved in vehicle before use. The data (mean ± SEM) were analyzed using one-way analysis of variance and Fisher's protected least-squares difference post hoc test.

(*R*,*S*)-ketamine, (2*R*,6*R*)-HNK (acute 10 mg/kg, intraperitoneal), or vehicle (NaCl, 0.9%) was administered 24 hours prior testing. On the next day (t24h), the FST was performed for 6 minutes during the 120 minutes of dialysate collection (Figure 1A). Similar to (*R*,*S*)-ketamine–elicited antidepressant-like effects at t24h as already reported (3), systemic (2*R*,6*R*)-HNK increased swimming duration (a serotonergic parameter) and extracellular levels of 5-HT in the mPFC (Figure 1B–D). Thirty minutes after its systemic administration, (2*R*,6*R*)-HNK plasma levels were five times higher than those of (*R*,*S*)-ketamine, but both drugs were no longer detected at t24h (Figure 1E), while they display a sustained antidepressant-like activity (8). These data agree with their pharmacokinetic parameters (9) and underline the presence of brain adaptive mechanisms.

To know whether the effects of (*R*,*S*)-ketamine and (2*R*,6*R*)-HNK in the mPFC were due to increases in Glu release and/or to changes in its reuptake, we performed the zero-net-flux method of quantitative microdialysis. The slope of zero-net-flux regression line is an in vivo estimate of Glu cellular uptake (10,11). (2*R*,6*R*)-HNK significantly increased basal Glu release (Figure 1F), while (*R*,*S*)-ketamine only trended to increase it (p = .09 vs. control mice). Glu uptake was not reduced by these two drugs because cortical slope/extracellular fraction of the probe did not change (Figure 1G and insert).

In a second cohort of mice, 1 nmol/side of (*R*,*S*)-ketamine or (2*R*,6*R*)-HNK or vehicle (cerebrospinal fluid) was perfused locally at 0.2 μL/min into the mPFC (bilateral) for 2 minutes. At t24h, both (*R*,*S*)-ketamine and (2*R*,6*R*)-HNK increased swimming duration and cortical extracellular levels of 5-HT (Figure 1H–J) and decreased Gln_{ext}/Glu_{ext} ratio in the mPFC (Figure 1K). (*R*,*S*)-ketamine, but not (2*R*,6*R*)-HNK, increased cortical extracellular levels of GABA (Figure 1L, M), while (2*R*,6*R*)-HNK increased Glu_{ext} (Figure 1N–O) versus vehicle-treated mice. (*R*,*S*)-ketamine only trended to increase area under the curve Glu_{ext} values (p = .13 vs. control mice).

Using ex vivo ^{1}H-[^{13}C]-nuclear magnetic resonance spectroscopy, changes in mPFC Glu/GABA/Gln cycling in rat brain tissues occurred 30 minutes, but not 24 hours post-injection of (*R*,*S*)-ketamine (from 1 to 80 mg/kg, intraperitoneal) (12). The nuclear magnetic resonance technique measures the Glu/GABA-Gln cycling, used as marker of glial and neuronal metabolism, whereas in vivo microdialysis can measure a Gln_{ext}/Glu_{ext} ratio following their neuronal/glial release and/or reuptake.

Our data suggest that (2*R*,6*R*)-HNK contributes to the neurochemical and behavioral effects of (*R*,*S*)-ketamine. (2*R*,6*R*)-HNK is the major active metabolite found in the plasma and brain of mice after (*R*,*S*)-ketamine administration (5). Brain tissue concentration of (2*R*,6*R*)-HNK was about 25% of that of (*R*,*S*)-ketamine (9). Unlike (*R*,*S*)-ketamine, (2*R*,6*R*)-HNK does not bind to NMDAR at antidepressant-relevant concentrations (13), but rather increases mPFC glutamatergic AMPAR activity. Here, activation of the mPFC results in an excitatory effect and increased Glu release by pyramidal cells (Figure 1F, N, O), without affecting its reuptake (Figure 1G): various 5-HT receptor subtypes on pyramidal neurons and GABA interneurons are known to modulate mPFC neuronal activity (14,15). This mechanism can, at least partially, support

https://doi.org/10.1016/j.biopsych.2017.10.020
ISSN: 0006-3223

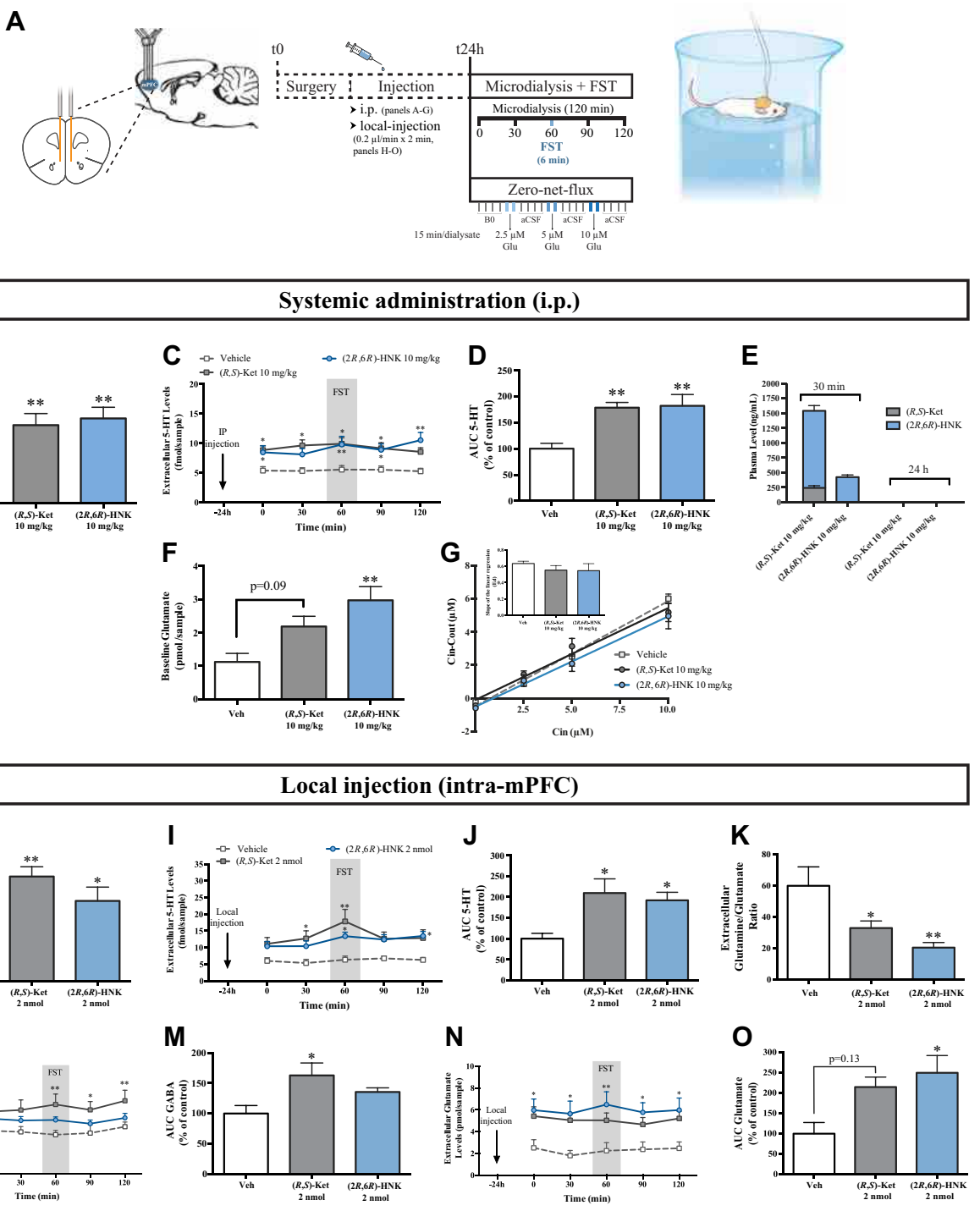

Figure 1. (2*R*,6*R*)-hydroxynorketamine (HNK) and (*R*,*S*)-ketamine (Ket) display sustained antidepressant-like activity. **(A)** Experimental protocol: the surgery and drugs administration (either intraperitoneal [i.p.] or locally into the medial prefrontal cortex [intra-mPFC]) were carried out 24 hours before testing. On the next day (t24h), the microdialysis coupled to the forced swim test (FST) was performed in the same mice. Samples were collected from the right and left cortex in each mouse for 120 minutes, i.e., before, during, and after the FST. Swimming duration was scored for the last 4 minutes of the 6-minute testing period. Systemic administration of vehicle (Veh), (*R*,*S*)-Ket, or (2*R*,6*R*)-HNK. **(B)** Similar to (*R*,*S*)-Ket, (2*R*,6*R*)-HNK increased the swimming duration in the FST ($F_{2,27}$ = 11.72, p = .0002; n = 10 mice per group). **(C)** Time course of drug effects on mPFC extracellular levels of 5-hydroxytryptamine (5-HT_{ext}): (*R*,*S*)-Ket and (2*R*,6*R*)-HNK increased cortical 5-HT_{ext} (in fmol/sample) vs. Veh-treated mice ($F_{2,264}$ = 22.64, $p < .0001$). The gray area indicates the duration of the FST. **(D)** (*R*,*S*)-Ket and (2*R*,6*R*)-HNK increased cortical 5-HT_{ext} (area under the curve [AUC] values as percentages of Veh group) ($F_{2,52}$ = 8.39, p = .0007). **(E)** Plasma levels of (*R*,*S*)-Ket and (2*R*,6*R*)-HNK were measured at two different time points, 30 minutes and 24 h after their systemic acute administration. (*R*,*S*)-Ket was quickly

(2*R*,6*R*)-HNK antidepressant-like activity. It should result in potentiation of excitatory neurotransmission in the mPFC, but (2*R*,6*R*)-HNK decreased Gln_{ext} and increased Glu_{ext}, thus leading to a decrease in Gln_{ext}/Glu_{ext} ratio. In agreement with these data, an increased cerebrospinal fluid Gln/Glu ratio was found in depressed patients, suggesting abnormalities in the glia-neuron communication in the brains of these subjects (16).

Consistent with the effects of AMPAR antagonists (3), our data suggest that AMPAR activation is required for ketamine's effects. We used the BALB/cJ strain of mice for its baseline anxiety phenotype (7), while Yang *et al.* (6) used a C57 strain. Behavioral effects may be mouse strain dependent because of regional differences in neurotransmitter metabolism across strains that have been previously described (17). (2*R*,6*R*)-HNK effects on mPFC Glu release by pyramidal neurons together with those of (*R*,*S*)-ketamine on cortical GABA release by interneurons led to a sustained antidepressant-like activity. Chronic stress yielding a depressed phenotype decreased brain tissue GABA levels, and a subanesthetic dose of (*R*,*S*)-ketamine normalized these changes (18). Furthermore, major depression is associated with low plasma and cerebrospinal fluid GABA concentrations and an increase in cortical GABA concentrations after selective serotonin reuptake inhibitor treatment of depressed patients (19).

In conclusion, this analysis of excitatory/inhibitory neurotransmitters' response to (*R*,*S*)-ketamine and its metabolites paves the way for further studies to decipher the molecular and cellular mechanisms underlying their sustained antidepressant-like activity, as new data suggest that (2*R*,6*R*)-HNK is an open-channel blocker of NMDAR (20).

Thu Ha Pham
Céline Defaix
Xiaoming Xu
Shi-Xian Deng
Nicolas Fabresse
Jean-Claude Alvarez
Donald W. Landry
Rebecca A. Brachman
Christine A. Denny
Alain M. Gardier

Acknowledgments and Disclosures

This work was supported by Université Paris-Sud (THP, AMG), INSERM (AMG), and Université Paris-Saclay (AMG); National Institutes of Health Grant No. DP5 OD017908-01 (to CAD); New York State Stem Cell Science Grant No. C-021957 (to CAD), and a NARSAD Young Investigator Grant from the Brain & Behavior Research Foundation, P&S Investigator (to CAD).

We would like to thank Laurent Tritschler, Jean-Philippe Guilloux, Indira Mendez-David, and Denis J. David for helpful discussions on the manuscript.

RAB and CAD are named on a nonprovisional patent application for the prophylactic use of ketamine against stress-related psychiatric disorders. All other authors report no biomedical financial interests or potential conflicts of interest.

Article Information

From the CESP/UMR-S 1178 (THP, CD, AMG), Université Paris-Sud, Faculté de Pharmacie, INSERM, Université Paris-Saclay, Châtenay Malabry; and Laboratoire de Pharmacologie-Toxicologie (NF, J-CA), Centre Hospitalier Universitaire Raymond Poincaré, AP-HP, Garches, France; and the Department of Medicine (XX, S-XD, DWL); Organic Chemistry Collaborative Center (XX, S-XD, DWL), Department of Medicine; and Department of Psychiatry (RAB, CAD), Columbia University; and Division of Integrative Neuroscience (CAD), Research Foundation for Mental Hygiene, Inc/New York State Psychiatric Institute, New York, New York.

CAD and AMG contributed equally to this work.

Address correspondence to Alain M. Gardier, Pharm.D., Ph.D., Laboratoire de Neuropharmacologie, CESP/UMR-S 1178 "Depression, Plasticity and Resistance to Antidepressant Drugs," Inserm, Univ. Paris-Sud, Fac. Pharmacie, 5 Rue J-B Clement, Tour D1, 2e etage, F-92296 Chatenay Malabry cedex, France; E-mail: alain.gardier@u-psud.fr.

Received Mar 9, 2017; revised Oct 14, 2017; accepted Oct 17, 2017.

References

1. Duman RS, Aghajanian GK, Sanacora G, Krystal JH (2016): Synaptic plasticity and depression: New insights from stress and rapid-acting antidepressants. Nat Med 22:238–249.
2. Brachman RA, McGowan JC, Perusini JN, Lim SC, Pham TH, Faye C, *et al.* (2016): Ketamine as a prophylactic against stress-induced depressive-like behavior. Biol Psychiatry 79:776–786.
3. Pham TH, Mendez-David I, Defaix C, Guiard BP, Tritschler L, David DJ, *et al.* (2017): Ketamine treatment involves medial prefrontal cortex serotonin to induce a rapid antidepressant-like activity in BALB/cJ mice. Neuropharmacology 112:198–209.

metabolized to (2*R*,6*R*)-HNK 30 minutes after its administration, but at t24h, plasma levels of both drugs were below the detection limit, thus no longer existing in the body of these mice (n = 10 mice per group). The zero-net-flux (ZNF) method of quantitative microdialysis measuring basal glutamate (Glu) dynamics [see (21) for the details of this experiment]. Briefly, the mPFC was perfused with increasing concentrations of Glu (0, 2.5, 5, and 10 μM) at 24-hour postsystemic administration of (*R*,*S*)-Ket and (2*R*,6*R*)-HNK [panel **(A)**]. **(F)** Values of basal extracellular levels of Glu (Glu_{ext}) (y-intercept), mean ± SEM of n = 5–6 mice per group. $^{**}p < .01$ compared with Veh using one-way analysis of variance ($F_{2,14} = 8.2$, $p = .004$) followed by a Bonferroni post hoc test. **(G and insert)** The dialysate Glu levels (Cout) obtained during perfusion of various micromolar (μM) Glu concentrations (Cin). The net change in Glu (Cin–Cout) was plotted on the y axis against Cin on the x axis. Slope of linear regression corresponds to the extracellular fraction of the probe (E_d). Basal Glu_{ext}, mean ± SEM for n = 5–6 mice per group. No differences were observed between the three groups studied regarding mean ± SEM of slope/E_d (one-way analysis of variance [$F_{2,14} = 0.73$, p = .5]). Local bilateral intra-mPFC injection of Veh, (*R*,*S*)-Ket, or (2*R*,6*R*)-HNK (n = 4, 6, and 8 mice, respectively). **(H)** (*R*,*S*)-Ket and (2*R*,6*R*)-HNK reproduced their systemic effects on swimming duration in the FST vs. Veh-treated mice ($F_{2,15} = 7.937$, $p = .0045$). **(I)** Time course of drugs effects on mPFC 5-HT_{ext}: (*R*,*S*)-Ket and (2*R*,6*R*)-HNK increased cortical 5-HT_{ext} (in fmol/sample) vs. Veh-treated mice ($F_{2,98} = 20.79$, $p < .001$). **(J)** (*R*,*S*)-Ket and (2*R*,6*R*)-HNK increased cortical AUC 5-HT_{ext} values vs. Veh-treated mice ($F_{2,21} = 5.472$, $p = .012$). **(K)** Ratio of mPFC extracellular glutamine/Glu levels as the ratio of AUC values at t24h in both groups ($F_{2,21} = 10.19$, $p = .0008$). The ratio was decreased in both groups, but to a lesser extent in the (*R*,*S*)-Ket group compared with the (2*R*,6*R*)-HNK group. **(L)** Time course of drugs effects on mPFC extracellular levels of gamma-aminobutyric acid (GABA): (*R*,*S*)-Ket, but not (2*R*,6*R*)-HNK, increased cortical extracellular levels of GABA (in fmol/sample) vs. Veh-treated mice ($F_{2,130} = 17.95$, $p < .001$). **(M)** (*R*,*S*)-Ket increased cortical AUC extracellular levels of GABA values vs. Veh-treated mice ($F_{2,26} = 4.527$, $p = .02$). **(N)** Time course of drugs effects on mPFC Glu_{ext}: (2*R*,6*R*)-HNK, but not (*R*,*S*)-Ket, increased cortical Glu_{ext} (in pmol/sample) vs. Veh-treated mice ($F_{2,108} = 18.66$, $p < .001$). **(O)** (2*R*,6*R*)-HNK increased cortical AUC Glu_{ext} values vs. Veh-treated mice ($F_{2,22} = 5.683$, $p = .0102$). $^{*}p < .05$; $^{**}p < .01$ vs. Veh-treated group. Data are shown as mean ± SEM (n = 4–8 mice per group). AUC values (% of the corresponding control group) were calculated as the amount of neurotransmitter outflow for the 0- to 120-minute period of samples collection. aCSF, artificial cerebrospinal fluid.

4. Moghaddam B, Adams B, Verma A, Daly D (1997): Activation of glutamatergic neurotransmission by ketamine: A novel step in the pathway from NMDA receptor blockade to dopaminergic and cognitive disruptions associated with the prefrontal cortex. J Neurosci 17: 2921–2927.
5. Zanos P, Moaddel R, Morris PJ, Georgiou P, Fischell J, Elmer GI, *et al.* (2016): NMDAR inhibition-independent antidepressant actions of ketamine metabolites. Nature 533:481–486.
6. Yang C, Qu Y, Abe M, Nozawa D, Chaki S, Hashimoto K (2017): (R)-ketamine shows greater potency and longer lasting antidepressant effects than its metabolite (2R,6R)-hydroxynorketamine. Biological Psychiatry 82:e43–e44.
7. Dulawa SC, Holick KA, Gundersen B, Hen R (2004): Effects of chronic fluoxetine in animal models of anxiety and depression. Neuropsychopharmacology 29:1321–1330.
8. Abe E, Ricard F, Darrouzain F, Alvarez JC (2013): An automated method for measurement of methoxetamine in human plasma by use of turbulent flow on-line extraction coupled with liquid chromatography and mass spectrometric detection. Anal Bioanal Chem 405:239–245.
9. Can A, Zanos P, Moaddel R, Kang KJ, Dossou KS, Wainer IW, *et al.* (2016): Effects of ketamine and ketamine metabolites on evoked striatal dopamine release, dopamine receptors, and monoamine transporters. J Pharmacol Exp Ther 359:159–170.
10. Gardier AM, David DJ, Jego G, Przybylski C, Jacquot C, Durier S, *et al.* (2003): Effects of chronic paroxetine treatment on dialysate serotonin in 5-HT1B receptor knockout mice. J Neurochem 86:13–24.
11. Deltheil T, Guiard BP, Cerdan J, David DJ, Tanaka KF, Reperant C, *et al.* (2008): Behavioral and serotonergic consequences of decreasing or increasing hippocampus brain-derived neurotrophic factor protein levels in mice. Neuropharmacology 55:1006–1014.
12. Chowdhury GM, Zhang J, Thomas M, Banasr M, Ma X, Pittman B, *et al.* (2017): Transiently increased glutamate cycling in rat PFC is associated with rapid onset of antidepressant-like effects. Mol Psychiatry 22:120–126.
13. Gould TD, Zanos P, Zarate CA Jr (2017): Ketamine mechanism of action: Separating the wheat from the chaff. Neuropsychopharmacology 42:368–369.
14. Mendez-David I, David DJ, Darcet F, Wu MV, Kerdine-Romer S, Gardier AM, *et al.* (2014): Rapid anxiolytic effects of a 5-HT(4) receptor agonist are mediated by a neurogenesis-independent mechanism. Neuropsychopharmacology 39:1366–1378.
15. Artigas F (2015): Developments in the field of antidepressants, where do we go now? Eur Neuropsychopharmacol 25:657–670.
16. Hashimoto K, Bruno D, Nierenberg J, Marmar CR, Zetterberg H, Blennow K, *et al.* (2016): Abnormality in glutamine-glutamate cycle in the cerebrospinal fluid of cognitively intact elderly individuals with major depressive disorder: A 3-year follow-up study. Transl Psychiatry 6:e744.
17. Calcagno E, Canetta A, Guzzetti S, Cervo L, Invernizzi RW (2007): Strain differences in basal and post-citalopram extracellular 5-HT in the mouse medial prefrontal cortex and dorsal hippocampus: Relation with tryptophan hydroxylase-2 activity. J Neurochem 103:1111–1120.
18. Perrine SA, Ghoddoussi F, Michaels MS, Sheikh IS, McKelvey G, Galloway MP (2014): Ketamine reverses stress-induced depression-like behavior and increased GABA levels in the anterior cingulate: An 11.7 T 1H-MRS study in rats. Prog Neuropsychopharmacol Biol Psychiatry 51:9–15.
19. Sanacora G, Mason GF, Rothman DL, Krystal JH (2002): Increased occipital cortex GABA concentrations in depressed patients after therapy with selective serotonin reuptake inhibitors. Am J Psychiatry 159:663–665.
20. Suzuki K, Nosyreva E, Hunt KW, Kavalali ET, Monteggia LM (2017): Effects of a ketamine metabolite on synaptic NMDAR function. Nature 546:E1–E3.
21. Miller BR, Dorner JL, Shou M, Sari Y, Barton SJ, Sengelaub DR, *et al.* (2008): Up-regulation of GLT1 expression increases glutamate uptake and attenuates the Huntington's disease phenotype in the R6/2 mouse. Neuroscience 153:329–337.

ARTICLE 3 : *Role of cortical and raphe $GABA_A$ and AMPA receptors in ketamine-induced fast antidepressant-like activity*

Type of paper: Research article

Title: Role of cortical and raphe $GABA_A$ and AMPA receptors in ketamine-induced fast antidepressant-like activity

(In preparation)

Thu Ha Pham, Céline Defaix, Laurent Tritschler, Denis J David and Alain M. Gardier

CESP/UMR-S 1178, Univ. Paris-Sud, Fac. Pharmacie, Inserm, Université Paris-Saclay, Chatenay Malabry, 92290, France.

Corresponding author:

Pr. Alain M. GARDIER

Laboratoire de Neuropharmacologie

CESP/UMR-S 1178, Univ. Paris-Sud, Fac Pharmacie, Inserm, Université Paris-Saclay

5, rue J-B Clement, Tour D1, 2e etage, F-92296 Chatenay Malabry cedex

tel: (33) 1 46 83 54 16

E-mail: alain.gardier@u-psud.fr

Abstract

Unlike classic serotonergic antidepressant drugs, ketamine, an NMDA receptor antagonist, exhibits a rapid and persistent antidepressant (AD) activity, at sub-anaesthetic doses in treatment-resistant depressed (TRD) patients and in preclinical studies in rodents. However, the initial targets by which ketamine produces glutamate bursts that triggers its fast antidepressant-like activity remain unclear.

Comorbid depression and anxiety disorders often occur in chronic diseases such as neuropathic pain. In addition, a number of GABAergic (benzodiazepines, BZD) and anti-glutamatergic treatments are used as adjunctive therapy in TRD. Is it appropriate? Such information is critical to establish efficacy or treatment restrictions to maximize clinical translation from animal models to TRD patients, effectiveness and safety.

Here, we assessed the specific role of excitatory and inhibitory neurotransmission in the PFC-DRN circuit in the sustained antidepressant-like activity of a sub-anaesthetic ketamine dose, i.e., 24 hours post-administration.

We administered an AMPA-R antagonist (intra-DRN), a $GABA_A$-R agonist (intra-mPFC) or antagonist (intra-DRN) or a selective glutamate transporter GLT-1 inhibitor before ketamine to study behavioral (the FST) and neurochemical consequences on extracellular levels of glutamate, GABA and 5-HT (Glu_{ext}, $GABA_{ext}$, and $5\text{-}HT_{ext}$, respectively) in the mPFC in BALB/cJ mice.

We found:

- intra-DRN NBQX prevented the effects of intra-mPFC ketamine injection in the FST and blunted its effects on mPFC $5\text{-}HT_{ext}$ and Glu_{ext} but not on cortical $GABA_{ext}$.

- intra-mPFC muscimol completely blocked ketamine antidepressant-like activity and its effects on cortical $5\text{-}HT_{ext}$, but had no effects on ketamine-induced increase in cortical Glu_{ext} and $GABA_{ext}$.

- intra-DRN bicuculline did not enhance ketamine effects but blocked ketamine-induced increase in cortical $GABA_{ext}$.

Interestingly, we found that antidepressant activity only occurred with a concomitant increase of Glu_{ext} and $5\text{-}HT_{ext}$ or of all neurotransmitters Glu_{ext}, $5\text{-}HT_{ext}$ and $GABA_{ext}$. However, the excitation-inhibition balance remained constant, highlighting the role of neuronal adaptation in these effects. The results of the present study contribute to a further understanding of the cellular mechanisms underlying ketamine antidepressant-like activity.

1. Introduction

Ketamine, a non-competitive antagonist of the N-methyl-D-aspartate receptor of glutamate (NMDA-R) elicited an antidepressant efficacy in treatment-resistant depression (TRD) (Berman *et al.*, 2000; Zarate *et al.*, 2006). Since this discovery, ketamine has been continuously demonstrating its efficacy in multiple randomized clinical trials (see meta-analysis reviews: Caddy *et al.*, 2014; Fond *et al.*, 2014; Newport *et al.*, 2015; Xu *et al.*, 2016). The search for a new treatment of TRD is important because ≈30% of depressed patients are classified as affected by refractory depression (Rush *et al.*, 2006). Furthermore, the delayed onset of action of classical antidepressant drugs (i.e., 4 to 6 weeks for selective serotonin reuptake inhibitor, SSRI) makes the rapid ketamine action (less than 24h in human and animals) of great value, but we need more details about its mechanism of action.

Comorbid depression and anxiety disorders occur in up to 25% of patients (Tiller, 2013). For example, chronic neuropathic pain often leads to anxiety and depression disorders (Sellmeijer *et al.*, 2018). Both disorders require appropriate treatment, e.g., an antidepressant drug for depression, and a benzodiazepine (BZD) for anxiety. In addition, a number of GABAergic (BZD) and anti-glutamatergic treatments are used as adjunctive therapy in TRD (Frye *et al.*, 2015). Thus, it is especially important to know whether or not we can associate ketamine and a BZD (an agonist of $GABA_A$ receptor – $GABA_A$-R). It was recently shown that concomitant BZD use attenuated ketamine response (Frye *et al.*, 2015). Such information is critical to establish efficacy or treatment restrictions to maximize clinical translation from animal models to TRD patients, effectiveness and safety.

Preclinical models, mostly rodents, contribute robustly to study ketamine's mechanism of action (reviewed by Pham *et al*., 2018, submitted). The medial prefrontal cortex (mPFC) plays a key role in ketamine's pharmacological effects, because NMDA-R, the main target with highest affinity to ketamine (F. Murray *et al.*, 2000), is widely expressed in this brain region (Kamiyama *et al.*, 2011; Sanz-Clemente *et al.*, 2013). Artigas's group demonstrated that 5-HT release in the mPFC depends on the excitatory glutamatergic transmission (Lopez-Gil *et al.*, 2012). Moreover, it has been shown that mPFC projections to the dorsal raphe nucleus (DRN) control stressful behaviour (Amat *et al.*, 2016). Ketamine in the mPFC triggers a cascade of neuronal adaptation involving the mammalian target of rapamycin (mTOR) pathway and induction of synaptogenesis, in an α-amino-3-hyroxy-5-methyl-4-isoxazolepropionic-acid-receptor-(AMPA-R)-dependent manner (Duman *et al.*,

2016; Li *et al.*, 2010). Furthermore, recent evidences have confirmed that ketamine requires an activation of AMPA-R to exert its antidepressant-like activity since NBQX, an AMPA-R antagonist, blocked ketamine antidepressant-like activity in rodents (Koike & Chaki, 2014; Koike *et al.*, 2011; Li *et al.*, 2010; Li *et al.*, 2011; Maeng *et al.*, 2008; Pham *et al.*, 2017b). However, the initial targets by which ketamine produces glutamate bursts that triggers its fast antidepressant-like activity remain unclear (Fuchikami *et al.*, 2015).

We recently described a positive correlation between mPFC 5-HT neurotransmission and ketamine-induced antidepressant-like activity in the forced swim test (FST, a serotonin-dependent test that predicts the antidepressant drug response in rodents (Pham *et al.*, 2017a; Pham *et al.*, 2017b). However, the origin of this increase in extracellular 5-HT levels still remains questionable. The cell bodies of 5-HT neurons are located in the DRN, a region receiving dense glutamatergic projections from the mPFC (Aghajanian & Marek, 1997; Hajos *et al.*, 1998; Peyron *et al.*, 1998). Since systemic administration of ketamine also increased c-Fos immunoreactivity in DRN 5-HT neurons, which were blocked by NBQX microinjection into the mPFC (Fukumoto *et al.*, 2016), the activation of these neurons modulated by the mPFC could contribute to ketamine mechanism of action. Still, information about the influence of the mPFC on the firing activity of DRN 5-HT neurones and *vice versa* in ketamine-induced antidepressant-like activities are missing.

Thus, we examined the behavioral and neurochemical effects of ketamine in experiments coupling microdialysis and FST in BALBc/J mice. In a pharmacological approach, we used a pre-treatment with AMPA-R antagonist (intra-DRN NBQX: 0.25 nmol according to Lopez-Gil *et al.*, 2007; Fukumoto *et al.*, 2016), $GABA_A$-R agonist (intra-mPFC muscimol: 8 nmol (or 1 µg) according to Amat *et al.*, 2016) or antagonist (intra-DRN bicuculline: 0.25 nmol according to Carreno *et al.*, 2016) administered 30 min before ketamine to study the specific role of excitatory and inhibitory neurotransmission in this circuit. The influence of these pre-treatments on extracellular levels of glutamate, GABA and 5-HT (Glu_{ext}, $GABA_{ext}$, and $5\text{-}HT_{ext}$, respectively) in the mPFC could bring more insights about the origin of each neurotransmitter modification. We also investigated neurochemical and behavioral consequences of glutamate transporter GLT-1 (or EAAT2) blockade after intra-mPFC perfusion of dihydrokainic acic (DHK), a selective inhibitor of GLT-1, present in astrocytes (Gasull-Camos *et al.*, 2017).

2. Materials and methods

2.1. Animals

Male BALB/cJ mice (9-12-weeks old) weighing 23-25g at the beginning of the experiments were purchased from Janvier Labs (Le Genest-Saint-Isle). The BALB/cJ strain of mice was chosen for its highly anxious phenotype (Dulawa *et al.*, 2004; Holick *et al.*, 2008). They were housed in groups of four in a temperature (21 ± 1°C) controlled room with a 12 h light: 12 h dark cycle (lights on at 06:00 h). Food and water were available *ad libitum* except during behavioral observations. Particular efforts were made to minimize the number of mice used in the experiments. Protocols were approved by the Institutional Animal Care and Use Committee in France (Council directive # 87-848, October 19, 1987, "Ministère de l'Agriculture et de la Forêt, Service Vétérinaire de la Santé et de la Protection Animale, permissions # 92-196" to A.M.G.) as well as with the European directive 2010/63/EU.

2.2. Drugs and treatments

Ketamine 10 mg/kg purchased from Sigma-Aldrich (Saint-Quentin Fallavier, France) were dissolved in vehicle (NaCl 0.9%) and administered intraperitoneally (i.p.) for optogenetic study or 2 nmol dissolved in artificial cerebrospinal fluid (aCSF) for pharmaclogic study at 24 h prior to the behavioral tests. Drug doses and pre-treatment times were based on previous studies performed in the literature for ketamine (Iijima *et al.*, 2012; Koike *et al.*, 2013; Li *et al.*, 2010; Liu *et al.*, 2012; Zanos *et al.*, 2015).

First, we performed an experiment using intra-DRN injection of NBQX, an AMPA-R antagonist at 0.25 nmol (NBQX disodium salt purchased from Tocris Bioscience, Lille, France). This dose was chosen based on previous studies in rodents (Lopez-Gil *et al.*, 2007; Fukumoto *et al.*, 2016). Second, we performed an experiment using intra-mPFC injection of muscimol (Sigma-Aldrich, Saint-Quentin Fallavier, France), a $GABA_A$-R agonist at 8 nmol (or 1 µg) according to Amat *et al.*, 2016). Third, bicuculline methochloride (Tocris Bioscience, Lille, France), a $GABA_A$-R antagonist, was injected intra-DRN at 0.25 nmol according to Carreno *et al.*, 2016). NBQX, bicuculline and muscimol were injected 30 min before a bilateral intra-mPFC ketamine injection (2 nmol: Pham *et al.*, 2017). Then, dialysate samples were collected in the mPFC 24 hours after (at t24h). Lastly, dihyrokainic acid (DHK, Tocris Bioscience, Lille, France), an inhibitor of GLT-1 glutamatergic transporter, was dissolved in the aCSF and perfused continuously at 5 mM for 2.5 hours according to Gasull-Camos *et al.*, 2017.

The swimming duration in the FST was measured in these mice when mPFC dialysates were collected as shown in protocols (Figure 1A – 3A).

2.3. Forced Swim Test (FST)

The mouse forced swim test procedure (FST) is one of the most useful tools for antidepressants screening. Swimming, climbing and immobility behaviors were distinguished from each other according to the procedure previously described (Dulawa *et al.*, 2004; Holick *et al.*, 2008). Swimming behavior relies on the serotonergic system, and climbing behavior on the noradrenergic system in mouse (Holick *et al.*, 2008). Mice were placed individually into glass cylinders (height: 25 cm, diameter: 10cm) containing 18 cm water, maintained at 23-25°C for 6 min. The predominant behavior (immobility, swimming) was scored for the last 4 min of the 6 min testing period manually by the experimenter (Pham et al., 2017).

2.4. Intracerebral in vivo microdialysis

Each mouse was anesthetized with chloral hydrate (400 mg/kg, i.p.) and implanted with two microdialysis probes (CMA7 model, Carnegie Medicine, Stockholm, Sweden) located in the medial prefrontal cortex (mPFC) and one microdialysis probe in the dorsal raphe nucleus (DRN). Stereotaxic coordinates in mm from bregma: mPFC : A= + 2.2, L= ± 0.2, V= - 3.4). On the same day, after awakening, mice received an acute dose of NBQX, muscimol or bicuculline at 30 min before a ketamine dose, or their vehicle intracerebrally for pharmacologic study. On the next day, ≈ 24h after ketamine administration, the probes were continuously perfused with aCSF (composition in mmol/L: NaCl 147, KCl 3.5, $CaCl_2$ 2.26, NaH_2PO_4 1.0, pH 7.4 ± 0.2) at a flow rate of 1.0 µl/min through the mPFC using CMA/100 pump (Carnegie Medicine, Stockholm, Sweden), while animals were awake and freely moving in their cage. One hour after the start of aCSF perfusion stabilization period, four fractions were collected (one every 25 min) to measure the basal 5-HT_{ext} levels in the mPFC by using a high-performance liquid chromatography (HPLC) system (column Ultremex 3µ C18, 75 X 4.60 mm, particle size 3 µm, Phenomenex, Torrance, CA) coupled to an amperometric detector (VT03; Antec Leyden, The Netherlands). In parallel, the basal Glu_{ext}, $GABA_{ext}$, Gln_{ext} were measured using liquid chromatography-tandem mass spectrometry (LC-MS/MS) as previously described (Defaix *et al.*, 2018). AUC values (% of baseline) were also calculated during the sample collections as previously described (Nguyen *et al.*, 2013). The limit of sensitivity for 5-HT was ≈ 0.5 fmol/sample (signal-to-noise ratio=2). The limit of quantification is ≈ 1.25 ng/ml for Glu, 0.63 ng/ml for GABA and 3.15 ng/ml for Gln (signal-to-noise ratio = 10). At the end of the experiments, localization of microdialysis probes was verified histologically (Bert *et al.*, 2004).

In the DHK protocol, after 4 points of baseline, DHK was perfused at 5 mM (dose chosen

based on the study of Gasull-Camos *et al.*, 2017) for 2.5 hours in the mPFC, equal 5 collected points, of which the FST was executed at the 3rd sample (Figure 4A). After the perfusion, 3 others samples were collected to re-establish the baseline level of 5-HT_{ext}, Glu_{ext}, $GABA_{ext}$ and Gln_{ext}.

2.5. Statistics

All experimental results are given as the mean ± SEM. Data were analyzed using Prism 6 software (GraphPad). Comparisons between groups were performed using one-way ANOVA followed by Fisher's PLSD *post hoc* analysis. A summary of statistical measures is included in Supplementary *Table S1*. Statistical significance was set at $p \leq 0.05$. A two-way ANOVA with pre-treatment (Vehicle vs NBQX or Vehicle vs muscimol or Vehicle vs bicuculline) and treatment (Vehicle vs Ketamine) factors was also used followed by Bonferroni *post hoc* test.

3. Results

3.1. Effects of local AMPA-R antagonist NBQX intra-DRN injection on ketamine-induced changes in neurotransmitters extracellular levels.

Microinfusion of AMPA-R antagonist NBQX (0.25 nmol) in the DRN 30 minutes before ketamine (1 nmol/side) intra-mPFC administration. At t24hr after these injections, ketamine alone increased swimming duration, together with 5-HT_{ext}, Glu_{ext} and $GABA_{ext}$ in the mPFC (AUC values by 159%, 168% and 162%, respectively compared to Vehicle) (Figure 1). **Intra-DRN NBQX prevented the effects of intra-mPFC ketamine injection on the swimming duration in the FST (Figure 1B), and blunted the effects of ketamine on mPFC 5-HT_{ext} (Figure 1C, 1D) and Glu_{ext} (Figure 1D). By contrast, intra-DRN NBQX had no effects on ketamine-induced increase in cortical $GABA_{ext}$.** Interestingly, increase in cortical 5-HT_{ext} after ketamine cortical injection was correlated (R^2=0.41) with its antidepressant-like activity as measured on swimming duration in the FST in the same mice (Figure 1E) as we previously described (Pham *et al.*, 2017b). The lower correlation was found in the NBQX/ketamine-treated group (R^2=0.19) highlight the role of AMPA-R in the DRN (Figure 1E). It suggests that activation of DRN AMPA-R exerts a key control of ketamine responses in these two serotonergic parameters, mPFC 5-HT_{ext} and swimming duration.

3.2. Effects of local bilateral $GABA_A$-R agonist muscimol intra-mPFC injection on ketamine-induced changes in neurotransmitters extracellular levels.

To determine the influence of neuronal silencing on ketamine responses, muscimol, a $GABA_A$-R agonist, was infused into the mPFC 30 minutes before intra-mPFC ketamine. Neurochemical and behavioral responses were assessed at t24hr post-injections to avoid the acute effects of drug treatments. The results demonstrate that ketamine increased swimming duration and mainly 5-HT_{ext} in the mPFC, while only a tendency to increase Glu_{ext} and $GABA_{ext}$ was observed (AUC values by 191% (p=0.0008), 144% (p=0.4), and 150% (p=0.11), respectively compared to Vehicle) (Figure 2). **Muscimol infusion into the mPFC completely blocked the antidepressant-like effects of ketamine in the FST (Figure 2B) and its effects on cortical 5-HT_{ext} too (Figure 2C, 2D). Intra-mPFC muscimol had no effects on ketamine-induced increase in cortical Glu_{ext} and $GABA_{ext}$.** Surprisingly here muscimol *per se* enhanced mPFC Glu_{ext} (244% vs Vehicle) in BALB/cJ mice. It suggests that $GABA_A$-R is tonically activated by endogenous GABA levels. Muscimol *per se* had no significant effect on the swimming duration as already described in rats by Fuchikami *et al.*, 2015 when the time point analysis was t24hr, but not when the analysis was performed immediately after intra-mPFC muscimol administration (Slattery *et al.*, 2011). In rat cortical neurons in culture, **muscimol** increases inhibitory neurotransmission by opening GABA-Cl(-)-channel, permitted inward Cl^- fluxes and **increased basal glutamate release by potentiating intracellular Ca^{2+}** (Farrant & Nusser, 2005), an effect reversed by bicuculline (Herrero *et al.*, 1999), **suggesting a role of $GABA_A$-R agonism in inducing neuronal excitation.** Here, this excessive increase in mPFC Glu_{ext} by muscimol could even cause an excitotoxicity and prevent beneficial stimulation of serotonergic neurons for antidepressant-like response of ketamine.

Interestingly, increases in cortical 5-HT_{ext} after ketamine cortical injection was correlated with its antidepressant-like activity as measured on swimming duration in the FST in the same mice (Figure 2E). The loss of such a correlation (R^2=0.13) in the muscimol/ketamine-treated group compared to the ketamine-treated group (R^2=0.94) likely suggests that **the release of endogenous GABA** by inhibitory interneurons located in the mPFC, and the subsequent activation of $GABA_A$-R may **limit ketamine responses**. It also indicates that serotonin release in the mPFC is a key component of this response, and NMDA-R blockade is not sufficient to produce an antidepressant response (Fuchikami *et al.*, 2015).

3.3. Effects of local bilateral $GABA_A$-R antagonist bicuculline intra-DRN injection on ketamine-induced changes in neurotransmitters extracellular levels.

To study the role of DRN $GABA_A$-R in ketamine's antidepressant-like activities, bicuculline, a $GABA_A$-R antagonist, was infused into the DRN (0.25 nmol) 30 minutes before intra-mPFC ketamine. Neurochemical and behavioral responses were assessed at t24hr post-injections. Ketamine increased swimming duration (Figure 3B), together with $5\text{-}HT_{ext}$ (Figure 3C), Glu_{ext} and $GABA_{ext}$ (Figure 3D) in the mPFC (AUC values by 172%, 190% and 135%, respectively compared to Vehicle). Intra-DRN bicuculline infusion did not alter or reinforce ketamine-induced increases in swimming duration and mPFC $5\text{-}HT_{ext}$ and Glu_{ext}. However, bicuculline blocked ketamine-induced increase in $GABA_{ext}$ in the mPFC. These results suggest that $GABA_A$-R in the DRN can control cortical GABA release induced by ketamine, regardless of its antidepressant-like activity. However, note that this blockade appeared with a lower baseline levels of all neurotransmitters in mice treated with bicuculline alone.

Increases in cortical $5\text{-}HT_{ext}$ after mPFC ketamine injection was correlated (R^2=0.89) with its antidepressant-like activity as measured on swimming duration in the FST in the same mice (Figure 3E).

3.4. Local perfusion of DHK intra-mPFC provoked an antidepressant-like effect

We then assessed the direct effects of enhancing glutamate tone in the mPFC using DHK (5 mM) to block GLT-1 glutamate transporter present in astrocytes (Gasull-Camos *et al.*, 2017). The behavioral and neurochemical consequences were assessed at t24hr post-injections. The FST was performed at the 3rd point of perfusion, revealed an increase in swimming duration in the same mice. DHK increased swimming duration in the FST (Figure 4). This response appears to be mediated by increases in all neurotransmitters levels in the mPFC, i.e., $5\text{-}HT_{ext}$ (Figure 4C), Glu_{ext} (Figure 4D), $GABA_{ext}$ (Figure 4E) and Gln_{ext}) (Figure 4I). The time course analysis showed that Gln_{ext} did not return to the baseline at the end of the experiment, as opposed to the levels of $5\text{-}HT_{ext}$, Glu_{ext} and $GABA_{ext}$. The AUC values increased by 475%, 462%, 236% and 198% of $5\text{-}HT_{ext}$, Glu_{ext}, $GABA_{ext}$ and Gln_{ext} (Figure 4F, 4G, 4H, 4J), respectively.

4. Discussion

Here, we have used pharmacologic (here) and optogenetic (see Supplementary data S1 & S2) approaches to study the specific role of the mPFC-DRN circuit in ketamine-induced antidepressant-like in BALBc/J mice. In the pharmacologic study, ketamine was injected locally into the mPFC, a brain region known to be involved in the fast antidepressant activity of

ketamine. This local injection strategy facilitates the analysis of the role of AMPA-R and $GABA_A$-R located in the circuit mPFC-DRN in ketamine responses. We found that ketamine-induced increase in swimming duration in the FST was blocked by pre-treatment of intra-DRN NBQX and intra-mPFC muscimol, while intra-DRN bicuculline did not enhance ketamine's effects. These data underline that the involvement of DRN AMPA-R and mPFC $GABA_A$-R in modulating ketamine antidepressant-like activity in BALB/cJ mice. DRN AMPA-R must be activated to facilitate ketamine antidepressant-like activity, while mPFC $GABA_A$-R may limit this response (see below).

Table 1. Summary of behavioral and neurochemical effects (in the mPFC) obtained in the study

Molecules	FST	5-HT_{ext}	Glu_{ext}	$GABA_{ext}$	Gln_{ext}/Glu_{ext} ratio	$Glu_{ext}/GABA_{ext}$ ratio
Ketamine	↑	↑	↑(tendency)	↑	↓	⊘
NBQX + KET (AMPA-R, DRN)	X	X (p=0.14)	X	⊘	⊘	↑
Muscimol + KET ($GABA_A$-R, mPFC)	X	X	⊘	↑	⊘	⊘
Bicuculline+KET ($GABA_A$-R, DRN)	↑	↑	↑	⊘	X	⊘
DHK (GLT-1 inhibitor)	↑	↑↑	↑↑	↑↑	⊘	⊘

X: blockade of the effect ; ⊘: No effect; ↑: increase or ↓: decrease effect.

AMPA-R are located on DRN 5-HT neurons and endogenous glutamate can activate this receptor subtype (Gartside *et al.*, 2007). Our results regarding intra-DRN NBQX injection agree with previous studies who described the blockade of the antidepressant-like effects of ketamine following a systemic NBQX administration 30 min prior to testing in rats (Koike *et al.*, 2011; Koike & Chaki, 2014) or in mice (Fukumoto *et al.*, 2016; Koike *et al.*, 2011; Pham *et al.*, 2017b). Taken together, these data suggest that activation of AMPA-R in the DRN would participate to the sustained antidepressant-like activity of ketamine (at t24h) by increasing mPFC serotonergic and glutamatergic neurotransmission. Interestingly, NBQX blocked ketamine-induced increase in 5-HT_{1B} receptor binding and decrease in SERT binding in primates (Yamanaka *et al.*, 2014). By contrast, ketamine-induced cortical GABA release was

not dependent on DRN AMPA-R activation, which thus poorly influenced the sustained antidepressant-like activity of ketamine.

Note that NBQX alone increased mPFC $GABA_{ext}$. Several factors could explain this effect. First, it could be due to the basal anxiety phenotype of BALB/cJ mice (Dulawa *et al.*, 2004; Holick *et al.*, 2008). Second, it is possible that the dose of NBQX (0.25 nmol/side) infused into the DRN was too high. Indeed, it was already shown that the decrease in the immobility duration in the FST induced by systemic administration of ketamine (30 mg/kg, i.p.) was blocked by a lower dose of NBQX (0.03 nmol/side into the mPFC) in C57BL/6J mice, while NBQX *per se* had no effects (Fukumoto *et al.*, 2016). Similarly, NBQX (30 nmol into the DRN 10 min before 25 mg/kg, s.c. ketamine) attenuated ketamine-induced 5-HT release in rat mPFC, while NBQX *per se* increased mPFC $5\text{-}HT_{ext}$ (Nishitani *et al.*, 2014). By contrast, when given alone in rats, higher dose of NBQX (300 µM into the mPFC) did not change $5\text{-}HT_{ext}$ and Glu_{ext} in the mPFC compared to controls (Lopez-Gil *et al.*, 2007). In these different studies, however, NBQX and NMDA-R antagonists were administered 30 min before neurochemical and behavioral tests, not at t24hr as in the present study. Third, the effect of NBQX *per se* suggests that a tonic activation of AMPA-R in the DRN by the endogenous glutamate may exert a negative feedback control on GABA release in the mPFC. Our experiment with a combination of microdialysis and FST in the same mice provided, for the first time, more insights into how the blockade of DRN AMPA-R interacts with ketamine's responses.

Our results of intra-mPFC muscimol pointed out that activation of mPFC $GABA_A$-R could limit ketamine's effects. Here, we found that when injected alone, muscimol increased robustly Glu_{ext} and when injected with ketamine, it improved ketamine-induced increase in $GABA_{ext}$. Injection of muscimol alone at higher dose (1.25 µg per side) induced no alteration in rat locomotion at 24h post-treatment (Fuchikami *et al.*, 2015), thus agreed with our observation. On the other hand, intra-infralimbic cortex (IL-PFC, a deep sub-region of the mPFC) injection of muscimol alone (200 pmol per side), 10 min prior to testing, reduced immobility time in the FST in rats (Slattery *et al.*, 2011). Moreover, a combination of low dose of muscimol (0.1 mg/kg, i.p., 30 min prior to ketamine) with a low dose of ketamine (0.1 mg/kg, i.p.) and tested at 1h post-injection resulted in antidepressant-like activity in mice in the tail suspension test (Rosa *et al.*, 2016). Thus, the time point of observation is crucial because an acute effect of muscimol could result in increasing locomotion and decreasing immobility in these behavioral tests, while at 24h post-injection muscimol-induced

inactivation of the mPFC by activating $GABA_A$-R could result in a hindrance of ketamine's effects.

The question then arises whether or not what was observed here in mice with a highly anxious phenotype, could also occur following a co-administration of BZD and ketamine in patients.

Bicuculline 0.25 nmol was injected into the DRN to see whether the inhibition of local $GABA_A$-R could enhance ketamine's action. According to the disynaptic downstream pathway from mPFC pyramidal cells to DRN 5-HT neurons via GABA interneurons, the inhibitory control of GABA interneurons could limit the function of 5-HT neurons. The injection of bicuculline was necessary to block the feedback pathway of this disynaptic mPFC-DRN connection in order to facilitate the antidepressant effects of mPFC-vHipp circuit activation by optogenetic (Carreno *et al.*, 2016). Bicuculline, by **decreasing inhibitory neurotransmission**, when injected alone did not alter rodents' behavior (intra-DRN: Carreno *et al.*, 2016 or intra-infralimbic: Slattery *et al.*, 2011), similar to our results. In addition, an increased firing in DRN 5-HT neurons induced by endogenous glutamate was enhanced by bicuculline, suggesting that glutamate can increase local GABA release (Gartside *et al.*, 2007).

Here, we did not see an enhancement of intra-mPFC ketamine-induced antidepressant activity by intra-DRN bicuculline pre-treatment, indicating that blocking the control of GABAergic inhibition in the DRN was not sufficient to boost excitatory activities in the mPFC. On the other hand, we found a tendency of increasing the Glu/GABA ratio by bicuculline, indicating an increased excitatory and decreased inhibitory neurotransmission, confirming the role of this $GABA_A$-R antagonist in suppressing GABA inhibition. However, systemic injection of bicuculline (5-8 mg/kg, i.p.) can induce tonic seizure in rats, which was reversed by ketamine (Irifune *et al.*, 2000; P. G. Schneider & Rodriguez de Lores Arnaiz, 2013), indicating complex activities of $GABA_A$-R in different brain regions. The choice of injection location must be precisely investigated in future studies, i.e., intra-mPFC, -vHipp or -amygdala injection.

On the other hand, inhibition of glutamatergic transporter GLT-1 by acute local intra-mPFC perfusion of DHK at 5 mM provoked a robust increase in extracellular levels of 5-HT, Glu, GABA and Gln. GLT-1 (or EAAT2), together with EAAT1, are two most abundant glutamatergic transporters in the forebrain (Gegelashvili *et al.*, 2000). In our previous study, ketamine was found to have no influence on the function of glutamatergic transporters (Pham *et al.*, 2017a), indicating that ketamine-induced increase in mPFC Glu_{ext} in microdialysis

experiments was of neuronal origin, rather than from astrocytes. DHK, an inhibitor of EAAT2, was already shown to increase swimming duration in the FST and mPFC Glu_{ext} and $5\text{-}HT_{ext}$ in rats (Gasull-Camos *et al.*, 2017). Thus, an acute increase of excitatory glutamate neurotransmission selectively in the mPFC triggers the sustained antidepressant-like activity of DHK in mice. A pharmacological approach using 5-HT synthesis inhibition in rats suggests that these DHK responses are mediated by the activation of mPFC-raphe pathways, which then induced a fast increase in serotonergic activity (Gasull-Camos *et al.*, 2017). The excessive increase in Glu_{ext} in cortical synapses induced by GLT-1 blockade seems to be the source of this neuronal excitation. However, this phenomenon occurred with a constant ratio of $Glu_{ext}/GABA_{ext}$, indicating that the excitation-inhibition balance was still maintained, which could be the key to the sustained antidepressant-like activity of ketamine in the FST in these mice.

In the present study, the increase in swimming duration in the FST was only observed when the glutamatergic and serotonergic systems are enhanced in the mPFC, indicating an increase in excitatory neurotransmission. Interestingly, in most cases (with the exception of DHK where both Glu_{ext} and Gln_{ext} were increased), this boost comes with a decrease in Gln_{ext}/Glu_{ext} ratio in the mPFC. On the other hand, in our experiments, the sustained antidepressant-like behavior of ketamine was associated with a stable balance of $Glu_{ext}/GABA_{ext}$ ratio in the mPFC, although Glu_{ext} increased, suggesting a neuronal adaptation after an antidepressant drug treatment that can boost the brain activity, but still preserving the excitation-inhibition balance.

In conclusion, we carried out here a pharmacologic approach to study the role of DRN AMPA-R and mPFC $GABA_A$-R in sustained antidepressant-like activity of ketamine. Our results suggest that $GABA_A$-R located in the DRN exert a minor control on the local intra-mPFC effects of ketamine. Interestingly, an increase in glutamate, i.e. glutamate bursts, could be involved in these effects. Ketamine and DHK (a GLT-1 glutamatergic transporter blocker) induced similar behavioral and neurochemical effects. However, our data pointed out the importance of the excitatory-inhibitory balance in the mPFC-DRN circuit, as this balance stayed constant even with the enhancement of glutamatergic neurotransmission in the mPFC. The results of the present study contribute to a further understanding of the cellular mechanisms underlying ketamine antidepressant-like activity.

Legend

Figure 1. Intra-DRN injection of AMPA-R antagonist, NBQX, blocked ketamine antidepressant-like activities

(A) Experimental protocol: after the surgery, NBQX 0.25 nmol was injected locally intra-DRN at 30 min prior to ketamine 2 nmol intra-mPFC. On the next day (t24h), the microdialysis-coupled-to the forced swim test (FST) was performed in the same mice. All dialysates were analysed for 5-HT, Glu and GABA extracellular level.

(B) NBQX blocked ketamine effects on the swimming duration in the FST and (C) 5-HT levels in the mPFC as shown in the time course t0-120 min. The gray area indicated the FST period.

(D) NBQX abolished ketamine-induced increase in 5-HT and Glu extracellular level, and augmented GABA extracellular level. The AUC values were calculated for the amount of 5-HT, Glu and GABA outflow collected during 0-120 min, and expressed as percentage of control group.

(E) The correlation between 5-HT extracellular levels in the mPFC at t60 min (i.e., during the FST) and the swimming duration is stronger in Vehicle/Ketamine than in NBQX/Ketamine mice in regard to their respective R^2 Pearson value.

*p<0.05; **p<0.01 vs Vehicle-treated group. #p<0.05 between compared groups. Data are presented as means ± S.E.M (n=5 mice per group).

Figure 1

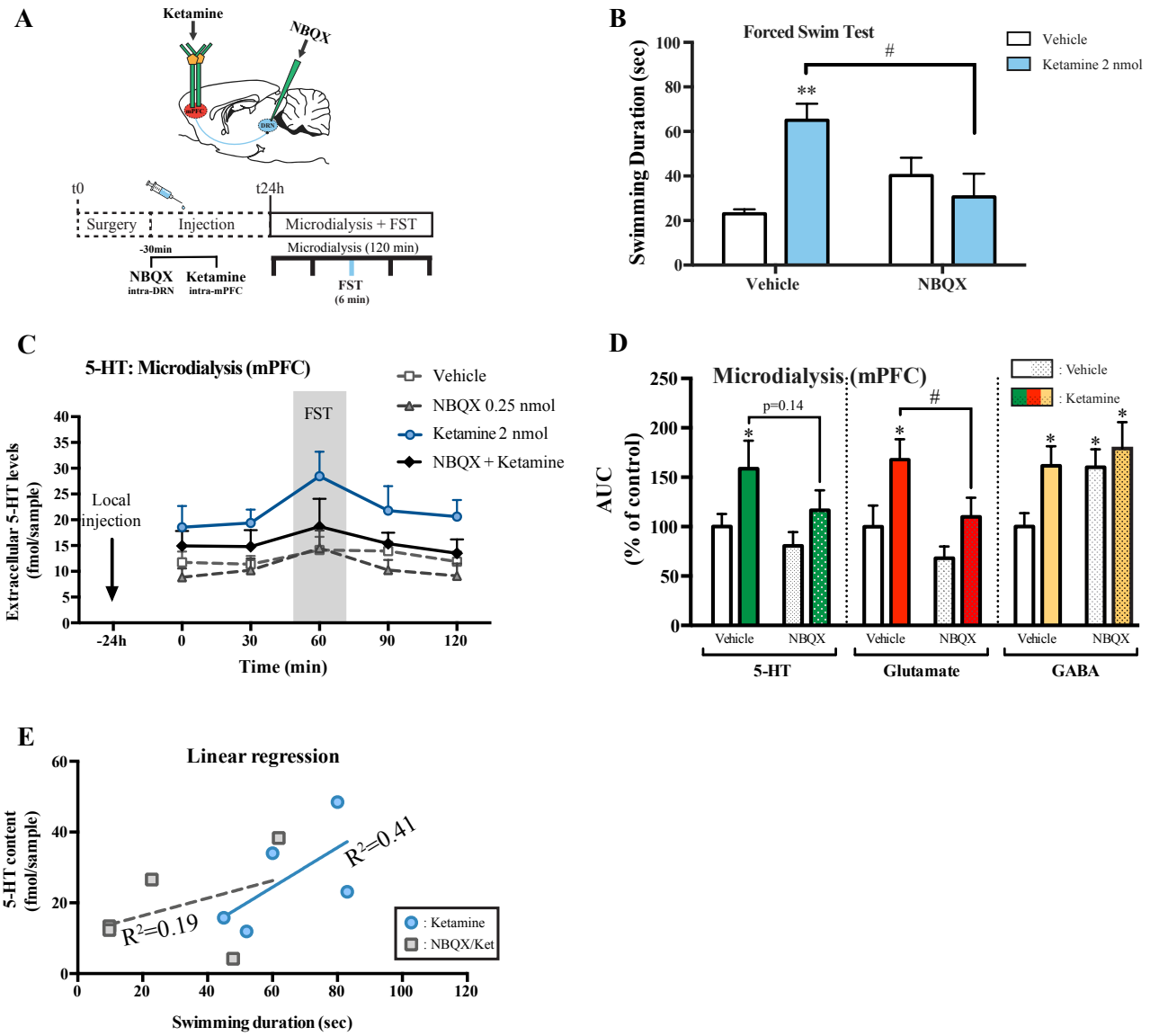
A
Ketamine
NBQX
mPFC
DRN
t0
t24h
Surgery
Injection
Microdialysis + FST
-30min
Microdialysis (120 min)
NBQX
intra-DRN
Ketamine
intra-mPFC
FST
(6 min)
B
Forced Swim Test
Vehicle
Ketamine 2 nmol
Swimming Duration (sec)
**
#
Vehicle
NBQX
C
5-HT: Microdialysis (mPFC)
Vehicle
NBQX 0.25 nmol
Ketamine 2 nmol
NBQX + Ketamine
FST
Local injection
Extracellular 5-HT levels (fmol/sample)
-24h
0
30
60
90
120
Time (min)
D
Microdialysis (mPFC)
: Vehicle
: Ketamine
p=0.14
#
AUC (% of control)
Vehicle
NBQX
5-HT
Glutamate
GABA
E
Linear regression
5-HT content (fmol/sample)
R²=0.41
R²=0.19
: Ketamine
: NBQX/Ket
Swimming duration (sec)

Figure 2. Intra-mPFC injection of $GABA_A$-R agonist, muscimol, blocked ketamine antidepressant-like activities

(A) Experimental protocol: after the surgery, muscimol (4 nmol per side) was injected bilaterally intra-mPFC at 30 min prior to ketamine (1 nmol per side) injected in the same site. On the next day (t24h), the microdialysis-coupled-to the forced swim test (FST) was performed in the same mice. All dialysates were analysed for 5-HT, Glu and GABA extracellular level.

(B) Muscimol blocked ketamine effects on the swimming duration in the FST and (C) 5-HT levels in the mPFC as shown in the time course t0-120 min. The gray area indicated the FST period.

(D) Muscimol abolished ketamine-induced increase in 5-HT extracellular level and robustly augmented Glu, and GABA extracellular level. The AUC values were calculated for the amount of 5-HT, Glu and GABA outflow collected during 0-120 min, and expressed as percentage of control group.

(E) The correlation between 5-HT extracellular levels in the mPFC at t60 min (i.e., during the FST) and the swimming duration is stronger in Vehicle/Ketamine than in Musicmol/Ketamine mice in regard to their respective R^2 Pearson value.

*p<0.05; **p<0.01 vs Vehicle-treated group. #p<0.05 between compared groups (ANOVA two-way). Data are presented as means ± S.E.M (n=4-5 mice per group).

Figure 2

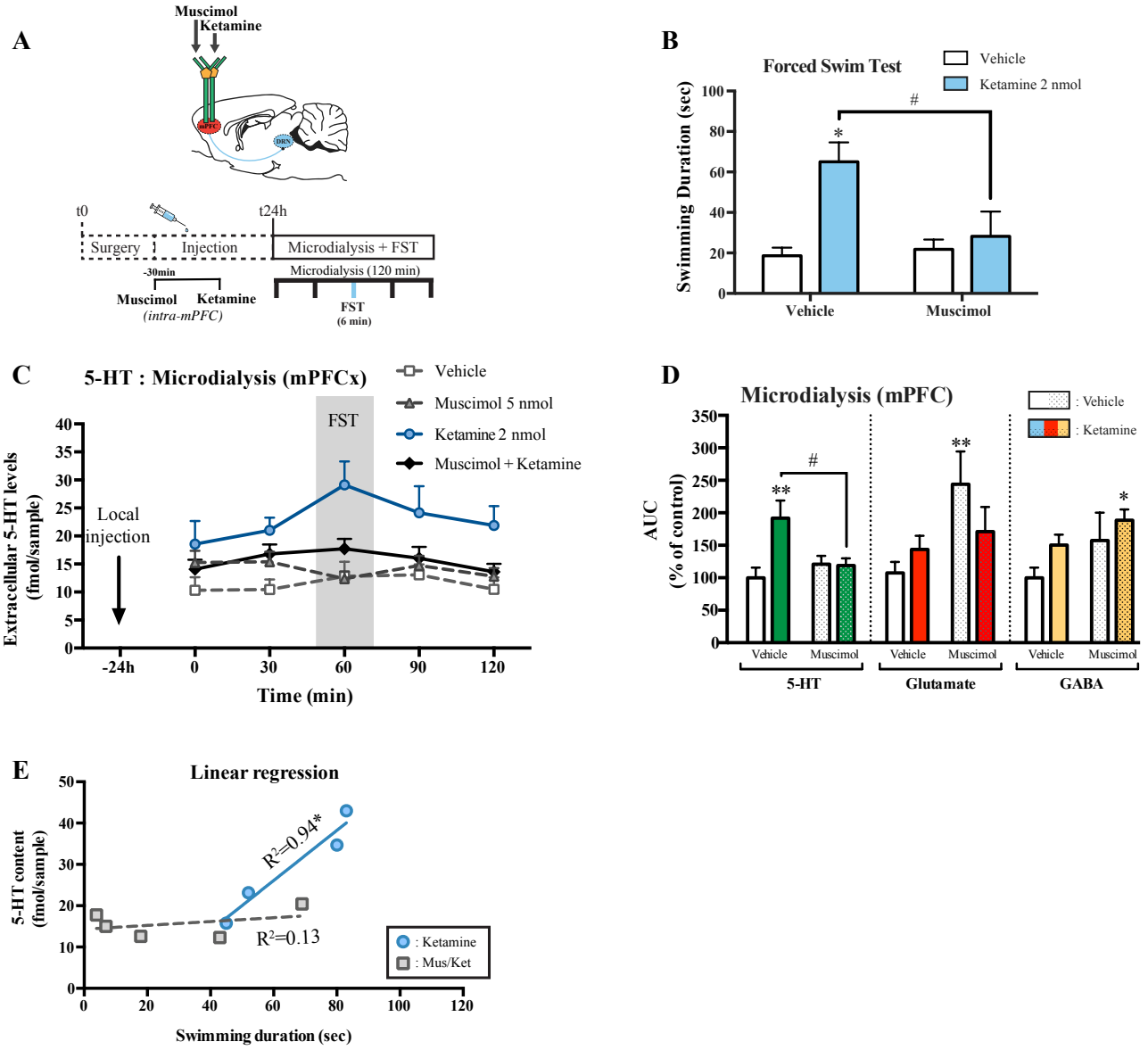
A
Muscimol
Ketamine
t0
t24h
Surgery
Injection
Microdialysis + FST
-30min
Muscimol
Ketamine
(intra-mPFC)
Microdialysis (120 min)
FST
(6 min)
B
Forced Swim Test
Vehicle
Ketamine 2 nmol
Swimming Duration (sec)
Vehicle
Muscimol
C
5-HT : Microdialysis (mPFCx)
Vehicle
Muscimol 5 nmol
Ketamine 2 nmol
Muscimol + Ketamine
FST
Local injection
Extracellular 5-HT levels (fmol/sample)
Time (min)
D
Microdialysis (mPFC)
: Vehicle
: Ketamine
AUC (% of control)
Vehicle
Muscimol
5-HT
Glutamate
GABA
E
Linear regression
5-HT content (fmol/sample)
R²=0.94*
R²=0.13
: Ketamine
: Mus/Ket
Swimming duration (sec)

Figure 3. Intra-DRN injection of $GABA_A$-R antagonist, bicuculline, did not abolish ketamine antidepressant-like activities

(A) Experimental protocol: after the surgery, bicuculline 0.25 nmol was injected locally intra-DRN at 30 min prior to ketamine 2 nmol intra-mPFC. On the next day (t24h), the microdialysis-coupled-to the forced swim test (FST) was performed in the same mice. All dialysates were analysed for 5-HT, Glu and GABA extracellular level.

(B) Bicuculline amplified ketamine effects on the swimming duration in the FST.

(C) Time course t0-120 min of 5-HT levels in the mPFC. The gray area indicated the FST period.

(D) Bicuculline tendentially decreased all the neurotransmitters levels but still maintained ketamine-induced increases in 5-HT and Glu extracellular level. Only ketamine effect on GABA extracellular level was abolished by bicuculline. The AUC values were calculated for the amount of 5-HT, Glu and GABA outflow collected during 0-120 min, and expressed as percentage of control group.

(E) The correlation between 5-HT extracellular levels in the mPFC at t60 min (i.e., during the FST) and the swimming duration is stronger in Vehicle/Ketamine than in Bicuculline/Ketamine mice in regard to their respective R^2 Pearson value.

*p<0.05; **p<0.01 vs Vehicle-treated group. #p<0.05; ##p<0.01 between compared groups. Data are presented as means ± S.E.M (n=4-5 mice per group).

Figure 3

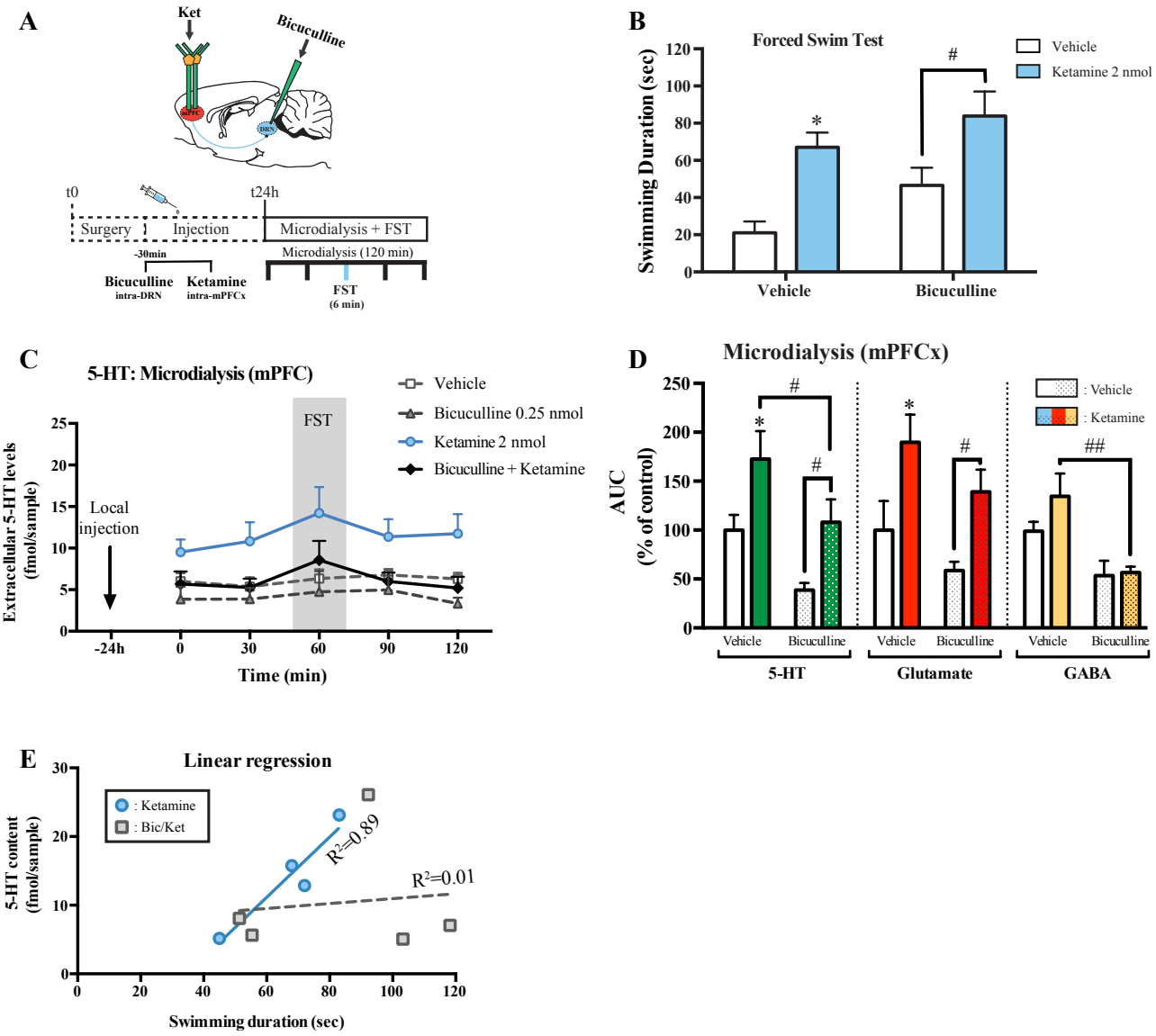
A
Ket
Bicuculline
mPFC
DRN
t0
t24h
Surgery
Injection
Microdialysis + FST
Microdialysis (120 min)
-30min
Bicuculline
intra-DRN
Ketamine
intra-mPFCx
FST
(6 min)
B
Forced Swim Test
Swimming Duration (sec)
Vehicle
Ketamine 2 nmol
Vehicle
Bicuculline
C
5-HT: Microdialysis (mPFC)
Extracellular 5-HT levels (fmol/sample)
Vehicle
Bicuculline 0.25 nmol
Ketamine 2 nmol
Bicuculline + Ketamine
FST
Local injection
-24h
Time (min)
D
Microdialysis (mPFCx)
AUC (% of control)
: Vehicle
: Ketamine
Vehicle
Bicuculline
5-HT
Glutamate
GABA
E
Linear regression
: Ketamine
: Bic/Ket
R²=0.89
R²=0.01
5-HT content (fmol/sample)
Swimming duration (sec)

Figure 4. Local perfusion of DHK intra-mPFC provoked an antidepressant-like effect

(A) Experimental protocol: after achieving 4 points of baseline, DHK 5 mM (dissolved in aCSF) was perfused during 2.5 hours (equal 5 collecting points of dialysats). The FST was executed at the 3rd point of DHK perfusion during 6 min. Then 3 other dialysats were collected.
(B) DHK induced an increase of swimming duration in the FST.
(C, D, E, I) Time course of 12 collecting points (30 min per point) of 5-HT, glutamate, GABA and glutamine levels in the mPFC, respectively. The gray areas indicated the FST session. Data are presented as fmol/sample for 5-HT and GABA levels, and as pmol/sample for glutamate and glutamine levels.
(F, G, H, J) DHK induced an increase in all neurotransmitters parameters. The AUC values were calculated for the amount of 5-HT, glutamate, GABA and glutamine, respectively, outflow collected during 5 points of DHK perfusion, and expressed as percentage of baseline levels.
* $p<0.05$, ** $p<0.01$ vs Vehicle-treated group. Data are presented as means ± S.E.M (n=4-6 mice per group).

Figure 4

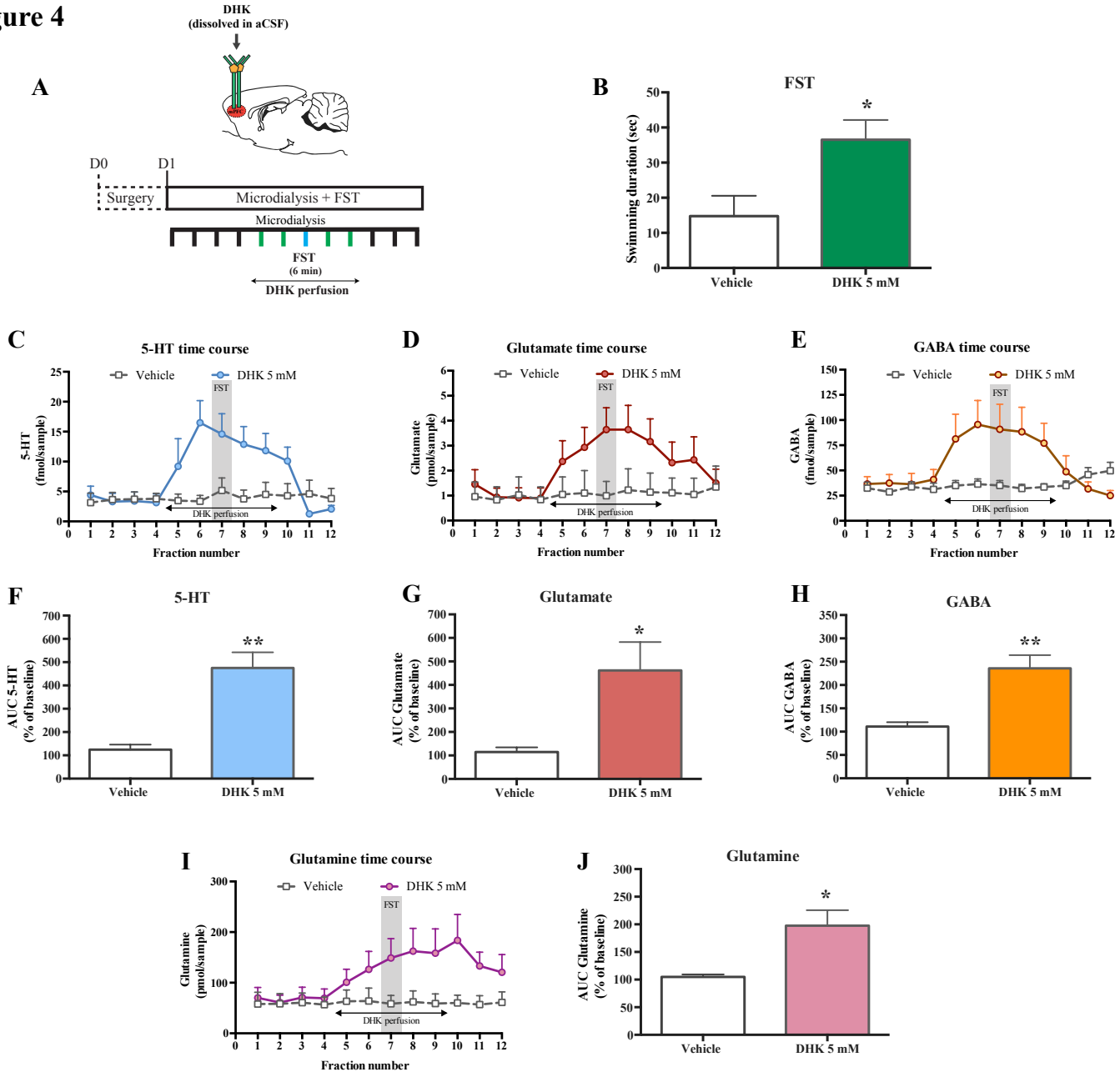
A
DHK
(dissolved in aCSF)
D0
D1
Surgery
Microdialysis + FST
Microdialysis
FST
(6 min)
DHK perfusion
B
FST
Swimming duration (sec)
Vehicle
DHK 5 mM
C
5-HT time course
Vehicle
DHK 5 mM
5-HT
(fmol/sample)
Fraction number
D
Glutamate time course
Glutamate
(pmol/sample)
E
GABA time course
GABA
(fmol/sample)
F
5-HT
AUC 5-HT
(% of baseline)
G
Glutamate
AUC Glutamate
(% of baseline)
H
GABA
AUC GABA
(% of baseline)
I
Glutamine time course
Glutamine
(pmol/sample)
J
Glutamine
AUC Glutamine
(% of baseline)

PRELIMINARY RESULTS REGARDING THE OPTOGENETIC APPROACH

Knowing the connectivity between the mPFC and raphe nuclei (Aghajanian & Marek, 1997; Hajos *et al.*, 1998; Peyron *et al.*, 1998; Varga *et al.*, 2001; Harandi *et al.*, 1987; Q. P. Wang *et al.*, 1992), particularly after verifying the role of this circuit by pharmacologic approach, we also used the optogenetic technique to selectively activate or inhibit the mPFC-DRN circuit in order to verify the extent of its implication in ketamine-induced antidepressant-like effects.

Using optogenetic, Fuchikami *et al.*, 2015 confirmed in rats that activation of the mPFC alone is sufficient to induce an antidepressant-like activity similar to ketamine. However, this study only used the optogenetic stimulation to reproduce ketamine's effects in the mPFC, thus no brain circuit was studied in this work. By contrast, Carreno *et al.*, 2016 highlighted the mPFC-ventral hippocampus (v-Hipp) circuit in ketamine responses, by using both optogenetic activation and inhibition of this brain circuit. Moreover, they combined a pharmacologic approach by using intra-dorsal raphe nucleus (DRN) injection of $GABA_A$ receptor ($GABA_A$-R) antagonist bicuculline, in order to identify the negative feedback in the DRN, controlled by GABAergic interneurons, that limit the response of optogenetic activation.

Materials and methods

1. Intracerebral in vivo microdialysis

Each mouse was anesthetized with chloral hydrate (400 mg/kg, i.p.) and implanted with two microdialysis probes (CMA7 model, Carnegie Medicine, Stockholm, Sweden) located in the medial prefrontal cortex (mPFC) and one microdialysis probe in the dorsal raphe nucleus (DRN). Stereotaxic coordinates in mm from bregma: mPFC : A= + 2.2, L= ± 0.2, V= - 3.4; DRN: A= - 4.5, L= + 1.2, V= - 4.7 with an angle of 15° (A, anterior; L, lateral; and V, ventral) (Calcagno & Invernizzi, 2010; Ferres-Coy *et al.*, 2013; Pham *et al.*, 2017b).

An acute i.p. dose of ketamine 10 mg/kg was used for the optogenetic inhibition study. Flow rate of 0.5 µl/min through the DRN using CMA/100 pump.

2. Optogenetic manipulation of the mPFC-DRN pathway, in combination with the FST-coupled microdialysis in the same mice

Construction of optical fibers. As we previously described, for all experiments, a 200 µm core, 0.37 numerical aperture multimode fiber (ThorLabs, Maison Laffitte, France) was used for

optical stimulation through a patch cable connected to a 100 mW 473 nm or 532 nm blue green laser diodes (OEM laser systems) (Tritschler *et al.*, 2017).

Virus injection and fiber implantation. For targeting opsin expression selectively to cortical glutamatergic terminals in the DRN, AAV5-CamKII-hChR2(H134R)-EYFP, AAV5-CaMKII-ArchT-GFP or AAV5-CaMKII-GFP, obtained from Karl Deisseroth and Ed Boyden (UNC Vector Core, NC, USA) was bilaterally injected into the mPFC of mice under anesthesia (chloral hydrate, 400 mg/kg, i.p). Mice receiving AAV5-CamKII-GFP were used as control. The viruses were microinjected bilaterally (0.4 µl per side) into the mPFC. Mice were allowed to recover for eight weeks before optogenetic studies to allow for robust gene expression in target regions (mPFC and DRN). Eight weeks later, mice were anesthesized (chloral hydrate 400 mg/kg, i.p.) and surgically implanted two special optic fibers coupled to microdialysis probes into the mPFC and one normal microdialysis probe into the DRN for the activation study; or two normal microdialysis probes into the mPFC and one optogenetic-coupled microdialysis probe in the DRN for the inactivation study. These probes were then secured to the skull with dental cement.

Activation study. The bilateral stimulation of pyramidal neurons in the mPFC, 24hr before the FST involved delivery of an average of 8 mW of blue light (473 nm, 10 ms pulses, 10 Hz, Master-8, A.M.P Instruments, Israel), 1 minute “ON” and 1 minute “OFF” for 1 hour (30 sequences).

Inactivation study. Optical fibers were connected to a 100 mW 532 nm laser diode (OEM laser systems), and green light was delivered continuously (15 mW) intra-DRN at the same time as the FST, which was excecuted at 24 hours post ketamine-administration. One day following ketamine administration, mice were tested in the FST. During the 6 minutes duration of swimming, the first 2 minutes were considered as adaptation of animals to the aqueous environment. During the next 2 minutes and the last 2 minutes, the green light was randomly applied to avoid sequential effects of the optogenetic inactivation process.

Verification of opsin expression in the mPFC and DRN was done by immunohistochemistry with anti-GFP anticorp from rabbit (Invitrogen) (Figure S1A and S2A).

Results

1. Bilateral photoactivation of the mPFC mimicks ketamine-induced antidepressant-like effects in the FST and -increased in 5-HT levels

Mice receiving the virus expressing ChR2 channel (AAV5-CamKII-ChR2-YFP) were compared to mice who received the control virus (AAV5-CamKII-GFP) (see the protocol in Figure S1A). Optogenetic activation of ChR2 channel by blue light for one hour at Day 1

induced a robust increase in swimming duration in the FST the day after, an effect similar to ketamine at 24h post-treatment.

In the mPFC: ChR2-eYFP-expressing mice induced an increase in 5-HT_{ext} (Figure S1C) compared to control mice at Day 2, i.e., 24 hours after optogenetic stimulation (AUC values: +92% of baseline in comparison to control mice, Figure S1D). This increase in 5-HT_{ext} was correlated with the swimming duration measured in the same BALB/cJ mice (Figure S1G), highlighting the predictive value of mPFC 5-HT_{ext} in this test.

In the DRN: no significant changes in 5-HT_{ext} were observed in this brain region (Figure S1E and S1F). It could be due to the distance of transmission since the activation was performed in the mPFC. However, the 5-HT_{ext} in this region still showed a strong correlation with the swimming duration of the same mice confirming the role of mPFC 5-HT_{ext} in predicting antidepressant-like activity in the FST (Figure S1H).

2. Photoinhibition of the mPFC-DRN circuit blocked partially ketamine-induced antidepressant-like effects in the FST and -increased in 5-HT levels

Mice receiving the virus expressing Arch channel (AAV5-CamKII-Arch-GFP) were compared to mice who received the control virus (AAV5-CamKII-GFP) (see the protocol in Figure S2A). Ketamine (10 mg/kg, i.p.) was injected to the Arch group at Day 1. On the next day, optogenetic inhibition of Arch channel by green laser for 2 min during the FST session blocked partially: 34% for reponded mice (n=10) compared to -20% for non-responded mice (n=2), ketamine-induced increase in the swimming duration (Figure S2B and S2C). There was no significant sequential difference between the light inhibition at 2-4 and 4-6 min, so we grouped the swimming duration of the “ON” or “OFF” sessions together. The scattergram inserted in Figure S2B indicated that among 12 animals, there were 2 mice that did not respond to the laser inhibition.

The microdialysis in these same mice showed a decrease in 5-HT_{ext} (t-test) during the point of laser inhibition compared to the baseline level of Day 2 in the mPFC (90% vs 111%, respectively) and in the DRN (112% vs 147%, respectively) (Figure S2 D-G). This means that 2min of inhibition by optogenetic was sufficient to increase mPFC 5-HT_{ext}, which is quite surprising.

Discussion

Our results of mPFC stimulation by optogenetic confirmed the data of Fuchikami *et al.*, 2015, who found that this neuronal activation, specifically targetting glutamatergic neurons in the mPFC was sufficient to replicate ketamine's antidepressant-like activity in the FST in rats, accompagnied with an increase in cFos (a marker of neuronal activation) expressed cells. Here, by coupling the FST with *in vivo* microdialysis in the same mice, we measured also 5-HT_{ext} at the moment of optogenetic stimulation and at 24h later in the mPFC. Our results showed that when the stimulation occurred, eventhough the mice responded to the laser with an increased locomotion, no increase in 5-HT_{ext} was observed in the mPFC or in the DRN, suggesting that the source of locomotion was due to another excitatory factor, such as an increase in Glu_{ext}. Meanwhile, at 24h later, 5-HT_{ext} of ChR2 groupe was increased significantly compared to control mice, which is similar to ketamine's effects. This indicates a neuronal adaptation after glutamate bursts that facilitated other excitatory neurotransmitter system, i.e. 5-HT. Although this increase in 5-HT_{ext} was only observed in the mPFC, we found a strong correlation between 5-HT_{ext} and the swimming behavior of each animal in both regions, which was not the case in control group, indicating that optogenetic stimulation generated a particular modification of the serotonergic system in a way that could predict the antidepressant-like activity of ketamine in the FST. Our data underlined the importance of the mPFC in ketamine's mechanism of action. Future works should be performed in nerve terminal originating from the mPFC to other brain regions such as the hippocampus, amygdala and DRN to understand better the circuit involved in ketamine's action.

Using optogenetic inhibition of the mPFC-DRN circuit, we found a 33% blocking of ketamine-induced increase in the swimming duration in the FST and 21% in mPFC 5-HT_{ext}. In our previous reports, we have seen an increase in 5-HT_{ext} during the FST session (Pham *et al.*, 2017a; Pham *et al.*, 2017b). Here, the 5-HT peak during the FST was totally blocked in the mPFC, as well as in the DRN, indicating an effect of the laser inhibition. However, the inhibition of the mPFC-DRN circuit was low (33%) and limited to a small number of mice on ketamine's effects, suggesting: (i)- either technical problems of virus injection (some immuno-histochemistry controls are in progress), or (ii)- a limited role of the mPFC-DRN circuit in ketamine responses, thus possibly the involvement of other circuits and brain regions in ketamine's mechanism of action, such as the mPFC-vHipp pathway as mentioned by Carreno *et al.*, 2016.

Legend

Figure S1. Optogenetic activation of mPFC induced antidepressant-like activities in the FST and increased 5-HT levels in the mPFC

(A) Experimental protocol: the viruses AAV5-CamKII-ChR2-YFP (ChR2) and AAV5-CamKII-GFP (control) were injected intra-mPFC of mice at 8 weeks before the experiment. After 8 weeks, mice were anesthesized and implanted with 2 fiber-optic-coupled-to microdialysis probes intra-mPFC and one conventional microdialysis probe intra-DRN (Day 0). On the next day (Day 1), the microdialysis procedure was performed in these mice. After 4 points of baseline (B0), mice received laser activation (473 nm, 8 mW, 10 Hz, 30 sequences of 1 min ON - 1 min OFF lasting for 1 hour) bilaterally through the 2 fiber optics in the mPFC. Another 4 points were collected after the activation (B1). On day 2, the microdialysis-coupled-to the forced swim test (FST) was performed in the same mice. All dialysates were analysed for 5-HT extracellular level. An exemple of the verification of virus expression by immunohistochemistry is presented.

(B) mPFC activation by optogenetic induced an increase of swimming duration in the FST in mice expressing ChR2 vs control group.

(C) Time course t0-180 min (Day 1) and t0-120 min (Day 2) of 5-HT levels in the mPFC. Only the average of 4 points of the baseline is presented. The gray areas indicated the laser activation and the FST period at Day 1 and Day 2, respectively.

(D) Activation of the ChR2 channel increased the 5-HT extracellular level in the mPFC. The AUC values were calculated for the amount of 5-HT collected during t0-120 min of Day 2, and expressed as percentages of Day 1 baseline levels for each mouse.

(E) Time course t0-180 min (Day 1) and t0-120 min (Day 2) of 5-HT levels in the DRN. Only the average of 4 points of the baseline is presented. The gray areas indicated the laser activation and the FST period at Day 1 and Day 2, respectively.

(F) Activation of the ChR2 channel did not increase the 5-HT extracellular level in the DRN. The AUC values were calculated for the amount of 5-HT collected during t0-120 min of Day 2, and expressed as percentages of Day 1 baseline levels for each mouse.

(G) The correlation between extracellular mPFC and (H) DRN 5-HT levels at Day 2 - t60 min (i.e., during the FST) and the swimming duration is stronger in ChR2-activated than in control-activated mice in regard to their respective R^2 Pearson value.

* $p<0.05$, ** $p<0.01$ vs control mice (t-test). Red points indicated mice in which virus (ChR2) expression has been verified by immunohistochemistry. Data are presented as means ± S.E.M (n=5-7 mice per group).

Figure S1

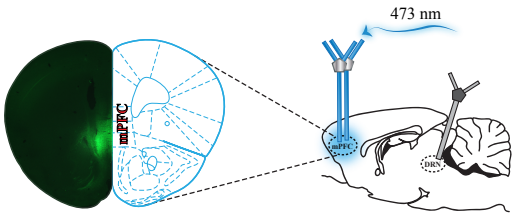
473 nm
mPFC
DRN

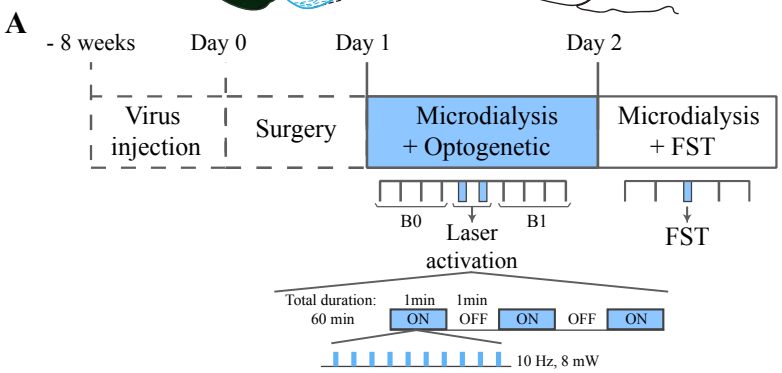
A
- 8 weeks
Day 0
Day 1
Day 2
Virus injection
Surgery
Microdialysis + Optogenetic
Microdialysis + FST
B0
Laser activation
B1
FST
Total duration: 60 min
1min ON
1min OFF
ON
OFF
ON
10 Hz, 8 mW

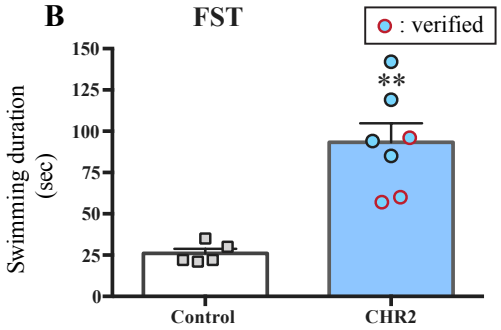
B
FST
: verified
Swimming duration (sec)
Control
CHR2

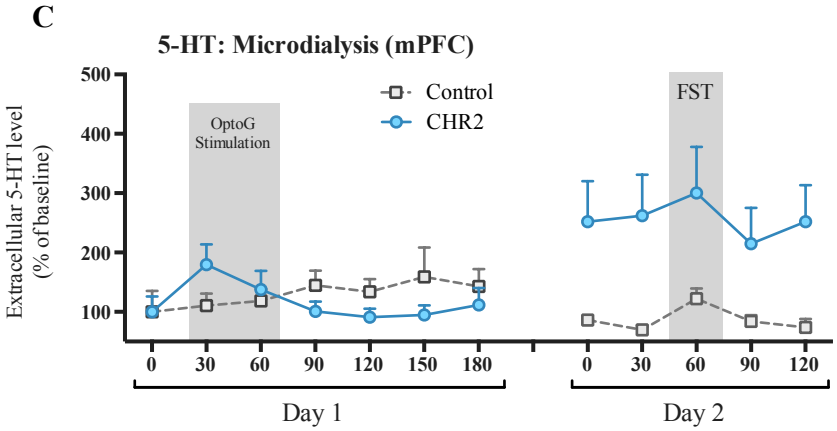
C
5-HT: Microdialysis (mPFC)
Extracellular 5-HT level (% of baseline)
Control
CHR2
OptoG Stimulation
FST
Day 1
Day 2

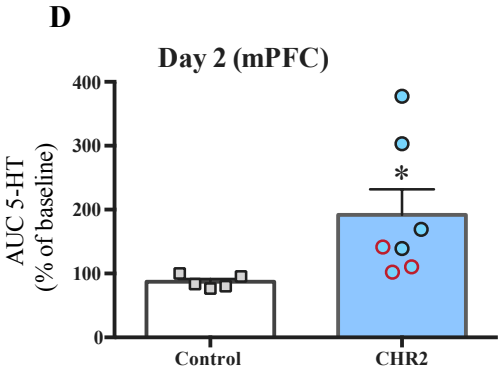
D
Day 2 (mPFC)
AUC 5-HT (% of baseline)
Control
CHR2

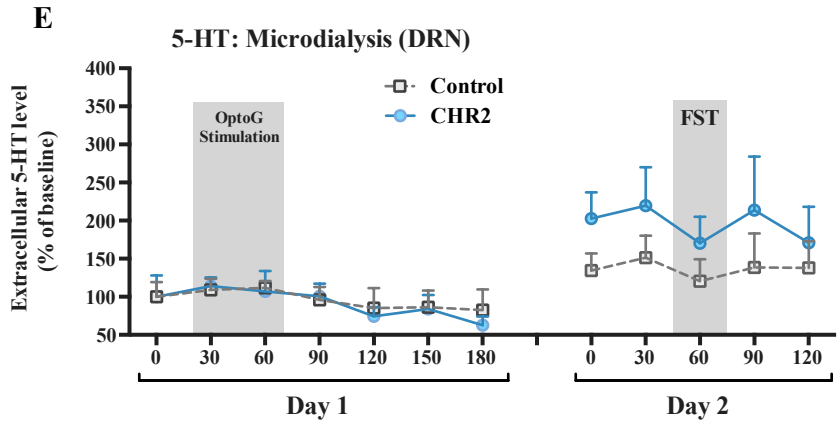
E
5-HT: Microdialysis (DRN)
Extracellular 5-HT level (% of baseline)
Control
CHR2
OptoG Stimulation
FST
Day 1
Day 2

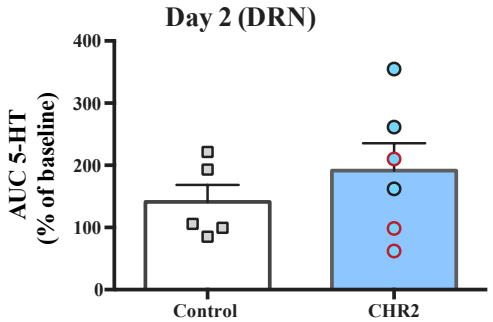
F
Day 2 (DRN)
AUC 5-HT (% of baseline)
Control
CHR2

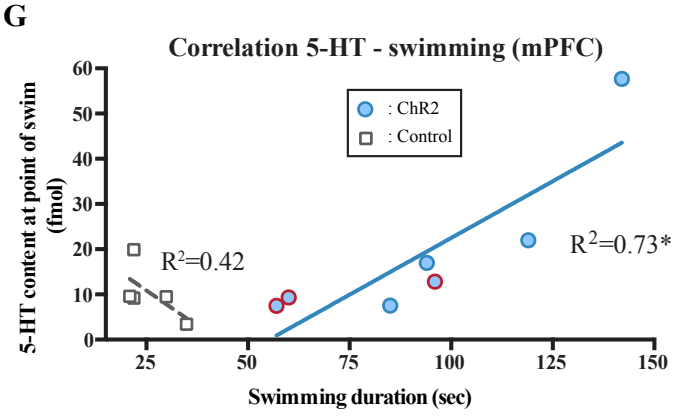
G
Correlation 5-HT - swimming (mPFC)
5-HT content at point of swim (fmol)
: ChR2
: Control
R²=0.42
R²=0.73*
Swimming duration (sec)

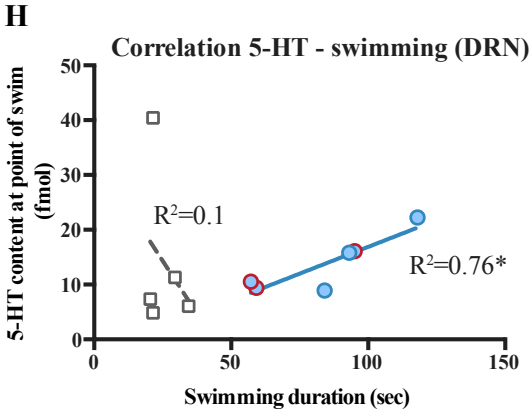
H
Correlation 5-HT - swimming (DRN)
5-HT content at point of swim (fmol)
R²=0.1
R²=0.76*
Swimming duration (sec)

Figure S2. Optogenetic inhibition of the mPFC-DRN circuit blocked partially ketamine-induced antidepressant-like activities in the FST and 5-HT increase in microdialysis in the mPFC

(A) Experimental protocol: the viruses AAV5-CamKII-Arch-YFP (Arch) and AAV5-CamKII-GFP (control) were injected intra-mPFC of mice at 8 weeks before the experiment. After 8 weeks, mice were anesthesized and implanted with two conventional microdialysis probes intra-mPFC and one fiber-optic-coupled-to microdialysis probe intra-DRN (Day 0). On the next day (Day 1), the microdialysis procedure was performed in these mice. After 4 points of baseline (B0), ketamine (10 mg/kg, i.p.) or vehicle (NaCl 0.9%) were injected in mice of Arch and vehicle (Veh) groups, respectively. On Day 2, the microdialysis-coupled-to the forced swim test (FST) was performed in the same mice. After 2 points of baseline, the FST was performed during 6 min. The first 2 min is for adaptation, for the next and the last 2 minutes, mice received randomly at 2-4 or 4-6 min the laser inhibition (532 nm, 15 mW) through the fiber optic in the DRN. Another 2 points were collected after the inhibition. All dialysates were analysed for 5-HT extracellular level (5-HT_{ext}). An exemple of the verification of virus expression by immunohistochemistry is presented.

(B) mPFC-DRN specific inhibition by optogenetic blocked ketamine-induced increase of swimming duration in the FST in mice expressing Arch (ANOVA two-way). Inserted figure: scattergram of each mouse with (ON) or without (OFF) laser inhibition.

(C) The magnitude of optogenetic inhibition on swimming duration in Arch groups presented as scattergram, in percentages. The responded and non-responded mice are separated.

(D, F) Time course t0-120 min (Day 1) and t0-120 min (Day 2) of 5-HT_{ext} in the mPFC. Only the average of 4 points of the baseline is presented. The gray areas indicated the laser inhibition and the FST session at Day 2.

(E, G) Activation of the Arch channel decreased the 5-HT_{ext} in the mPFC (E) and DRN (F) (t-test). The AUC values were calculated for the 5-HT_{ext} collected at the point of injection at Day 1 (Veh D1 and Ket D1 for mice receiving vehicle and ketamine, respectively), for the baseline of Day 2 (Veh D2 and Ket D2) and during the FST of Day 2 (Veh Laser and Ket Laser), and expressed as percentages of Day 1 baseline levels for each mouse. Inserted figure: scattergram of each mouse with (ON) or without (OFF) laser inhibition.

(H, I) The correlation between 5-HT_{ext} in the mPFC (H) and in the DRN (I) at Day 2 t60 min (i.e., during the FST) and the swimming duration.

* $p<0.05$ between selected groups. Red points indicated mice in which virus (Arch) expression has been verified by immunohistochemistry. Data are presented as means ± S.E.M (n=6 and 12 mice for Veh and Ket groups, respectively).

Figure S2

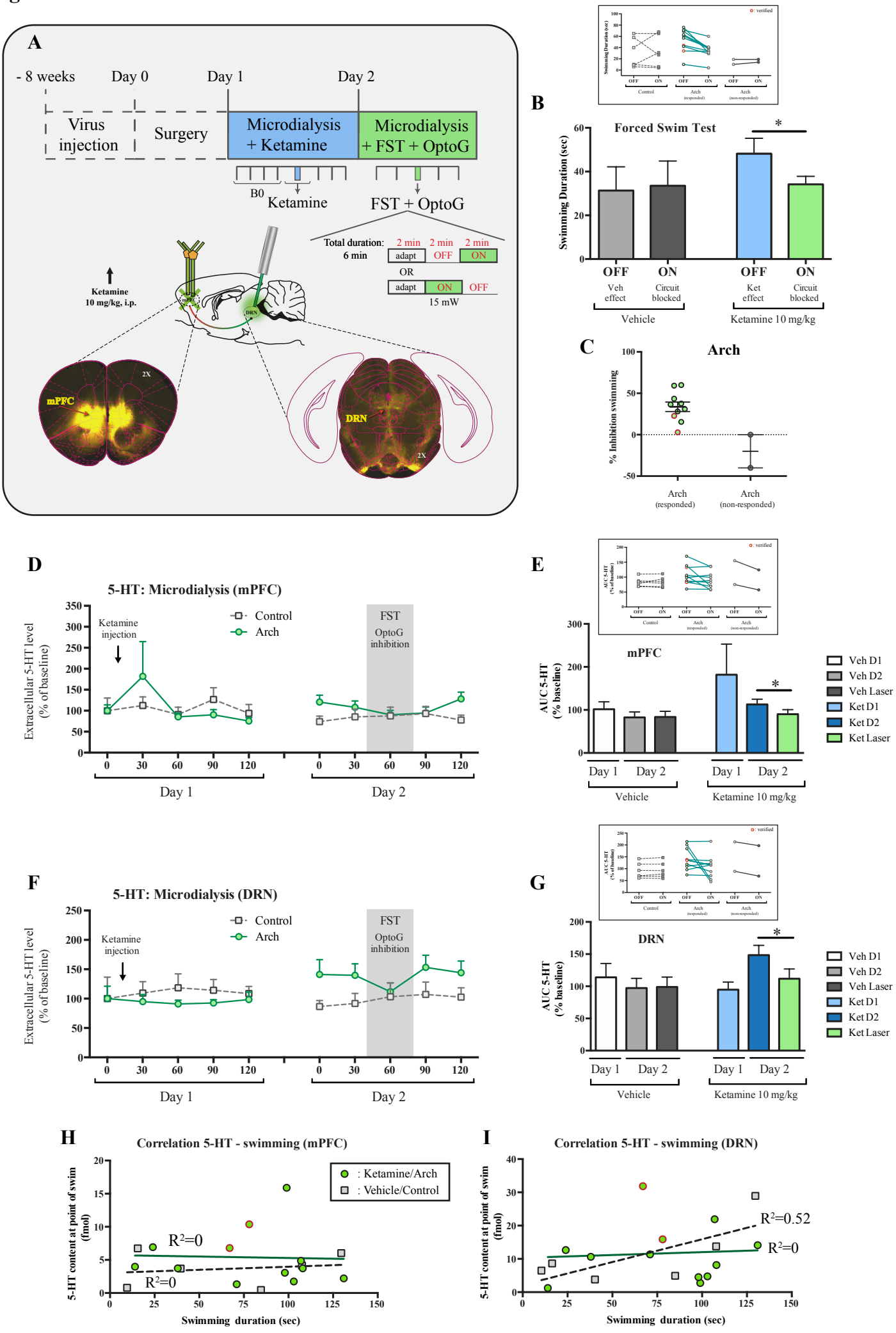
A
- 8 weeks
Day 0
Day 1
Day 2
Virus injection
Surgery
Microdialysis + Ketamine
Microdialysis + FST + OptoG
B0
Ketamine
FST + OptoG
Total duration: 6 min
2 min adapt
2 min OFF
2 min ON
OR
adapt ON OFF
15 mW
Ketamine 10 mg/kg, i.p.
mPFC
DRN
2X
B
Forced Swim Test
Swimming Duration (sec)
OFF ON OFF ON
Veh effect
Circuit blocked
Ket effect
Circuit blocked
Vehicle
Ketamine 10 mg/kg
C
Arch
% Inhibition swimming
Arch (responded)
Arch (non-responded)
D
5-HT: Microdialysis (mPFC)
Extracellular 5-HT level (% of baseline)
Ketamine injection
Control
Arch
FST
OptoG inhibition
Day 1
Day 2
E
mPFC
AUC 5-HT (% baseline)
Veh D1
Veh D2
Veh Laser
Ket D1
Ket D2
Ket Laser
Day 1 Day 2 Day 1 Day 2
Vehicle
Ketamine 10 mg/kg
F
5-HT: Microdialysis (DRN)
G
DRN
H
Correlation 5-HT - swimming (mPFC)
5-HT content at point of swim (fmol)
: Ketamine/Arch
: Vehicle/Control
R²=0
R²=0
Swimming duration (sec)
I
Correlation 5-HT - swimming (DRN)
R²=0.52
R²=0

Supplemental table 1. Complete statistical summary analysis for behavioral and microdialysis data

Tests	Measurement	Statistical Test	Comparison	Statistics	Degrees of freedom	p	Fig.
NBQX - Forced swim test	Swimming duration	2-way ANOVA	Interaction	F=10.1	1, 15	0.0062 **	**1B**
			Row factor (ketamine treatment)	F=1.123	1, 15	0.3061	
			Column factor (NBQX treatment)	F=3.984	1, 15	0.0644	
		Bonferroni post-hoc test	Veh/Veh vs Veh/Ket			0.0029 **	
			Veh/Veh vs NBQX/Veh			0.1659	
			Veh/Veh vs NBQX/Ket			0.5296	
			Veh/Ket vs NBQX/Veh			0.0417 *	
			Veh/Ket vs NBQX/Ket			0.0075 **	
			NBQX/Veh vs NBQX/Ket			0.4022	
NBQX - Microdialysis (intra-DRN injection)	mPFC AUC $[5\text{-HT}]_{ext}$	2-way ANOVA	Interaction	F=0.3188	1, 29	0.5767	**1D**
			Row factor (ketamine treatment)	F=2.399	1, 29	0.1323	
			Column factor (NBQX treatment)	F=5.706	1, 29	0.0236 *	
		Bonferroni post-hoc test	Veh/Veh vs Veh/Ket			0.0486 *	
			Veh/Veh vs NBQX/Veh			0.498	
			Veh/Veh vs NBQX/Ket			0.5515	
			Veh/Ket vs NBQX/Veh			0.0103 *	
			Veh/Ket vs NBQX/Ket			0.1403	
			NBQX/Veh vs NBQX/Ket			0.201	
	mPFC AUC $[Glu]_{ext}$	2-way ANOVA	Interaction	F=0.176	1, 28	0.678	
			Row factor (ketamine treatment)	F=5.852	1, 28	0.0223 *	
			Column factor (NBQX treatment)	F=6.081	1, 28	0.0201 *	
		Bonferroni post-hoc test	Veh/Veh vs Veh/Ket			0.0437 *	
			Veh/Veh vs NBQX/Veh			0.1734	
			Veh/Veh vs NBQX/Ket			0.9709	
			Veh/Ket vs NBQX/Veh			0.0037 **	
			Veh/Ket vs NBQX/Ket			0.0517	
			NBQX/Veh vs NBQX/Ket			0.1723	
	mPFC AUC $[GABA]_{ext}$	2-way ANOVA	Interaction	F=1.234	1, 28	0.2761	
			Row factor (ketamine treatment)	F=4.068	1, 28	0.0534	
			Column factor (NBQX treatment)	F=4.361	1, 28	0.046 *	

		Bonferroni post-hoc test	Veh/Veh vs Veh/Ket			0.0223 *	
			Veh/Veh vs NBQX/Veh			0.0353 *	
			Veh/Veh vs NBQX/Ket			0.0071 **	
			Veh/Ket vs NBQX/Veh			0.9601	
			Veh/Ket vs NBQX/Ket			0.5268	
			NBQX/Veh vs NBQX/Ket			0.5199	
Muscimol - Forced swim test	Swimming duration	2-way ANOVA	Interaction	F=5.724	1, 15	0.03 *	**2B**
			Row factor (ketamine treatment)	F=4.039	1, 15	0.06	
			Column factor (muscimol treatment)	F=9.973	1, 15	0.0065 *	
		Bonferroni post-hoc test	Veh/Veh vs Veh/Ket			0.01 *	
			Veh/Veh vs Mus/Veh			> 0.99	
			Veh/Veh vs Mus/Ket			> 0.99	
			Veh/Ket vs Mus/Veh			0.0174 *	
			Veh/Ket vs Mus/Ket			0.051	
			Mus/Veh vs Mus/Ket			> 0.99	
Muscimol - Microdialysis (intra-mPFC injection)	mPFC AUC $[5\text{-HT}]_{ext}$	2-way ANOVA	Interaction	F=6.977	1, 30	0.013*	**2D**
			Row factor (ketamine treatment)	F=2.141	1, 30	0.15	
			Column factor (muscimol treatment)	F=6.366	1, 30	0.0172 *	
		Bonferroni post-hoc test	Veh/Veh vs Veh/Ket			0.0008 ***	
			Veh/Veh vs Mus/Veh			0.438	
			Veh/Veh vs Mus/Ket			0.414	
			Veh/Ket vs Mus/Veh			0.0146 *	
			Veh/Ket vs Mus/Ket			0.0041 **	
			Mus/Veh vs Mus/Ket			0.935	
	mPFC AUC $[Glu]_{ext}$	2-way ANOVA	Interaction	F=2.471	1, 30	0.1264	
			Row factor (ketamine treatment)	F=5.575	1, 30	0.0249 *	
			Column factor (muscimol treatment)	F=0.281	1, 30	0.599	
		Bonferroni post-hoc test	Veh/Veh vs Veh/Ket			0.467	
			Veh/Veh vs Mus/Veh			0.0093 **	
			Veh/Veh vs Mus/Ket			0.134	
			Veh/Ket vs Mus/Veh			0.082	
			Veh/Ket vs Mus/Ket			0.581	

			Mus/Veh vs Mus/Ket			0.148	
	mPFC AUC $[GABA]_{ext}$	2-way ANOVA	Interaction	F=0.187	1, 30	0.6685	
			Row factor (ketamine treatment)	F=4.693	1, 30	0.0383 *	
			Column factor (muscimol treatment)	F=3.445	1, 30	0.0733	
		Bonferroni post-hoc test	Veh/Veh vs Veh/Ket			0.1084	
			Veh/Veh vs Mus/Veh			0.0935	
			Veh/Veh vs Mus/Ket			0.0037 *	
			Veh/Ket vs Mus/Veh			0.8413	
			Veh/Ket vs Mus/Ket			0.1998	
			Mus/Veh vs Mus/Ket			0.3322	
Bicuculline - Forced swim test	Swimming duration	2-way ANOVA	Interaction	F=0.1849	1, 14	0.67	**3B**
			Row factor (ketamine treatment)	F=4.293	1, 14	0.0572	
			Column factor (muscimol treatment)	F=16.53	1, 14	0.0012**	
		Bonferroni post-hoc test	Veh/Veh vs Veh/Ket			0.0093**	
			Veh/Veh vs Bic/Veh			0.0986	
			Veh/Veh vs Bic/Ket			0.0007***	
			Veh/Ket vs Bic/Veh			0.1804	
			Veh/Ket vs Bic/Ket			0.265	
			Bic/Veh vs Bic/Ket			0.0164*	
Bicuculline - Microdialysis (intra-DRN injection)	mPFC AUC $[5\text{-}HT]_{ext}$	2-way ANOVA	Interaction	F=0.005	1, 30	0.9462	**3D**
			Row factor (ketamine treatment)	F=8.018	1, 30	0.0082**	
			Column factor (muscimol treatment)	F=10.21	1, 30	0.0033**	
		Bonferroni post-hoc test	Veh/Veh vs Veh/Ket			0.0271*	
			Veh/Veh vs Bic/Veh			0.0745	
			Veh/Veh vs Bic/Ket			0.7926	
			Veh/Ket vs Bic/Veh			0.0003***	
			Veh/Ket vs Bic/Ket			0.0349*	
			Bic/Veh vs Bic/Ket			0.036*	
	mPFC AUC $[Glu]_{ext}$	2-way ANOVA	Interaction	F=0.009	1, 28	0.9257	
			Row factor (ketamine treatment)	F=5.107	1, 28	0.0318*	
			Column factor (muscimol treatment)	F=15.47	1, 28	0.0005***	
		Bonferroni post-hoc test	Veh/Veh vs Veh/Ket			0.0136*	
			Veh/Veh vs Bic/Veh			0.1177	

			Veh/Veh vs Bic/Ket			0.2485	
			Veh/Ket vs Bic/Veh			0.0001***	
			Veh/Ket vs Bic/Ket			0.1249	
			Bic/Veh vs Bic/Ket			0.0065**	
	mPFC AUC $[GABA]_{ext}$	2-way ANOVA	Interaction	F=1.075	1, 28	0.3087	
			Row factor (ketamine treatment)	F=15.26	1, 28	0.0005***	
			Column factor (muscimol treatment)	F=1.508	1, 28	0.2296	
		Bonferroni post-hoc test	Veh/Veh vs Veh/Ket			0.1205	
			Veh/Veh vs Bic/Veh			0.066	
			Veh/Veh vs Bic/Ket			0.0686	
			Veh/Ket vs Bic/Veh			0.0011**	
			Veh/Ket vs Bic/Ket			0.0008***	
			Bic/Veh vs Bic/Ket			0.8933	
DHK – Forced swim test	Swimming duration	Unpaired t-test (two-tailed) with Welch's correction		t=2.685 df=7.411		0.0297*	**4B**
DHK - Microdialysis (local perfusion)	Microdialysis: mPFC AUC $[5\text{-}HT]_{ext}$	Unpaired t-test (two-tailed) with Welch's correction		t=4.970 df=5.947		0.0026**	**4F**
	Microdialysis: mPFC AUC $[Glu]_{ext}$	Unpaired t-test (two-tailed) with Welch's correction		t=2.838 df=5.266		0.0343*	**4G**
	Microdialysis: mPFC AUC $[GABA]_{ext}$	Unpaired t-test (two-tailed) with Welch's correction		t=4.236 df=6.028		0.0054**	**4H**
	Microdialysis: mPFC AUC $[Gln]_{ext}$	Unpaired t-test (two-tailed) with Welch's correction		t=3.281 df=5.248		0.0204*	**4J**
Optogenetic-microdialysis-FST: **activation**	Forced Swim Test: Swimming duration	Unpaired t-test (two-tailed) with Welch's correction		t=5.697 df=6.687		0.0009 ***	**S1B**
	Microdialysis: mPFC AUC $[5\text{-}HT]_{ext}$	Unpaired t-test (two-tailed) with Welch's correction		t=2.6 df=6.154		0.0397 *	**S1D**
	Microdialysis: DRN AUC $[5\text{-}HT]_{ext}$	Unpaired t-test (two-tailed) with Welch's correction		t=0.9732 df=8.131		0.3585	**S1F**
	Linear regression - **ChR2**: mPFC 5-HT content - swimming			R^2=0.73		0.0141 *	**S1G**
	Linear regression – **ChR2**: DRN 5-HT content - swimming			R^2=0.76		0.0239 *	**S1H**

	Linear regression - **Control**: mPFC 5-HT content - swimming			R^2=0.42		0.2386	**S1G**
	Linear regression - **Control**: DRN 5-HT content - swimming			R^2=0.1		0.6017	**S1H**
Optogenetic-microdialysis-FST: **inhibition**	Forced Swim Test: Swimming duration	ANOVA two-way	Interaction	F=3.12	1, 15	0.0977	**S2B**
			Row factor (ketamine treatment)	F=0.7539	1, 15	0.3989	
			Column factor (laser inhibition)	F=1.671	1, 15	0.2156	
			Subjects (matching)	F=4.865	15,15	0.002 *	
		Bonferroni post-hoc test	Control			>0.9999	
			Arch			0.0423 *	
	Microdialysis: mPFC AUC $[5\text{-HT}]_{ext}$	Paired t-test (two-tailed) Wilcoxon	Ket Laser vs Ket D2			0.0289 *	**S2E**
	Microdialysis: DRN AUC $[5\text{-HT}]_{ext}$	Paired t-test (two-tailed) Wilcoxon	Ket Laser vs Ket D2			0.0171 *	**S2G**
	Linear regression - **Arch**: mPFC 5-HT content - swimming			R^2=0		0.9057	**S2H**
	Linear regression - **Arch**: DRN 5-HT content - swimming			R^2=0		0.8239	**S2I**
	Linear regression - **Conrol**: mPFC 5-HT content - swimming			R^2=0.03		0.7348	**S2H**
	Linear regression - **Control**: DRN 5-HT content - swimming			R^2=0.52		0.104	**S2I**

Résultats complémentaires

1- Comparer l'effet antidépresseur du (2*R*,6*R*)-hydroxynorkétamine avec celui de son isomère (2*S*,6*S*)-hyrdoxynorkétamine

2- L'effet de la kétamine intra-mPFC dans le test de microdialyse couplée avec le Novelty Suppressed Feeding (NSF)

1 – Comparer l'effet antidépresseur rapide du (2*R*,6*R*)-HNK avec celui du (2*S*,6*S*)-HNK

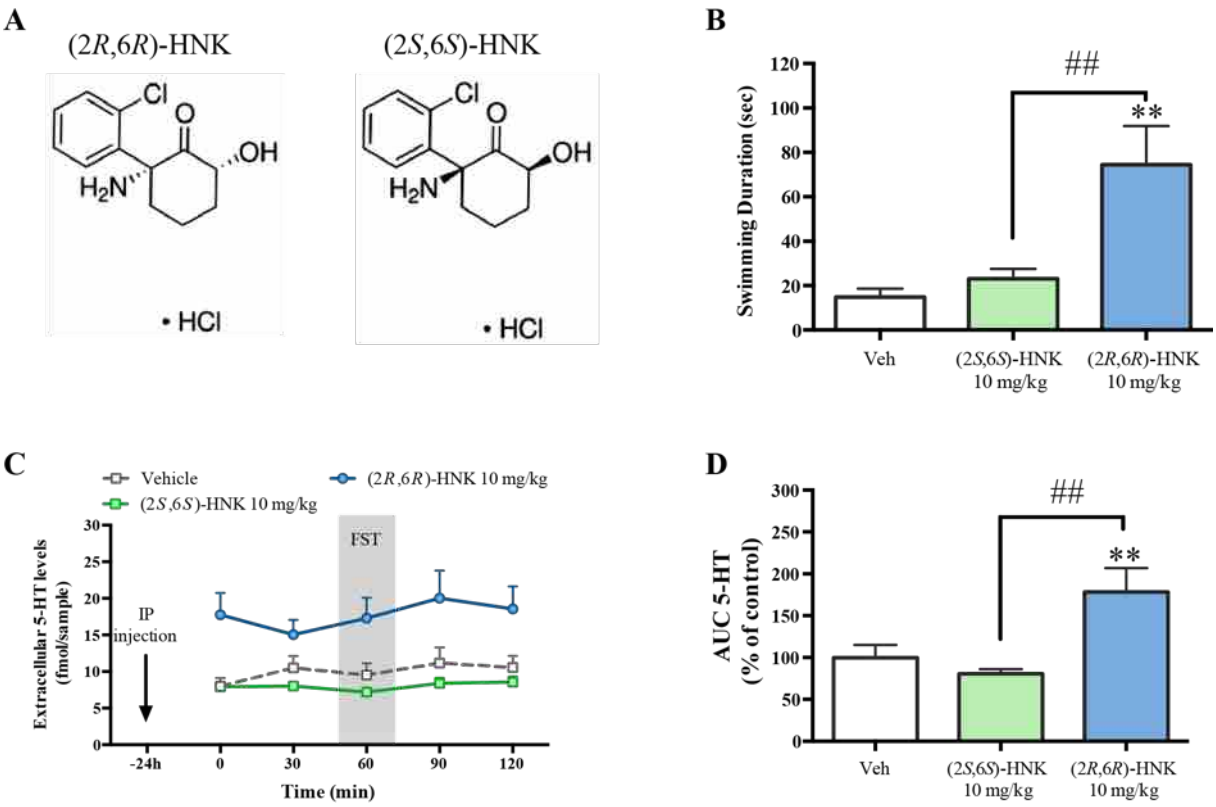

Figure 24. Le (2S,6S)-hyrodxynorkétamine (HNK) n'as pas d'effet antidépresseur comme son isomère, le (2R,6R)-HNK

A) Les structures chimiques de deux molécules

B) Différent du (2R,6R)-HNK (10 mg/kg, i.p.), le (2S,6S)-HNK (10 mg/kg, i.p.), injecté à 24h avant l'expérience n'augmente pas la durée de nage dans la nage forcée (forced swim test – FST) chez la souris.

C) La course du temps des effets de deux molécules sur le taux de 5-HT dans le cortex médian préfrontal (mPFC), mesurée par la microdialyse *in vivo* chez la même souris de FST. La carrée grise indique le moment de FST (à t60 min).

D) Les valeurs des aires sous la courbe (AUC) du taux de 5-HT à partir de la course du temps.

** p<0,01 vs le groupe véhicule (Veh)

p<0,01 entre groupes sélectionnés

Les détails de statistiques :

Expérience	Test statistique	Les valeurs de F	*Post-hoc* test	
FST	ANOVA one-way	$F_{2,13}$ = 9,836 p = 0,0025**	Veh vs (2R,6R)-HNK	p = 0,0041**
			(2R,6R)-HNK vs (2S,6S)-HNK	p = 0,0089**
Microdialyse	ANOVA one-way	$F_{2,27}$ = 7,876 p = 0,002**	Veh vs (2R,6R)-HNK	p = 0,0075**
			(2R,6R)-HNK vs (2S,6S)-HNK	p = 0,0008**

Commentaires :

La comparaison de deux isomères de HNK dans ce test de microdialyse couplé le FST montre que :

Des deux molécules, le (2*R*,6*R*)-HNK est le seul isomère actif pouvant exercer un effet antidépresseur similaire à celui de la molécule mère.

Le (2*R*,6*R*)-HNK est plus intéressant à étudier dans les futures études, en comparaison avec la kétamine, afin de mieux comprendre leurs propriétés particulières produisant ces effets thérapeutiques.

2- L'effet de la kétamine intra-mPFC dans le test de microdialyse couplée avec le Novelty Suppressed Feeding (NSF)

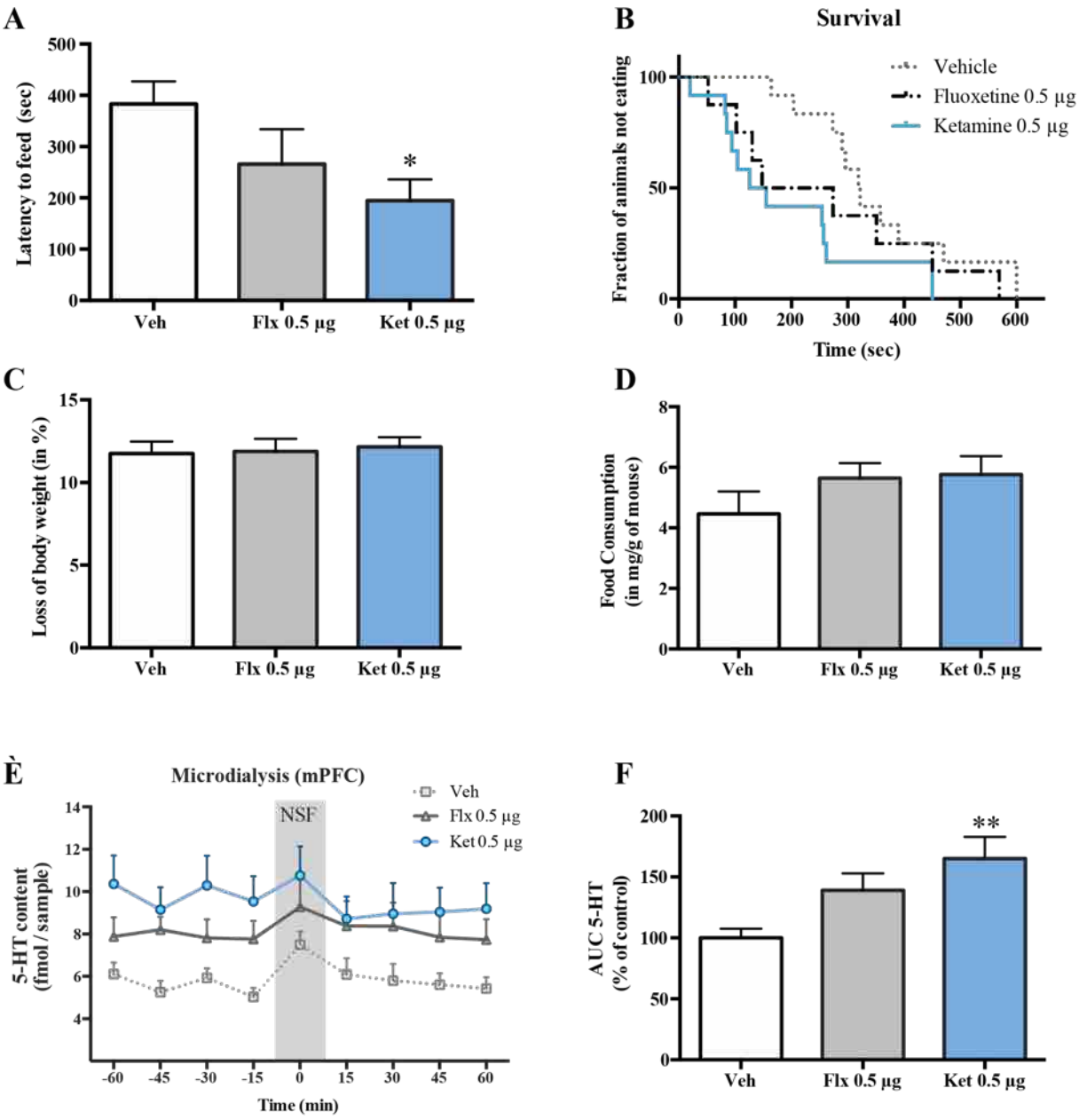

Figure 25. La kétamine intra-mPFC induit un effet antidépresseur dans le test de microdialyse couplée avec le NSF

A, B) La kétamine (0,5 µg intra-mPFC) injectée 24h avant l'expérience, a diminué la latence à se nourrir de façon plus potentielle que celle de la fluoxétine injectée dans la même condition.

C, D) Il n'y a pas de différence statistique de la perte du poids corporel et de la consommation de nourriture entre 3 groupes de traitements.

E) La course du temps des effets de deux molécules sur le taux de 5-HT dans le mPFC, mesurée par la microdialyse *in vivo* chez la même souris de NSF. La carrée grise indique le moment de NSF (à t0).

D) Les valeurs des aires sous la courbe (AUC) du taux de 5-HT à partir de la course du temps. La kétamine augmente la concentration extracellulaire de la 5-HT de façon plus potentielle que celle de la fluoxétine.

* p<0,05 ; **p<0,01 vs le groupe véhicule (Veh)

Les détails de statistiques :

Expérience	Test statistique	Les valeurs de F	*Post-hoc* test	
NSF : Latence à se nourrir	ANOVA one-way	$F_{2,29} = 4,236$ $p = 0,024$*	Veh vs Ket	p = 0,0217*
	Mantel-Cox survival test	p = 0.0464*		
NSF: Perte de poids corporel	ANOVA one-way	$F_{2,29} = 0,089$ $p = 0,91$		
NSF: Consommation de nourriture	ANOVA one-way	$F_{2,29} = 1,372$ $p = 0,269$		
Microdialyse	ANOVA one-way	$F_{2,54} = 6,472$ $p = 0,003$**	Veh vs Ket	p = 0,0023**

Commentaires :

Le NSF permet de prédire des activités de type anxiolytique/antidépresseur chez la souris. L'effet antidépresseur d'une seule dose de la kétamine (0,5 µg) injectée intra-mPFC dans ce test valide, encore une fois, l'activité de type antidépresseur de cette molécule. En plus, le couplage du NSF avec la microdialyse nous a permis de suivre les changements de la 5-HT dans le mPFC. Nous avons retrouvé l'augmentation de la 5-HT dans cette région 24h après l'injection de la kétamine, similaire aux résultats de test de la microdialyse couplée avec le FST (voir les 3 articles au-dessus).

La mise au point de ce test a ouvert effectivement des possibilités de coupler la microdialyse *in vivo* avec des tests comportementaux différents pour récupérer au maximum les données expérimentales chez l'animal et associer ces résultats pour mieux expliquer l'origine de ces comportements.

Un point difficile à noter pour cette expérience est que la mise à jeun de l'animal est en même temps que l'implantation des sondes de microdialyse. Donc, 24h après, l'effet de la faim est plus important, ce qui a rendu l'animal plus agressif. Le couplage des sondes de microdialyse a aussi modifié la latence à se nourrir chez ces animaux comme il y avait plusieurs animaux qui avaient commencé à manger après 10 minutes (le temps théorique maximum dans le protocole original). Nous avons mis tous ces animaux qui ont mangé après 10 minutes à 600 secondes pour ne pas perturber le test original. Diminuer la durée de la faim pourrait probablement diminuer ces effets irritants et la souffrance des animaux.

Discussion

Ces travaux de thèse ont permis d'étudier l'effet antidépresseur rapide de la kétamine chez la souris, impliquant les neurotransmissions glutamatergique, GABAergique et sérotoninergique.

L'hypothèse actuelle de la désinhibition corticale indirecte concernant la cascade d'événements cellulaires et moléculaires conduisant à une activité antidépressive rapide d'une dose aiguë de kétamine peut être résumée comme suit: la kétamine se lie au R-NMDA situé sur les interneurones GABAergiques et induit un blocage sélectif de ces interneurones inhibiteurs, augmentant ainsi la libération de glutamate (potentialisation à long terme - LTP) à partir des cellules pyramidales situées dans le mPFC. Suite à cette libération, le R-AMPA, un canal Na^+/Ca^{2+} ligand-dépendant, situé sur les neurones glutamatergiques post-synaptiques, est activé comme cela a été décrit par plusieurs auteurs (voir Duman *et al.*, 2016; Miller *et al.*, 2016; Rantamaki & Yalcin, 2016). Il résulte de cette activation une augmentation de la synthèse et de la libération de BDNF, ce qui active la voie de signalisation TrkB/Akt, puis celle de mTORC1 dans le mPFC (groupe de Duman: Li *et al.*, 2010), mais désactive celle de la kinase eEF2 dans l'hippocampe ventral (groupe de Monteggia: Autry *et al.*, 2011). Finalement, ces cascades conduisent à la maturation des synapses et à la synaptogenèse, elles-mêmes responsables de la plasticité synaptique et de l'activité rapide de type antidépresseur.

Cependant, plusieurs points doivent être clarifiés. L'un d'entre eux est de savoir si, en plus du glutamate, la libération de GABA et de 5-HT participe à cette voie. La kétamine est susceptible d'augmenter ces trois neurotransmetteurs, notamment dans le mPFC, mais plusieurs autres circuits cérébraux spécifiques pourraient également contribuer à son activité antidépressive. En utilisant la technique de microdialyse chez la souris vigile, nous avons trouvé une augmentation des concentrations extracellulaires de glutamate, GABA et 5-HT (Glu_{ext}, $GABA_{ext}$ et $5\text{-}HT_{ext}$, respectivement) dans le mPFC concomitamment à une augmentation de la durée de nage dans le FST chez la même souris (**Article 1 et 2**), alors que plusieurs auteurs ont rapporté une augmentation de seulement un ou deux de ces quatre paramètres. De ce fait, la question de savoir quel neurotransmetteur est affecté en premier pour conduire à la modification des autres reste méconnue.

Libération du glutamate

Dans les études de microdialyse, l'augmentation de Glu_{ext} après l'administration d'une dose unique et infra-anesthésique de kétamine a été observée dans le mPFC, soit

immédiatement après son administration (chez le rat: Lopez-Gil *et al.*, 2007; Lorrain *et al.*, 2003; Moghaddam *et al.*, 1997), soit 24h après (chez les souris: Pham *et al.*, 2017a – **Article 2**). Ainsi, l'effet de type antidépresseur rapide de la kétamine conduirait à une libération rapide de glutamate qui déclencherait une cascade d'événements ultérieurs impliquant la stimulation de la neurotransmission GABAergique et sérotoninergique. Puisque la kétamine se lie au R-NMDA du glutamate, la libération de glutamate dans le circuit mPFC/hippocampe/NRD est probablement le premier neurotransmetteur à déclencher la cascade cellulaire responsable de la plasticité synaptique, puis de l'activité antidépressive rapide. Ainsi, si la libération de glutamate est nécessaire aux neurones pyramidaux pour activer les interneurones GABAergiques comme suggéré par Duman *et al.*, 2016, la kétamine, en tant qu'antagoniste du R-NMDA, pourrait affaiblir les connexions entre les cellules pyramidales et les interneurones GABAergiques. Toutefois, il n'est pas certain que ce mécanisme que nous avons décrit comme responsable des effets rapides de type antidépresseur de la kétamine soit également impliqué dans ses effets prophylactiques (Brachman *et al.*, 2016), antalgiques ou psychotomimétiques. En effet, il est probable que les régions cérébrales, les circuits (amygdale et émotion) ou encore les neurotransmetteurs impliqués dans ces différentes propriétés soient différents.

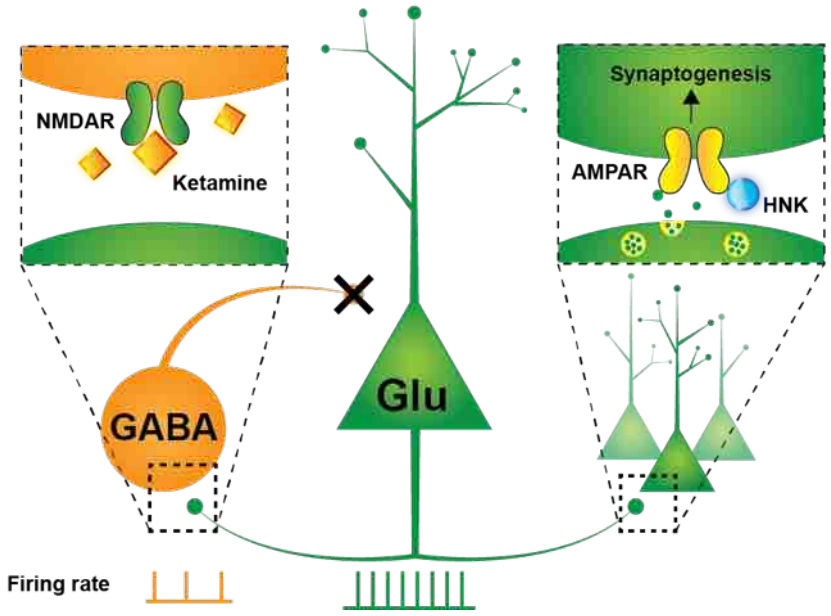

Figure 26. Comparaison du mécanisme d'action de (R,S)-ketamine vs (2R,6R)-HNK sur le système glutamatergique

La kétamine bloquerait le R-NMDA (X) situé sur les interneurones GABAergiques pour les désinhiber. Cela permettrait une augmentation indirecte de l'activité électrique des neurones glutamatergiques pyramidaux du mPFC. À l'inverse, le HNK se fixerait sur le R-AMPA post-synaptique situé sur les neurones glutamatergiques corticaux afin de les activer directement.

À faible dose, quand les effets antidépresseurs sont observables, son métabolite principal, le (2*R*,6*R*)-HNK, est capable d'activer directement le R-AMPA du glutamate (Figure 26), sans se lier au R-NMDA (Zanos *et al.*, 2016). Dans notre laboratoire, nous avons confirmé son effet dans le FST et sur la 5-HT_{ext} corticale, mais nous avons aussi trouvé que le (2*R*,6*R*)-HNK est plus efficace pour augmenter la Glu_{ext} corticale que la (*R,S*)-kétamine. Cela se justifie par sa propriété glutamatergique activatrice directe du R-AMPA post-synaptique entraînant la LTP et la décharge neuronale. Par conséquent, le (2*R*,6*R*)-HNK pourrait potentialiser les effets de sa molécule mère en facilitant la neurotransmission glutamatergique et ainsi renforcer l'excitation corticale.

Libération du GABA

Les résultats concernant les changements de $GABA_{ext}$ après administration de kétamine ont montré soit une augmentation dans le mPFC chez les souris BALB/cJ (Pham *et al.*, 2017a), soit aucun effet dans plusieurs régions du cerveau de rat (Lindefors *et al.*, 1997; Littlewood *et al.*, 2006). Cette dernière réponse de la kétamine chez les souris stressées est difficile à concilier avec l'hypothèse du déficit GABAergique de l'équipe de Duman, expliquant le bénéfice thérapeutique de la kétamine. De manière intéressante, la vortioxétine, nouvel antidépresseur multimodal, inhibe la neurotransmission GABAergique dans certaines régions du cerveau (mPFC, vHipp) via un mécanisme dépendant de l'antagonisme des récepteurs 5-HT_3 et en conséquence désinhibe les neurones pyramidaux et améliore la signalisation glutamatergique (Dale *et al.*, 2017; Riga *et al.*, 2016). Cependant, chez la souris, le stress induit par un stress chronique affaiblit la libération et la recapture de GABA en régulant positivement des micro-ARNs et négativement l'expression corticale de GAD67 (Ma *et al.*, 2016). Il serait donc intéressant d'identifier le type d'interneurones GABAergiques inhibés par la kétamine (parvalbumine - PV, somatostatine – SST ou récepteur 5-HT_{3A}). Par exemple, la vulnérabilité cellulaire au stress est exacerbée dans les interneurones GABAergiques SST-positifs (Lin & Sibille, 2015). Une potentialisation fonctionnelle de la transmission inhibitrice des interneurones GABAergiques SST-positifs sur les cellules pyramidales entraîne une réduction du rapport excitation-inhibition synaptique et est suffisante pour déclencher un phénotype antidépresseur (Fuchs *et al.*, 2017). Ainsi, la balance excitation-inhibition, traduite par le

rapport des concentrations extracellulaires glutamate/GABA retrouvés en microdialyse renforce cette affirmation (Pham *et al.*, 2017a). Ces données confirment les hypothèses du groupe de G. Sanacora concernant le déficit GABAergique dans le TDM et l'amélioration de la transmission synaptique GABAergique par les traitements antidépresseurs. Des augmentations des deux neurotransmetteurs Glu_{ext} et de $GABA_{ext}$ pourraient aider à équilibrer la neurochimie du cerveau puisque l'atrophie neuronale et la diminution du volume de l'hippocampe sont régulièrement décrits chez les patients atteints de TDM (Duman, 2009). Toutefois, une activation prolongée de la neurotransmission glutamatergique dans le cortex et/ou l'hippocampe peut conduire à une augmentation de la Glu_{ext} et à une excitotoxicité rétrograde, une dégénération neuronale ou une susceptibilité aux crises d'épilepsie (Morales *et al.*, 2013). L'étude de la contribution du R-NMDA synaptique *vs* extrasynaptique dans la réponse à la kétamine pourrait rassurer sur cette question. Dans notre étude (Pham *et al.*, 2017a – **Article 2**), la kétamine a augmenté la Glu_{ext} (+100% par rapport au groupe témoin, en pmol/échantillon) de manière plus conséquente que la $GABA_{ext}$ (+50% vs groupe témoin, fmol/échantillon). Ainsi, cette gamme de concentration pourrait se traduire par un rôle pharmacologique (activité antidépressive) ou pathologique (mort neuronale) de Glu_{ext} (Moussawi *et al.*, 2011).

Par ailleurs, notre étude avec le (2*R*,6*R*)-HNK a montré que ce métabolite n'agirait probablement pas de la même manière que sa molécule mère sur le système GABAergique. En effet, alors que la (*R,S*)-kétamine a augmenté la $GABA_{ext}$ corticale, le (2*R*,6*R*)-HNK n'a quant à lui pas eu d'effet sur ce paramètre. De plus, le (2*R*,6*R*)-HNK a induit une augmentation plus importante de Glu_{ext} que la (*R,S*)-kétamine. Enfin, le (2*R*,6*R*)-HNK a augmenté la $5\text{-}HT_{ext}$ corticale dans les mêmes proportions que la (*R,S*)-kétamine. Cela met donc en évidence une différence mécanistique intéressante entre ces deux molécules, dont l'une est antagoniste du R-NMDA et l'autre agoniste du R-AMPA du glutamate. De ce fait, les conséquences sur le système GABAergique pourrait s'expliquer par les différences de propriétés pharmacodynamiques de ces deux molécules. Nous pouvons aussi penser que les effets neurochimiques de la (*R,S*)-kétamine et du (2*R*,6*R*)-HNK se complètent et donc que c'est la combinaison de ces deux molécules qui produit l'effet antidépresseur.

L'altération du système GABAergique induite par la kétamine dépend du type de stress. En effet, un stress chronique diminue la neurotransmission GABAergique tandis qu'une thérapie antidépressive répétée (par exemple, antidépresseurs, ECT ou kétamine) corrige ce

déficit. Cependant, l'augmentation des taux de GABA semble inhabituelle puisque le GABA est le principal neurotransmetteur régulant l'inhibition neurale du cerveau. Cela pourrait s'expliquer par une exacerbation de la libération de glutamate, qui a pour conséquence une augmentation de l'activité électrique rapide des interneurones GABAergiques, puis une augmentation de la libération de GABA par des vésicules GABAergiques. Cependant, cela pourrait ne pas être le cas, du moins dans le PFC et l'hippocampe, puisque la kétamine diminue l'expression de GAD67 dans ces régions cérébrales (N. Wang *et al.*, 2014; Zhou *et al.*, 2015). La GAD67 est l'enzyme qui dégrade le glutamate en GABA au niveau de la synapse tripartite glutamine-glutamate-GABA. La régulation négative de l'expression de GAD67 suggère que la synthèse de GABA n'est pas la cause de l'augmentation de $GABA_{ext}$ que nous avons observée dans le mPFC. Cependant, ceci ne pourrait s'appliquer qu'aux interneurones PV-positifs (fast-spiking), et non pas à d'autres classes d'interneurones (par exemple, SST), étant donné que l'expression de PV est également réduite dans ces études. La diminution de l'expression de la PV facilite les courants synaptiques chez la souris (Caillard *et al.*, 2000), accélérant ainsi la neurotransmission glutamatergique. D'autre part, cette augmentation de $GABA_{ext}$ pourrait aussi s'expliquer par une augmentation de l'utilisation du glucose, qui métabolise le glutamate - le précurseur du GABA (Bonvento *et al.*, 2017), ou encore par un blocage de la recapture du GABA par les transporteurs situés sur les neurones pré-synaptiques ou sur les cellules gliales.

Libération de la sérotonine

Il est probable que l'altération de l'équilibre cortical glutamate/GABA induite par les antagonistes du R-NMDA entraîne des modifications en aval d'autres neurotransmetteurs. Plusieurs groupes de recherche ont décrit des augmentations de la durée de nage dans le FST, un paramètre sérotoninergique (Cryan *et al.*, 2002a), et de la $5\text{-}HT_{ext}$ dans le mPFC après l'administration de kétamine par voie systémique, mais sur des cohortes d'animaux différentes. Dans notre projet (**Article 1, 2 et 3**), nous avons réussi à coupler le FST avec la microdialyse chez une même souris. L'obtention de données comportementales et neurochimiques ont ainsi permis de confirmer l'existence d'une corrélation positive entre la $5\text{-}HT_{ext}$ du mPFC et la durée de nage mesurée chez le même animal, soulignant l'importance de ce test comportemental prédictif de l'activité de type antidépresseur sérotonine-dépendent. Cette corrélation, associée à l'absence d'effet de la kétamine sur la nage chez des souris déplétées en 5-HT centrale (par la pCPA, un inhibiteur de synthèse de la 5-HT), a confirmé

l'implication du système sérotoninergique, en particulier dans le mPFC, dans le mécanisme d'action antidépressive de la kétamine.

Cependant, le mécanisme à la base de l'augmentation de la neurotransmission sérotoninergique induite par la kétamine est intrigant. En effet, il semblerait impliquer une diminution, et non pas une augmentation de l'activité électrique des neurones sérotoninergiques du NRD (Pham *et al.*, 2017b – **Article 1**), un effet similaire à ce qui a été décrit suite à un traitement avec un ISRS (Blier *et al.*, 1988; Le Poul *et al.*, 1995). Toutefois, l'activité électrique des neurones 5-HT revient au niveau basal lors d'un traitement chronique par ISRS, ce qui s'explique par une désensibilisation progressive des autorécepteurs 5-HT_{1A} du NRD (Chaput *et al.*, 1986; Hanoun *et al.*, 2004). L'activation du R-AMPA situé sur les neurones 5-HT dans le NRD pourrait faciliter la libération de 5-HT dans le mPFC, puisque des études précliniques ont montré que les antagonistes sélectifs du R-AMPA bloquent l'activité antidépressive de la kétamine sur la 5-HT_{ext} dans le mPFC. Du mPFC part un dense réseau de projections vers le NRD, soit directement, soit indirectement via des interneurones GABAergiques. Lorsque Gartside *et al.*, 2007 ont évalué les effets de l'activation du récepteur du glutamate sur l'activité des neurones 5-HT du NRD sur des coupes de cerveau de rat, ils ont mis en évidence que le blocage sélectif des récepteurs 5-HT_{1A} somatodendritiques améliorait les effets de l'AMPA et du NMDA sur la réponse excitatrice des neurones 5-HT du NRD. Ces données suggèrent que la 5-HT pourrait être modifiée *a posteriori* par une libération de glutamate induite par la kétamine dans le mPFC, sans pour autant impliquer une activation tonique des autorécepteurs 5-HT_{1A} dans le NRD.

La balance excitation-inhibition glutamatergique/GABAergique

La modification de la neurotransmission glutamatergique et GABAergique par la kétamine, ainsi que l'hypothèse glutamatergique et GABAergique de la dépression, soulignent l'importance de la balance excitation-inhibition dans la MDD et son traitement. La modification de cette balance semble être la clé des thérapies antidépressives, comme le montre une étude récente (Fuchs *et al.*, 2017). Nous pensons que la kétamine est capable d'augmenter à la fois les concentrations de glutamate et de GABA dans le cerveau. L'augmentation de l'excitabilité permet au cerveau de renforcer sa fonction en augmentant la neurotransmission et en renforçant les connexions entre les régions du cerveau. L'élévation du taux de GABA pourrait atténuer les augmentations excessives de glutamate et ainsi

maintenir l'homéostasie du cerveau. Cependant, la manière dont la kétamine induit une telle augmentation reste encore à éclaircir. Les interneurones PV-positifs ciblent préférentiellement les régions à proximité des corps cellulaires des neurones pyramidaux, tandis que les interneurones SST-positifs ciblent plutôt les dendrites (Kuki *et al.*, 2015). Une régulation négative de l'expression de la PV, protéine liant le calcium et contrôlant la synchronisation des potentiels d'action des cellules pyramidales, a été observée après un traitement avec la kétamine. Cependant, peu de données sont disponibles sur la façon dont la kétamine interagit avec les interneurones SST-positifs dans le cerveau. Cette altération induite par la kétamine a déjà été décrite, mais seulement à dose anesthésique (Pongdhana *et al.*, 1987). On peut imaginer que la régulation négative de l'expression de la PV favorise l'émission des potentiels d'action des cellules pyramidales, ce qui conduirait à une augmentation de la libération de glutamate. Cependant, la manière dont les interneurones SST-positifs interagissent avec les dendrites des cellules pyramidales pour transmettre les informations dans les régions sous-corticales nécessite d'être approfondie. Comprendre la manière dont la kétamine est capable d'interagir avec un sous-type particulier d'interneurone GABAergique est un point essentiel à la caractérisation du rôle de la balance excitation-inhibition dans l'activité de type antidépresseur rapide de la kétamine.

Molécules	**FST (nage)**	**5-HT$_{ext}$**	**Glu$_{ext}$**	**GABA$_{ext}$**	**Gln/Glu ratio**	**Glu/GABA ratio**
Ket	↑	↑	↑ (tendance)	↑	↓	∅
HNK	↑	↑	↑	∅	↓	∅
NBQX + Ket (AMPA-R, DRN)	X	X (p=0.14)	X	∅	∅	↑
Muscimol + Ket (GABA$_A$-R, mPFC)	X	X	∅	↑	∅	∅
Bicuculline+Ket (GABA$_A$-R, DRN)	↑	↑	↑	∅	X	∅
DHK	↑	↑↑	↑↑	↑↑	∅	∅
OptoG activation	↑	↑	n/a	n/a	n/a	n/a

Tableau 8. Résumé des résultats expérimentaux obtenus

X: bloqué; ∅: pas d'effet ; ↑: augmenté ; ↓: diminué et n/a : non-inclu

D'après nos résultats résumés (Tableau 8), l'effet de type antidépresseur de la kétamine dans le test de la nage forcée est observé lorsqu'il y a une augmentation simultanée dans le mPFC de 5-HT, glutamate ou des trois neurotransmetteurs : 5-HT, glutamate, GABA. L'augmentation des concentrations extracellulaires corticales soit du glutamate, soit du GABA n'est pas suffisante pour induire un effet antidépresseur de la kétamine. De façon intéressante, nous constatons que dans les cas où l'effet antidépresseur est observé dans le FST, le rapport $Glu_{ext}/GABA_{ext}$, c'est-à-dire la balance excitation-inhibition reste constante dans le cortex. Cela indique une adaptation neuronale flexible pour assurer l'homéostasie centrale et limiter le risque d'excitotoxicité. Pour ces raisons, nous supposons que la balance excitation-inhibition serait un paramètre clé des futurs travaux de recherche visant à examiner les molécules ayant un effet antidépresseur rapide comme la kétamine.

Neurotransmission complexe entre les récepteurs R-NMDA, R-AMPA, R-GABAA et le système sérotoninergique

Le mécanisme des effets antidépresseurs de la kétamine implique de nombreux récepteurs, formant un important réseau dont il faut détailler les éléments. Ici, nous nous sommes concentrés sur les récepteurs R-NMDA, R-AMPA, $R\text{-}GABA_A$ et sérotoninergiques.

La kétamine est un bloqueur du canal calcique du R-NMDA. Bien que le rôle de la sous-unité GluN1 dans les effets antidépresseurs de la kétamine soit toujours un sujet débattu, les sous-unités GluN2A et GluN2B semblent en revanche être essentielles à cet effet car la kétamine bloque les R-NMDA contenant les sous-unités GluN2A et GluN2B (Kotermanski & Johnson, 2009). De ce fait, l'implication de ces deux sous-unités devrait être étudiée en parallèle de l'activité antidépressive de la kétamine. La théorie de la désinhibition de l'activité de type antidépresseur de la kétamine suggère un blocage sélectif du R-NMDA situé sur les interneurones GABAergiques, conduisant à une levée d'inhibition des neurones pyramidaux du cortex, améliorant ainsi leur activité électrique excitatrice. Cette voie est considérée comme indirecte. Puisque les interneurones PV-positifs sont enrichis en sous-unité GluN2A du R-NMDA, et que la régulation négative de l'activité des neurones PV-positifs est fortement impliquée dans les effets de la kétamine, il est possible que celle-ci mobilise davantage cette sous-unité du R-NMDA pour induire son effet désinhibiteur. La sous-unité GluN2B serait plutôt impliquée dans une voie directe participer à l'activité antidépressive de la kétamine. Cette voie directe, selon l'équipe de Miller *et al.*, 2016, a lieu au niveau des dendrites des neurones

pyramidaux, qui, contrairement à la voie indirecte, pourrait ne pas impliquer l'augmentation de Glu_{ext} et 5-HT_{ext}. Le blocage sélectif ou l'élimination de cette sous-unité située sur les neurones pyramidaux participe à l'augmentation rapide des influx excitateurs synaptiques sur ces neurones pour induire des effets antidépresseurs. Cette hypothèse est intéressante puisque les antagonistes sélectifs de GluN2B ont montré des résultats hétérogènes dans les essais cliniques. Des études complémentaires sur les sous-unités GluN2B situées sur les cellules pyramidales permettrait une meilleure compréhension.

Actuellement, tout laisse à penser que l'activation de R-AMPA est essentielle à l'activité antidépresseur de la kétamine. Cependant, la manière dont la kétamine exerce ses effets, à savoir en agissant directement sur R-AMPA ou indirectement par blocage du R-NMDA situé sur les interneurones GABAergiques, reste méconnue. L'activation du R-AMPA pourrait être nécessaire à l'activité rapide de la kétamine (c'est-à-dire lorsque l'administration a lieu 30 minutes avant le test) pour déclencher la libération de glutamate, tandis que le blocage du R-NMDA pourrait plutôt être impliqué dans ses effets prolongés. Le processus de trafic du R-AMPA s'avère essentiel pour expliquer les effets durables de la kétamine, car il améliore la synaptogenèse et la connectivité fonctionnelle entre les régions du cerveau (Duman & Aghajanian, 2012). De plus, l'altération de l'expression des sous-unités du R-NMDA chez les souris knock-out de GluA1 et l'altération de l'expression des sous-unités du R-AMPA chez les souris knock-out pour la sous-unité GluN2B ont confirmé l'existence d'une interaction entre ces deux sous-types de récepteurs glutamatergiques. Ces deux récepteurs modulent également la décharge des neurones 5-HT et la libération locale de GABA dans le NRD.

Nous ne savons toujours pas dans quelle mesure les connexions monosynaptiques (ou directes) et disynaptiques – ou indirectes *via* les interneurones GABAergiques entre le mPFC et le NRD sont impliquées dans les effets centraux de la kétamine. La connexion monosynaptique entre les neurones glutamatergiques du mPFC et les neurones sérotoninergiques du NRD pourraient moduler directement l'augmentation de la libération de 5-HT présynaptique. En revanche, la voie disynaptique via les interneurones GABAergiques pourrait impliquer des phénomènes plus complexes dans lesquels les R-AMPA, R-NMDA et R-$GABA_A$ interagiraient de manière concomitante pour induire une augmentation des taux corticaux de GABA (Figure 27). Ceci pourrait impliquer les interneurones des deux régions, du mPFC et du NRD, puisque la kétamine corrige le déficit de neurotransmission GABAergique, de

manière plus efficace dans le mPFC, région connue pour ses projections denses vers les neurones GABAergiques du NRD.

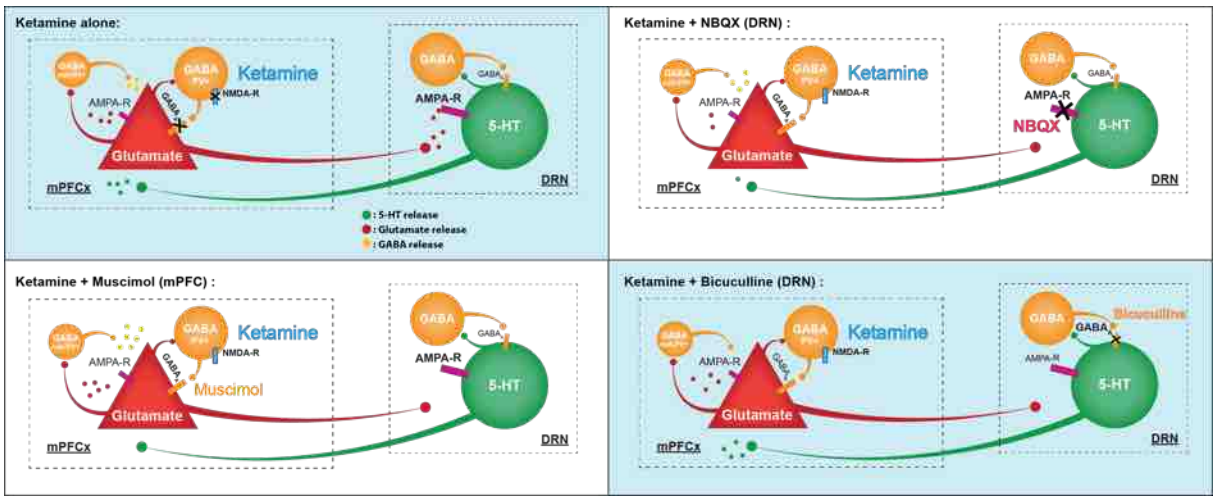

Figure 27. Résumé de l'effet de la kétamine en combinaison avec différentes molécules
(NBQX : antagoniste du R-AMPA, muscimol : agoniste du R-GABA$_A$ et bicuculline : antagoniste du R-GABA$_A$)

La technique d'optogénétique devrait aider à différencier efficacement ces deux voies monosynaptiques et disynaptiques distinctes. Cette approche innovante est largement utilisée aujourd'hui pour étudier les circuits cérébraux. En utilisant des récepteurs photosensibles, cette technique permet aux neurobiologistes d'activer ou inhiber des voies neuronales spécifiques avec une sélectivité élevée des types neuronaux. Des études utilisant une approche par optogénétique, en combinaison avec des techniques conventionnelles (par exemple, la microdialyse, l'électrophysiologie) devraient être menées pour examiner le rôle spécifique de chaque type neuronal (glutamate, GABA, 5-HT) de certains circuits tels que le mPFC-NRD et le mPFC-vHipp. Cela permettrait de mieux comprendre les connexions entre les neurones de ces régions et l'ordre dans lequel elles sont mobilisées dans l'activité antidépressive de la kétamine.

Selon nos résultats (**Article 3**), le R-AMPA du NRD et le R-GABA$_A$ du mPFC semblent fortement impliqués dans le mécanisme d'action de la kétamine. Après un prétraitement par la bicuculline (antagoniste du R-GABA$_A$) dans le NRD, nous n'avons pas observé d'influence sur les effets de la kétamine. Cela pourrait s'expliquer par le choix de la dose, bien qu'elle soit couramment utilisée dans la littérature (Carreno *et al.*, 2016). Dans cet article, l'équipe de Carreno a montré une hypothèse intéressante du contrôle négative des interneurones GABAergiques du NRD sur la voie indirecte du circuit mPFC-vHipp. Le blocage de ces

interneurones pourrait faciliter l'effet activateur de ce circuit par optogénétique. Dans notre étude du circuit mPFC-NRD, nous pensions observer un effet potentialisateur de la bicuculline intra-DRN sur la kétamine, mais cette molécule n'a ni bloqué, ni renforcé les effets de la kétamine. Il serait donc intéressant d'injecter la bicuculline à une dose plus forte ou dans une autre région cérébrale pour apporter des informations supplémentaires qui pourraient soutenir ces résultats.

Par optogénétique, nous avons montré que la stimulation des neurones glutamatergiques du mPFC a induit un effet antidépresseur et activé la neurotransmission sérotoninergique corticale. Les résultats de l'inhibition optogénétique du circuit mPFC-NRD sont en cours de validation. D'autres circuits pourraient bien sûr participer au mécanisme d'action de la kétamine.

Conclusions

Conclusion

Dans ces travaux expérimentaux, nous avons principalement mis en évidence l'effet antidépresseur "soutenu" (i.e., 24h après administration) d'une dose unique et infra-anesthésique de la kétamine chez la souris BALB/cJ présentant un phénotype anxio-dépressif. Ces effets sont accompagnés d'une augmentation des concentrations de 5-HT_{ext}, Glu_{ext} et $GABA_{ext}$ dans le mPFC. Son métabolite, le (2*R*,6*R*)-HNK possède également une activité antidépressive chez la souris en augmentant la 5-HT_{ext} et la Glu_{ext} mais sans effet sur la $GABA_{ext}$ ce qui le distingue de la molécule mère.

D'autre part, nos résultats pharmacologiques et ceux préliminaires d'optogénétique (en cours de validation) sur l'étude du circuit mPFC-NRD montrent **un rôle importante des récepteurs $GABA_A$ (il ne faut pas les activer dans le mPFC) et AMPA (il faut les activer dans le NRD),** mais aussi le recrutement du système glutamatergique dans l'effet antidépresseur de la kétamine. La **balance excitation-inhibition corticale** semble être un paramètre clé dans les futures études visant à examiner de nouveaux agents antidépresseurs rapides et efficaces.

Perspectives

Les suites de ce travail peuvent s'articuler selon plusieurs axes :

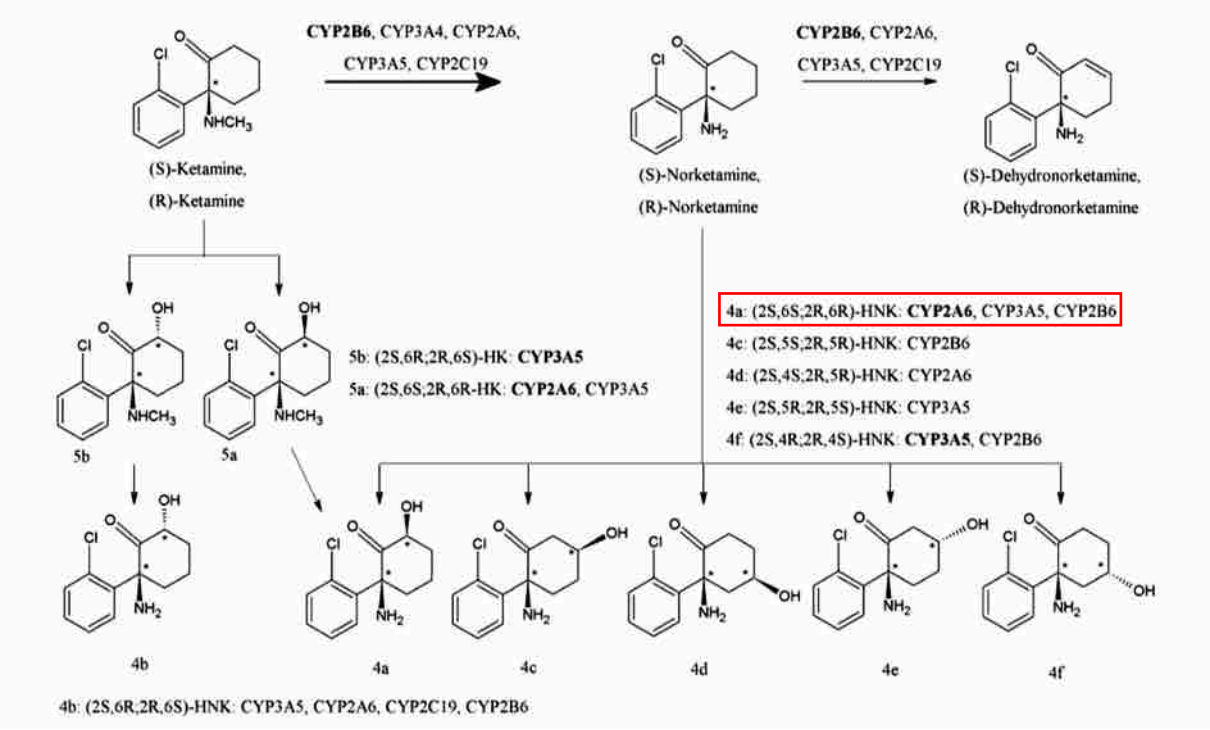

Figure 28. Les transformations métaboliques de la kétamine in vitro (Desta et al., 2012)

- Étudier l'effet du métabolisme de la kétamine vers le HNK en inhibant le métabolisme hépatique (blocage du CYP3A4 par exemple) pour confirmer la forte implication de ce métabolite dans les effets de la kétamine (Figure 28).

- Définir les répondeurs de kétamine et les non-répondeurs dans des modèles d'anxiété/dépression chez les rongeurs, ce qui pourrait apporter des informations pertinentes en ligne avec l'intérêt clinique de la kétamine dans le DRT. L'expression des protéines représentant une combinaison de marqueurs associés au maintien des animaux dans un état réfractaire, ou associés à une amélioration du comportement (Mekiri *et al.*, November 2015; Mendez-David *et al.*, 2017).

- Étudier les interneurones GABAergiques PV- et SST-positifs dans les régions spécifiques comme le mPFC et l'hippocampe.

Références bibliographiques

(La liste des références ci-dessous n'inclut pas toutes les références de la revue et des articles)

1. Aghajanian, G. K., & Marek, G. J. (**1997**). Serotonin induces excitatory postsynaptic potentials in apical dendrites of neocortical pyramidal cells. *Neuropharmacology, 36*(4-5), 589-599.

2. Amat, J., Dolzani, S. D., Tilden, S., Christianson, J. P., Kubala, K. H., Bartholomay, K., Sperr, K., Ciancio, N., Watkins, L. R., & Maier, S. F. (**2016**). Previous Ketamine Produces an Enduring Blockade of Neurochemical and Behavioral Effects of Uncontrollable Stress. *J Neurosci, 36*(1), 153-161.

3. Autry, A. E., Adachi, M., Nosyreva, E., Na, E. S., Los, M. F., Cheng, P. F., Kavalali, E. T., & Monteggia, L. M. (**2011**). NMDA receptor blockade at rest triggers rapid behavioural antidepressant responses. *Nature, 475*(7354), 91-95.

4. Berman, R. M., Cappiello, A., Anand, A., Oren, D. A., Heninger, G. R., Charney, D. S., & Krystal, J. H. (**2000**). Antidepressant effects of ketamine in depressed patients. *Biol Psychiatry, 47*(4), 351-354.

5. Bert, L., Favale, D., Jego, G., Greve, P., Guilloux, J. P., Guiard, B. P., Gardier, A. M., Suaud-Chagny, M. F., & Lestage, P. (**2004**). Rapid and precise method to locate microdialysis probe implantation in the rodent brain. *J Neurosci Methods, 140*(1-2), 53-57.

6. Blier, P., Chaput, Y., & de Montigny, C. (**1988**). Long-term 5-HT reuptake blockade, but not monoamine oxidase inhibition, decreases the function of terminal 5-HT autoreceptors: an electrophysiological study in the rat brain. *Naunyn Schmiedebergs Arch Pharmacol, 337*(3), 246-254.

7. Bodnoff, S. R., Suranyi-Cadotte, B., Aitken, D. H., Quirion, R., & Meaney, M. J. (**1988**). The effects of chronic antidepressant treatment in an animal model of anxiety. *Psychopharmacology (Berl), 95*(3), 298-302.

8. Bonvento, G., Valette, J., Flament, J., Mochel, F., & Brouillet, E. (**2017**). Imaging and spectroscopic approaches to probe brain energy metabolism dysregulation in neurodegenerative diseases. *J Cereb Blood Flow Metab, 37*(6), 1927-1943.

9. Brachman, R. A., McGowan, J. C., Perusini, J. N., Lim, S. C., Pham, T. H., Faye, C., Gardier, A. M., Mendez-David, I., David, D. J., Hen, R., & Denny, C. A. (**2016**). Ketamine as a Prophylactic Against Stress-Induced Depressive-like Behavior. *Biol Psychiatry, 79*(9), 776-786.

10. Bromet, E., Andrade, L. H., Hwang, I., Sampson, N. A., Alonso, J., de Girolamo, G., de Graaf, R., Demyttenaere, K., Hu, C., Iwata, N., Karam, A. N., Kaur, J., Kostyuchenko, S., Lepine, J. P., Levinson, D., Matschinger, H., Mora, M. E., Browne, M. O., Posada-Villa, J., Viana, M. C., Williams, D. R., & Kessler, R. C. (**2011**). Cross-national epidemiology of DSM-IV major depressive episode. *BMC Med, 9*, 90.

11. Caddy, C., Giaroli, G., White, T. P., Shergill, S. S., & Tracy, D. K. (**2014**). Ketamine as the prototype glutamatergic antidepressant: pharmacodynamic actions, and a systematic review and meta-analysis of efficacy. *Ther Adv Psychopharmacol, 4*(2), 75-99.

12. Caillard, O., Moreno, H., Schwaller, B., Llano, I., Celio, M. R., & Marty, A. (**2000**). Role of the calcium-binding protein parvalbumin in short-term synaptic plasticity. *Proc Natl Acad Sci U S A, 97*(24), 13372-13377.

13. Calcagno, E., & Invernizzi, R. W. (**2010**). Strain-dependent serotonin neuron feedback control: role of serotonin 2C receptors. *J Neurochem, 114*(6), 1701-1710.

14. Carreno, F. R., Donegan, J. J., Boley, A. M., Shah, A., DeGuzman, M., Frazer, A., & Lodge, D. J. (**2016**). Activation of a ventral hippocampus-medial prefrontal cortex pathway is both necessary and sufficient for an antidepressant response to ketamine. *Mol Psychiatry, 21*(9), 1298-1308.

15. Chaput, Y., de Montigny, C., & Blier, P. (**1986**). Effects of a selective 5-HT reuptake blocker, citalopram, on the sensitivity of 5-HT autoreceptors: electrophysiological studies in the rat brain. *Naunyn Schmiedebergs Arch Pharmacol, 333*(4), 342-348.

16. Crick, F. (**1999**). The impact of molecular biology on neuroscience. *Philos Trans R Soc Lond B Biol Sci, 354*(1392), 2021-2025.

17. Cryan, J. F., Markou, A., & Lucki, I. (**2002a**). Assessing antidepressant activity in rodents: recent developments and future needs. *Trends Pharmacol Sci, 23*(5), 238-245.

18. Cryan, J. F., & Mombereau, C. (**2004**). In search of a depressed mouse: utility of models for studying depression-related behavior in genetically modified mice. *Mol Psychiatry, 9*(4), 326-357.

19. Cryan, J. F., Page, M. E., & Lucki, I. (**2002b**). Noradrenergic lesions differentially alter the antidepressant-like effects of reboxetine in a modified forced swim test. *Eur J Pharmacol, 436*(3), 197-205.

20. Dale, E., Grunnet, M., Pehrson, A. L., Frederiksen, K., Larsen, P. H., Nielsen, J., Stensbol, T. B., Ebert, B., Yin, H., Lu, D., Liu, H., Jensen, T. N., Yang, C. R., & Sanchez, C. (**2017**). The multimodal antidepressant vortioxetine may facilitate pyramidal cell firing by inhibition of 5-HT3 receptor expressing interneurons: An in vitro study in rat hippocampus slices. *Brain Res*

21. David, D. J., Samuels, B. A., Rainer, Q., Wang, J. W., Marsteller, D., Mendez, I., Drew, M., Craig, D. A., Guiard, B. P., Guilloux, J. P., Artymyshyn, R. P., Gardier, A. M., Gerald, C., Antonijevic, I. A., Leonardo, E. D., & Hen, R. (**2009**). Neurogenesis-dependent and -independent effects of fluoxetine in an animal model of anxiety/depression. *Neuron, 62*(4), 479-493.

22. Defaix, C., Solgadi, A., Pham, T. H., Gardier, A. M., Chaminade, P., & Tritschler, L. (**2018**). Rapid analysis of glutamate, glutamine and GABA in mice frontal cortex microdialysis samples using HPLC coupled to electrospray tandem mass spectrometry. *J Pharm Biomed Anal, 152*, 31-38.

23. Deisseroth, K. (**2011**). Optogenetics. *Nat Methods, 8*(1), 26-29.

24. Deisseroth, K., Feng, G., Majewska, A. K., Miesenbock, G., Ting, A., & Schnitzer, M. J. (**2006**). Next-generation optical technologies for illuminating genetically targeted brain circuits. *J Neurosci, 26*(41), 10380-10386.

25. Delgado, J. M., DeFeudis, F. V., Roth, R. H., Ryugo, D. K., & Mitruka, B. M. (**1972**). Dialytrode for long term intracerebral perfusion in awake monkeys. *Arch Int Pharmacodyn Ther, 198*(1), 9-21.

26. Desta, Z., Moaddel, R., Ogburn, E. T., Xu, C., Ramamoorthy, A., Venkata, S. L., Sanghvi, M., Goldberg, M. E., Torjman, M. C., & Wainer, I. W. (**2012**). Stereoselective and regiospecific hydroxylation of ketamine and norketamine. *Xenobiotica, 42*(11), 1076-1087.

27. Dugue, G. P., Akemann, W., & Knopfel, T. (**2012**). A comprehensive concept of optogenetics. *Prog Brain Res, 196*, 1-28.

28. Dugue, G. P., & Tricoire, L. (**2015**). [Principles and applications of optogenetics in neuroscience]. *Med Sci (Paris), 31*(3), 291-303.

29. Dulawa, S. C., Holick, K. A., Gundersen, B., & Hen, R. (**2004**). Effects of chronic fluoxetine in animal models of anxiety and depression. *Neuropsychopharmacology, 29*(7), 1321-1330.

30. Duman, R. S. (**2009**). Neuronal damage and protection in the pathophysiology and treatment of psychiatric illness: stress and depression. *Dialogues Clin Neurosci, 11*(3), 239-255.

31. Duman, R. S., & Aghajanian, G. K. (**2012**). Synaptic dysfunction in depression: potential therapeutic targets. *Science, 338*(6103), 68-72.

32. Duman, R. S., Aghajanian, G. K., Sanacora, G., & Krystal, J. H. (**2016**). Synaptic plasticity and depression: new insights from stress and rapid-acting antidepressants. *Nat Med, 22*(3), 238-249.

33. Duman, R. S., & Voleti, B. (**2012**). Signaling pathways underlying the pathophysiology and treatment of depression: novel mechanisms for rapid-acting agents. *Trends Neurosci, 35*(1), 47-56.

34. Duric, V., Banasr, M., Licznerski, P., Schmidt, H. D., Stockmeier, C. A., Simen, A. A., Newton, S. S., & Duman, R. S. (**2010**). A negative regulator of MAP kinase causes depressive behavior. *Nat Med, 16*(11), 1328-1332.

35. Farrant, M., & Nusser, Z. (**2005**). Variations on an inhibitory theme: phasic and tonic activation of GABA(A) receptors. *Nat Rev Neurosci, 6*(3), 215-229.

36. Ferres-Coy, A., Santana, N., Castane, A., Cortes, R., Carmona, M. C., Toth, M., Montefeltro, A., Artigas, F., & Bortolozzi, A. (**2013**). Acute 5-HT(1)A autoreceptor knockdown increases antidepressant responses and serotonin release in stressful conditions. *Psychopharmacology (Berl), 225*(1), 61-74.

37. Fond, G., Loundou, A., Rabu, C., Macgregor, A., Lancon, C., Brittner, M., Micoulaud-Franchi, J. A., Richieri, R., Courtet, P., Abbar, M., Roger, M., Leboyer, M., & Boyer, L. (**2014**). Ketamine administration in depressive disorders: a systematic review and meta-analysis. *Psychopharmacology (Berl), 231*(18), 3663-3676.

38. Frye, M. A., Blier, P., & Tye, S. J. (**2015**). Concomitant benzodiazepine use attenuates ketamine response: implications for large scale study design and clinical development. *J Clin Psychopharmacol, 35*(3), 334-336.

39. Fuchikami, M., Thomas, A., Liu, R., Wohleb, E. S., Land, B. B., DiLeone, R. J., Aghajanian, G. K., & Duman, R. S. (**2015**). Optogenetic stimulation of infralimbic PFC reproduces ketamine's rapid and sustained antidepressant actions. *Proc Natl Acad Sci U S A, 112*(26), 8106-8111.

40. Fuchs, T., Jefferson, S. J., Hooper, A., Yee, P. H., Maguire, J., & Luscher, B. (**2017**). Disinhibition of somatostatin-positive GABAergic interneurons results in an anxiolytic and antidepressant-like brain state. *Mol Psychiatry, 22*(6), 920-930.

41. Fukumoto, K., Iijima, M., & Chaki, S. (**2016**). The Antidepressant Effects of an mGlu2/3 Receptor Antagonist and Ketamine Require AMPA Receptor Stimulation in the mPFC

and Subsequent Activation of the 5-HT Neurons in the DRN. *Neuropsychopharmacology, 41*(4), 1046-1056.

42. Gartside, S. E., Cole, A. J., Williams, A. P., McQuade, R., & Judge, S. J. (**2007**). AMPA and NMDA receptor regulation of firing activity in 5-HT neurons of the dorsal and median raphe nuclei. *Eur J Neurosci, 25*(10), 3001-3008.

43. Gasull-Camos, J., Tarres-Gatius, M., Artigas, F., & Castane, A. (**2017**). Glial GLT-1 blockade in infralimbic cortex as a new strategy to evoke rapid antidepressant-like effects in rats. *Transl Psychiatry, 7*(2), e1038.

44. Geeraerts, T., Duranteau, J., & Vigué, B. (**2008**). Microdialyse cérébrale : méthodologie et applications cliniques. *Réanimation, 17*, 702-707.

45. Gegelashvili, G., Dehnes, Y., Danbolt, N. C., & Schousboe, A. (**2000**). The high-affinity glutamate transporters GLT1, GLAST, and EAAT4 are regulated via different signalling mechanisms. *Neurochem Int, 37*(2-3), 163-170.

46. Gentsch, C., Lichtsteiner, M., & Feer, H. (**1981**). Locomotor activity, defecation score and corticosterone levels during an openfield exposure: a comparison among individually and group-housed rats, and genetically selected rat lines. *Physiol Behav, 27*(1), 183-186.

47. Hajos, M., Richards, C. D., Szekely, A. D., & Sharp, T. (**1998**). An electrophysiological and neuroanatomical study of the medial prefrontal cortical projection to the midbrain raphe nuclei in the rat. *Neuroscience, 87*(1), 95-108.

48. Hanoun, N., Mocaer, E., Boyer, P. A., Hamon, M., & Lanfumey, L. (**2004**). Differential effects of the novel antidepressant agomelatine (S 20098) versus fluoxetine on 5-HT1A receptors in the rat brain. *Neuropharmacology, 47*(4), 515-526.

49. Harandi, M., Aguera, M., Gamrani, H., Didier, M., Maitre, M., Calas, A., & Belin, M. F. (**1987**). gamma-Aminobutyric acid and 5-hydroxytryptamine interrelationship in the rat nucleus raphe dorsalis: combination of radioautographic and immunocytochemical techniques at light and electron microscopy levels. *Neuroscience, 21*(1), 237-251.

50. Herrero, M. T., Oset-Gasque, M. J., Lopez, E., Vicente, S., & Gonzalez, M. P. (**1999**). Mechanism by which GABA, through its GABA(A) receptor, modulates glutamate release from rat cortical neurons in culture. *Neurochem Int, 34*(2), 141-148.

51. Hirschfeld, R. M. (**2000**). History and evolution of the monoamine hypothesis of depression. *J Clin Psychiatry, 61 Suppl 6*, 4-6.

52. Holick, K. A., Lee, D. C., Hen, R., & Dulawa, S. C. (**2008**). Behavioral effects of chronic fluoxetine in BALB/cJ mice do not require adult hippocampal neurogenesis or the serotonin 1A receptor. *Neuropsychopharmacology, 33*(2), 406-417.

53. Iijima, M., Fukumoto, K., & Chaki, S. (**2012**). Acute and sustained effects of a metabotropic glutamate 5 receptor antagonist in the novelty-suppressed feeding test. *Behav Brain Res, 235*(2), 287-292.

54. Irifune, M., Sato, T., Kamata, Y., Nishikawa, T., Dohi, T., & Kawahara, M. (**2000**). Evidence for GABA(A) receptor agonistic properties of ketamine: convulsive and anesthetic behavioral models in mice. *Anesth Analg, 91*(1), 230-236.

55. Kamiyama, H., Matsumoto, M., Otani, S., Kimura, S. I., Shimamura, K. I., Ishikawa, S., Yanagawa, Y., & Togashi, H. (**2011**). Mechanisms underlying ketamine-induced

synaptic depression in rat hippocampus-medial prefrontal cortex pathway. *Neuroscience, 177*, 159-169.

56. Koike, H., & Chaki, S. (**2014**). Requirement of AMPA receptor stimulation for the sustained antidepressant activity of ketamine and LY341495 during the forced swim test in rats. *Behav Brain Res, 271*, 111-115.

57. Koike, H., Iijima, M., & Chaki, S. (**2011**). Involvement of AMPA receptor in both the rapid and sustained antidepressant-like effects of ketamine in animal models of depression. *Behav Brain Res, 224*(1), 107-111.

58. Koike, H., Iijima, M., & Chaki, S. (**2013**). Effects of ketamine and LY341495 on the depressive-like behavior of repeated corticosterone-injected rats. *Pharmacol Biochem Behav, 107*, 20-23.

59. Kotermanski, S. E., & Johnson, J. W. (**2009**). Mg2+ imparts NMDA receptor subtype selectivity to the Alzheimer's drug memantine. *J Neurosci, 29*(9), 2774-2779.

60. Krishnan, V., Han, M. H., Graham, D. L., Berton, O., Renthal, W., Russo, S. J., Laplant, Q., Graham, A., Lutter, M., Lagace, D. C., Ghose, S., Reister, R., Tannous, P., Green, T. A., Neve, R. L., Chakravarty, S., Kumar, A., Eisch, A. J., Self, D. W., Lee, F. S., Tamminga, C. A., Cooper, D. C., Gershenfeld, H. K., & Nestler, E. J. (**2007**). Molecular adaptations underlying susceptibility and resistance to social defeat in brain reward regions. *Cell, 131*(2), 391-404.

61. Kuki, T., Fujihara, K., Miwa, H., Tamamaki, N., Yanagawa, Y., & Mushiake, H. (**2015**). Contribution of parvalbumin and somatostatin-expressing GABAergic neurons to slow oscillations and the balance in beta-gamma oscillations across cortical layers. *Front Neural Circuits, 9*, 6.

62. Le Poul, E., Laaris, N., Doucet, E., Laporte, A. M., Hamon, M., & Lanfumey, L. (**1995**). Early desensitization of somato-dendritic 5-HT1A autoreceptors in rats treated with fluoxetine or paroxetine. *Naunyn Schmiedebergs Arch Pharmacol, 352*(2), 141-148.

63. Li, N., Lee, B., Liu, R. J., Banasr, M., Dwyer, J. M., Iwata, M., Li, X. Y., Aghajanian, G., & Duman, R. S. (**2010**). mTOR-dependent synapse formation underlies the rapid antidepressant effects of NMDA antagonists. *Science, 329*(5994), 959-964.

64. Li, N., Liu, R. J., Dwyer, J. M., Banasr, M., Lee, B., Son, H., Li, X. Y., Aghajanian, G., & Duman, R. S. (**2011**). Glutamate N-methyl-D-aspartate receptor antagonists rapidly reverse behavioral and synaptic deficits caused by chronic stress exposure. *Biol Psychiatry, 69*(8), 754-761.

65. Lin, L. C., & Sibille, E. (**2015**). Somatostatin, neuronal vulnerability and behavioral emotionality. *Mol Psychiatry, 20*(3), 377-387.

66. Lindefors, N., Barati, S., & O'Connor, W. T. (**1997**). Differential effects of single and repeated ketamine administration on dopamine, serotonin and GABA transmission in rat medial prefrontal cortex. *Brain Res, 759*(2), 205-212.

67. Littlewood, C. L., Jones, N., O'Neill, M. J., Mitchell, S. N., Tricklebank, M., & Williams, S. C. (**2006**). Mapping the central effects of ketamine in the rat using pharmacological MRI. *Psychopharmacology (Berl), 186*(1), 64-81.

68. Liu, R. J., Lee, F. S., Li, X. Y., Bambico, F., Duman, R. S., & Aghajanian, G. K. (**2012**). Brain-derived neurotrophic factor Val66Met allele impairs basal and ketamine-stimulated synaptogenesis in prefrontal cortex. *Biol Psychiatry, 71*(11), 996-1005.

69. Lonnroth, P., Jansson, P. A., & Smith, U. (**1987**). A microdialysis method allowing characterization of intercellular water space in humans. *Am J Physiol, 253*(2 Pt 1), E228-231.

70. Lopez-Gil, X., Babot, Z., Amargos-Bosch, M., Sunol, C., Artigas, F., & Adell, A. (**2007**). Clozapine and haloperidol differently suppress the MK-801-increased glutamatergic and serotonergic transmission in the medial prefrontal cortex of the rat. *Neuropsychopharmacology, 32*(10), 2087-2097.

71. Lopez-Gil, X., Jimenez-Sanchez, L., Romon, T., Campa, L., Artigas, F., & Adell, A. (**2012**). Importance of inter-hemispheric prefrontal connection in the effects of non-competitive NMDA receptor antagonists. *Int J Neuropsychopharmacol, 15*(7), 945-956.

72. Lorrain, D. S., Baccei, C. S., Bristow, L. J., Anderson, J. J., & Varney, M. A. (**2003**). Effects of ketamine and N-methyl-D-aspartate on glutamate and dopamine release in the rat prefrontal cortex: modulation by a group II selective metabotropic glutamate receptor agonist LY379268. *Neuroscience, 117*(3), 697-706.

73. Ma, K., Xu, A., Cui, S., Sun, M. R., Xue, Y. C., & Wang, J. H. (**2016**). Impaired GABA synthesis, uptake and release are associated with depression-like behaviors induced by chronic mild stress. *Transl Psychiatry, 6*(10), e910.

74. MacQueen, G., & Frodl, T. (**2011**). The hippocampus in major depression: evidence for the convergence of the bench and bedside in psychiatric research? *Mol Psychiatry, 16*(3), 252-264.

75. Maeng, S., Zarate, C. A., Jr., Du, J., Schloesser, R. J., McCammon, J., Chen, G., & Manji, H. K. (**2008**). Cellular mechanisms underlying the antidepressant effects of ketamine: role of alpha-amino-3-hydroxy-5-methylisoxazole-4-propionic acid receptors. *Biol Psychiatry, 63*(4), 349-352.

76. Matsuno-Yagi, A., & Mukohata, Y. (**1977**). Two possible roles of bacteriorhodopsin; a comparative study of strains of Halobacterium halobium differing in pigmentation. *Biochem Biophys Res Commun, 78*(1), 237-243.

77. Mekiri, M., Gardier, A. M., David, D. J., & Guilloux, J. P. (**November 2015**). *Resistance to chronic antidepressant treatment: A behavioural and neurogenic study in a neuroendocrine-based mice model of anxiety/depression.* Paper presented at the 45th Annual Meeting of Neuroscience, Chicago, U.S.A.

78. Mendez-David, I., Boursier, C., Domergue, V., Colle, R., Falissard, B., Corruble, E., Gardier, A. M., Guilloux, J. P., & David, D. J. (**2017**). Differential Peripheral Proteomic Biosignature of Fluoxetine Response in a Mouse Model of Anxiety/Depression. *Front Cell Neurosci, 11*, 237.

79. Mendez-David, I., David, D. J., Darcet, F., Wu, M. V., Kerdine-Romer, S., Gardier, A. M., & Hen, R. (**2014**). Rapid anxiolytic effects of a 5-HT(4) receptor agonist are mediated by a neurogenesis-independent mechanism. *Neuropsychopharmacology, 39*(6), 1366-1378.

80. Miller, O. H., Moran, J. T., & Hall, B. J. (**2016**). Two cellular hypotheses explaining the initiation of ketamine's antidepressant actions: Direct inhibition and disinhibition. *Neuropharmacology, 100*, 17-26.

81. Moghaddam, B., Adams, B., Verma, A., & Daly, D. (**1997**). Activation of glutamatergic neurotransmission by ketamine: a novel step in the pathway from NMDA receptor blockade to dopaminergic and cognitive disruptions associated with the prefrontal cortex. *J Neurosci, 17*(8), 2921-2927.

82. Morales, I., Sabate, M., & Rodriguez, M. (**2013**). Striatal glutamate induces retrograde excitotoxicity and neuronal degeneration of intralaminar thalamic nuclei: their potential relevance for Parkinson's disease. *Eur J Neurosci, 38*(1), 2172-2182.

83. Moussawi, K., Riegel, A., Nair, S., & Kalivas, P. W. (**2011**). Extracellular glutamate: functional compartments operate in different concentration ranges. *Front Syst Neurosci, 5*, 94.

84. Murray, C. J., & Lopez, A. D. (**1996**). Evidence-based health policy--lessons from the Global Burden of Disease Study. *Science, 274*(5288), 740-743.

85. Murray, F., Kennedy, J., Hutson, P. H., Elliot, J., Huscroft, I., Mohnen, K., Russell, M. G., & Grimwood, S. (**2000**). Modulation of [3H]MK-801 binding to NMDA receptors in vivo and in vitro. *Eur J Pharmacol, 397*(2-3), 263-270.

86. Nagel, G., Ollig, D., Fuhrmann, M., Kateriya, S., Musti, A. M., Bamberg, E., & Hegemann, P. (**2002**). Channelrhodopsin-1: a light-gated proton channel in green algae. *Science, 296*(5577), 2395-2398.

87. Newport, D. J., Carpenter, L. L., McDonald, W. M., Potash, J. B., Tohen, M., Nemeroff, C. B., Biomarkers, A. P. A. C. o. R. T. F. o. N., & Treatments. (**2015**). Ketamine and Other NMDA Antagonists: Early Clinical Trials and Possible Mechanisms in Depression. *Am J Psychiatry, 172*(10), 950-966.

88. Nguyen, H. T., Guiard, B. P., Bacq, A., David, D. J., David, I., Quesseveur, G., Gautron, S., Sanchez, C., & Gardier, A. M. (**2013**). Blockade of the high-affinity noradrenaline transporter (NET) by the selective 5-HT reuptake inhibitor escitalopram: an in vivo microdialysis study in mice. *Br J Pharmacol, 168*(1), 103-116.

89. Nishitani, N., Nagayasu, K., Asaoka, N., Yamashiro, M., Shirakawa, H., Nakagawa, T., & Kaneko, S. (**2014**). Raphe AMPA receptors and nicotinic acetylcholine receptors mediate ketamine-induced serotonin release in the rat prefrontal cortex. *Int J Neuropsychopharmacol, 17*(8), 1321-1326.

90. Otte, C., Gold, S. M., Penninx, B. W., Pariante, C. M., Etkin, A., Fava, M., Mohr, D. C., & Schatzberg, A. F. (**2016**). Major depressive disorder. *Nat Rev Dis Primers, 2*, 16065.

91. Pastrana, E. (**2010**). Optogenetics: controlling cell function with light. *Nature Methods, 8*, 24.

92. Pellow, S., & File, S. E. (**1986**). Anxiolytic and anxiogenic drug effects on exploratory activity in an elevated plus-maze: a novel test of anxiety in the rat. *Pharmacol Biochem Behav, 24*(3), 525-529.

93. Peyron, C., Petit, J. M., Rampon, C., Jouvet, M., & Luppi, P. H. (**1998**). Forebrain afferents to the rat dorsal raphe nucleus demonstrated by retrograde and anterograde tracing methods. *Neuroscience, 82*(2), 443-468.

94. Pham, T. H., Defaix, C., Xu, X., Deng, S.-X., Fabresse, N., Alvarez, J.-C., Landry, D. W., Brachman, R. A., Denny, C. A., & Gardier, A. M. (**2017a**). Common neurotransmission recruited in (R,S)-ketamine and (2R,6R)-hydroxynorketamine-induced sustained antidepressant-like effects. *Biol Psychiatry*

95. Pham, T. H., Mendez-David, I., Defaix, C., Guiard, B. P., Tritschler, L., David, D. J., & Gardier, A. M. (**2017b**). Ketamine treatment involves medial prefrontal cortex serotonin to induce a rapid antidepressant-like activity in BALB/cJ mice. *Neuropharmacology, 112*, 198-209.

96. Pongdhana, K., Ogawa, N., Hirose, Y., Ono, T., Kosaka, F., & Mori, A. (**1987**). Effects of ketamine on the cholecystokinin, somatostatin, substance P, and thyrotropin releasing hormone in discrete regions of rat brain. *Neurochem Res, 12*(1), 73-77.

97. Porsolt, R. D., Bertin, A., & Jalfre, M. (**1977**). Behavioral despair in mice: a primary screening test for antidepressants. *Arch Int Pharmacodyn Ther, 229*(2), 327-336.

98. Porsolt, R. D., Chermat, R., Lenegre, A., Avril, I., Janvier, S., & Steru, L. (**1987**). Use of the automated tail suspension test for the primary screening of psychotropic agents. *Arch Int Pharmacodyn Ther, 288*(1), 11-30.

99. Price, R. B., Nock, M. K., Charney, D. S., & Mathew, S. J. (**2009**). Effects of intravenous ketamine on explicit and implicit measures of suicidality in treatment-resistant depression. *Biol Psychiatry, 66*(5), 522-526.

100. Rantamaki, T., & Yalcin, I. (**2016**). Antidepressant drug action--From rapid changes on network function to network rewiring. *Prog Neuropsychopharmacol Biol Psychiatry, 64*, 285-292.

101. Riga, M. S., Sanchez, C., Celada, P., & Artigas, F. (**2016**). Involvement of 5-HT3 receptors in the action of vortioxetine in rat brain: Focus on glutamatergic and GABAergic neurotransmission. *Neuropharmacology, 108*, 73-81.

102. Rosa, P. B., Neis, V. B., Ribeiro, C. M., Moretti, M., & Rodrigues, A. L. (**2016**). Antidepressant-like effects of ascorbic acid and ketamine involve modulation of GABAA and GABAB receptors. *Pharmacol Rep, 68*(5), 996-1001.

103. Rush, A. J., Trivedi, M. H., Wisniewski, S. R., Nierenberg, A. A., Stewart, J. W., Warden, D., Niederehe, G., Thase, M. E., Lavori, P. W., Lebowitz, B. D., McGrath, P. J., Rosenbaum, J. F., Sackeim, H. A., Kupfer, D. J., Luther, J., & Fava, M. (**2006**). Acute and longer-term outcomes in depressed outpatients requiring one or several treatment steps: a STAR*D report. *Am J Psychiatry, 163*(11), 1905-1917.

104. Santarelli, L., Saxe, M., Gross, C., Surget, A., Battaglia, F., Dulawa, S., Weisstaub, N., Lee, J., Duman, R., Arancio, O., Belzung, C., & Hen, R. (**2003**). Requirement of hippocampal neurogenesis for the behavioral effects of antidepressants. *Science, 301*(5634), 805-809.

105. Sanz-Clemente, A., Nicoll, R. A., & Roche, K. W. (**2013**). Diversity in NMDA receptor composition: many regulators, many consequences. *Neuroscientist, 19*(1), 62-75.

106. Schneider, M. B., Gradinaru, V., Zhang, F., & Deisseroth , K. (**2008**). Controlling Neuronal Activity. *American Journal of Psychiatry, 165*(5), 562-562.

107. Schneider, P. G., & Rodriguez de Lores Arnaiz, G. (**2013**). Ketamine prevents seizures and reverses changes in muscarinic receptor induced by bicuculline in rats. *Neurochem Int, 62*(3), 258-264.

108. Seligman, M. E., Rosellini, R. A., & Kozak, M. J. (**1975**). Learned helplessness in the rat: time course, immunization, and reversibility. *J Comp Physiol Psychol, 88*(2), 542-547.

109. Sellmeijer, J., Mathis, V., Hugel, S., Li, X. H., Song, Q., Chen, Q. Y., Barthas, F., Lutz, P. E., Karatas, M., Luthi, A., Veinante, P., Aertsen, A., Barrot, M., Zhuo, M., & Yalcin, I. (**2018**). Hyperactivity of anterior cingulate cortex areas 24a/24b drives chronic pain-induced anxiodepressive-like consequences. *J Neurosci*

110. Serafini, G., Howland, R. H., Rovedi, F., Girardi, P., & Amore, M. (**2014**). The role of ketamine in treatment-resistant depression: a systematic review. *Curr Neuropharmacol, 12*(5), 444-461.

111. Slattery, D. A., Neumann, I. D., & Cryan, J. F. (**2011**). Transient inactivation of the infralimbic cortex induces antidepressant-like effects in the rat. *J Psychopharmacol, 25*(10), 1295-1303.

112. Sparta, D. R., Stamatakis, A. M., Phillips, J. L., Hovelso, N., van Zessen, R., & Stuber, G. D. (**2011**). Construction of implantable optical fibers for long-term optogenetic manipulation of neural circuits. *Nat Protoc, 7*(1), 12-23.

113. Stuber, G. D., & Mason, A. O. (**2013**). Integrating optogenetic and pharmacological approaches to study neural circuit function: current applications and future directions. *Pharmacol Rev, 65*(1), 156-170.

114. Sugiyama, Y., Maeda, M., Futai, M., & Mukohata, Y. (**1989**). Isolation of a gene that encodes a new retinal protein, archaerhodopsin, from Halobacterium sp. aus-1. *J Biol Chem, 264*(35), 20859-20862.

115. Tiller, J. W. (**2013**). Depression and anxiety. *Med J Aust, 199*(6 Suppl), S28-31.

116. Tritschler, L., Kheirbek, M. A., Dantec, Y. L., Mendez-David, I., Guilloux, J. P., Faye, C., Doan, J., Pham, T. H., Hen, R., David, D. J., & Gardier, A. M. (**2017**). Optogenetic activation of granule cells in the dorsal dentate gyrus enhances dopaminergic neurotransmission in the Nucleus Accumbens. *Neurosci Res*

117. Trivedi, M. H., Rush, A. J., Wisniewski, S. R., Nierenberg, A. A., Warden, D., Ritz, L., Norquist, G., Howland, R. H., Lebowitz, B., McGrath, P. J., Shores-Wilson, K., Biggs, M. M., Balasubramani, G. K., Fava, M., & Team, S. D. S. (**2006**). Evaluation of outcomes with citalopram for depression using measurement-based care in STAR*D: implications for clinical practice. *Am J Psychiatry, 163*(1), 28-40.

118. Ungerstedt, U. (**1991**). Microdialysis--principles and applications for studies in animals and man. *J Intern Med, 230*(4), 365-373.

119. Varga, V., Szekely, A. D., Csillag, A., Sharp, T., & Hajos, M. (**2001**). Evidence for a role of GABA interneurones in the cortical modulation of midbrain 5-hydroxytryptamine neurones. *Neuroscience, 106*(4), 783-792.

120. Wang, N., Zhang, G. F., Liu, X. Y., Sun, H. L., Wang, X. M., Qiu, L. L., Yang, C., & Yang, J. J. (**2014**). Downregulation of neuregulin 1-ErbB4 signaling in parvalbumin interneurons in the rat brain may contribute to the antidepressant properties of ketamine. *J Mol Neurosci, 54*(2), 211-218.

121. Wang, Q. P., Ochiai, H., & Nakai, Y. (**1992**). GABAergic innervation of serotonergic neurons in the dorsal raphe nucleus of the rat studied by electron microscopy double immunostaining. *Brain Res Bull, 29*(6), 943-948.

122. WHO. (**2012**). Depression: A Global Crisis. *World Health Organisation - World Federation for Mental Health*

123. Willner, P. (**2005**). Chronic mild stress (CMS) revisited: consistency and behavioural-neurobiological concordance in the effects of CMS. *Neuropsychobiology, 52*(2), 90-110.

124. Xu, Y., Hackett, M., Carter, G., Loo, C., Galvez, V., Glozier, N., Glue, P., Lapidus, K., McGirr, A., Somogyi, A. A., Mitchell, P. B., & Rodgers, A. (**2016**). Effects of Low-Dose and Very Low-Dose Ketamine among Patients with Major Depression: a Systematic Review and Meta-Analysis. *Int J Neuropsychopharmacol, 19*(4)

125. Yamanaka, H., Yokoyama, C., Mizuma, H., Kurai, S., Finnema, S. J., Halldin, C., Doi, H., & Onoe, H. (**2014**). A possible mechanism of the nucleus accumbens and ventral pallidum 5-HT1B receptors underlying the antidepressant action of ketamine: a PET study with macaques. *Transl Psychiatry, 4*, e342.

126. Yan, H. C., Cao, X., Das, M., Zhu, X. H., & Gao, T. M. (**2010**). Behavioral animal models of depression. *Neurosci Bull, 26*(4), 327-337.

127. Yang, C., Qu, Y., Abe, M., Nozawa, D., Chaki, S., & Hashimoto, K. (**2016**). (R)-ketamine shows greater potency and longer lasting antidepressant effects than its metabolite (2R,6R)-hydroxynorketamine. *Biol Psychiatry*

128. Zanos, P., Moaddel, R., Morris, P. J., Georgiou, P., Fischell, J., Elmer, G. I., Alkondon, M., Yuan, P., Pribut, H. J., Singh, N. S., Dossou, K. S., Fang, Y., Huang, X. P., Mayo, C. L., Wainer, I. W., Albuquerque, E. X., Thompson, S. M., Thomas, C. J., Zarate, C. A., Jr., & Gould, T. D. (**2016**). NMDAR inhibition-independent antidepressant actions of ketamine metabolites. *Nature, 533*(7604), 481-486.

129. Zanos, P., Piantadosi, S. C., Wu, H. Q., Pribut, H. J., Dell, M. J., Can, A., Snodgrass, H. R., Zarate, C. A., Jr., Schwarcz, R., & Gould, T. D. (**2015**). The Prodrug 4-Chlorokynurenine Causes Ketamine-Like Antidepressant Effects, but Not Side Effects, by NMDA/GlycineB-Site Inhibition. *J Pharmacol Exp Ther, 355*(1), 76-85.

130. Zarate, C. A., Jr., Singh, J. B., Carlson, P. J., Brutsche, N. E., Ameli, R., Luckenbaugh, D. A., Charney, D. S., & Manji, H. K. (**2006**). A randomized trial of an N-methyl-D-aspartate antagonist in treatment-resistant major depression. *Arch Gen Psychiatry, 63*(8), 856-864.

131. Zhou, Z., Zhang, G., Li, X., Liu, X., Wang, N., Qiu, L., Liu, W., Zuo, Z., & Yang, J. (**2015**). Loss of phenotype of parvalbumin interneurons in rat prefrontal cortex is involved in antidepressant- and propsychotic-like behaviors following acute and repeated ketamine administration. *Mol Neurobiol, 51*(2), 808-819.

université PARIS-SACLAY | ÉCOLE DOCTORALE Innovation thérapeutique : du fondamental à l'appliqué

Titre : Mécanisme d'action antidépresseur rapide de la kétamine et de son principal métabolite (2*R*,6*R*)-hydroxynorkétamine: rôle de la balance excitation-inhibition chez la souris

Mots clés : kétamine, (2R,6R)-hydroxynorkétamine, glutamate, récepteur NMDA, 5-HT, cortex

Résumé : Selon l'OMS, les troubles dépressifs majeurs (TDM) seront la 2ème cause d'incapacité dans le monde en 2020 et deviendront la 1ère en 2030. Les antidépresseurs classiques ont des effets thérapeutiques retardés et de nombreux patients sont résistants. La kétamine, antagoniste du récepteur N-methyl-D-aspartate (R-NMDA) du L-glutamate, possède un effet antidépresseur rapide chez les patients résistants à un traitement classique. Le mécanisme de cette activité étonnante n'est pas bien compris. En couplant la microdialyse intracérébrale à un test comportemental prédictif d'une activité antidépressive dans un modèle de souris BALB/cJ de phénotype anxieux, nous montrons que cette activité de la kétamine dépend de la balance excitation-inhibition entre les systèmes glutamate/R-NMDA et R-AMPA, GABA/R-$GABA_A$, sérotonine du circuit cortex préfrontal/noyau du raphé. Nos résultats suggèrent également que ce serait la combinaison [kétamine-(2*R*,6*R*)-hydroxy-norkétamine, son principal métabolite cérébral] qui porterait l'effet antidépresseur. Mes travaux de thèse contribuent à une meilleure compréhension de l'effet rapide antidépresseur de la kétamine.

Title : Mechanism of rapid antidepressant action of ketamine and its principal metabolite (2R,6R)-hydroxynorketamine: role of the excitation-inhibition balance in mice

Keywords : ketamine, (2R,6R)-hydroxynorketamine, glutamate, NMDA receptor, 5-HT, cortex

Abstract : According to the WHO, major depressive disorder (MDD) will be the second leading cause of disability in the world in 2020 and will become the first in 2030. Conventional antidepressant drugs have delayed therapeutic effects and many patients are resistant. Ketamine, an N-methyl-D-aspartate (NMDA-R) receptor antagonist of L-glutamate, exerts a rapid antidepressant effect in patients who are resistant to standard therapy. The mechanism of this amazing activity is not well understood. By coupling intracerebral microdialysis to a predictive behavioral test of antidepressant activity in a BALB/cJ mouse model with an anxious phenotype, we show that this ketamine activity is dependent on the excitation-inhibition balance between glutamate/NMDA-R and AMPA-R, GABA/$GABA_A$-R, serotonin systems in the prefrontal cortex/raphe nucleus circuit. Our results also suggest that it would be the combination [ketamine-(*2R,6R*)-hydroxy-norketamine, its main brain metabolite] that would carry the antidepressant effect. My thesis work pave the way for the development of new fast-acting antidepressant drugs.

Université Paris-Saclay
Espace Technologique / Immeuble Discovery
Route de l'Orme aux Merisiers RD 128 / 91190 Saint-Aubin, France